

Corrosion of Steel at High Temperature in Naphthenic Acid and Sulfur Containing  
Crude Oil Fractions

A dissertation presented to  
the faculty of  
the Russ College of Engineering and Technology of Ohio University

In partial fulfillment  
of the requirements for the degree  
Doctor of Philosophy

Gheorghe M. Bota

November 2010

© 2010 Gheorghe M. Bota. All Rights Reserved.

This dissertation titled  
Corrosion of Steel at High Temperature in Naphthenic Acid and Sulfur Containing  
Crude Oil Fractions

by

GHEORGHE M. BOTA

has been approved for  
the Department of Chemical and Biomolecular Engineering  
and the Russ College of Engineering and Technology by

---

Srdjan Nesic

Professor of Chemical and Biomolecular Engineering

---

Dennis Irwin

Dean, Russ College of Engineering and Technology

**ABSTRACT**

BOTA, GHEORGHE M., Ph.D., November 2010, Chemical Engineering

Corrosion of Steel at High Temperature in Naphthenic Acid and Sulfur Containing  
Crude Oil Fractions

Director of Dissertation: Srdjan Nestic

Increasing oil prices and limited availability of light sweet crudes on oil markets sparked a new interest for oil companies in heavy crude oils in spite of the disadvantages of processing such oils. Well known for their high acidic and sulfur content, heavy crude oils have strong corrosive effects at high temperatures and therefore studying and understanding corrosion mechanism of naphthenic acids in sulfur environments became a necessity in designing and operating efficiently the refinery equipment. Thus in 2004 Institute of Corrosion and Multiphase Technology started the Naphthenic Acids Project financed by ExxonMobil Research and Engineering Company (EMRE), project that had as final goals: improved understanding of naphthenic acid corrosion and construction of a model for this particular type of corrosion.

Naphthenic acids corrosion occurs usually when acidic oils are processed at high temperatures (220-340°C) and because these oils also have a natural sulfur content which is high and corrosive, it become difficult to separate these two types of corrosions. Considering all the above it was decided that first part of the project will focus exclusively on sulfur compounds corrosive effects at high temperatures. Thus the experimental tests were run using a model oil with a given sulfur content. During these

“sulfidation” tests, the oil sulfur compounds not only corroded the metal samples but they also formed a protective iron sulfide (FeS) scale on metal surface.

The second part of the project investigated the iron sulfide scale protection against naphthenic acids attack and during these tests the performance of FeS scales was “challenged” with low sulfur model oils spiked with different concentrations of naphthenic acids.

Third part of the project was similar to the second except for using real crude oil fractions for generating the iron sulfide scales that were then challenged with model oil spiked with naphthenic acids. All these tests results were finally used in building the model of naphthenic acids corrosion in sulfur containing crude oil environments, a model that has practical applicability for refineries.

Approved: \_\_\_\_\_

Srdjan Nesic

Professor of Chemical and Biomolecular Engineering

## PREFACE

The Naphthenic Acid Project at the Institute for Corrosion and Multiphase Technology was financed in part by ExxonMobil Research and Engineering Company (EMRE) as the sole industrial sponsor, who also provided the experimental equipment and necessary technical expertise for using it. All experimental results were presented to EMRE experts during annual project Advisory Board meetings and in yearly reports (internal confidential documents). These reports will be further cited as references: Progress Reports 2005<sup>1</sup> 2006<sup>2</sup>, and 2008<sup>3</sup>. For a complete overview of the experimental results that were collected during the three years on the Naphthenic Acid Project, a complete sets of test results is included in the two appendices of this dissertation. The final goal of the project was the model of naphthenic acids corrosion used to build prediction software CRUDECORP V5.0 that will be also cited as a reference in this dissertation.

## ACKNOWLEDGMENTS

I would like to thank first my academic adviser Dr. Srdjan Nesic who had the intuition in assigning me to the Naphthenic Acids Project and then guided me in achieving the goals of this challenging scientific research. His scientific, practical, philosophical and social insight as well as his sharp but fair criticism influenced my becoming a corrosion specialist and therefore they were and are invaluable.

All my scientific and experimental work would have not been possible without the financial and material support of ExxonMobil Research and Engineering Company (EMRE) that started the NAP project at Ohio University and to whom I am thoroughly indebted. It was H. Alan Wolf, the EMRE representative for OU who guided and encouraged me through the first stages of this project and latter with his diplomacy, humor and patience helped me learn the working style of a big company and overcome the inherent mistakes in presenting my weekly reports. Josh Varon from EMRE did most of the SEM work of this project and therefore I thank him here also.

My gratitude is also due to the technical staff of Institute for Corrosion and Multiphase Technology: Al Schubert, John Goettge, and Daniel Cain who regardless of their other special responsibilities always provided me the necessary technical assistance and support. Assistance from NAP group students Vijaya Kanunkuntla, Nicolas Jauseau, and postdoctoral fellow Dr.Dingrong Qu is also gratefully acknowledged.

It was a great privilege meeting and working with all the people who helped and supported me along my years as graduate student at Ohio University, in the Institute of Corrosion and Multiphase Technology. Without their constant guidance, help, and

encouragements this current work would have not been possible and therefore my gratitude is due to all of them.

Last, but not least I would like to thank my family who constantly and unconditionally supported and encouraged me through all my life and particularly these years spent in graduate school far away from them.

**TABLE OF CONTENTS**

	Page
Abstract.....	3
Preface.....	5
Acknowledgments.....	6
List of Tables .....	13
List of Figures.....	14
Chapter 1: Introduction.....	26
Chapter 2: Literature Review.....	30
2.1 Identifying Naphthenic Acid Types and Structures.....	32
2.2 Corrosive Attack Morphology .....	35
2.3 The Effect of Naphthenic Acid Concentration .....	35
2.4 Effect of Sulfur Content.....	37
2.5 Effect of Temperature.....	40
2.6 Effect of Acid Structure .....	42
2.7 Effect of Velocity.....	42
2.8 Effect of NAP Vaporization and Condensation.....	43
2.9 Effect of Pressure.....	44
Chapter 3: Research Objectives.....	45
3.1 Research Objectives.....	45
3.2 Research Project Milestones.....	45
Chapter 4: Sulfidation Experiments.....	48
4.1 Introduction.....	48

	9
4.2 Experimental .....	48
4.2.1 Instrumentation - High Velocity Rig (HVR) .....	48
4.2.2 Materials .....	51
4.3 Test Conditions .....	52
4.3.1 Reactive Species Concentrations .....	53
4.3.2 Test Duration .....	53
4.3.3 Specimens Arrangement for Test.....	54
4.4 Sample Preparation .....	55
4.5 Evaluation of Metal Loss .....	56
4.6 Results and Discussion .....	57
4.6.1 HVR Quality Control Run Test .....	57
4.6.2 Test Matrix.....	58
4.6.3 Sulfidation Tests Results.....	59
4.6.3 Summary .....	82
Chapter 5: Sulfidation – Challenge Experiments.....	83
5.1 Introduction.....	83
5.2 Experimental .....	83
5.2.1 Instrumentation .....	84
5.2.2 Materials .....	84
5.2.3 Test Conditions .....	85
5.3 Results and Discussion .....	87
5.3.1 Sulfidation Tests .....	88

	10
5.3.2 TAN 2 Results.....	88
5.3.3 TAN 3.5 Results.....	93
5.3.4 TAN 5 Results.....	97
5.3.5 TAN 6.5 Results.....	103
5.3.6 TAN 8 Results.....	107
5.3.7 Comparison of 24 hr Test Results.....	112
5.3.8 Low Velocity Experiment Results.....	115
5.3.9 Sulfidation at Lower Temperature - 287°C (550°F).....	117
5.3.10 Summary.....	119
Chapter 6: Sulfidation-Challenge Experiments Using Real Crude Oil Fractions.....	123
6.1 Introduction.....	123
6.2 Crude Oil Fractions.....	123
6.3 Experimental.....	125
6.3.1 Experimental Considerations.....	125
6.3.2 Instrumentation.....	126
6.3.3 Materials.....	126
6.3.4 Test Conditions.....	128
6.4 Results and Discussion.....	129
6.4.1 Real Crude Oil Fractions Testing Matrix.....	130
6.4.2 Sulfidation Reference Test.....	131
6.4.3 Diluted Fractions Tests Results.....	136
6.4.4 “Neat” Fractions Experimental Results.....	145

	11
6.4.5 High TAN Spiked Crude Oil Fractions Tests .....	160
6.4.6 Special Corrosion Tests Using Only Naphthenic Acids .....	174
Chapter 7: Mechanistic Model of Naphthenic Acid Corrosion .....	179
7.1 Introduction.....	179
7.2 Corrosion model.....	184
7.2.1 Sulfidation Rate (SR).....	184
7.2.2 Sulfidation Rate – Physico-Chemical Model.....	184
7.2.3 Sulfidation Rate – Mathematical Model .....	185
7.2.4 Naphthenic Acid Corrosion Rate (NAP) .....	190
7.2.5 Naphthenic Acid Corrosion – Physico-Chemical Model.....	190
7.2.6 Naphthenic Acid Corrosion – Mathematical Model .....	192
7.3 Verification of the Model.....	195
7.3.1 CS Corrosion Rate Comparison.....	196
7.3.2 5Cr Corrosion Rate Comparison.....	196
Chapter 8: Conclusions .....	198
Chapter 9: Recommendation and Future Work .....	200
References.....	201
Appendix A: Initial Test Matrix for Sulfidation Tests Done in the High Velocity Rig (HVR) Fall 2005 .....	207
Appendix B: Test Matrix for Sulfidation-Challenge Tests Done in the High Velocity Rig (HVR) .....	208

Appendix C: Experimental Results and SEM Images for Sulfidation-Challenge Tests Done in the High Velocity Rig (HVR) .....	209
Appendix D: Test Matrix for NAP Acids Challenges Against Scales Formed with Real Crude Oil Fractions.....	210
Appendix E: Experimental Results and SEM Images for NAP Acids Challenges Against Scales Formed with Real Crude Oil Fractions.....	211

## LIST OF TABLES

	Page
Table 1. <i>Chemical Structures of Naphthenic Acids Most Frequently Identified in Crude Oils</i> <sup>13-15,19</sup> .....	34
Table 2. <i>Main Organic Sulfur Compounds in Crude Oils</i> <sup>8,14,38,41</sup> .....	38
Table 3. <i>Physical Properties of Mineral Oils</i> .....	52
Table 4. <i>Experimental Conditions for the First Set of HVR Tests using Carbon Steel (CS A106) and Mild Steel (F5-A 182) Specimens</i> .....	54
Table 5. <i>HVR QC Run results and experimental conditions at EMRE and OU Corrosion Center</i> .....	58
Table 6. <i>General test conditions for sulfidation-challenge tests</i> .....	86
Table 7. <i>Summary of sulfidation – challenge tests. Challenge time series vs. different TAN solutions. (TAN - Total Acid Number)</i> .....	86
Table 8. <i>Oil Fractions Separated in Atmospheric Distilling Units</i> <sup>45</sup> .....	124
Table 9. <i>Oil Fractions Separated in Vacuum Distilling Units</i> <sup>45</sup> .....	124
Table 10. <i>NAP Acids and Sulfur Concentrations of Main Model Oils and Crude oil fractions Used for Generating and Challenging FeS Scales</i> .....	127
Table 11. <i>General Test Conditions Used in Sulfidation and Challenge Tests Done with Real Crude oil fractions</i> .....	129
Table 12. <i>Dimensionless factor <math>\xi_{geo}</math> for various piping configuration</i> <sup>71</sup> .....	189
Table 13. <i>Kinetic constant <math>A_{RCOOH}</math> and activation energy <math>E_{RCOOH}</math> for NAP corrosion attack as function of metallurgy</i> <sup>70</sup> .....	195

## LIST OF FIGURES

	Page
Figure 1. Modified McConomy curves are diagrams used in refineries to predict sulfidic corrosion. These diagrams are taken from Kane, R.D.; Cayard, M.S.; Understanding Critical Factors that Influence Refinery Crude Corrosiveness. <i>Mater. Perform.</i> 1999, July, 48-54. ....	39
Figure 2. High Velocity Rig used for NAP corrosion tests under high velocity and temperature conditions. ....	49
Figure 3. Cutout through HVR autoclave reactor. Fluid is pumped through the bottom of the reactor (fluid inlet) fills completely the autoclave volume and leaves the reactor through the top (fluid outlet). ....	55
Figure 4. Integral corrosion rate for sulfidation tests on carbon steel. 6, 15, 24, 48, and 96 h tests using Yellow oil (S = 0.25% wt; TAN 0.1). Points are average values while errors bars indicate the highest and lowest value obtained on multiple samples exposed in the same experiment. ....	62
Figure 5. Differential corrosion rate for sulfidation tests on carbon steel. 6, 15, 24, 48, and 96 h tests using Yellow oil (S = 0.25% wt; TAN 0.1). Points are average values while errors bars indicate the highest and lowest value obtained on multiple samples exposed in the same experiment, with propagation of error accounted for. ....	62
Figure 6. Integral Scale Formation Rate for CS specimens evaluated for sulfidation tests using Yellow oil. Points are average values while errors bars indicate the highest and lowest value obtained on multiple samples exposed in the same experiment. ....	64
Figure 7. Differential Scale Formation Rate for CS specimens evaluated for sulfidation tests using Yellow oil. Points are average values while errors bars indicate the highest and lowest value obtained on multiple samples exposed in the same experiment, with propagation of error accounted for. ....	65
Figure 8. Moles of Fe and FeS (integral values) Plot represents the moles of Fe used (lost by the metal) during the tests and the moles of FeS that represented the adherent scale found at the end of every test. Error bars represent absolute values for maximum and minimum of differences between individual and average corrosion rates of samples. ....	68
Figure 9. Moles of Fe and FeS (differential) Plot represents the moles of Fe used (lost by the metal) during the tests and the moles of FeS that represented the adherent scale found on the CS at the end of every test. Points are average values while errors bars indicate the highest and lowest value obtained on multiple samples exposed in the same experiment, with propagation of error accounted for. ....	69
Figure 10. SEM Analysis of iron sulfide scale formed on CS specimens after the 6 h test. The image represents a cross-section of the interface metal-iron sulfide scale, metal being at the bottom part of the picture. Several FeS scale layers are visible some of them are compact (bottom layer), others fragmented (top layers). ....	70

- Figure 11. SEM Analysis of iron sulfide scale formed on CS specimens after the 24 h test. The image represents a cross-section of the interface metal-iron sulfide scale, metal being at the bottom part of the picture. Multiple FeS scale layers are visible presenting a much fragmented structure which made the scale very porous..... 71
- Figure 12 SEM image of the FeS scale formed on the CS specimen surface in a 24 h sulfidation test. The FeS scale shows a multilayer structure with the top layer cracked and partially removed under the effect of high velocity. The SEM image has a 500X magnification. .... 72
- Figure 13 SEM image of the FeS scale formed on the CS specimen surface in a 48 h sulfidation test. The FeS scale shows a multilayer structure with the top layer cracked and partially removed under the effect of high velocity. The SEM image has a 100X magnification. .... 73
- Figure 14. Integral corrosion rate for sulfidation tests on 5Cr steel. Tests were done using Yellow oil (S = 0.25% wt) spiked with NAP to TAN 0.1 and run for 6, 24, 48, and 96 h. Points are average values while errors bars indicate the highest and lowest value obtained on multiple samples exposed in the same experiment..... 74
- Figure 15. Differential corrosion rate for sulfidation tests on 5Cr steel. Tests were done using Yellow oil (S = 0.25% wt) spiked with NAP to TAN 0.1 and run for 6, 24, 48, and 96 h. Points are average values while errors bars indicate the highest and lowest value obtained on multiple samples exposed in the same experiment, with propagation of error accounted for. .... 74
- Figure 16. Integral Scale Formation Rate for 5Cr specimens. FeS scale was formed in sulfidation tests using Yellow oil (TAN = 0.1, S = 0.25% wt). Points are average values while errors bars indicate the highest and lowest value obtained on multiple samples exposed in the same experiment. .... 75
- Figure 17. Differential Scale Formation Rate for 5Cr specimens. FeS scale was formed in sulfidation tests using Yellow oil (TAN = 0.1, S = 0.25% wt). Points are average values while errors bars indicate the highest and lowest value obtained on multiple samples exposed in the same experiment, with propagation of error accounted for..... 76
- Figure 18. Moles of Fe and FeS (integral values) Plot represents the moles of Fe used (lost by the metal) during the tests and the moles of FeS - the adherent scale found at the end of every test. Points are average values while errors bars indicate the highest and lowest value obtained on multiple samples exposed in the same experiment..... 77
- Figure 19. Moles of Fe and FeS (differential) Plot represents the moles of Fe used (lost by the metal) during the tests and the moles of FeS - the adherent scale found at the end of every test. Points are average values while errors bars indicate the highest and lowest value obtained on multiple samples exposed in the same experiment, with propagation of error accounted for. .... 77
- Figure 20. CS vs. 5Cr- Integral corrosion rates for sulfidation tests. Tests were done separately for each type of steel using Yellow oil (S = 0.25% wt) spiked with NAP to TAN 0.1 and they were run for 6, 15, 24, 48, and 96 h. Points are average

- values while errors bars indicate the highest and lowest value obtained on multiple samples exposed in the same experiment. .... 78
- Figure 21. CS vs. 5Cr- Integral scale formation rates for sulfidation tests. Tests were done separately for each type of steel using Yellow oil (S = 0.25% wt) spiked with NAP to TAN 0.1 and they were run for 6, 15, 24, 48, and 96 h. Points are average values while errors bars indicate the highest and lowest value obtained on multiple samples exposed in the same experiment. .... 79
- Figure 22. Comparison of the 6 h experiments made in HVR and in FTMA. HVR experiments were done under different test conditions, i.e. normal conditions - rotation of the specimens and flushing at the end of the experiment (6 hr R&F), 6 h with no flush at the end of the experiment (6 h No Flushing), 6 h and no rotation of the specimens (6 h No Rotation). Points are average values while errors bars indicate the highest and lowest value obtained on multiple samples exposed in the same experiment. .... 81
- Figure 23. CS vs. 5Cr steel. Corrosion rates for 24 hr and 60 hr challenge tests using TAN 2 white oil. Number 7 above the error bars for the sulfidation point represents the number of experiments that were averaged for calculating the respective value. Points are average values while errors bars indicate the highest and lowest value obtained on multiple samples exposed in the same experiment. .... 89
- Figure 24. CS vs. 5Cr steel. Scale thickness comparison for 24 h and 60 h TAN 2 challenge tests. Graph includes total scale (loose) and adherent scale found at the end of the tests. Number 7 above the sulfidation reference represents the number of sulfidation test replicates. Points are average values while errors bars indicate the highest and lowest value obtained on multiple samples exposed in the same experiment..... 90
- Figure 25. SEM surface analysis for FeS scale on the 5Cr specimens in TAN 2, 60 h challenge test. SEM picture reveals the consecutive layers of FeS scale that were formed during the test. .... 92
- Figure 26. EDX analysis for FeS scale generated on 5Cr specimens that had been challenged with TAN 2 for 60 h. The high peaks correspond to iron and sulfur respectively which are the main components of FeS scale..... 93
- Figure 27. CS vs. 5Cr steel. Corrosion rates for 24, 60, and 120 h challenge tests using TAN 3.5 white oil. Number 7 above the error bars for sulfidation point represents the number of experiments that were averaged for calculating the respective value..... 94
- Figure 28. CS vs. 5Cr steel. Scale thickness comparison for 24, 60 and 120 h TAN 3.5 challenge tests. Graph includes total scale (loose) and adherent scale found at the end of the tests. Number 7 above the sulfidation reference represents the number of sulfidation test replicates. Points are average values while errors bars indicate the highest and lowest value obtained on multiple samples exposed in the same experiment..... 95

- Figure 29. SEM surface analysis for scale formed on CS specimens after 24 h challenge with TAN 3.5. Top layer of FeS scale was partially removed (*a*) and bottom FeS layer can be observed through a hole in the top layer (*b*). ..... 96
- Figure 30. SEM surface analysis for 5Cr specimens after 24 hr challenge TAN 3.5 test. Significant cracks can be seen in image (*a*) for 1000X magnification whereas image (*b*) collected at 5000X magnification reveals torn edges for FeS crystals. 97
- Figure 31. CS vs. 5Cr steel. Corrosion rates for 6, 12, 24, and 50 h challenge tests using TAN 5 white oil. Number 7 above the error bars for sulfidation point represents the number of experiments that were averaged for calculating the respective value. Points are average values while errors bars indicate the highest and lowest value obtained on multiple samples exposed in the same experiment..... 98
- Figure 32. CS vs. 5Cr steel. Scale thickness comparison for 6, 12, 24, and 50 h TAN 5 challenge tests. Graph includes total scale (loose) and adherent scale found at the end of the tests. Number 7 above the sulfidation reference represents the number of sulfidation test replicates. Points are average values while errors bars indicate the highest and lowest value obtained on multiple samples exposed in the same experiment..... 99
- Figure 33. SEM surface analysis for CS specimens after 24 h challenge TAN 5 test. FeS crystals have torn and rounded edges and large parts of scale peeled off leaving only fragments from the superficial layer. .... 100
- Figure 34. EDX analysis along cross-section of the FeS scale on CS specimens after 24 hr challenge TAN 5 test. The analysis compares concentrations of main chemical elements along the cross-section of the FeS layers..... 101
- Figure 35. SEM surface analysis for 5Cr specimens after 24 h challenge TAN 5 test. FeS crystals have torn and rounded edges and the scale surface has regions where crystals have been removed. .... 101
- Figure 36. EDX analysis for cross-section through FeS scale on 5Cr specimens after 24 h challenge TAN 5 test. Sulfur has two distinct peaks suggesting a multiple layer structure for the scale. .... 102
- Figure 37. Corrosion rates for CS and 5Cr in 24hr and 50hr challenge tests using TAN 6.5. Number 7 above the error bars for sulfidation point represents the number of experiments that were averaged for calculating the respective reference value. Points are average values while errors bars indicate the highest and lowest value obtained on multiple samples exposed in the same experiment. .... 103
- Figure 38. CS vs. 5Cr steel. Scale thickness comparison for 24 and 50 h TAN 6.5 challenge tests. Graph includes total scale (loose) and adherent scale found at the end of the tests. Number 7 above the sulfidation reference represents the number of sulfidation test replicates. Points are average values while errors bars indicate the highest and lowest value obtained on multiple samples exposed in the same experiment..... 104
- Figure 39. (*a*) SEM surface analysis for CS specimens after 24 h challenge TAN 6.5 test. FeS crystals have torn and rounded edges and large parts of scale peeled off from metal surface. (*b*) Cross-section through FeS scale on CS specimens after 24 h

	challenge TAN 6.5 test. FeS scale presents large empty spaces between scale fragments (high porosity).....	105
Figure 40.	(a) SEM surface analysis for 5Cr specimens after 24 h challenge TAN 6.5 test. SEM surface image shows large parts of scale peeled off from metal surface. (b) Cross-section through FeS scale on 5Cr specimens after 24 h challenge TAN 6.5 test. FeS scale presents large empty spaces between scale fragments (high porosity). .....	107
Figure 41.	Corrosion rates for CS and 5Cr in 6, 12, and 24h challenge tests using TAN 8. Number 7 above the error bars for sulfidation point represents the number of experiments that were averaged for calculating the respective reference value. Points are average values while errors bars indicate the highest and lowest value obtained on multiple samples exposed in the same experiment. ....	108
Figure 42.	CS vs. 5Cr steel. Scale thickness comparison for 6, 12, and 24 h TAN 8 challenge tests. Graph includes total scale (loose) and adherent scale found at the end of the tests. Number 7 above the sulfidation reference represents the number of sulfidation test replicates. Points are average values while errors bars indicate the highest and lowest value obtained on multiple samples exposed in the same experiment.....	109
Figure 43.	SEM surface analysis for CS specimens after 24 h challenge TAN 8 test. FeS crystals have torn rounded edges and large cracks in the scale revealed its multiple layer structure. ....	110
Figure 44.	SEM cross-section for FeS scale formed CS specimens after 24 h challenge TAN 8 test. SEM analysis shows distribution of main scale components across the FeS scale. ....	110
Figure 45.	SEM surface analysis for 5Cr specimens after 24 h challenge TAN 8 test. FeS crystals have torn rounded edges and large cracks in the scale revealed its multiple layer structure. ....	111
Figure 46.	Cross-section through FeS scale on 5Cr specimens after 24 h challenge TAN 8 test. Picture shows a grainy characteristic structure of FeS scale. The EDX analysis was run across the white line and shows main components detected in that region of the FeS scale.....	112
Figure 47.	Comparison for corrosion rates of CS and 5Cr specimens in 24 h challenge tests with different NAP concentrations (TAN 2 to TAN 8). Points are average values while errors bars indicate the highest and lowest value obtained on multiple samples exposed in the same experiment. ....	113
Figure 48.	Total and adherent scale thickness formed on CS specimens during 24 h challenge tests with different NAP concentrations (TAN 2 to TAN 8). Points are average values while errors bars indicate the highest and lowest value obtained on multiple samples exposed in the same experiment. ....	114
Figure 49.	Total and adherent scale thickness formed on 5Cr specimens during 24 h challenge tests with different NAP concentrations (TAN 2 to TAN 8). Points are average values while errors bars indicate the highest and lowest value obtained on multiple samples exposed in the same experiment. ....	114

- Figure 50. Comparison of corrosion rates on CS under different rotation conditions. Lower point represents the corrosion rate corresponding to low velocity test (500 rpm). Points are average values while errors bars indicate the highest and lowest value obtained on multiple samples exposed in the same experiment. Number 7 above the sulfidation reference represents the number of sulfidation test replicates. .... 116
- Figure 51. Comparison of corrosion rates on 5Cr under different rotation conditions. Lower point represents the corrosion rate corresponding to low velocity test (500 rpm). Points are average values while errors bars indicate the highest and lowest value obtained on multiple samples exposed in the same experiment. Number 7 above the sulfidation reference represents the number of sulfidation test replicates. .... 117
- Figure 52. Comparison of corrosion rates for CS specimens presulfided at 650°F with corrosion rates for CS specimens presulfided at (287°C) 550°F – lower points. Points are average values while errors bars indicate the highest and lowest value obtained on multiple samples exposed in the same experiment. .... 118
- Figure 53. Comparison of corrosion rates for 5Cr specimens presulfided at 343°C (650°F) with corrosion rates for 5Cr specimens presulfided at 287°C (550°F) – lower points. Number 7 above the sulfidation reference represents the number of sulfidation test replicates. Points are average values while errors bars indicate the highest and lowest value obtained on multiple samples exposed in the same experiment..... 119
- Figure 54. Comparison of corrosion rates for CS generated during sulfidation-challenge tests. TAN challenge series are plotted as function of time. All TAN challenge series were done at the same temperature 343°C (650°F). Number 7 above the sulfidation reference represents the number of sulfidation test replicates. Points are average values while errors bars indicate the highest and lowest value obtained on multiple samples exposed in the same experiment. .... 120
- Figure 55. Comparison of corrosion rates for 5Cr generated during sulfidation-challenge tests. All TAN challenge series were done at the same temperature 343°C (650°F). Number 7 above the sulfidation reference represents the number of sulfidation test replicates. Points are average values while errors bars indicate the highest and lowest value obtained on multiple samples exposed in the same experiment..... 121
- Figure 56. Expanded view for comparison of corrosion rates for 5Cr generated during sulfidation-challenge tests. All TAN challenge series were done at the same temperature 343°C (650°F). Number 7 above the sulfidation reference represents the number of sulfidation test replicates. Points are average values while errors bars indicate the highest and lowest value obtained on multiple samples exposed in the same experiment. .... 121
- Figure 57. Corrosion rates for CS specimens presulfided with Yellow oil and then challenged with NAP at TAN = 3.5 and TAN = 6.5. Points are average values while errors bars indicate the highest and lowest value obtained on multiple samples exposed in the same experiment. .... 132

- Figure 58. Scale thickness formed on CS specimens presulfided with Yellow oil and then challenged with NAP at TAN = 3.5 and TAN = 6.5. Points are average values while errors bars indicate the highest and lowest value obtained on multiple samples exposed in the same experiment. .... 132
- Figure 59. SEM backscattered images represent cross-sections on CS specimens presulfided with Yellow oil and then challenged with NAP acids. FeS scale was challenged with TAN 3.5 (image *a*) and with TAN 6.5 (image *b*). In both images the metal is on the bottom side. .... 134
- Figure 60. Corrosion rates for 5Cr specimens presulfided with Yellow oil and then challenged with NAP at TAN = 3.5 and TAN = 6.5. Points are average values while errors bars indicate the highest and lowest value obtained on multiple samples exposed in the same experiment. .... 135
- Figure 61. Scale thickness formed on 5Cr specimens presulfided with Yellow oil and then challenged with NAP at TAN = 3.5 and TAN = 6.5. Points are average values while errors bars indicate the highest and lowest value obtained on multiple samples exposed in the same experiment. .... 136
- Figure 62. Corrosion rates for CS and 5Cr steel specimens presulfided with *diluted* DDD VGO and then challenged with NAP at TAN = 3.5 and TAN = 6.5. Points are average values while errors bars indicate the highest and lowest value obtained on multiple samples exposed in the same experiment. .... 137
- Figure 63. Scale thickness formed on CS specimens presulfided with *diluted* DDD VGO and then challenged with NAP at TAN = 3.5 and TAN = 6.5. Points are average values while errors bars indicate the highest and lowest value obtained on multiple samples exposed in the same experiment. .... 138
- Figure 64. SEM backscattered images represent cross-sections on CS specimens presulfided with *diluted* DDD VGO and then challenged with NAP. FeS scale was challenged with TAN 3.5 (image *a*) and with TAN 6.5 (image *b*). In both images the metal is on the bottom side. .... 139
- Figure 65. Scale thickness formed on 5Cr specimens presulfided with *diluted* DDD VGO and then challenged with NAP at TAN = 3.5 and TAN = 6.5. Points are average values while errors bars indicate the highest and lowest value obtained on multiple samples exposed in the same experiment. .... 140
- Figure 66. SEM backscattered images represent cross-sections on 5Cr specimens presulfided with *diluted* DDD VGO and then challenged with NAP. FeS scale was challenged with TAN 3.5 (image *a*) and with TAN 6.5 (image *b*). In both images the metal is on the bottom side. .... 140
- Figure 67. Corrosion rates for CS and 5Cr steel specimens that were presulfided with *diluted* HH1 VGO and then challenged with NAP at TAN = 3.5 and TAN = 6.5. Points are average values while errors bars indicate the highest and lowest value obtained on multiple samples exposed in the same experiment. .... 141
- Figure 68. Total and adherent scale measured on CS specimens presulfided with *diluted* HH1 VGO. Scale values cover similar ranges in TAN 3.5 as in TAN 6.5 challenges. Points are average values while errors bars indicate the highest and lowest value obtained on multiple samples exposed in the same experiment. ... 142

- Figure 69. Total and adherent scale measured on 5Cr specimens presulfidized with *diluted* HH1 VGO. Scale values cover similar ranges in TAN 3.5 as in TAN 6.5 challenges. Points are average values while errors bars indicate the highest and lowest value obtained on multiple samples exposed in the same experiment. ... 143
- Figure 70. SEM images of cross-sections on CS specimens sulfidized with *diluted* HH1 VGO. SEM image *a* represents the scale that was found at the end of TAN 3.5 challenge and image *b* the scale at the end of TAN 6.5 challenge. In image *b* the scale had only one layer compared to image *a* where two layer are visible. .... 143
- Figure 71. SEM images of scales formed with *diluted* HH1 VGO on 5Cr specimens. Image *a* presents the scale challenged with TAN 3.5 and image *b* corresponds to TAN 6.5 challenged scale. In Both images scales had multiple layers with porous structures. .... 144
- Figure 72. Corrosion rates for CS and 5Cr steel specimens that were presulfidized with DDD VGO (*neat*) and then challenged with naphthenic acids at TAN = 3.5 and TAN = 6.5. Points are average values while errors bars indicate the highest and lowest value obtained on multiple samples exposed in the same experiment. ... 146
- Figure 73. FeS scale thickness on CS specimens that were presulfidized with DDD VGO (*neat*) and then challenged with NAP at TAN = 3.5 and TAN = 6.5. Points are average values while errors bars indicate the highest and lowest value obtained on multiple samples exposed in the same experiment. .... 146
- Figure 74. FeS scale thickness on 5Cr steel specimens that were presulfidized with DDD VGO (*neat*) and then challenged with NAP at TAN = 3.5 and TAN = 6.5. Points are average values while errors bars indicate the highest and lowest value obtained on multiple samples exposed in the same experiment. .... 147
- Figure 75. SEM backscattered images represent cross-sections on CS and 5Cr specimens presulfidized with DDD VGO (*neat*) and then challenged with NAP. FeS scale was challenged with TAN 6.5. Image *a* shows scale formed on CS and image *b* scale formed on 5Cr steel. In both images the metal is on the bottom side. .... 148
- Figure 76. Corrosion rates for CS and 5Cr steel specimens that were presulfidized with HH1 VGO (*neat*) and then challenged with NAP at TAN = 3.5 and TAN = 6.5. Points are average values while errors bars indicate the highest and lowest value obtained on multiple samples exposed in the same experiment. .... 149
- Figure 77. Scale thickness measured on CS at the end of TAN 3.5 and TAN 6.5 challenge tests. The scale was formed with HH1 VGO undiluted (*neat*). Points are average values while errors bars indicate the highest and lowest value obtained on multiple samples exposed in the same experiment. .... 149
- Figure 78. Scale thickness measured on CS at the end of TAN 3.5 and TAN 6.5 challenge tests. The scale was formed with HH1 VGO undiluted (*neat*). Points are average values while errors bars indicate the highest and lowest value obtained on multiple samples exposed in the same experiment. .... 150
- Figure 79. SEM images represent cross-sections on CS specimens presulfidized with HH1 VGO (*neat*) and then challenged with NAP. FeS scale was challenged with TAN 3.5 (image *a*) and with TAN 6.5 (image *b*). In both images the metal is on the bottom side. .... 151

- Figure 80. Corrosion rates for CS and 5Cr steel specimens that were presulfided with BBB VGO (*neat*) and then challenged with NAP at TAN = 3.5 and TAN = 6.5. Points are average values while errors bars indicate the highest and lowest value obtained on multiple samples exposed in the same experiment. .... 152
- Figure 81. Scale thickness on CS specimens that were presulfided with BBB VGO (*neat*) and then challenged with NAP at TAN = 3.5 and TAN = 6.5. Points are average values while errors bars indicate the highest and lowest value obtained on multiple samples exposed in the same experiment. .... 153
- Figure 82. Scale thickness on 5Cr steel specimens that were presulfided with BBB VGO (*neat*) and then challenged with NAP at TAN = 3.5 and TAN = 6.5. Points are average values while errors bars indicate the highest and lowest value obtained on multiple samples exposed in the same experiment. .... 153
- Figure 83. SEM images represent cross-sections on CS and 5Cr presulfided with BBB VGO (*neat*) and then challenged with NAP. FeS scale was challenged with TAN 6.5 Image *a* represents the scale formed on CS and image *b* the scale formed on 5Cr. In both images the metal is on the bottom side. Magnification in both images was 1000 X. .... 154
- Figure 84. Corrosion rates for CS and 5Cr steel specimens that were presulfided with AAA VGO (*neat*) and then challenged with NAP at TAN = 3.5 and TAN = 6.5. Points are average values while errors bars indicate the highest and lowest value obtained on multiple samples exposed in the same experiment. .... 155
- Figure 85. Scale thickness on CS specimens that were presulfided with AAA VGO (*neat*) and then challenged with NAP at TAN = 3.5 and TAN = 6.5. Points are average values while errors bars indicate the highest and lowest value obtained on multiple samples exposed in the same experiment. .... 156
- Figure 86. Corrosion rates for CS and 5Cr steel specimens that were presulfided with AAA VGO (*neat*) and then challenged with NAP at TAN = 3.5 and TAN = 6.5. Points are average values while errors bars indicate the highest and lowest value obtained on multiple samples exposed in the same experiment. .... 156
- Figure 87. SEM images represent cross-sections on CS and 5Cr presulfided with AAA VGO (*neat*) and then challenged with NAP (TAN 6.5). Image *a* represents the scale formed on CS and image *b* the scale formed on 5Cr. In both images metal is on the bottom side. .... 157
- Figure 88. Corrosion rates for CS and 5Cr steel specimens that were with CCC 650+ (*neat*) and then challenged with NAP at TAN = 3.5 and TAN = 6.5. Points are average values while errors bars indicate the highest and lowest value obtained on multiple samples exposed in the same experiment. .... 158
- Figure 89. Scale thickness for CS specimens that were presulfided with CCC 650+ (*neat*) and then challenged with NAP at TAN = 3.5 and TAN = 6.5. Points are average values while errors bars indicate the highest and lowest value obtained on multiple samples exposed in the same experiment. .... 159
- Figure 90. Corrosion rates for CS and 5Cr steel specimens that were presulfided with CCC 650+ (*neat*) and then challenged with NAP at TAN = 3.5 and TAN = 6.5.

	Points are average values while errors bars indicate the highest and lowest value obtained on multiple samples exposed in the same experiment. ....	159
Figure 91.	SEM images represent cross-sections on CS and 5Cr presulfided with CCC 650+ ( <i>neat</i> ) and then challenged with NAP (TAN 6.5). Image <i>a</i> represents the scale formed on CS and image <i>b</i> the scale formed on 5Cr. In both images metal is on the bottom side. ....	160
Figure 92.	Corrosion rates for CS and 5Cr steel specimens that were presulfided with Yellow oil spiked to TAN 1.75 and then challenged with NAP at TAN = 3.5 and TAN = 6.5. Points are average values while errors bars indicate the highest and lowest value obtained on multiple samples exposed in the same experiment. ...	162
Figure 93.	Scale thickness measured on CS specimens presulfided with Yellow oil spiked to TAN 1.75 and then challenged with NAP at TAN = 3.5 and TAN = 6.5. Points are average values while errors bars indicate the highest and lowest value obtained on multiple samples exposed in the same experiment. ....	162
Figure 94.	Scale thickness measured on 5Cr specimens that were presulfided with Yellow oil spiked to TAN 1.75 and then challenged with NAP at TAN = 3.5 and TAN = 6.5. Points are average values while errors bars indicate the highest and lowest value obtained on multiple samples exposed in the same experiment. ...	163
Figure 95.	SEM images represent cross-sections on CS and 5Cr presulfided with Yellow oil spiked to TAN 1.75 and then challenged with NAP (TAN 6.5). Image <i>a</i> represents the scale formed on CS and image <i>b</i> the scale formed on 5Cr. In both images metal is on the bottom side. ....	164
Figure 96.	Corrosion rates for CS and 5Cr steel specimens that were presulfided with HH1 VGO spiked to TAN 1.75 and then challenged with NAP at TAN = 3.5 and TAN = 6.5. Points are average values while errors bars indicate the highest and lowest value obtained on multiple samples exposed in the same experiment. ...	165
Figure 97.	Scale thickness on CS specimens presulfided with HH1 VGO spiked to TAN 1.75 and then challenged with NAP at TAN = 3.5 and TAN = 6.5. Points are average values while errors bars indicate the highest and lowest value obtained on multiple samples exposed in the same experiment. ....	165
Figure 98.	Scale thickness on 5Cr steel specimens that were presulfided with HH1 VGO spiked to TAN 1.75 and then challenged with NAP at TAN = 3.5 and TAN = 6.5. Points are average values while errors bars indicate the highest and lowest value obtained on multiple samples exposed in the same experiment. ....	166
Figure 99.	SEM images represent cross-sections on CS and 5Cr presulfided with HH1 VGO spiked to TAN 1.75 and then challenged with NAP acids (TAN 6.5). Image <i>a</i> represents the scale formed on CS and image <i>b</i> the scale formed on 5Cr. In both images the metal is on the bottom side. ....	167
Figure 100.	Corrosion rates for CS and 5Cr steel specimens that were presulfided with BBB VGO spiked to TAN 1.75 and then challenged with NAP at TAN = 3.5 and TAN = 6.5. Points are average values while errors bars indicate the highest and lowest value obtained on multiple samples exposed in the same experiment. ...	168
Figure 101.	Scale thickness measured on CS specimens that were presulfided with BBB VGO spiked to TAN 1.75 and then challenged with NAP at TAN = 3.5 and TAN	

- = 6.5. Points are average values while errors bars indicate the highest and lowest value obtained on multiple samples exposed in the same experiment..... 169
- Figure 102. Scale thickness measured 5Cr steel specimens that were presulfided with BBB VGO spiked to TAN 1.75 and then challenged with NAP at TAN = 3.5 and TAN = 6.5. Points are average values while errors bars indicate the highest and lowest value obtained on multiple samples exposed in the same experiment. ... 169
- Figure 103. SEM images represent cross-sections on CS and 5Cr presulfided with BBB VGO spiked to TAN 1.75 and then challenged with NAP acids (TAN 6.5). Image *a* represents the scale formed on CS and image *b* the scale formed on 5Cr. In both images the metal is on the bottom side. .... 170
- Figure 104. Corrosion rates for CS and 5Cr steel specimens that were presulfided with CCC 650+ spiked to TAN 1.75 and then challenged with NAP at TAN = 3.5 and TAN = 6.5. Points are average values while errors bars indicate the highest and lowest value obtained on multiple samples exposed in the same experiment. ... 171
- Figure 105. Scale thickness on CS specimens that were with CCC 650+ spiked to TAN 1.75 and then challenged with NAP at TAN = 3.5 and TAN = 6.5. Points are average values while errors bars indicate the highest and lowest value obtained on multiple samples exposed in the same experiment. .... 172
- Figure 106. Scale thickness on 5Cr steel specimens that were presulfided with CCC 650+ spiked to TAN 1.75 and then challenged with NAP at TAN = 3.5 and TAN = 6.5. Points are average values while errors bars indicate the highest and lowest value obtained on multiple samples exposed in the same experiment..... 172
- Figure 107. SEM images represent cross-sections on CS and 5Cr presulfided with BBB VGO spiked to TAN 1.75 and then challenged with NAP acids (TAN 6.5). Image *a* represents the scale formed on CS and image *b* the scale formed on 5Cr. In both images the metal is on the bottom side. .... 173
- Figure 108. Comparison of corrosion rates for CS and 5Cr steel specimens challenged with different TAN concentrations in the absence of sulfur compounds. Tests were run for 24 h at 343°C (650°F). Points are average values while errors bars indicate the highest and lowest value obtained on multiple samples exposed in the same experiment. .... 176
- Figure 109. NAP corrosion of presulfided CS specimens vs. NAP corrosion of CS specimens in the absence of sulfur. Tests were run for 24 hr at 343°C (650°F). Points are average values while errors bars indicate the highest and lowest value obtained on multiple samples exposed in the same experiment. .... 176
- Figure 110. NAP corrosion of presulfided 5Cr specimens vs. NAP corrosion of 5Cr specimens in the absence of sulfur. Tests were run for 24 hr at 343°C (650°F). Points are average values while errors bars indicate the highest and lowest value obtained on multiple samples exposed in the same experiment. .... 177
- Figure 111. Mechanism of sulfidation at the metal-oil interface. Initial attack of sulfur species (RS) on the metal surface causing formation of successive layers of iron sulfide scale (FeS). .... 180
- Figure 112. Mechanism of sulfidation at the metal-oil interface. Formation of cracks and new scale. FeS scale cracking is caused by internal stresses. Cracks in the scale

- allow new attacks of sulfur species on the metal exposed surface. As a result of these attacks new FeS scale is formed. .... 181
- Figure 113. Mechanism of sulfidation at the metal-oil interface. FeS scale becomes thick and porous due to repeated forming, cracking and peeling off processes. The thick scale reduces the corrosion rate by slowing down the transport of species. .... 181
- Figure 114. Mechanism of sulfidation at the metal-oil interface. Combined mechanism of sulfidation and acid attack. Turbulent flow removes layers of porous scale enabling naphthenic acids to attack the metal increasing the corrosion rate. .... 182
- Figure 115. Kinetic constant  $A_{RS}$  and activation energy  $E_{RS}$  as function of metallurgy. For different steel types were included as most used as construction materials in refineries<sup>70</sup> ..... 188
- Figure 116. Mechanism of naphthenic acid corrosion. Naphthenic acid attack rate is limited by diffusion mechanism (convective, molecular, and solid state) as acids are transported from bulk solution towards steel surface. .... 191
- Figure 117. Comparison between model prediction and measured corrosion rates on CS during sulfidation-challenge experiments. Model predictions are plotted as continuous thick lines whereas experimental data are points connected by lines. .... 196
- Figure 118. Comparison between model prediction and measured co-rrosion rates on 5Cr during sulfidation-challenge experiments. Model predictions are plotted as continuous thick lines whereas experimental data are points connected by lines. .... 197

## CHAPTER 1: INTRODUCTION

Oil extraction, transport, and its processing in refineries raises a multitude of challenges for the industry, and all of them can be expressed in economic costs and benefits. Reducing production costs entices oil companies to process “opportunity crudes” - low quality corrosive crude oils with high naphthenic acid and sulfur contents that are cheaper than the so called “sweet crudes”, the former of which are readily available on the oil market. Processing of these acidic crudes at high temperatures in refineries forced the refinery engineers to adopt special strategies for mitigating their corrosive effects. These strategies included blending crudes, selecting better materials for various critical refinery components. Part of the strategy for identifying better materials includes an investment into better understanding the mechanism of naphthenic acid corrosion and its interaction with sulfidic corrosion.

Naphthenic acid (NAP) corrosion was identified in refineries for the first time in 1920's according to W.A. Derungs<sup>4</sup>, the author of the first systematic case study of NAP corrosion published in 1956. Starting from Derungs' results, further research studies done by Gutzeit<sup>5</sup> and Piehl<sup>6</sup> described the NAP corrosion process in a more comprehensive manner and gave the first model of naphthenic corrosion. Based on case studies and laboratory tests it was an empirical model but it was used as a basic reference for NAP corrosion rate predictions in refineries.

Although the classical model of NAP corrosion based on Derungs, Gutzeit, and Piehl research work was used in oil industry for characterizing the acidity of crude oils, it had some limitations when certain specific highly acidic crudes that were processed have

proven not to be as corrosive as the model predicted<sup>7</sup>. Therefore, efforts were made to investigate other important factors like the interaction with sulfur compounds, naphthenic acid molecular weight and structure, etc. According to the literature, engineers currently use different methods for predicting NAP corrosion rates in refineries. The most common models are McConomy curves<sup>8</sup>, iso-corrosion curves.<sup>8</sup> Both methods predict corrosion rates related to oil sulfur content, “iron powder test”<sup>9-11</sup> based on the interactions between naphthenic acids and sulfur compounds. All of these methods were based on empirical observation of real cases and laboratory tests and did not take into consideration any physical aspects and phenomena that evolved on the metal surface during scale formation and acidic attack. Therefore this project offered a different approach of naphthenic acid corrosion.

It is already known from practical refinery experience that when “opportunity crudes” are processed, the naphthenic acid corrosion and sulfur corrosion occur together mainly in distilling towers and their adjacent transfer lines. The two corrosive groups i.e. naphthenic acids and sulfur compounds influence each other and their effect cannot be simply separated. Both are very reactive at high temperatures while naphthenic acid seems to be most aggressive at high velocity encountered in refinery transfer lines. Therefore, our study started from the hypothesis that sulfur compounds formed in sulfur corrosion can mitigate naphthenic acid corrosion in some cases due to the iron sulfide scales on metal surfaces, however these scales may lose their protective properties under combined effect of strong acidic attack and high velocity. In order to verify this hypothesis it was decided to divide the experimental activities in three successive phases.

The first project phase included a preliminary study focusing on iron sulfide scale formation under high temperature and high velocity conditions. It also included a detailed investigation of iron sulfide scale morphology using scanning electronic microscopy. These preliminary tests were done using “yellow oil” which is a mineral oil with a natural sulfur content of 0.25wt% (0.25g S/100g oil). The yellow oil used for sulfidation tests was spiked with a low a low naphthenic acids concentration that was from experience considered favorable for better iron sulfide scale formation.

The second phase of the project was a more extensive study of the protective iron sulfide scales formed in yellow oil using similar procedures as in the first phase, with the added effect of being “challenged” by exposing them to sulfur-free “white” oils containing naphthenic acids at high temperatures and velocities. Temperature and velocity conditions were selected as close as possible to those of real refinery cases. The final results of the second phase were used for validating the model of naphthenic acid corrosion.

While the first and second phase of this project relied on the use of model oils in the tests (yellow and white oil), the third phase of the project relied on real crude oil fractions. Iron sulfide scales formed at high temperatures in real crude oil fraction cuts with different acidic and sulfur contents were challenged in a similar way as was done in the second phase using a white oil with high acid content.

The developed NAP corrosion model takes into consideration the successive reactions of sulfur containing compounds in the oil and the steel surface, the ensuing

formation of the iron sulfide (FeS) scale and the NAP attack on the scale and the base metal.

## CHAPTER 2: LITERATURE REVIEW

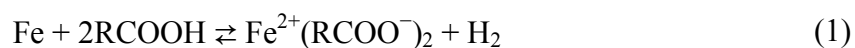
Opportunity crudes are characterized by high TAN (Total Acid Number), high sulfur content, and high pour point (PP). Although they are cheap and readily available, processing opportunity crudes is always associated with high corrosion rates in atmospheric and vacuum distillation columns, side strippers, furnaces, piping, and overhead systems.<sup>12</sup> Opportunity crudes also produce fouling with corrosion products in heat-exchangers, atmospheric and vacuum units. Corrosion products containing metals can also poison the catalytic conversion units and cause their breakdown. In spite of all these disadvantages related to opportunity crudes, processing them is still attractive for industry because of the recent evolution of oil supply markets.

Solving the corrosion problems associated with processing of opportunity crude oils is a serious challenge. Among the most typical corrosive agents in oil, NAPs proved to be one of the most aggressive and as a consequence numerous studies focused on investigating their corrosive effects. Derungs wrote the first paper about NAP corrosion in 1956 and set the most important guidelines for addressing these acidic corrosion phenomena.<sup>4</sup> He also wrote in his paper that both NAP and sulfur corrosion processes became aggressive at high temperatures and that it was difficult to differentiate between the two corrosion types. Derungs identified acidic concentration in oils, high temperatures and high velocity conditions as the most important factors influencing NAP corrosion. Starting from Derungs results and observations, Gutzeit did the first laboratory tests related to corrosion kinetics of NAP corrosion and tried correlating them to refinery corrosion data.<sup>5</sup> He confirmed Derungs' observations about factors influencing NAP

corrosion and added that this corrosion process occurred only in liquid phase and that pressure had little influence on it.<sup>5</sup>

Interactions between NAP corrosion and sulfur corrosion were first mentioned in 1987 by Piehl who wrote in his paper that FeS scales formed in distilling towers and heat exchangers had a protective role against NAP corrosive attacks.<sup>6</sup> Starting from this field observation Piehl suggested that H<sub>2</sub>S generated at high temperatures in distilling units, attacked the metal and built insoluble iron sulfide scales. Under the same high temperature conditions naphthenic acids corroded the metal, thus forming iron naphthenates which were oil soluble. Thus, Piehl concluded that there was a competition between the two corrosion processes and variations in corrosion rates were dependent of sulfur and naphthenic acids concentrations in processed crudes.

The combined corrosive effects of naphthenic acids and sulfur compounds were described in following chemical reactions:<sup>6-8</sup>



According to reaction (1), naphthenic acids directly attacks the metal to generate iron naphthenates  $\text{Fe}^{2+}(\text{RCOO}^-)_2$ , that are soluble in oil and could be entrained by the fluid flow. Sulfur compounds in oil decomposed at high temperatures, forming hydrogen sulfide that is corrosive and attacked the metal generating insoluble iron sulfide (FeS) according to reaction (2). Iron sulfide is insoluble in oil and forms a film on the metal

surface, thereby offering some protection against acidic attack. Iron naphthenates dissolved in oil can react with hydrogen sulfide regenerating naphthenic acids and forming more iron sulfide as in reaction (3).

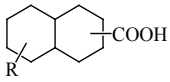
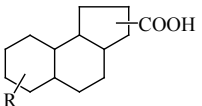
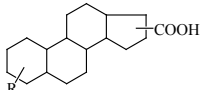
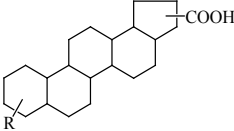
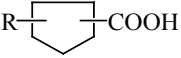
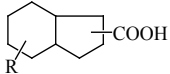
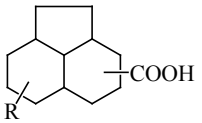
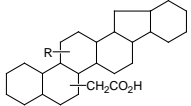
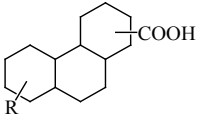
These reactions represent the NAP corrosion mechanism influenced by combined effects of many factors such as acidic concentration, temperature, velocity, and sulfur compound concentration. All these influences will be discussed in detail in the following paragraphs.

## **2.1 Identifying Naphthenic Acid Types and Structures**

Naphthenic acids were identified as the main corrosive species in acidic crudes although they represent less than 3% wt. They are organic acids with general formula  $R-(CH_2)_n-COOH$  where R is a radical including one or more cyclopentane or cyclohexane rings. Due to NAP corrosivity effects and their biological marker role in geochemistry many studies were focused on identifying NAP structures that were present in different crudes.<sup>15</sup> This challenge proved to be very difficult because naphthenic acids were extremely complicated mixtures. Some references mentioned that only in a single Californian crude approximately 1500 different organic acids were identified with molecular weights in range from 200 to 700.<sup>6</sup> More recent works on some crude oils identified NAPs over a mass range of 115-1500 with a carbon content of C20 to C33.<sup>13-15</sup> Progress of analytical techniques made also possible to provide a thorough description of many naphthenic structures. Thus in 1988 Dzidic et al. were able to identify the NAP structures in California crudes and refinery wastewaters using gas-chromatography coupled with chemical ionization mass spectrometry (GC/MS).<sup>16</sup> In further NAP studies

done by Fan<sup>15</sup>, Fast Atom Bombardment Mass Spectrometry (FAB/MS) was used as an analytical technique more suitable to characterize products with high molecular weights and low volatility such as naphthenic acids. Table 1 summarizes the results of these studies and others<sup>13-27</sup> grouping the main naphthenic acids as they were identified in crude oils.

**Table 1.** Chemical Structures of Naphthenic Acids Most Frequently Identified in Crude Oils<sup>13-15,19</sup>

1 ring	2 rings	3 rings	4 rings	5 rings	6 rings	C22 – C33
						$C_nH_{2n-2}O_2$
						$C_nH_{2n-4}O_2$
						$C_nH_{2n-6}O_2$
						$C_nH_{2n-8}O_2$

## 2.2 Corrosive Attack Morphology

Both NAPs and sulfur in heavy crudes are corrosive at high temperatures and as a consequence it is difficult to differentiate naphthenic acid corrosion from sulfur corrosion. However investigations of some cases of refineries that processed the same type of high acidic crudes for a long period time made possible to characterize the morphology of corrosive acidic attack. Thus NAP corrosion is characterized by sharp-edged holes or sharp-edged streamlined groves in places where the vapor streams had high velocities.<sup>4,28-33</sup> In other refinery equipment sections like trays and downcomers where the vapor condensed, the metal was only thinned by the acidic attack and the surface showed an “orange peel” aspect.<sup>28</sup>

Morphology of sulfidic corrosion is very different from that produced by NAP. In case of sulfur attack there is a general mass loss all over the metal surface followed by formation of iron sulfide scale directly on the metal.<sup>8</sup> Sulfidic corrosion will be described in a further section of this work.

## 2.3 The Effect of Naphthenic Acid Concentration

Measuring NAP concentration in oils was one of the first tasks for NAP corrosion studies. Currently, NAP concentrations are measured by titrating them with an alcoholic solution of potassium hydroxide (KOH) therefore they are expressed by the total acid number (TAN) that represents the milligrams of KOH used to neutralize the acids in one gram of oil. TAN was also called neutralization number or acid number by some authors.<sup>5,28</sup>

Standard ASTM tests used for measuring the TAN are ASTM D 974 which is a colorimetric method and ASTM D 664 which is a potentiometric method.<sup>5,6</sup> ASTM D

974, the colorimetric procedure considers the end point of the titration the color change of the indicator.<sup>34</sup> ASTM D 664 is the potentiometric method used for TAN determination and it considers the inflection point in the titration curve as end point for acid titration.<sup>35</sup> Although ASTM D 664 is the most commonly used method in refineries, this method is less accurate because it measures not only the organic acids but also the acidity generated by H<sub>2</sub>S, CO<sub>2</sub>, MgCl<sub>2</sub>, and CaCl<sub>2</sub> that are present in crudes and may hydrolyze.<sup>5,6</sup> According to Piehl, due to the presence of these compounds in the crudes, measured TAN values using the potentiometric method (ASTM D 664) are 80% higher than values obtained using the colorimetric method ASTM D 974 for the same oils.<sup>6</sup>

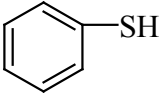
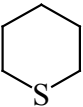
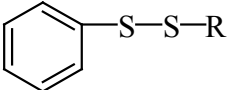
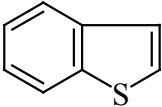
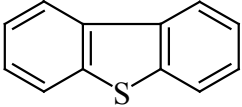
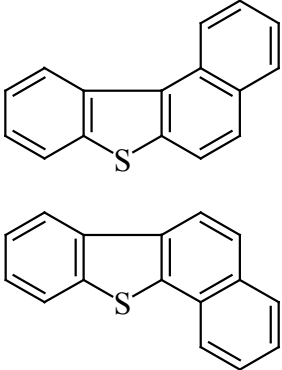
The TAN number alone is not sufficient for explaining the corrosivity of crude oils because in some cases different crudes having the same TAN value generated different corrosion rates.<sup>4</sup> Therefore it was concluded that differences in corrosion rate were affected by the different nature of the naphthenic acids.<sup>7,30</sup> In spite of these findings, TAN is still largely used in refineries for assessing the corrosivity of processed crudes. Crude oils with TAN values higher than 0.5 mg KOH are considered corrosive when processed in atmospheric distilling towers at temperature ranges of 220-400°C.<sup>5,6,28</sup> For vacuum distilling towers crudes become corrosive when the TAN values are between 1.5 and 2 mg KOH.<sup>6,7,33</sup> Some authors tried finding correlations between TAN values, corrosivity, and molecular weight of naphthenic acids and their results will be discussed in the section on temperature effects.<sup>4,5,31,32</sup>

## 2.4 Effect of Sulfur Content

Sulfidic corrosion is caused by sulfur compounds present in crude oils and their corrosive effects were investigated and described in different research papers.<sup>37-42</sup> The most important organic sulfur compounds that have been identified in oils are included in Table 2. They have been identified and characterized using different analytical techniques such as: cation exchange resin chromatography<sup>41</sup>, gas chromatography (GC) with flame photometric detectors (FID and FPD)<sup>38</sup>, gas chromatography (GC) with atomic emission detection (AED)<sup>42</sup>, gas chromatography (GC) coupled with sulfur chemiluminescence detection (SCD)<sup>40</sup>.

Although not all sulfur compounds are corrosive, it was widely accepted for practical reasons that crude oils can be classified according to their sulfur content. Thus, oils with less than 1% wt content named “sweet crudes” are considered to be of good quality whereas “sour crudes” containing about 6% wt sulfur are termed “heavy crudes” of low quality that represent the main cause of sulfidic corrosion in refineries.<sup>7,43,45,47</sup>

**Table 2.** *Main Organic Sulfur Compounds in Crude Oils*<sup>8,14,38,41</sup>

$\text{R-SO}_3\text{H}$	Aliphatic Sulfites
$\text{H}_2\text{S}$	Hydrogen Sulfide
$\text{R-SH}$	Thiols (Mercaptans)
	Thiophenols (Aromatic Mercaptans)
$\text{R-S-R}$	Sulfides
	Cyclic Sulfides
$\text{R-S-S-R}$	Disulfides (Aliphatic)
	Disulfides (Aromatic)
$\text{R-(S)}_n\text{-R}$	Polysulfides
	Thiophene
	Benzothiophene
	Dibenzothiophene
	Naphthobenzothiophene

Due to complex composition of oil it is difficult to predict the rate of sulfidic corrosion using the total sulfur content in oils. However, for practical purposes in refineries sulfidic corrosion rates are still predicted using the modified McConey curves (Figure 1) which provide a correlation between sulfur content in oil, temperature range, chromium content of steel and corrosion.<sup>8,46,48,50</sup> McConey curves have some limitations because they were generated from field data<sup>7</sup> without taking into consideration the velocity effect or some other specific factors like  $H_2$  content. Therefore a new type of diagrams, the Couper-Gorman diagrams was developed to predict sulfidic corrosion rates for different  $H_2$  containing environments.

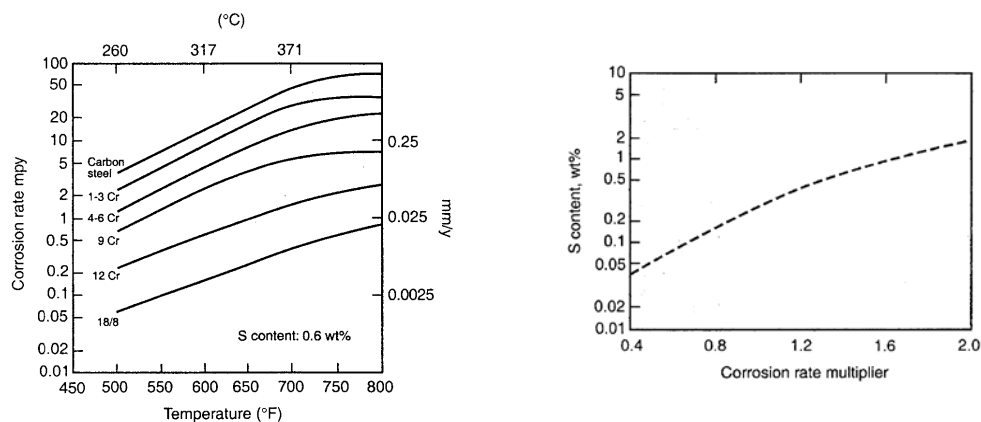


**Figure 1.** Modified McConey curves are diagrams used in refineries to predict sulfidic corrosion. These diagrams are taken from Kane, R.D.; Cayard, M.S.; Understanding Critical Factors that Influence Refinery Crude Corrosiveness. *Mater. Perform.* **1999**, July, 48-54.

Field surveys<sup>5,6,46-50</sup> indicate that high concentrations of hydrogen sulfide ( $H_2S$ ) had an inhibiting effect on naphthenic acid corrosion. These observations regarding inhibiting role of  $H_2S$  were later confirmed by experimental studies done both with model oils and crude oil fractions. At high temperatures ( $>260^\circ C$ ) in distilling towers some oil

sulfur compounds decompose and generate  $H_2S$  which is generally a highly corrosive compound.<sup>31</sup> Although  $H_2S$  is corrosive and attacks the metal, it forms an iron sulfide scale (FeS) which is oil-insoluble and is deposited on the metal offering some protection against further corrosion.<sup>31,46</sup>

Sulfidic corrosion and naphthenic acid corrosion proceed simultaneously, interact but lead to lower corrosion rates than it was predicted.<sup>7,31</sup> The explanation for this behavior is related to the solubility differences between the two corrosion products: oil-insoluble iron sulfide and oil-soluble iron naphthenates, respectively, and to the different concentrations of NAP and sulfur in crude oil. Although both NAP and  $H_2S$  attacked the metal there was a competition between formation and destroying of iron sulfide scale during corrosion processes. Iron sulfide scale formed on the metal surface but was attacked by increased NAP concentrations whereby the FeS layer was removed and could no longer offer the protective effect against corrosion. Thus it was possible that when crude oils with low sulfur content were processed, the NAP corrosion rates were high whereas when high sulfur crude oils were processed corrosion rates decreased significantly.

## **2.5 Effect of Temperature**

Temperature is one of the most important factors affecting naphthenic acid corrosion.<sup>4,8,50-55</sup> Based on field data, Derungs identified the lower temperature limit  $220^{\circ}C$  ( $430^{\circ}F$ ) when NAPs become corrosive. Their corrosive effect is very intense in a temperature range between  $220^{\circ}C$  and  $350^{\circ}C$  ( $430-660^{\circ}F$ ) and decreases with a further temperature increase. Over  $400^{\circ}C$  ( $750^{\circ}F$ ) no evidence of NAP corrosion was found and

this was attributed to naphthenic acid decomposition in that temperature range.<sup>4,5</sup> Gutzeit did some of the first experiments investigating the effect of temperature on NAP corrosion. He found that the corrosion rate triples with every 55°C increase in temperature and for a given temperature the corrosion rate is dependent on NAP content. He suggested that NAP corrosion kinetics follows the Arrhenius equation and it is controlled by a chemisorption mechanism.<sup>5</sup> Using these assumptions for NAP corrosion kinetics, Gutzeit calculated the activation energy at temperatures over 288°C (550°F) to be 68.5 kJ·mol<sup>-1</sup>.<sup>5</sup> However these data were later contradicted by tests done by Slavcheva et al. who took into consideration the structures of naphthenic acids in their studies.<sup>7</sup> They found different activation energy values for a single acid (31.8 kJ·mol<sup>-1</sup>) and for an acid mixture (23.8 kJ·mol<sup>-1</sup>) with both values being lower than the value obtained by Gutzeit. Slavcheva suggested that the oil composition is the main factor influencing the activation energy values and thus controlling corrosion kinetics.<sup>31</sup>

Piehl proposed a different way of analyzing correlations between temperature and NAP corrosion. He started by analyzing the NAP distribution in crude oils as a function of their True Boiling Points (TBP). TBP is a parameter used in refineries that is determined from ASTM D86 boiling curve.<sup>6,45</sup> In atmospheric distillation columns, NAP will boil at temperatures close to their TBP whereas in vacuum distilling units the under vacuum conditions the boiling points of NAPs decrease by 111°C to 166°C (200°F to 300°F). Thus if TBP's of naphthenic acids in oil are known, it would be possible to predict where in the plant they will reach the highest concentrations and cause corrosion.

## 2.6 Effect of Acid Structure

Slavcheva, Shone, and Turnbull studied the corrosivity of different single naphthenic acids and their mixtures.<sup>7</sup> Their hypothesis was that NAP carboxylic group activity was influenced by the rest of the molecule which included one or more rings. Experimental results showed a maximum in reactivity in medium molecular weight NAP. The assumption was that as molecular weight increased, the corresponding NAP structures were bigger and complicated preventing the adsorption of the molecule on metal surface. Thus the steric hindrance decreased the adsorption of acid molecules and the naphthenic acid corrosion decreased too. Based on these assumptions the authors explained in an empirical way the differences in corrosivity of crude oils with similar or identical TAN values. This theory of steric factors influencing NAP corrosion was later used to evaluate the corrosivity of Athabasca oil-sands crudes that had a high naphthenic acid and sulfur content.<sup>32</sup>

## 2.7 Effect of Velocity

The effect of flow in naphthenic corrosion is directly related to the mass transfer of corrosive species to metal surfaces and of corrosion products from metal to the bulk fluid.

Under severe flow conditions, the protective iron sulfide film can be physically removed by the shear stresses, thereby exposing the metal surface to further NAP attack. High corrosion rates caused by high flow rates and turbulence were identified in return bends, tube inlets of furnaces, and bends of transfer lines.<sup>4,7,12,51-57</sup> The first investigations of the flow effect in NAP corrosion were strictly related to case histories<sup>4,6</sup>. Derungs

mentioned volatility of the product, pressure, and steam injection as principal factors influencing fluid velocities in distilling units.<sup>4</sup> Experimental tests done by Gutzeit showed that naphthenic acid in the vapor phase were more corrosive as velocity increased (from 0 to  $0.12 \text{ m}\cdot\text{s}^{-1}$ ) as long as vapors could form a film on the metal surface. For higher velocities ( $4 \text{ m}\cdot\text{s}^{-1}$ ) acid vapors could not condense on the metal surface and the corrosion rate decreased.<sup>5</sup>

Other authors investigated the role of shear stress on scale integrity in acidic and sulfur corrosion and found that oils with a high sulfur and NAP content vaporized less and were more sensitive to velocity effects.<sup>49-51</sup>

Based on his laboratory flow tests compared to real case data Craig<sup>51,54</sup> determined that NAP corrosion is controlled by the diffusion of species from solution to the metal (acids) or from the metal surface to bulk solution (iron naphthenates).

Some authors tried to mimic flow conditions from transfer lines or tube inlets of distilling towers on laboratory scale using flow rigs,<sup>55,57</sup> rotating cylinders in autoclaves,<sup>56,57</sup> and jet impingement devices.<sup>58-62</sup> Jet impingement tests results were compared to specific locations in refineries (bends, feeding lines) where NAP corrosion was very aggressive under the combined effect of velocity and high temperature.

## **2.8 Effect of NAP Vaporization and Condensation**

Naphthenic acids had the most severe effects at high temperature close to their boiling points. Therefore it was important to find if the change of physical state of NAPs influenced their corrosion rates. Based on field observations and laboratory tests, Derungs determined that highest corrosion rates of naphthenic acids occurred at their

condensation points. He also noticed that corrosion did not occur when NAPs were totally transformed into a vapor phase.<sup>4</sup> Gutzeit also did vaporization-condensation experiments with naphthenic acids and found that the vapor phase corrosion was caused by the formation of a condensate film on the metal surface and not by the vapors.<sup>5</sup>

In summary NAPs are corrosive only in the liquid phase as it was presented in other research studies focusing on corrosion at high temperatures.<sup>62-67</sup> However, Slavcheva et al. suggested that even if naphthenic acids were close to their boiling points, their corrosivity was influenced by the dilution of the acids in hydrocarbons with similar boiling points.<sup>7</sup>

## **2.9 Effect of Pressure**

According to the literature pressure has little or no effect on NAP corrosion.<sup>5-7</sup> However in vacuum distilling units any pressure variation (i.e. by steam injection) can influence the vaporization of naphthenic acids and consequently their corrosion rates. Thus as it was already mentioned when NAP are in vapor phase they lose their corrosive effects.

## CHAPTER 3: RESEARCH OBJECTIVES

### 3.1 Research Objectives

NAP corrosion is a complex phenomenon with many different influential factors (i.e. sulfur content, velocity, temperature). No source in the current literature has yet offered a comprehensive basis for a model of corrosion. The current research project tried to compile the known facts and combine them with additional experimentation in order to make a significant contribution to understanding, explaining, and modeling of NAP corrosion. The work started from a hypothesis that naphthenic acid and sulfur corrosion are intertwined and that the model should describe both corrosive processes. Thus the research objective was formulated as:

*“Build and implement a physico-chemical model of naphthenic acid corrosion including both formation and damage of protective iron sulfide films on steel surfaces.”*

### 3.2 Research Project Milestones

In order to achieve the main goal of the project, the research activity was divided into specific tasks that represented real milestones of the project. Project tasks were completed successively over a period of three years and their corresponding results were presented during annual Advisory Board meetings and published in reports submitted to ExxonMobil Research and Engineering Company.

These project milestones are listed below in the order they were accomplished:

- **Sulfidation experiments** were performed focusing on iron sulfide scale formation in order to obtain corrosion and scale formation rates as references for the general model. Experiments were run using the yellow

model oil with a given sulfur content (0.25% wt), “spiked” with commercially available naphthenic acids (TAN 0.1). Scale growth and corrosion rates were evaluated as function of time. Variables such as temperature and velocity were kept constant in every sulfidation test.

- **Sulfidation-challenge experiments** were done in order to determine the extent of protectiveness offered by the iron sulfide scale under NAP attack and high velocity conditions. These test conditions required a separate pre-sulfidation experimental phase for building the FeS protective scale in a yellow oil, followed by the challenge phase when white oils with different NAP concentrations were used to challenge the protectiveness of the preformed sulfide scales.
- **Sulfidation-challenge experiments** were completed where real crude oil fractions having different sulfur content and NAP concentrations were used to preform the sulfide scale. These FeS scales were then challenged with white oils spiked at high and low NAP concentrations for testing the scale protectiveness.
- **Building of a model**, calibration and verification of the performance with experimental results of sulfidation and challenge tests.

Each of the following chapters will present in a comprehensive manner the various phases of the project so that the reader can follow and understand easily the building of the model of NAP corrosion which is presented in the end. In real time, the

model was developed concurrently with the execution of the experimental part of the project as the understanding developed.

In order to offer the reader an easier way to follow the results and the line of arguments each chapter covering various stages of the project is structured in the same way:

**Introduction** – provides basic information about the chapter topic.

**Experimental** – includes details about instrumentation, testing materials and conditions, as well as the experimental procedures.

**Results and Discussion** – presents in a comprehensive manner the testing matrices, experimental results and their analysis.

**Summary** – expresses the main findings in a concise manner.

## CHAPTER 4: SULFIDATION EXPERIMENTS

### 4.1 Introduction

Reactive sulfide species in oil attack the metal through a solid state reaction generating iron sulfide scales. One of the first goals of this current research work was to understand the sulfidation mechanism and build a physico-chemical model of this process. Initial tests focused on generating iron sulfide scales from model oils of given sulfur content and under high temperature and high velocity conditions. The protective properties of FeS scale vary as a function of experimental time were also investigated. NAPs had only a minor role in sulfidation tests. They were used only in small concentration (TAN = 0.1) as that amount is considered beneficial for FeS scale generation.

### 4.2 Experimental

#### *4.2.1 Instrumentation - High Velocity Rig (HVR)*

A high velocity rig (HVR) was used as an experimental unit for NAP corrosion tests under continuous flow conditions. It was designed to reproduce the flow, pressure, temperature, and shear stress conditions usually encountered in a refinery (i.e. transfer lines, furnaces, distilling towers). A schematic representation of the HVR is presented in Figure 2.

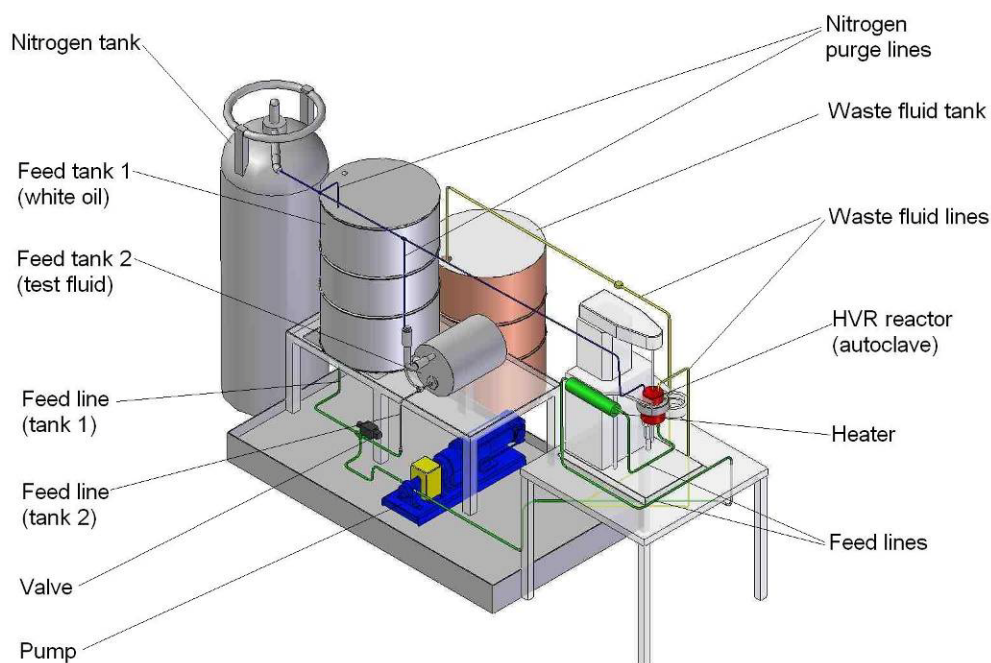


**Figure 2.** High Velocity Rig used for NAP corrosion tests under high velocity and temperature conditions.

The HVR was designed and built by Parr Instrument Company IL according to specifications requested by EMRE. The HVR consists of an experimental flow through system made of Inconel and 316 SS (stainless steel with 20% Cr), and consists of an autoclave situated in a box that can be sealed during experiments, a metering pump, a feeding tank for the experimental fluid, a flushing tank containing white oil, an electromagnetic valve, a sample box for fluid sampling during experiments, a heat exchanger situated between the pump and the autoclave, and a waste tank at the end of the rig. The whole system is pressurized with nitrogen provided from an outer tank, preventing oxygen contact of the specimens and the auto ignition of the fluids due to high temperature during experiments. Normal nitrogen pressure for running an experiment is

40 psig. The operating pressure of the autoclave was from 0 to 500 psig and temperature from 20°C to 371°C. The autoclave vessel and fluid contained within are heated with two ring electric heaters and the rest of the rig parts are heated with electric tape during the experiments. The autoclave has a rotor on which ring specimens can be attached for the experiments. Ring specimens can be rotated in the autoclave during experiments with velocities up to 2500 rpm. The autoclave is fed with fluids by an inlet situated on the bottom of the vessel. The fluid flow rate provided by the pump can be controlled by the control panel and varies from 5 to 20 cm<sup>3</sup>/min.

A complete run in the HVR had five main operating phases. The first phase of the test cycle is termed “preheating” of the testing equipment (i.e. autoclave with specimens and feeding lines) using white oil as the heating fluid. During “preheating” which lasts almost 2 hours, the oil temperature increases from 20°C to the preset experimental condition (usually 340-370°C). The increase in temperature is manually controlled by the operator using the temperature controller of the HVR. The second phase is called the “warm up” when the experimental rig is heated further by the oil that runs through the entire rig. This step has a 30 min duration and starts when the preset temperature is reached. When “warm up” phase ends, the “run” starts. The “run” phase of the tests is the real experimental part of the test cycle. The run starts when the electromagnetic valve of the rig switches the feed from the white oil over to the experimental fluid. During the run phase, the test oil flushes the steel specimens at a preset testing temperature for a certain period of time. When the experimental time elapses, the control switches the valve back from the test fluid to the white oil and continues with the fourth test phase called

“flushing”. During the “flushing” phase, the heated white oil is pumped into the rig again for cleaning purposes. The fifth and final phase is the “cooling down” when the heating is turned off and the system is flushed for 30 min more only with white oil.

#### ***4.2.2 Materials***

The materials used for this research project were selected so that the experiments should be able to reproduce real field conditions as close as possible. Thus the test specimens were made of the same steel types as those types used for building refinery equipment. Test fluids were mineral oils that could be spiked with corresponding chemicals and brought to physico-chemical properties close to real crude oil fractions.

##### ***4.2.2.1 Steel types***

Two types of steel specimens are commonly used in NAP corrosion experiments: carbon steel (CS A106) and 5-Cr steel (F5-A 182). Specimens used in the HVR experiments had a ring form with OD = 81.76 mm ID = 70.43 mm and height = 5 mm.

##### ***4.2.2.2 Mineral Oils***

The mineral oils used for sulfidation and challenge tests were white oil and yellow oil respectively. White oil is a clear petroleum distillate with light paraffinic content and is considered a chemically inert fluid. It was used both for preheating and flushing the HVR rig and as a test fluid when it was spiked with commercial naphthenic acids. The physical properties of white oil are summarized in Table 3. The other mineral oil used for NAP corrosion tests was yellow oil, an “Americas CORE basestock”. The reason for using yellow oil was its natural 0.25 %wt sulfur content which provided a good source for building sulfide scales during the tests. In the following sections the

sulfur content of any oils used in the tests will be denoted using the symbol “S”. Physical properties of yellow oil are included also in Table 3.

**Table 3.** *Physical Properties of Mineral Oils*<sup>1</sup>

<b>Properties</b>	<b>White oil</b>	<b>Yellow Oil</b>
Appearance	Clear liquid	Clear liquid
Density, 15°C, kg·m <sup>-3</sup>	0.9	0.879
Flash Point, COC, °C	268	270
Viscosity, Kinematic, cst, 100°C	11.4	11.8
Viscosity, Kinematic, cst, 40°C	98.6	111.5

In order to correctly evaluate the final corrosion rates after the experiments, the scales formed on the steel specimens were removed by mechanical and chemical means. Chemical removal of iron sulfide scale was done using a Clarke solution. It was prepared from 84 mL hydrochloric acid (HCl 12.1 N, analytical purity, Fisher A 144c-212), 5 g stannous chloride (SnCl<sub>2</sub>·2H<sub>2</sub>O, 99.99%, Fluka 98529), and 2 g antimony (III) oxide 99.999%, Sigma-Aldrich) according to ASTM G 1-90.<sup>68</sup>

### 4.3 Test Conditions

Test conditions for the sulfidation experiments were selected so that they would be similar or identical to operation conditions in refineries. The main selected temperature was 343°C (650°F). This temperature was high enough to produce sulfidation and NAP corrosion and it gets below temperature limit of 371°C (700°F) where naphthenic acids decompose. The flow rate of the fluids through the test autoclave

<sup>1</sup> CITGO Tufflo Naphthenic Process Oil Product Information

was 5-7 ccm and rotation of specimens was set to 2000 rpm. Pressure in the autoclave was kept constant at 150 psig for every test.

#### ***4.3.1 Reactive Species Concentrations***

The reactive species for sulfidation experiments were sulfur and naphthenic acids. Yellow oil had a natural sulfur concentration of 0.25 % wt that was considered sufficient to corrode the metal and generate the iron sulfide scale. Naphthenic acids in small concentrations accelerate the sulfidation processes therefore yellow oil was spiked with commercial naphthenic acids to the low TAN 0.1.

#### ***4.3.2 Test Duration***

Sulfidation processes were studied as a function of time at high temperatures and velocities. Therefore time was the only variable that was modified for each sulfidation experiment. Tests had durations of 6, 15, 24, 48 and 96 hours. All test conditions for sulfidation tests are summarized in Table 4.

**Table 4.** *Experimental Conditions for the First Set of HVR Tests using Carbon Steel (CS A106) and Mild Steel (F5-A 182) Specimens*

Test number*	Time (h)	Ring Material	Sulfur content (% wt)	TAN	RPM	Press (psig)	Temp. (°F)
#4	6	CS A106	0.25	0.1	2000	150	343 (650°F)
#5	24	CS A106	0.25	0.1	2000	150	343 (650°F)
#6	48	CS A106	0.25	0.1	2000	150	343 (650°F)
#10	15	CS A106	0.25	0.1	2000	150	343 (650°F)
#11	6	<b>F5-A 182</b>	0.25	0.1	2000	150	343 (650°F)
#14	24	<b>F5-A 182</b>	0.25	0.1	2000	150	343 (650°F)
#13	48	<b>F5-A 182</b>	0.25	0.1	2000	150	343 (650°F)
GB 10	96	CS A106 + <b>F5-A 182</b>	0.25	0.1	2000	150	343 (650°F)

\*Tests are presented in their chronological order.

#### **4.3.3 Specimens Arrangement for Test**

The HVR was designed in such a way to expose tests samples to high velocities and high temperatures conditions. Samples had a ring form as it was already presented and were stacked up on the autoclave rotor.

Figure 3 which is a cross-section of the HVR autoclave, shows the arrangement of the ring specimens on the autoclave rotor, the fluid inlet, fluid route through the autoclave, and the fluid inlet and outlet. Rotation of cylindrical rotor incurs a shear stress on the specimens outer surface. The heated oil enters through inlet at the bottom of the autoclave. Then the oil flows between the rotating specimens and the inner surface of the autoclave vessel. Finally the oil exits the autoclave through the outlet at the top.

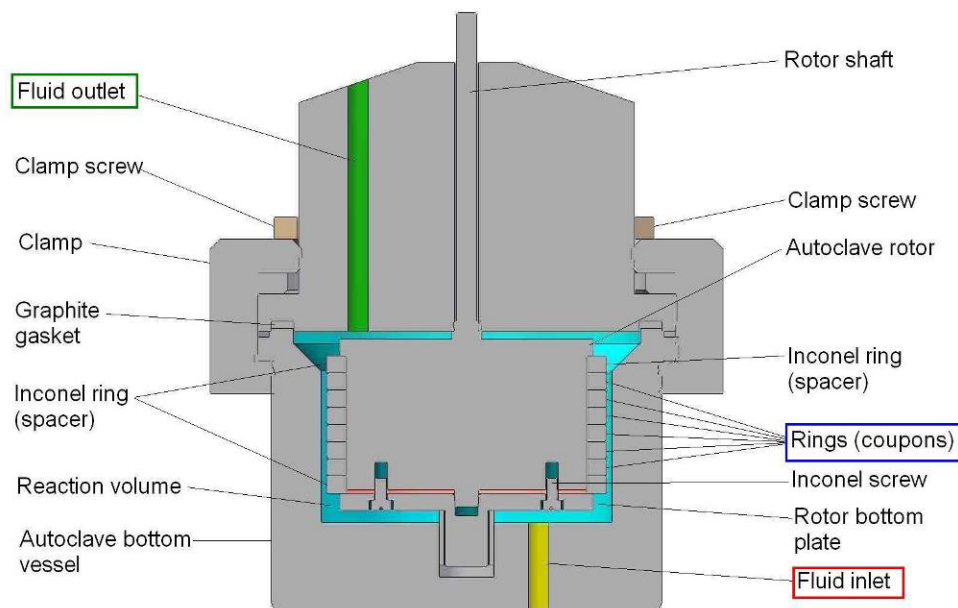


**Figure 3.** Cutout through HVR autoclave reactor. Fluid is pumped through the bottom of the reactor (fluid inlet) fills completely the autoclave volume and leaves the reactor through the top (fluid outlet).

#### 4.4 Sample Preparation

Specimen surfaces were prepared in the same way before every test so that they were oxide free, had the same roughness, etc., to maintain the reproducibility of the tests.

First, every specimen was marked with a number registered in the lab-book. After marking the specimens were polished with 400 and 600 grit papers under isopropanol flushing. Isopropanol minimized oxide formation on the steel specimens during the polishing procedure. Finally specimens were rinsed with toluene and acetone and dried under a dry nitrogen stream. Then the specimens were weighed using an analytical balance and their corresponding values were registered. Finally the specimens were

inserted into the HVR according to the experimental procedure. The assembly of the HVR is presented in Appendix C (Figure 1).

#### **4.5 Evaluation of Metal Loss**

The HVR autoclave was disassembled after each test was finished. The specimens were taken out, rinsed with toluene and acetone, dried under dry nitrogen flow and weighed. Because it was noticed that some of the scale was easily removed during rinsing the specimens with solvents, it was decided to evaluate the amount of the loose scale. Thus specimens were first rinsed with solvents and weighed. Then they were rubbed with paper towels, rinsed again and weighed again. In this way the difference between these two successive procedures (rinsing and rubbing) represented the amount of loose iron sulfide scale. Therefore the term *RW* used in the formulae for corrosion and scale formation calculations represented the weight after rubbing. Rinsing and rubbing mechanically removed the scale from the specimens. The iron sulfide scale could only be removed completely from the surface of the specimens by chemical means. The FeS scale was chemically removed by using the ASTM G 1-90 solution or Clarke solution, which contains concentrated hydrochloric acid (HCl, 12.1 N), 2% antimony trioxide (Sb<sub>2</sub>O<sub>3</sub>), and 5% stannous chloride (SnCl<sub>2</sub>). All chemicals were purchased from Fisher Scientific. Each specimen was dipped in the Clarke solution for 20 s and then rinsed with deionized water. Specimens were dried with nitrogen and weighed. This “clarking” procedure was repeated 4-5 times until no significant weight change ( $\Delta W < 0.0005$  g) was noticed between two consecutive “clarkings”. Final weight loss represented the metal loss used to calculate the final corrosion rate.

## **4.6 Results and Discussion**

Evaluation of sulfidation and corrosion rates in the HVR was done for two types of steel commonly used as construction materials in refinery equipment. These two types of steel were carbon steel (CS A106) and 5-Cr steel (F5-A182) each steel type being evaluated in separate experimental sets. The following sections of this chapter will present in detail the experimental results.

### ***4.6.1 HVR Quality Control Run Test***

As it was mentioned above, the ExxonMobil Research and Engineering Company (EMRE) provided the financial and the technical support for this research project. In order to connect our research work to previous EMRE experimental data it was decided to run a Quality Control Run (QC Run) test before starting any other tests using the HVR. The main purpose of this QC Run test was to compare the Ohio University Corrosion Center results to previous QC Run results done at EMRE laboratories. Test conditions such as temperature, rotation speed, and time were similar at OU to those of EMRE labs. White oil spiked to TAN = 4 with commercial naphthenic acids was used as test fluid in the QC Run. Table 5 summarizes the experimental conditions and final results (i.e. corrosion and scale formation rates) for the two QC Runs (OU vs. EMRE).

**Table 5.** *HVR QC Run results and experimental conditions at EMRE and OU Corrosion Center*

Test Location	Steel Type	S (%wt)	TAN	RPM	Pres (bar)	Temp. (°C)	Time (h)	Corros. Rate (mm/y)
EMRE	CS A106	0	4	2000	200	315 (600°F)	15	6.55
OU	CS A106	0	4	2000	150	315 (600°F)	15	4.81

Both experimental results of the QC Runs (OU vs. EMRE) were considered to be in reasonable agreement when compared to the typical scatter in experimental results seen in these types of environments. In addition, according to EMRE evaluation, the QC Run results were considered to be in the same range when compared to real field data. Therefore it was decided that the HVR was ready for use in further experiments.

#### **4.6.2 Test Matrix**

The test matrix presented in Appendix A was designed to meet the research goals of the project. Thus the tests should cover sulfidation and NAP corrosion processes under high temperature and high velocity conditions. Therefore the first tests had to establish the quality and kinetics of scale growth in model oils. Then the tenacity of FeS scales against NAP attack had to be tested in “sulfidation-challenge tests”, and finally quality and kinetics of FeS scales formed from real crude oil fractions were established. Based on this initial test matrix all other phases of this research project were developed.

### 4.6.3 Sulfidation Tests Results

Sulfidation experiments were designed to establish the quality and kinetics of scale growth in model fluids that had a “typical” sulfur content. The tests were done separately for carbon steel (CS) and 5Cr steel specimens respectively. It was decided to use only one type of steel in every experiment to prevent any interference between the two different steels. Therefore the final results are presented separately for CS and 5Cr.

#### 4.6.3.1 Sulfidation Test Results for CS

The first set of three experiments used a model oil (yellow oil) with a low acid concentration (TAN = 0.1) and a low sulfur content (S  $\approx$  0.25% wt) for building the FeS scales on CS specimens. Experimental conditions such as pressure, temperature and rotation speed are presented in Table 4. The initial test matrix did not include the 15 hour test (test # 10) which was run later to determine whether evolution of corrosion rate versus time was linear or parabolic.

Corrosion rates of the specimens were evaluated by weight loss, calculating the difference of specimens weight before and after the test. It was expressed in both mm/year and mils (1 mil = 0.001 in) per year (mpy). Two types of corrosion rates were calculated, integral corrosion rate (CR) and differential corrosion rate (DCR). The integral corrosion rate is an average corrosion rate that evaluates the process on certain period of time and it is calculated with Equation 4:

$$CR = \frac{(IW - FW)}{\rho_{Fe} \times A_c \times t} \times 0.1 \times 24 \times 365 \quad (4)$$

where

$CR$  is the corrosion rate [mm/y]

$IW$  – initial weight (before the experiment) [g]

$FW$  – final weight (after final clarkking) [g]

$\rho_{Fe}$  – iron density [g/cm<sup>3</sup>], ( $\rho_{Fe} = 7.87$  g/cm<sup>3</sup>)

$A_c$  – specimen area exposed to Yellow oil [cm<sup>2</sup>]

$t$  – time of the experiment [h]

$0.1$  – multiplication factor used to obtain the final result in mm/y when all other terms are expressed with the above measurement units

$24$  – hours in a day

$365$  – days in a year

The integral corrosion rate, being a time-average, does not provide good information about any transients in the corrosion processes and therefore the differential corrosion rate was also measured.

The differential corrosion rate evaluates the intensity of the corrosion process in different experimental time periods. By comparing corrosion rates from one experiment to another, DCR showed more precisely when corrosion increased or decreased.

Therefore it provides a more accurate temporal description of the corrosion process evolution. DCR is calculated according to Equation 5:

$$DCR = \frac{(CR_f \times t_f) - (CR_i \times t_i)}{(t_f - t_i)} \quad (5)$$

where

$DCR$  is the differential corrosion rate [mm/y],

$CR_f$  is the average corrosion rate of the last test (test  $n+1$ ) [mm/y],

$CR_i$  is the corrosion rate of a previous test (test  $n$  - considered as reference) [mm/y],

$t_f$  represents running time of last test [h] and

$t_i$  represents running time of previous test [h].

Errors for every test were calculated using the individual corrosion rate of every specimen and the average corrosion rate of the test. Thus the error bars on the graphs represent absolute values for maximum and minimum of differences between individual and average corrosion rates of samples. Figure 4 presents the integral corrosion and Figure 5 presents differential corrosion rates for carbon steel specimens during sulfidation tests. The integral corrosion rate plot shows that corrosion rate decreases with time. The differential corrosion rate completes the picture of the process by showing that corrosion was very intense during the first 6 hours and then decreased and became constant as time increased. The value obtained for *DCR* on the 96 h test was negative because the average value of *CR* calculated for the 48 h test and used in Equation 2, was bigger than the *CR* average value obtained in the 96 h test. This highlights the problem with using differential corrosion rates – the propagation of errors can be significant and may eventually compromise the quality of the data presented.

The decrease of corrosion rates (detected with both integral and differential) was caused by the protective action of the iron sulfide film (FeS) that was formed on the specimen surface and mitigated corrosive reactions. For the shorter time test (6 h) the film was not completely formed and therefore its protective action was not very efficient, the result being a high *CR*. For the longer time experiments (15, 24, 48, and 96 h) the FeS film was completely formed protecting the metal surfaces and the corrosion rate decreased.

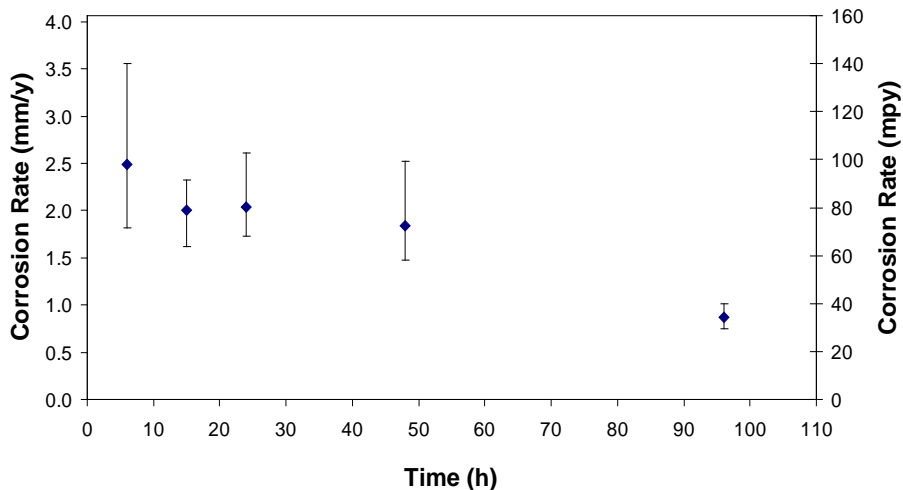


**Figure 4.** Integral corrosion rate for sulfidation tests on carbon steel. 6, 15, 24, 48, and 96 h tests using Yellow oil ( $S = 0.25\%$  wt; TAN 0.1). Points are average values while errors bars indicate the highest and lowest value obtained on multiple samples exposed in the same experiment.

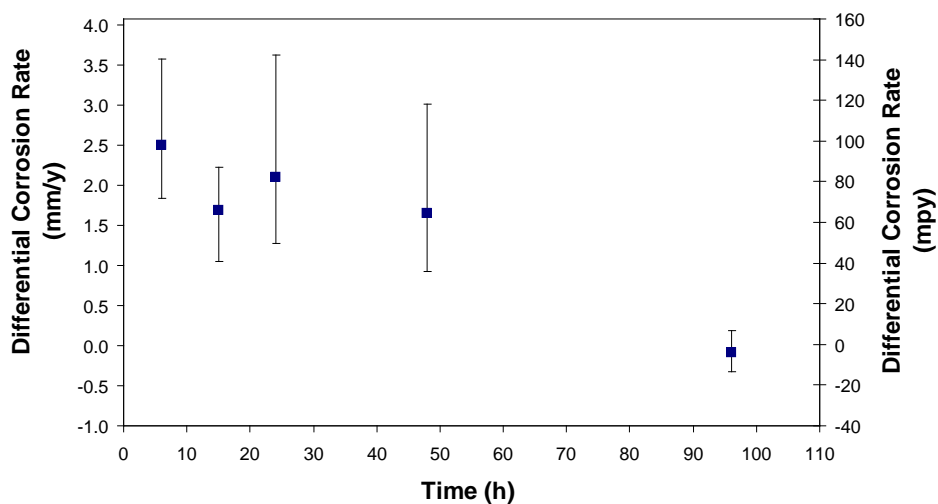


**Figure 5.** Differential corrosion rate for sulfidation tests on carbon steel. 6, 15, 24, 48, and 96 h tests using Yellow oil ( $S = 0.25\%$  wt; TAN 0.1). Points are average values while errors bars indicate the highest and lowest value obtained on multiple samples exposed in the same experiment.

The iron sulfide scale formation rate was determined by weight loss of the specimens in a similar way as the corrosion rates were calculated. After each experiment specimens were rinsed with toluene and acetone for removing all oil residues, then dried and weighed. Specimen weight after rinsing with organic solvents was the recorded as the initial value ( $RW$ ) used for calculating the scale formation rate. After solvent rinsing, specimens were “clarked”, dried and weighed 4-5 times. When there was no significant weight difference ( $\Delta W < 0.0005$  g) it was considered that scale was completely removed from the metal and last weighted value represented the final weight ( $FW$ ). Scale formation rate was calculated both as integral and differential formation rates in similar way as corrosion rates calculations. Scale Formation Rate ( $SFR$ ) is an average value and was calculated with (6):

$$SFR = \frac{(RW - FW)}{\rho_{FeS} \times A_c \times t} \times 0.1 \times 24 \times 365 \quad (6)$$

where

$SFR$  is the scale formation rate [mm/y],

$RW$  is rinse weight before any clarking [g],

$FW$  – final weight after last clarking [g],

$\rho_{FeS}$  is iron sulfide density [ $\text{g}/\text{cm}^3$ ], ( $\rho_{FeS} = 4.84 \text{ g}/\text{cm}^3$ ),

$A_c$  is specimen area exposed to Yellow Oil [ $\text{cm}^2$ ], and

$t$  is the time of the experiment [h]

0.1 – multiplication factor used to obtain the final result in mm/y when all other terms are expressed with the above measurement units.

24 – hours in a day

365 - days in a year.

The differential scale formation rate (*DSFR*) was used to evaluate the scale formation process as in the case of transient corrosion rate. It was calculated in a similar way as DCR according to Equation 7:

$$DSFR = \frac{(SFR_f \times t_f) - (SFR_i \times t_i)}{(t_f - t_i)} \quad (7)$$

$SFR_f$  is the average scale formation rate of the last test (test  $n+1$ ) [mm/y],

$SFR_i$  is the scale formation rate of a previous test (test  $n$  - considered as reference) [mm/y],

$t_f$  represents running time of last test [h] and

$t_i$  represents running time of previous test [h].

Integral scale formation rates for CS specimens are presented in Figure 6. Differential scale formation rates for the same tests are shown in Figure 7.

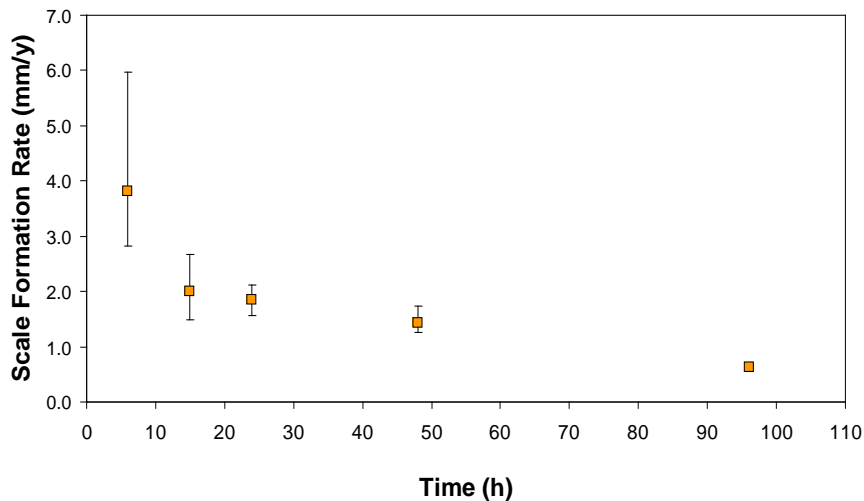


**Figure 6.** Integral Scale Formation Rate for CS specimens evaluated for sulfidation tests using Yellow oil. Points are average values while errors bars indicate the highest and lowest value obtained on multiple samples exposed in the same experiment.

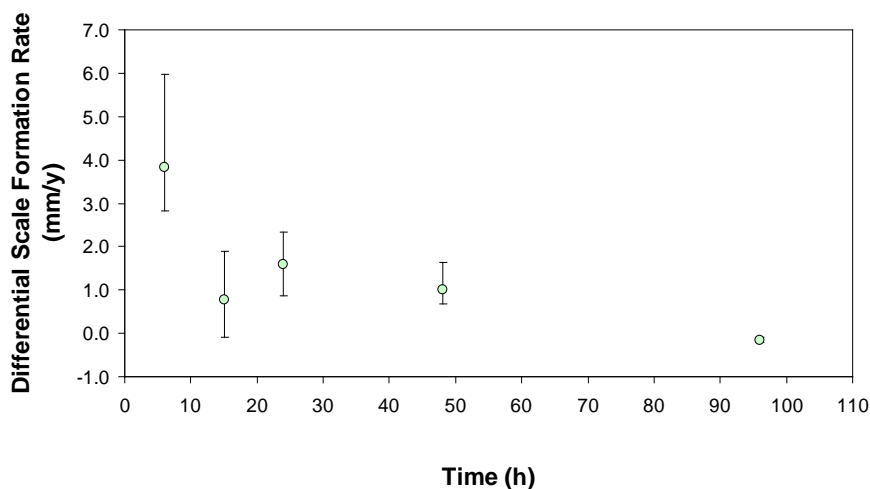


**Figure 7.** Differential Scale Formation Rate for CS specimens evaluated for sulfidation tests using Yellow oil. Points are average values while errors bars indicate the highest and lowest value obtained on multiple samples exposed in the same experiment, with propagation of error accounted for.

The 6 h sulfidation experiment was a relatively short experiment. Comparing the FeS scale formed in the 6 h test to those scales that were evaluated in longer tests (15, 24, 48, and 96 h) it is obvious that the scale formation rate decreased as time increased. Apparently, as the FeS scale went continuously through a cyclic process of growth, cracking, and delamination, under continuous flow and rotation conditions part of the scale spalled off and was removed by the fluid current. Only the strongly adherent scale survived on the specimens. This cyclic process of growth, cracking and delamination was also supported by the SEM images of the FeS scale found on the specimens at the end of tests (see the images in the appendices). With time increase less scale is formed on the steel surface which corresponds to the lower corrosion (sulfidation) rate. Differential scale formation (*DSFR*) plot shows that after 15 h the formation/removal of the scale remained more or less constant.

A different characterization of the corrosion process and scale formation was determined by estimating the moles of iron lost by the metal (corrosion) and moles of iron used in iron sulfide film growth (sulfidation). As in the previous evaluations of corrosion rate and scale formation rate, iron molar consumption/production rate was calculated in both ways, integral and differential respectively.

Iron moles lost by the metal were calculated using the weight difference of the specimens, before and after the test, according to Equation 8:

$$n_{Fe} = \frac{(IW - FW)}{M_{Fe} \times A_c \times t} \times 0.0001 \times 24 \times 365 \quad (8)$$

where

$n_{Fe}$  – number of moles of iron [moles/m<sup>2</sup>/y]

$IW$  - initial weight of the specimens [g]

$FW$  - final (after last clarkking) weight of the specimens [g]

$M_{Fe}$  - molecular weight of iron [g/mol] ( $M_{Fe} = 55.8$  g/mol)

$A_c$  - specimen exposed area of each specimen [cm<sup>2</sup>]

$t$  - experiment time [h].

0.0001 – multiplication factor used to obtain the final result in moles/m<sup>2</sup>/y when all other terms are expressed with the above measurement units.

24 – hours in a day

365 - days in a year.

Equation 9 gives the number of FeS moles:

$$n_{FeS} = \frac{(RW - FW)}{M_{FeS} \times A_c \times t} \times 0.0001 \times 24 \times 365 \quad (9)$$

where

$n_{FeS}$  – number of moles of FeS [moles/m<sup>2</sup>/y],

$RW$  - rinse weight of the specimens [g],

$FW$  - final weight of the specimens after clarkking [g],

$M_{FeS}$  iron sulfide molecular weight [g/mol], ( $M_{FeS} = 87.8$  g/mol)

$A_c$  - specimen exposed area of each specimen [cm<sup>2</sup>],

$t$  - experiment time [h],

0.0001 – multiplication factor used to obtain the final result in moles/m<sup>2</sup>/y when all other terms are expressed with the above measurement units,

24 – hours in a day,

365 - days in a year.

Differential number of iron moles and iron sulfide moles were calculated with (10) and (11) in a similar way as for previous differential rates calculations. Thus Equation 10 calculates moles of iron lost by the metal:

$$n_{Fe} = \frac{[(n_{Fe})_f \times t_f] - [(n_{Fe})_i \times t_i]}{(t_f - t_i)} \quad (10)$$

where

$n_{Fe}$  – number of moles of iron [moles/m<sup>2</sup>/y],

$(n_{Fe})_f$  – moles of iron in last test (test  $n+1$ ) [moles/m<sup>2</sup>/y],

$(n_{Fe})_i$  - moles of iron in previous test (test  $n$  - considered as reference) [moles/m<sup>2</sup>/y],

$t_f$  - running time of last test [h],

$t_i$  - running time of previous test [h].

and Equation 11 is used to calculate moles of FeS scale:

$$n_{FeS} = \frac{[(n_{FeS})_f \times t_f] - [(n_{FeS})_i \times t_i]}{(t_f - t_i)} \quad (11)$$

where

$n_{FeS}$  – number of moles of iron [moles/m<sup>2</sup>/y],

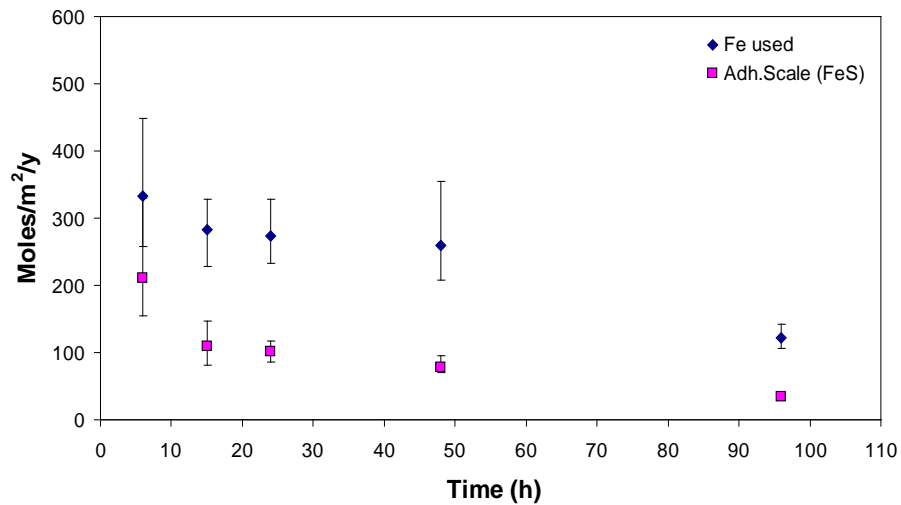
$(n_{FeS})_f$  – moles of FeS in last test (test  $n_{+1}$ ) [moles/m<sup>2</sup>/y],

$(n_{FeS})_i$  – moles of FeS in previous test (test  $n$  – considered as reference) [moles/m<sup>2</sup>/y],

$t_f$  – running time of last test [h],

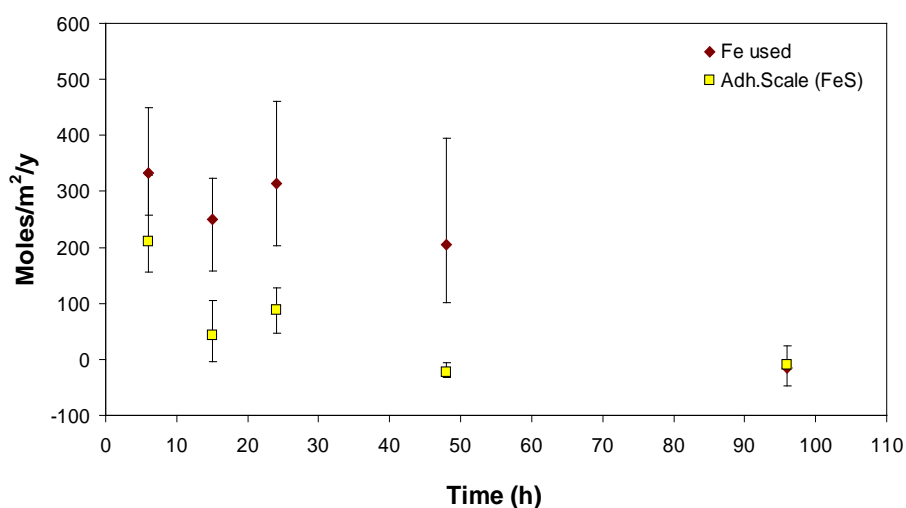
$t_i$  – running time of previous test [h].

Figure 8 shows the integral values for moles of iron used and the FeS scale that was found on the CS specimen surfaces at the end of sulfidation tests.



**Figure 8.** Moles of Fe and FeS (integral values) Plot represents the moles of Fe used (lost by the metal) during the tests and the moles of FeS that represented the adherent scale found at the end of every test. Error bars represent absolute values for maximum and minimum of differences between individual and average corrosion rates of samples.

Figure 9 shows the plot for differential values of moles for both species. In spite of the big error bars of differential values the trends are similar to those showed by the integral moles values Figure 8. Both moles of iron and FeS showed similar decreasing trends as testing time increased. According to reactions (1), the number of moles lost by the metal during sulfidation should be equal to the number of moles of FeS formed. However scale formation plots (Figure 8 and Figure 9) showed significant differences between the moles of iron and FeS. These differences are generated by the losses due to FeS scale that spalled and was removed from the metal and carried away by the flow as well as (to a smaller extent) by NAP corrosion which forms soluble iron naphthenates.



**Figure 9.** Moles of Fe and FeS (differential) Plot represents the moles of Fe used (lost by the metal) during the tests and the moles of FeS that represented the adherent scale found on the CS at the end of every test. Points are average values while errors bars indicate the highest and lowest value obtained on multiple samples exposed in the same experiment, with propagation of error accounted for.

### Scanning Electron Microscopy Analysis

Scanning Electron Microscopy (SEM) analysis offered a view of the iron sulfide scales that formed on the metal surface. SEM also provided details about how continuous scale growth/regeneration processes influenced the scale structure. Thus at the end of the 6 hr test the FeS scale had a multilayered structure as it is showed in Figure 10. The bottom FeS layer appears to be rather compact and adherent to the metal (partial delamination probably occurred during sample preparation), however, all other layers above it are fragmented. Voids between the scale fragments allowed the diffusion of reactive species like H<sub>2</sub>S and naphthenic acids to inner scale compact layer as well as counter-current diffusion of iron naphthenates from the metal to the bulk liquid.

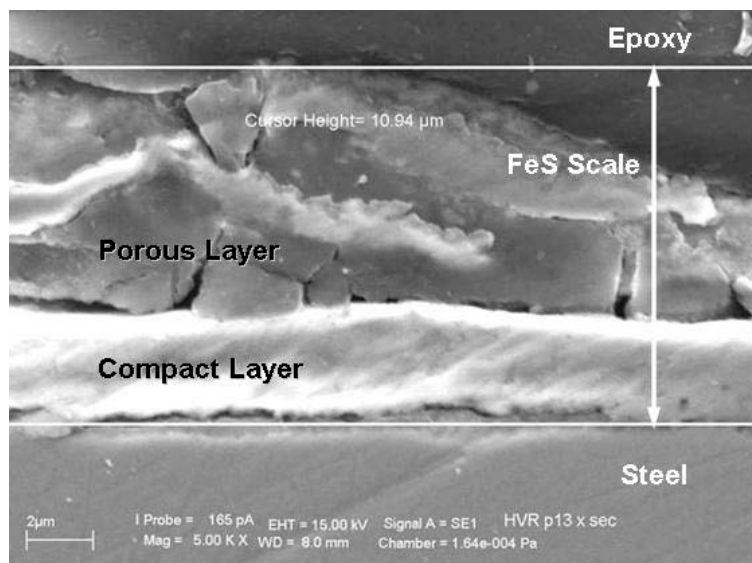


**Figure 10.** SEM Analysis of iron sulfide scale formed on CS specimens after the 6 h test. The image represents a cross-section of the interface metal-iron sulfide scale, metal being at the bottom part of the picture. Several FeS scale layers are visible some of them are compact (bottom layer), others fragmented (top layers).

As the experimental time increased the scale was more affected by the growth/regeneration processes and the continuous oil flow and specimen rotation. Figure 11 shows a cross-section of specimen after the 24 hr test and shows a very fragmented scale structure. Thus the scale became porous and fragile making it prone to delamination and spalling off. By comparing information provided by SEM pictures to data calculated for scale formation it became clear how scale thickness decreased as experimental time increased.

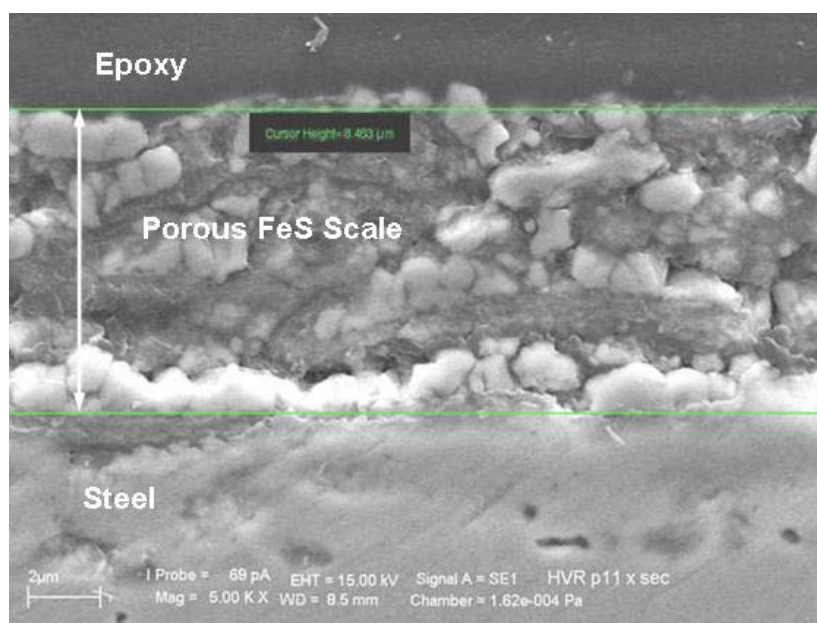


**Figure 11.** SEM Analysis of iron sulfide scale formed on CS specimens after the 24 h test. The image represents a cross-section of the interface metal-iron sulfide scale, metal being at the bottom part of the picture. Multiple FeS scale layers are visible presenting a much fragmented structure which made the scale very porous.

As it was mentioned before the FeS scale goes continuously through a cyclic process of growth, cracking and delamination and the effects of this cyclic process are shown in the SEM scale surfaces images. Thus Figure 12 shows the SEM image of the FeS scale

formed on CS samples in a 24 h sulfidation test. The scale has multiple layers and the top one is already cracked and partially removed. The top layer of the FeS scale reproduces the “pattern” of the original metal surface on which it was formed. Under the top layer can be noticed the next FeS layer that was formed on the metal surface.

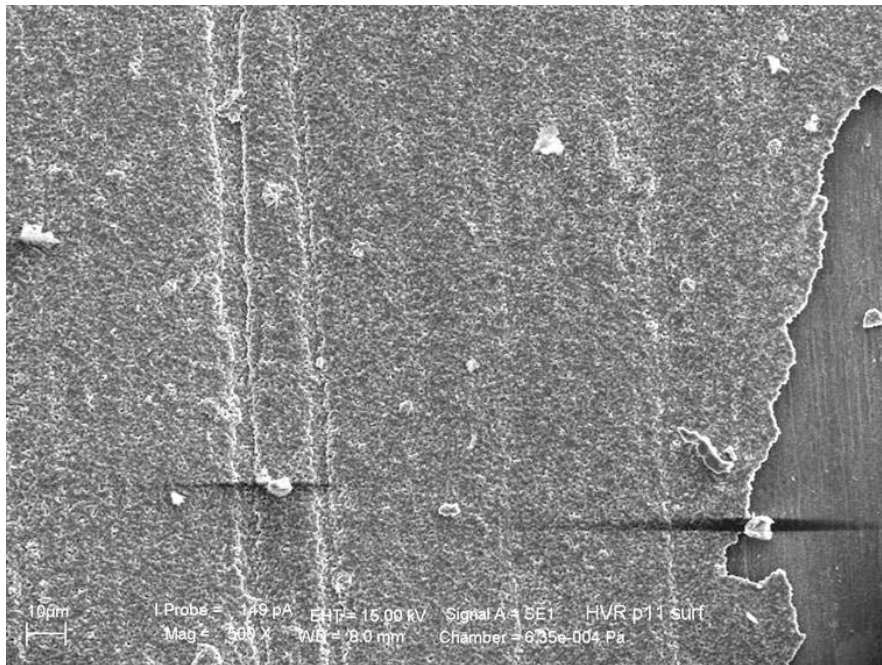


**Figure 12** SEM image of the FeS scale formed on the CS specimen surface in a 24 h sulfidation test. The FeS scale shows a multilayer structure with the top layer cracked and partially removed under the effect of high velocity. The SEM image has a 500X magnification.

Figure 13 shows also an SEM image of the surface of the FeS scale formed in 48 h sulfidation test. Although the testing time was double compared to 24 h test and the FeS scale was submitted for a longer time to high velocity aggression, the top layer still covers partially the metal surface. This top layer is worn but the original pattern of the metal surface can still be recognized on the FeS scale. This proves that the scale top layer was first formed and next new layers formed underneath.

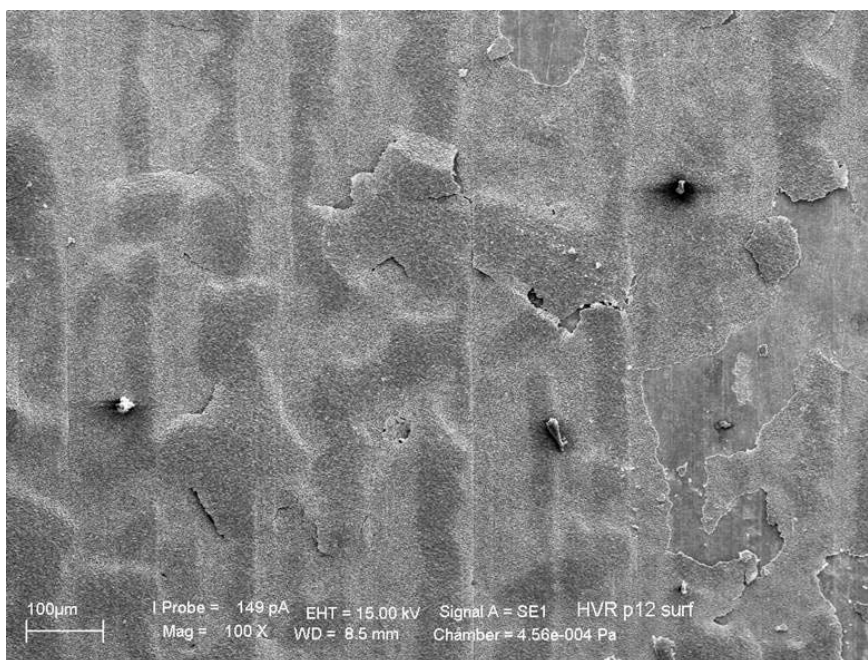


**Figure 13** SEM image of the FeS scale formed on the CS specimen surface in a 48 h sulfidation test. The FeS scale shows a multilayer structure with the top layer cracked and partially removed under the effect of high velocity. The SEM image has a 100X magnification.

#### ***4.6.3.2 Sulfidation Test Results for 5Cr Steel***

After the sulfidation test series with CS were completed, the next step was testing the 5Cr steel using the same experimental test fluids and conditions as for carbon steel. Thus the same yellow oil ( $S \approx 0.25\%$  wt) spiked to TAN = 0.1 was used with temperature, pressure and rotation already listed in Table 1. Time series for 5Cr included 6, 24, 48, and 96 h tests, the 15 h test being eliminated due to project time deadlines.

As in the case of CS tests corrosion and scale formation rates were calculated for 5Cr steel using the same equations. All terms of these equations were already explained in previous section therefore only the corresponding plots will be presented and analyzed

in current section. Integral and differential corrosion rates for 5Cr steel are presented in Figure 14 and Figure 15.

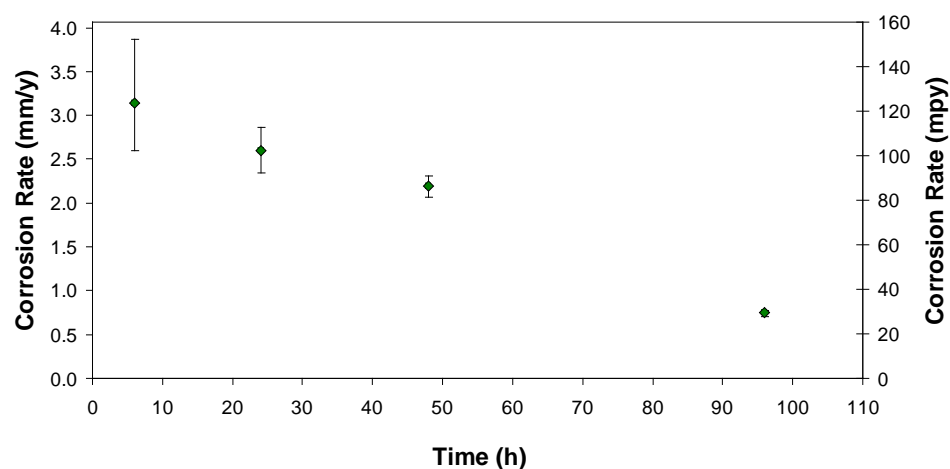


**Figure 14.** Integral corrosion rate for sulfidation tests on 5Cr steel. Tests were done using Yellow oil (S = 0.25% wt) spiked with NAP to TAN 0.1 and run for 6, 24, 48, and 96 h. Points are average values while errors bars indicate the highest and lowest value obtained on multiple samples exposed in the same experiment.

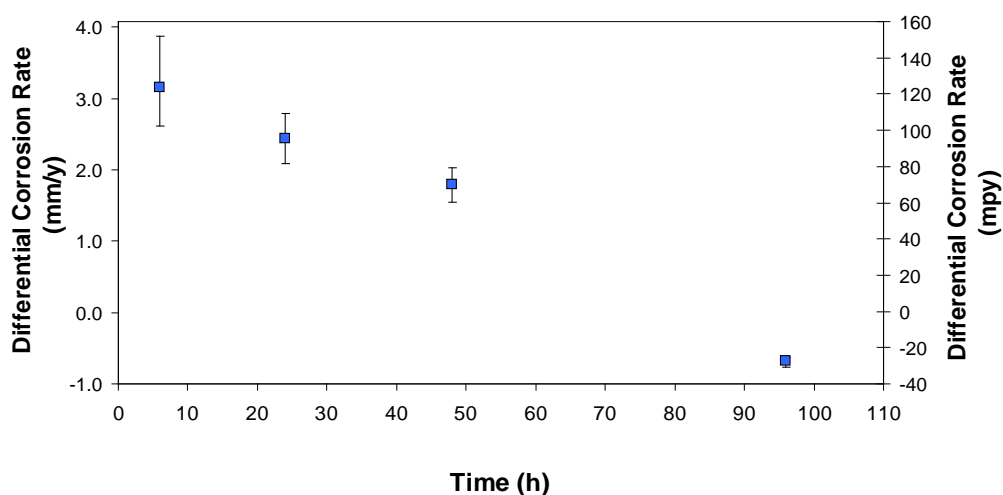


**Figure 15.** Differential corrosion rate for sulfidation tests on 5Cr steel. Tests were done using Yellow oil (S = 0.25% wt) spiked with NAP to TAN 0.1 and run for 6, 24, 48, and 96 h. Points are average values while errors bars indicate the highest and lowest value obtained on multiple samples exposed in the same experiment, with propagation of error accounted for.

The corrosion rates measured on 5Cr specimens indicated a steady decrease as testing time increased. This trend was similar both for integral corrosion rates and for differential corrosion rates, with the differential rate showing that after 48 h corrosion was only half of the value corresponding to 6 h test. This proved that corrosion was very intense only during the first hours of the test and then was mitigated by the protective FeS scale that formed on the metal surface. Substantial iron sulfide scale formed in short time test (6 h) as it is shown in both scale formation plots Figure 16 (integral values) and Figure 17 (differential values). As the experimental time increased (24 - 96 h) less scale was formed (as the corrosion rate decreased) and remained adherent on the metal surface.

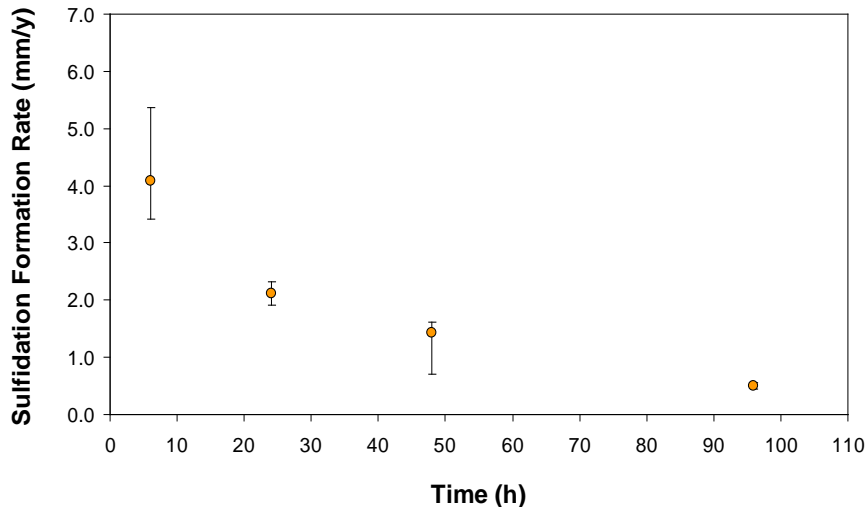


**Figure 16.** Integral Scale Formation Rate for 5Cr specimens. FeS scale was formed in sulfidation tests using Yellow oil (TAN = 0.1, S = 0.25% wt). Points are average values while errors bars indicate the highest and lowest value obtained on multiple samples exposed in the same experiment.

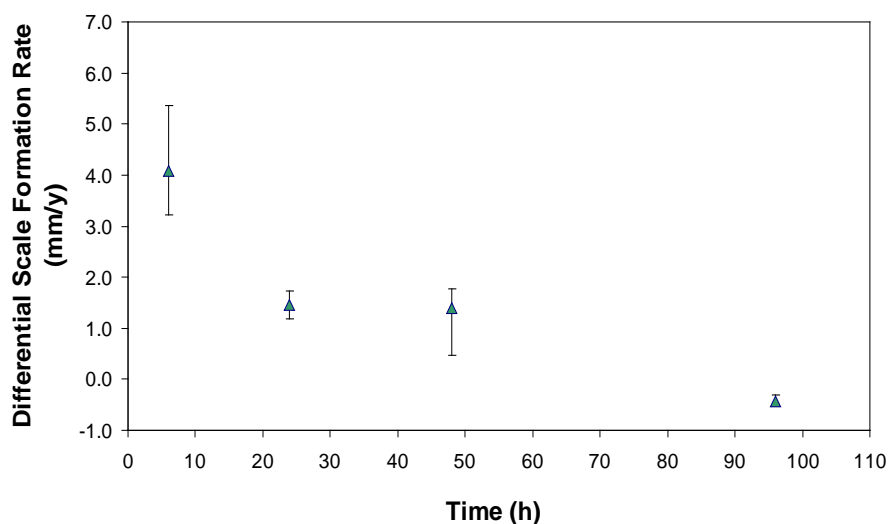


**Figure 17.** Differential Scale Formation Rate for 5Cr specimens. FeS scale was formed in sulfidation tests using Yellow oil (TAN = 0.1, S = 0.25% wt). Points are average values while errors bars indicate the highest and lowest value obtained on multiple samples exposed in the same experiment, with propagation of error accounted for.

In terms of moles of iron and iron sulfide, the corrosion and scale formation rates showed similar results decreasing as testing time decreased. These trends for moles of iron and FeS are presented in Figure 18 (integral values) and Figure 19 (differential values).

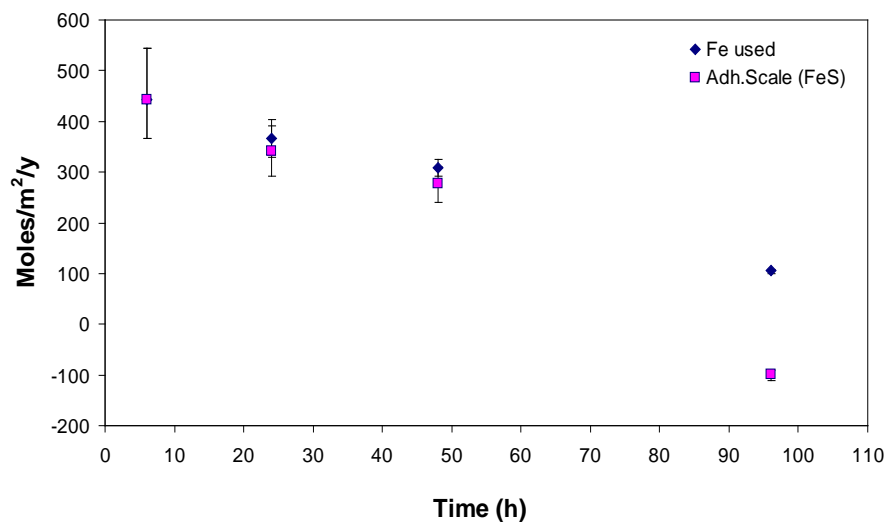


**Figure 18.** Moles of Fe and FeS (integral values) Plot represents the moles of Fe used (lost by the metal) during the tests and the moles of FeS - the adherent scale found at the end of every test. Points are average values while errors bars indicate the highest and lowest value obtained on multiple samples exposed in the same experiment.

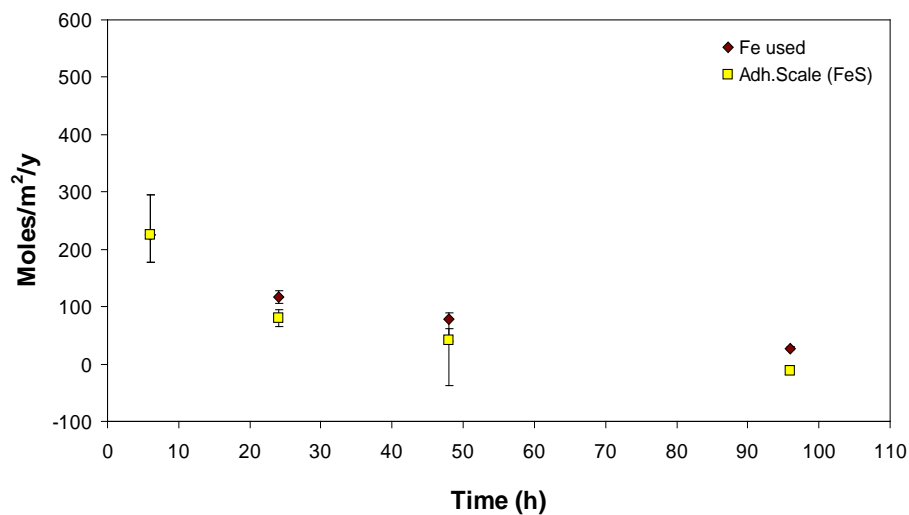


**Figure 19.** Moles of Fe and FeS (differential) Plot represents the moles of Fe used (lost by the metal) during the tests and the moles of FeS - the adherent scale found at the end of every test. Points are average values while errors bars indicate the highest and lowest value obtained on multiple samples exposed in the same experiment, with propagation of error accounted for.

#### 4.6.3.3 CS vs. 5-Cr Comparison

Sulfidation data analysis included the comparison of corrosion rates CS vs. 5Cr steel Figure 20. Corrosion rates were generated in sulfidation experiments under identical testing conditions. Although tests were run separately for each type of steel both CS and 5Cr had similar tendencies, i.e. corrosion rates and scale formation rates decreased as time increased. Error ranges made it difficult to present a clear separation between CS and 5Cr values. However it can be noticed that 5Cr generated higher corrosion rates than CS with the exception of the 96 h test where results overlap. It was concluded that both steels corroded at a similar rate in sulfidation experiments. This similar behavior of CS and 5Cr steel is also sustained by the scale formation rates data as they were almost the same for both steel types as it is shown in Figure 21.

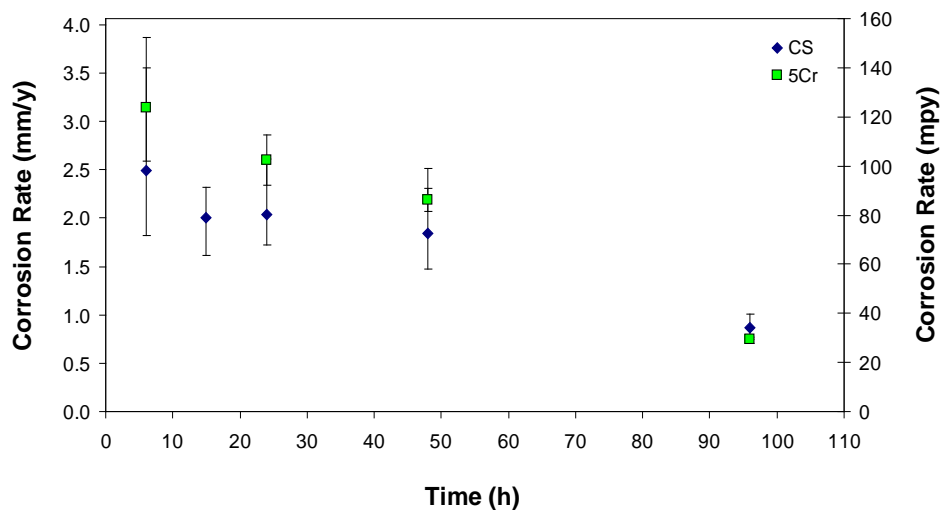


**Figure 20.** CS vs. 5Cr- Integral corrosion rates for sulfidation tests. Tests were done separately for each type of steel using Yellow oil (S = 0.25% wt) spiked with NAP to TAN 0.1 and they were run for 6, 15, 24, 48, and 96 h. Points are average values while errors bars indicate the highest and lowest value obtained on multiple samples exposed in the same experiment.

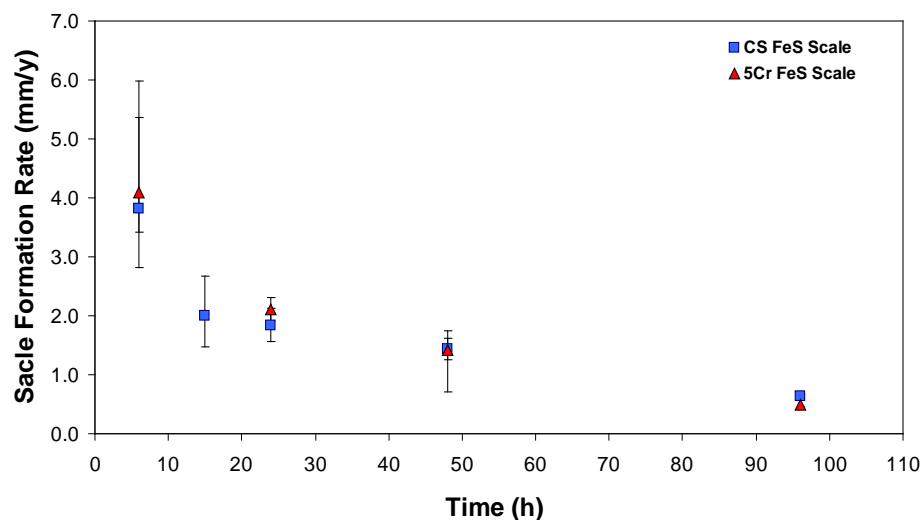


**Figure 21.** CS vs. 5Cr- Integral scale formation rates for sulfidation tests. Tests were done separately for each type of steel using Yellow oil ( $S = 0.25\%$  wt) spiked with NAP to TAN 0.1 and they were run for 6, 15, 24, 48, and 96 h. Points are average values while errors bars indicate the highest and lowest value obtained on multiple samples exposed in the same experiment.

#### 4.6.3.4 No Rotation and No Flushing HVR Experiments

Differences between number of Fe moles lost by the metal and Fe moles used to form iron sulfide film prompted a different experiment in order to better understand the amount of iron sulfide scale loss due to flow. The operating hypothesis in the previous experiments was that some of the loose FeS scale was removed from the specimens and entrained by the fluid flow and flushed out with the oil residues. Losing the FeS protective scale due to flow resulted in increasing corrosion rates.

Two different experiments were done to test this hypothesis further. One experiment was done without the final “flushing phase” when specimens are “washed” with white oil for 5 hours at  $343^{\circ}\text{C}$  ( $650^{\circ}\text{F}$ ). It was hypothesized that by eliminating the flushing, less FeS will be removed preserving the protective scale and therefore corrosion rates should decrease. This test was named the “No Flushing Test” and was run 6 h.

In the second test it was thought that by decreasing the shear stress, less FeS scale would be removed and thus the corrosion rates would decrease, too. Therefore a 6 hr test was performed without rotating the specimens so that the only movement of the test fluid would be generated by the slow continuous flow of yellow oil forming the scale. This so called “No Rotation Test” was considered to be very close to the experimental conditions executed in different experimental rigs in the same lab such as: the Flow Through Mini Autoclave (FTMA) and the static autoclaves. FTMA was an experimental unit used by other researchers to run sulfidation tests under very slow (creeping) flow conditions. FTMA tests were also part of the same NAP research project conducted by other students.

All other experimental conditions in these two “special” tests were otherwise identical to the 6 h sulfidation test i.e.  $T = 343^{\circ}\text{C}$  ( $650^{\circ}\text{F}$ ),  $p = 150$  psig,  $\text{TAN} = 0.1$ , and  $\text{S} = 0.25\%$  wt. The two “special” tests were done using only the carbon steel specimens.

Final corrosion rates of special tests are presented in Figure 22. For comparison, a 6 h “normal” sulfidation test result was included in the graph as well as a 6 h sulfidation test result from an experiment conducted in the FTMA with identical temperature and reactive species concentrations.

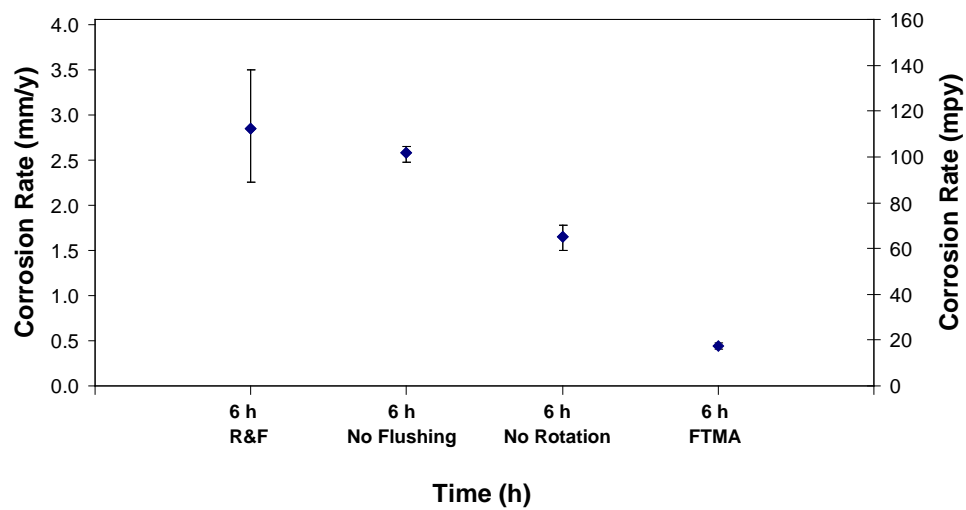


**Figure 22.** Comparison of the 6 h experiments made in HVR and in FTMA. HVR experiments were done under different test conditions, i.e. normal conditions - rotation of the specimens and flushing at the end of the experiment (6 hr R&F), 6 h with no flush at the end of the experiment (6 h No Flushing), 6 h and no rotation of the specimens (6 h No Rotation). Points are average values while errors bars indicate the highest and lowest value obtained on multiple samples exposed in the same experiment.

The final results did not show a significant difference between a test including the “final flushing” and a similar test without this flushing. This led us to conclusion that most of the scale was lost during the sulfidation testing time when most of corrosion took place.

The corrosion rate of the “No Rotation Test” was much lower than the experiment with rotation which was as expected. This result however, appears to be much higher than the FTMA corrosion rate. Thus it seems difficult to compare the results generated in two different experimental units: the HVR vs. FTMA due to the different geometry and procedure used in the experiments.

### ***4.6.3 Summary***

Sulfidation tests proved that iron sulfide scale was formed on both types of steel equally (CS and 5Cr steel) and had a protective effect against the corrosive sulfur containing species in longer experiments. The corrosion rates decreased as experimental time increased. The decrease in corrosion rates suggested that FeS scale was continuously formed on the metal surfaces reducing the diffusion of corrosive species towards the metal surface during the tests.

The SEM analysis of the specimens revealed that the FeS scale structure consisted of successive scale layers proving that scale regeneration was a continuous process. Thus repeated processes of growth, cracking and delamination made the FeS scale more porous. Due to its porous structure the FeS scale became a weak diffusion barrier allowing the exchange of reactive species and reaction products from the metal surfaces to bulk solution. Flow was able to partially remove the loose iron sulfide scale and contribute to higher corrosion rates under these conditions.

Further experiments were designed to investigate the protectiveness of FeS scale against NAP attack by challenging it with white oil without sulfur but with different naphthenic acids concentrations. This new experimental series will be discussed in detail in the following chapter.

## CHAPTER 5: SULFIDATION – CHALLENGE EXPERIMENTS

### 5.1 Introduction

Sulfidation – Challenge tests represented the second phase of this research project focusing mainly on naphthenic acid corrosive processes. The main goal of this experimental phase was to understand NAP corrosion and the interaction with FeS scales previously formed on the metal surfaces. The pure sulfidation tests generated sufficient data regarding the scale formation and its cyclic process of growth, cracking, and delamination, that generated the outer sulfide scale. In order to test the protectiveness of the FeS scales they were “challenged” with white sulfur-free oil containing naphthenic acids at different concentrations during in the so called challenge tests. Particularly important aspect of these tests was that the FeS scale was generated *in situ* using yellow oil (as it was done in the first phase of this project) followed by a switch of feed to a white oil containing naphthenic acids. The following sections in this chapter will describe in detail this part of the project.

### 5.2 Experimental

The experimental procedures and methods of the Sulfidation-Challenge tests were similar or even identical to those adopted in the sulfidation tests as described in the previous chapter. Therefore the following sections will describe in detail only those procedures, conditions, and experimental set-up that were different compared to the previous experiments.

### **5.2.1 Instrumentation**

The HVR was used for every experiment during this project phase but it was slightly modified to accommodate the new test requirements. Both test parts (“sulfidation” and “challenge”) had to be done in the same experimental unit to avoid cooling the specimen and exposing them to air, so that the FeS scales could be generated *in-situ*. Therefore a second 5 gal drum was added as a feeding tank. The first feeding tank was filled with yellow oil and used in the sulfidation part of the experiment. The second feeding tank was filled with a white oil spiked with naphthenic acids and was used in the challenge part of the experiment. Switching the feed from one tank to the other allowed running an experiment without interruption. The rest of the equipment was identical to that described in the sulfidation tests previously.

### **5.2.2 Materials**

#### **5.2.2.1 Steel types**

The metal specimens were made of the same steel types used in the sulfidation tests. They were carbon steel (CS A106) and 5Cr steel (F5-A182). The specimens had the same ring form with identical dimensions: outer diameter - OD = 81.76 mm, inner diameter - ID = 70.43 mm, and height = 5 mm.

#### **5.2.2.2 Mineral oils**

The iron sulfide scales were generated using the same yellow oil, an Americas CORE basestock with a natural sulfur content of S = 0.25% w/w. The preformed FeS scales were challenged with a solution consisting of white oil spiked with commercial naphthenic acids, covering a concentration range from TAN = 2 to TAN = 8. This NAP

concentration range was selected having as a reference the real refinery conditions where current TAN concentrations of the crude oil feeds are between 0.5 – 4. Even though TAN 8 is much higher than the usual TAN concentrations found in refinery, it was selected to represent a very aggressive condition which tests the limits of protection offered by the FeS scales. All physical properties of these mineral oils were presented previously in Chapter 5.

### **5.2.3 Test Conditions**

Generating the FeS scales *in-situ* and then challenging them imposed not only special experimental set-up but also special test procedures. It was decided that every experiment should include a sulfidation phase followed by challenge without any “break” between the two test phases. The test conditions for sulfidation had to be identical for each experiment so that the FeS scales would be generated under the same conditions regardless of the challenge conditions that followed. Thus sulfidation time was set to 24 h for every test, and the temperature was set to 343°C (650°F). Only one special sulfidation test was run at 287°C (550°F) which will be discussed in a later section of this chapter. Preformed FeS scales were challenged with different TAN concentrations for different periods of time. Both in sulfidation and in challenge tests specimens were rotated in the autoclave with 2000 rpm which corresponds to a peripheral velocity of  $v = 8.5$  m/s. The general testing conditions for the sulfidation-challenge tests are presented in Table 6.

**Table 6.** General test conditions for sulfidation-challenge tests

Test phase	Sulfur content (%w/w)	TAN	Temp. (°C)	Time (h)	Pressure (psig)	Peripheral Velocity (m/s)
Sulfidation	0.25	0.1	343 (650°F)	24	150	8.5
Challenge	0	2 – 8	343 (650°F)	6 - 120	150	8.5

A detailed summary of challenge vs. time series is presented in Table 7.

**Table 7.** Summary of sulfidation – challenge tests. Challenge time series vs. different TAN solutions. (TAN - Total Acid Number)

Challenge time TAN	6 h	12 h	24 h	50 h	60 h	120 h	Special Tests	
							Low velocity test	Sulfidation at 287°C (550°F)
TAN 2			X		X			
TAN 3.5			X		X	X		60 hr Challenge at 343°C (650°F)
TAN 5	X	X	X	X			24 hr Challenge at 500 rpm	
TAN 6.5			X	X				
TAN 8	X	X	X					

TAN 2 and 3.5 were considered as “low” NAP concentrations that would not affect the sulfide scale. Therefore it was decided to run a short (24 h) challenge and a longer (60 h) one. In the case of TAN 3.5, one test lasted 120 h because TAN 3.5 was assumed to be closer to the critical TAN limit in the real cases met in refineries.

Challenge with TAN 5 was more aggressive and it was decided to cover a more detailed time series starting from a short time (6 h) to a longer time (50 h). Based on the TAN 5 challenge series results for TAN 6.5 only two challenges were run for 24 h and 50 h respectively. Both tests provide enough information for modeling. The TAN 8 challenge was considered the most aggressive against FeS scale therefore only three tests were necessary (6, 12, and 24 h) for testing scale protectiveness.

Two special experiments were added to the initial test matrix and they were designed to investigate: NAP attack on FeS scale at low velocities (500 rpm) and the scale tenacity when it was formed at lower temperature 287°C (550°F). These test results and conclusions will be discussed in detail in latter sections of this chapter.

### **5.3 Results and Discussion**

In the sulfidation-challenge tests both processes: - sulfidation and challenge of FeS scale by NAP acids -, were run in the same experimental unit. To be able to separate the effect of NAP challenge from sulfidation, it was necessary to run some pure sulfidation tests that could be used as a reference for further combined sulfidation-challenge tests. Metal weight losses and scale weight gains generated in sulfidation reference tests were first averaged and then subtracted from metal weight losses and scale weight gains measured at the end of every sulfidation-challenge test to reveal what happened in the challenge phase only. All the results presented in this section were calculated by subtracting the reference sulfidation tests from the overall results.

In the sulfidation-challenge study, both types of steel specimens were used together in the same autoclave to save time. Thus three rings of each type (CS and 5Cr

steel) were tested simultaneously in every test. However the results of corresponding TAN and time series will be presented and analyzed separately for each type of steel.

### **5.3.1 Sulfidation Tests**

The sulfidation reference tests were repeated many times. The results from the seven successful sulfidation tests were averaged and the final results were used for calculating the differences in the sulfidation-challenge tests. The average value of weight losses for each type of steel (CS and 5Cr) obtained during the seven sulfidation tests were subtracted from the weight loss for every specimen that was exposed in the longer sulfidation – challenge tests. In this way it was possible to evaluate only the effects of the second phase of the tests. On every plot below, the sulfidation reference tests results will be presented separately (on the left) from the challenge tests results (on the right).

### **5.3.2 TAN 2 Results**

TAN 2 was considered to be low enough as a starting point for challenging the FeS scale and high enough to create damage to the scale. The first test with TAN 2 was a 24 h challenge and it was followed by a second longer test (60 h) with the same TAN concentration. Final corrosion rates for CS and 5Cr evaluated for TAN 2 challenge tests are presented in Figure 23. The plot for corrosion rates was divided in two separate regions “Sulfidation” and “Challenge” this style being repeated in all subsequent graphs for an easier comparison of data. Figure 23 shows that the average corrosion rates decreased for both steel types over time. However the decreasing trend of CRs was still within the error limits of sulfidation reference corrosion rates and as a consequence it can be considered that the corrosion rates did not change much in the TAN 2 challenge tests.

It was concluded that FeS scale preformed during sulfidation offered a good protection under these conditions and challenge concentrations had to be increased to the next TAN level.

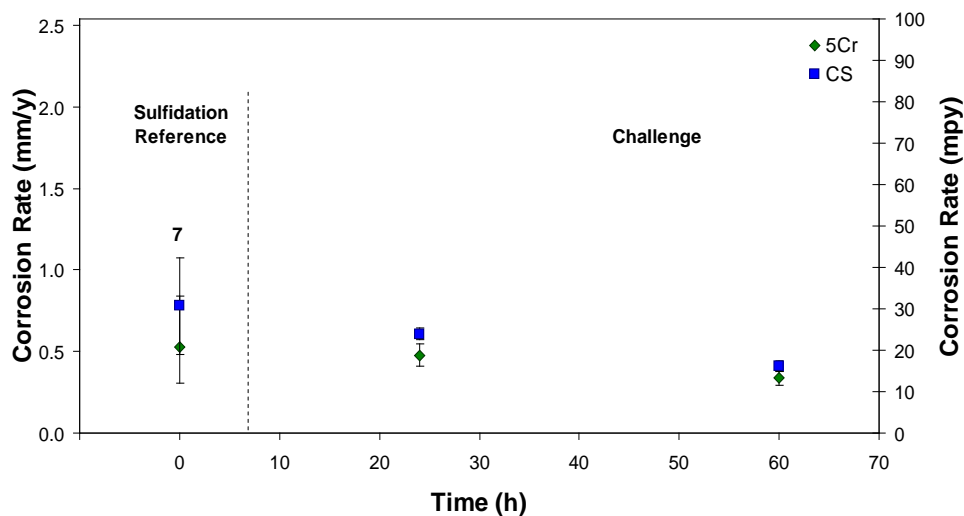


**Figure 23.** CS vs. 5Cr steel. Corrosion rates for 24 hr and 60 hr challenge tests using TAN 2 white oil. Number 7 above the error bars for the sulfidation point represents the number of experiments that were averaged for calculating the respective value. Points are average values while errors bars indicate the highest and lowest value obtained on multiple samples exposed in the same experiment.

The scale thickness was evaluated after the specimen rings were taken out of the autoclave. Some of the scale was very loose and could be removed easily by rinsing the rings with organic solvents. However rinsing did not remove all of the scale and it became clear that the loose scale can be further removed by some mechanical means like brushing with a stiff plastic brush or wiping the rings with a paper towel. The strongly adherent scale was removed from specimen surfaces only by chemical means (Clarke solutions). Both scales (loose and adherent) had to be evaluated because they were formed with iron that was lost by the metal during corrosive processes. Thus the term

“total scale” includes both loose and adherent scale formed on the metal. The total scale was quantified as a difference between the weight of the specimens after they had been rinsed with organic solvents and the final weight after specimens had been clarked. The adherent scale was evaluated as a difference between weight of specimens after loose scale mechanical removal and final weight after clarking. For both metals (CS and 5Cr steel) total and adherent scales were presented in Figure 24. The scale thickness graph for CS and 5Cr (Figure 24) shows that some scale was still formed on both steel types during the challenge phase because sulfur residues remained in the system after sulfidation. Although some FeS scale was formed from sulfur residues during the challenge phase, data in Fig 31 show that the scale remained in the same range as the sulfidation reference test even after being exposed to the 60 h challenge. Therefore it can be concluded that the amount of scale didn't change much during the TAN 2 challenge tests.

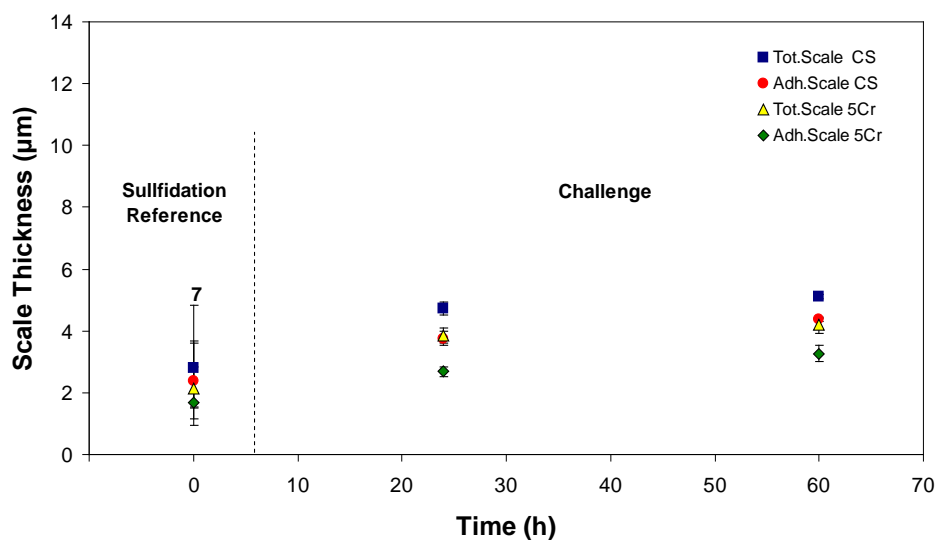


**Figure 24.** CS vs. 5Cr steel. Scale thickness comparison for 24 h and 60 h TAN 2 challenge tests. Graph includes total scale (loose) and adherent scale found at the end of the tests. Number 7 above the sulfidation reference represents the number of sulfidation test replicates. Points are average values while errors bars indicate the highest and lowest value obtained on multiple samples exposed in the same experiment.

All the results of these TAN 2 tests, the SEM pictures are included in Appendix C.

The number of moles of iron which were consumed (used) during corrosive processes was considered to have two parts: part of the iron reacted with sulfur compounds forming the iron sulfide scale while the other part was consumed in reacting with NAP forming iron naphthenates. These rates were calculated from metal weight loss using Equation 5 which was already presented in Chapter 5. Moles of FeS were calculated with Equation 6 for both total and adherent scales. The moles of Fe used follow the same trend as corrosion rates decreasing as experimental time increased. Similarly moles of FeS decreased with increasing the time, and the scale formation rate was higher for the 24 h test than for the 60 h test (see Appendix C).

An interesting view of challenging effects on FeS scales was provided by SEM analysis. The SEM surface analysis showed a scale that was layered and was reproducing almost as an imprint the irregular shape of the metal surface beneath it (see Figure 12). This raised the question whether the scale was formed on the metal surface from the “outside” by adding new layers (by “precipitation”) or generated from the metal surface and grew outward by some sort of a solid-state reaction. The SEM surface view of 5Cr surface after 60 h challenge test offered some interesting information about the FeS structure and formation mechanism. It can be seen in Figure 25 that the scale was fractured by a crack revealing its multi-layer structure. It is assumed that the crack was a consequence of stresses generated during the scale formation processes. Cracks generated on scale surface allowed the reactive species such as acids to penetrate closer to the metal surface and attack it. The cracks also allow the sulfur compounds to reach the metal

surface and corrode it, thereby generating more FeS. It appears that the scale regeneration was clearly possible even during the TAN 2 challenge tests due to the small amount of sulfur residues remaining in the rig from the sulfidation phase.

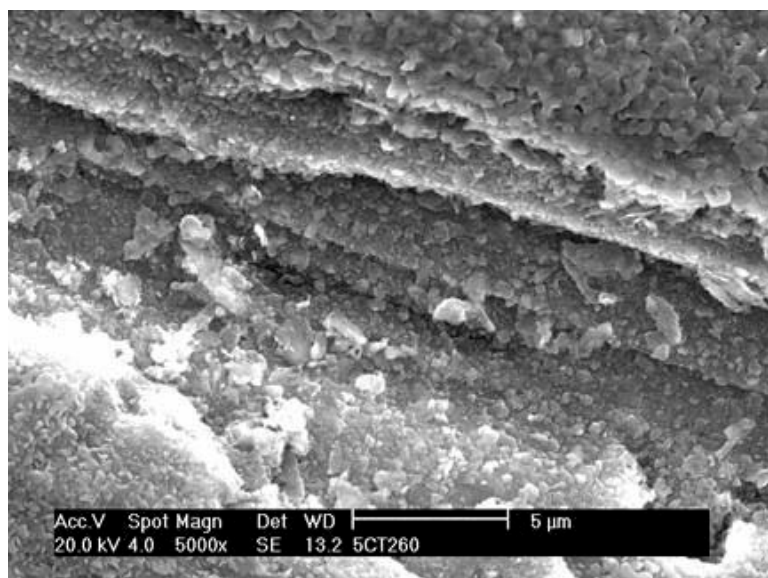


**Figure 25.** SEM surface analysis for FeS scale on the 5Cr specimens in TAN 2, 60 h challenge test. SEM picture reveals the consecutive layers of FeS scale that were formed during the test.

Energy Dispersive X-ray (EDX) analysis of the sample is shown in Figure 26 for a FeS scale that survived a 60 hr challenge with TAN 2.

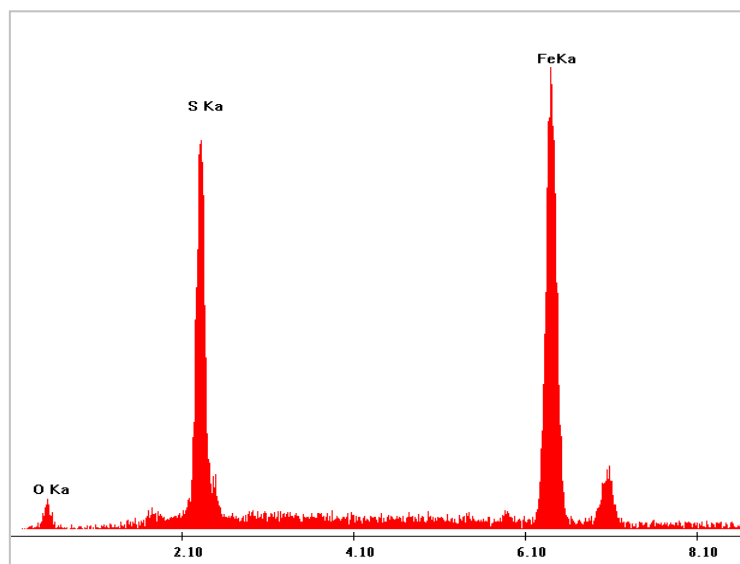


**Figure 26.** EDX analysis for FeS scale generated on 5Cr specimens that had been challenged with TAN 2 for 60 h. The high peaks correspond to iron and sulfur respectively which are the main components of FeS scale.

### 5.3.3 TAN 3.5 Results

Based on field experience, TAN 3.5 was considered rather high for challenging the FeS scale when compared to TAN 2 challenge results and more damage was expected. Figure 27 presents the corrosion rates for CS and 5Cr specimens in the TAN 3.5 time series. For the CS specimens corrosion rates decreased from 24 h to 60 h and stayed at a similar level even at 120 h proving that in long time experiments corrosion rates reached a constant level. The same tendency in decreasing corrosion rates towards a stable low level was noticed for 5Cr steel specimens as well. Corrosion rates for the 5Cr steel specimens had lower values than for corresponding CS specimens which revealed a better resistance of this alloy under identical testing conditions. However corrosion rates for both CS and 5Cr in all challenge tests were in the same range with corresponding corrosion rates of the sulfidation reference tests. These corrosion rates demonstrated that

the FeS scale was still generally effective in protecting the metal surface against naphthenic acid corrosive attack.

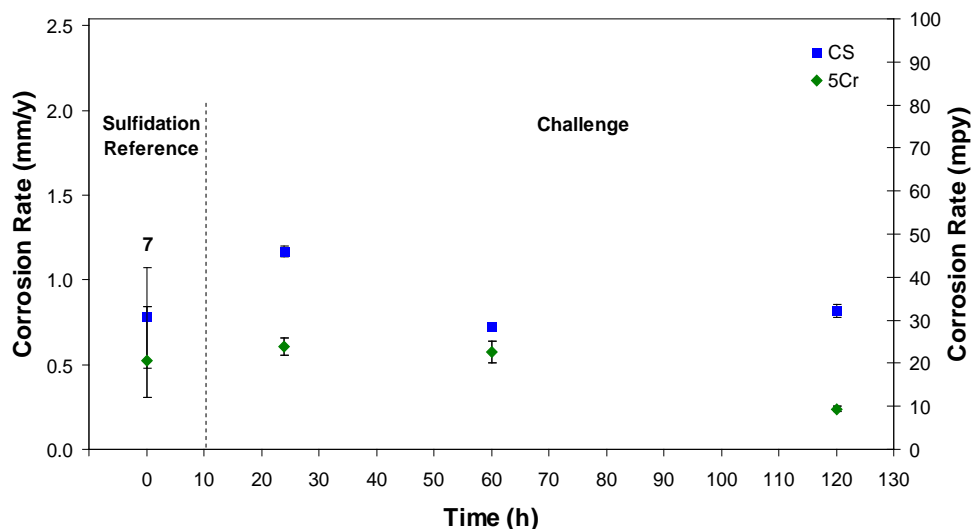


**Figure 27.** CS vs. 5Cr steel. Corrosion rates for 24, 60, and 120 h challenge tests using TAN 3.5 white oil. Number 7 above the error bars for sulfidation point represents the number of experiments that were averaged for calculating the respective value.

The thicknesses of the total and adherent scales are presented in Figure 28 for both CS and 5Cr steel. As Figure 28 shows there was a slight tendency in forming new FeS scale during the TAN 3.5 challenge tests. The sources for generating new scale were sulfur residues remaining in the system after the sulfidation phase of the test. In the case of the CS specimens, the scale growth was constant even in the 120 h tests. For 5Cr specimens the FeS scale had a different evolution. It was formed constantly in 24 and 60 h tests but decreased when experimental time was very long (120 h). However decreasing in scale thickness at 120 h exposure did not affect scale protectiveness (see Figure 27).

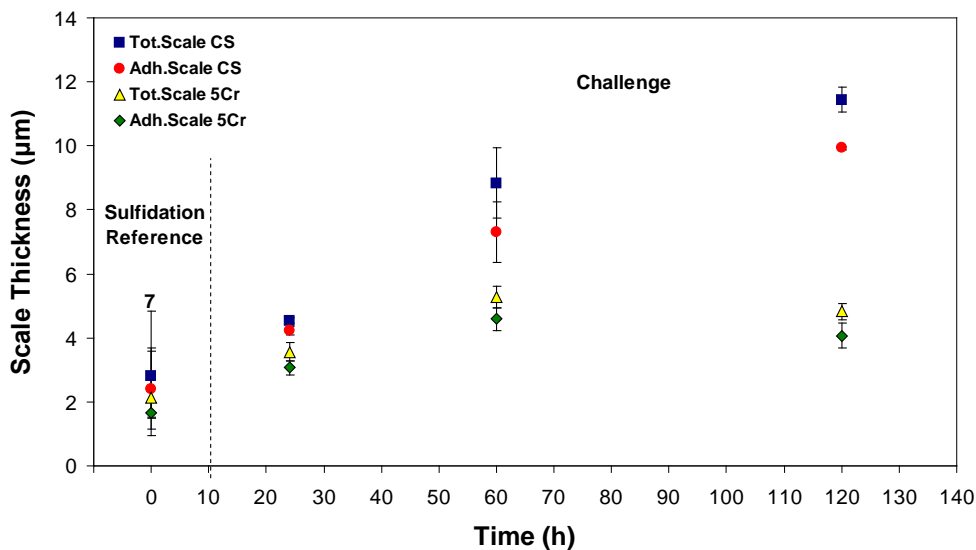
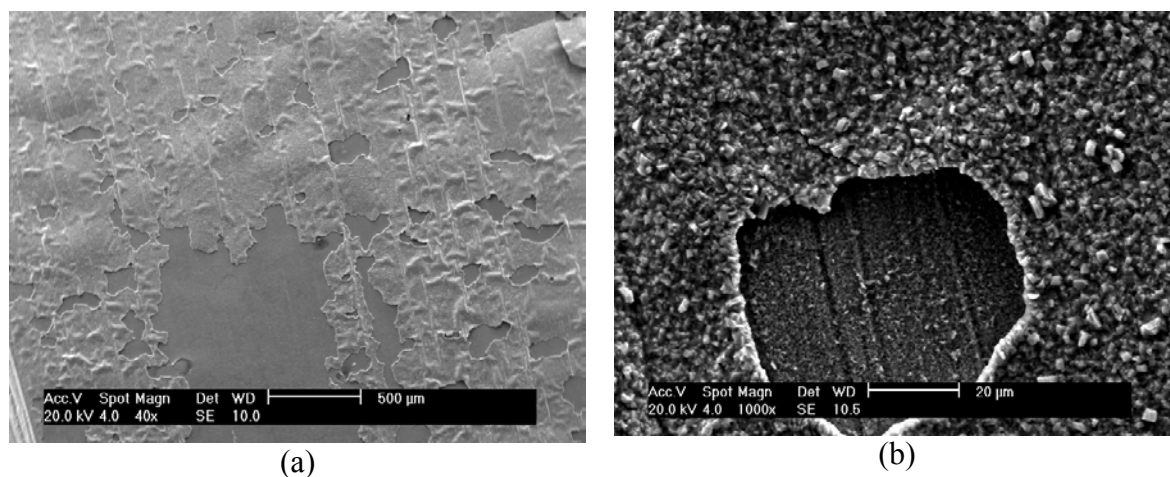


**Figure 28.** CS vs. 5Cr steel. Scale thickness comparison for 24, 60 and 120 h TAN 3.5 challenge tests. Graph includes total scale (loose) and adherent scale found at the end of the tests. Number 7 above the sulfidation reference represents the number of sulfidation test replicates. Points are average values while errors bars indicate the highest and lowest value obtained on multiple samples exposed in the same experiment.

Analysis of the moles of Fe consumed and FeS produced showed a similar evolution in the TAN 3.5 challenging tests as before. The rates of moles of “Fe used” decreased constantly with time, reaching lowest values for the 120 h test. Scale formation rates during challenge tests were almost equal to those formation rates evaluated for sulfidation and they correspond to the FeS scale measured at the end of each test.

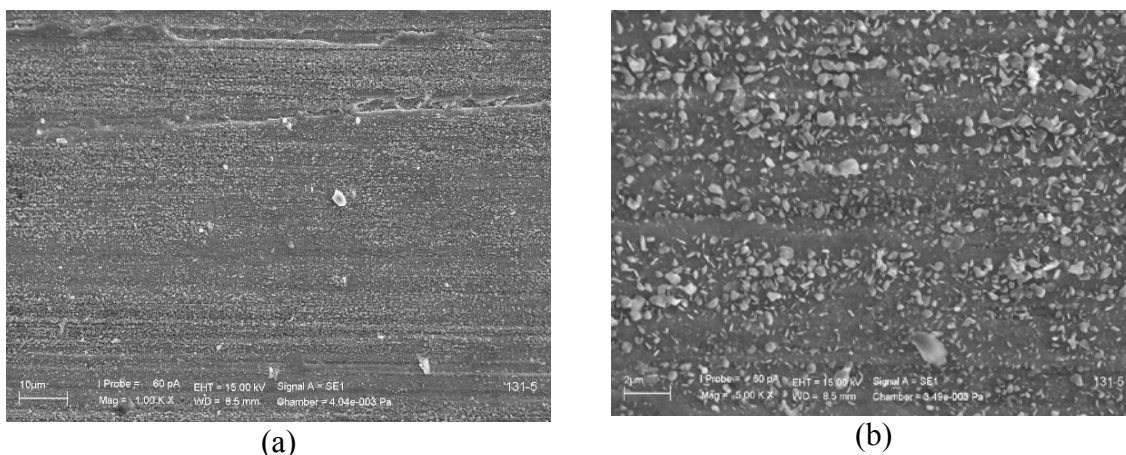
The SEM analysis of TAN 3.5 challenge tests offered extra details about the effect of NAP attack against the scales previously formed on the two metal surfaces. Thus on CS specimens FeS scale became loose and peeled off as a consequence of NAP attack. Figure 29 presents the scale surface that survived the 24 h challenge with TAN 3.5. The FeS scale was partially removed from the specimen (image *a*) but the enlarged

image *b* shows the FeS bottom layer that was adherent to the metal protecting it against acidic attack.



**Figure 29.** SEM surface analysis for scale formed on CS specimens after 24 h challenge with TAN 3.5. Top layer of FeS scale was partially removed (*a*) and bottom FeS layer can be observed through a hole in the top layer (*b*).

The scale formed on the 5Cr specimens that was challenged for 24 h with TAN 3.5 is presented in Figure 30. This FeS scale did not peel off as much as the scale on CS specimens but the acidic attack combined with flow effects removed some of the FeS crystals of the top scale layer. In spite of this worn aspect of the scale it still kept its protective qualities and the 5Cr steel which had a smaller corrosion rate than the CS specimens used in this test.



**Figure 30.** SEM surface analysis for 5Cr specimens after 24 hr challenge TAN 3.5 test. Significant cracks can be seen in image (a) for 1000X magnification whereas image (b) collected at 5000X magnification reveals torn edges for FeS crystals.

The TAN 3.5 challenge results showed that FeS scales formed on both types of steel and offered good protection against challenging naphthenic acids even for long exposure times. As a consequence further tests were done using TAN 5 oils.

### 5.3.4 TAN 5 Results

The TAN 5 is considered a rather high value and therefore time series tests started with short challenges time (6 and 12 h) and continued with 24 and 50 h tests. All other test parameters during this time series were identical to the previous tests. The CS corrosion rates for the TAN 5 challenge series are presented in Figure 31 and, as it can be noticed, a significant increase of corrosion rate was obtained for the 6 h challenge test, a value almost double that of the sulfidation reference test. For both 12 and 24 h challenge tests the corrosion rates were constant and almost equal to that of the 6 hr test. To increase the NAP attack effects against protective scales the challenge time was doubled for the next test. The corrosion rate obtained in the 50 h test was higher than in the

previous shorter TAN 5 tests and this challenge were considered to be high and long enough to compromise the FeS scale protection.

The 5Cr specimens displayed a different behavior during the TAN 5 test series compared to the CS specimens, as it is shown in same Figure 31. The corrosion rate for the 6 h challenge test was high and almost identical to the corresponding value for CS steel. The 5Cr corrosion rates in the longer TAN 5 challenge tests (12, 24, and 50 h) decreased constantly reaching the lowest value for the 50 h challenge. Comparison and analysis of the CR results for the steel types illustrated that 5Cr showed a better resistance against the TAN 5 challenge compared to CS.

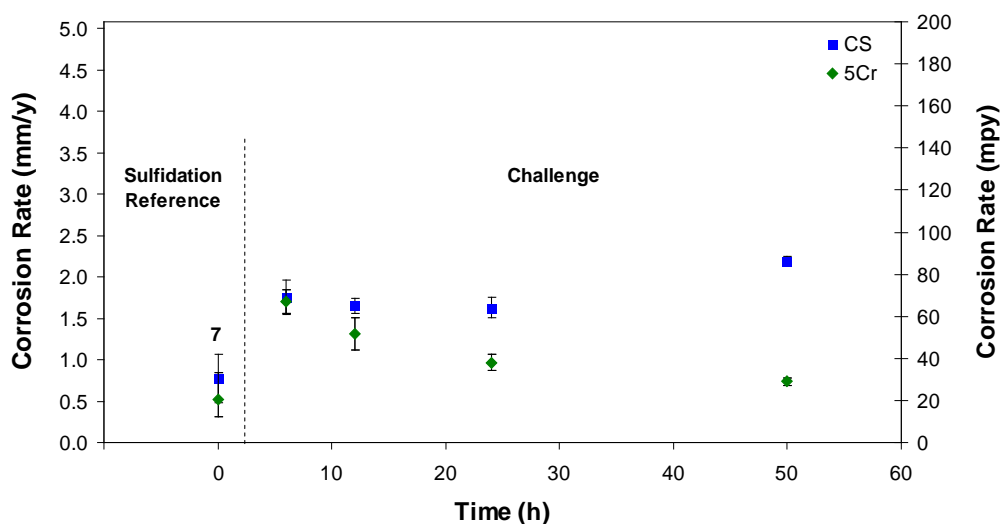


**Figure 31.** CS vs. 5Cr steel. Corrosion rates for 6, 12, 24, and 50 h challenge tests using TAN 5 white oil. Number 7 above the error bars for sulfidation point represents the number of experiments that were averaged for calculating the respective value. Points are average values while errors bars indicate the highest and lowest value obtained on multiple samples exposed in the same experiment.

The FeS scale offered some limited protection for CS and protected the 5Cr steel very well. However, as it is shown in Figure 32, the FeS scale thickness increased as

experimental time increased during the TAN 5 challenge tests and it even continued to grow during the 50 h challenge test. Similarly to previous challenge series, sulfur residues from the sulfidation phase were causing scale formation on both metal types during the challenging phases. Corrosion and scale formation rates were analyzed in terms of moles and the corresponding figure was included in Appendix C.

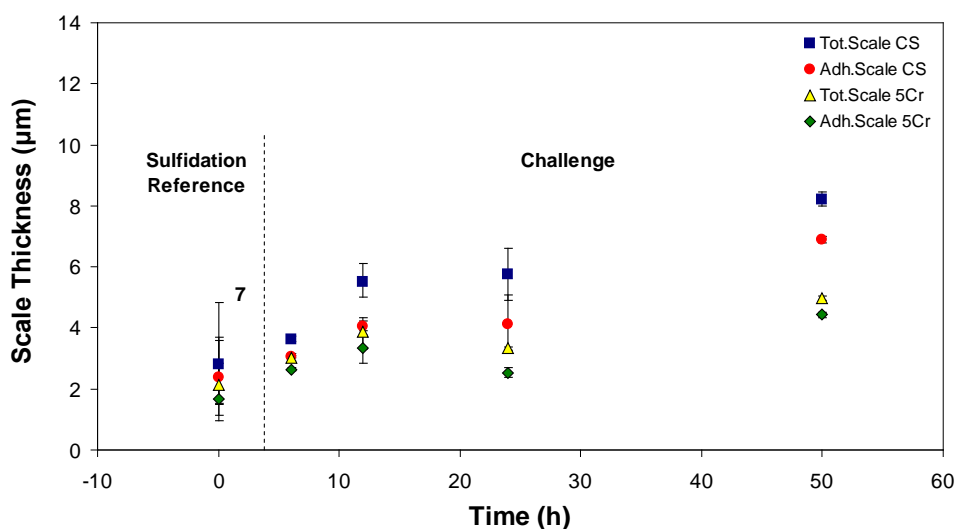


**Figure 32.** CS vs. 5Cr steel. Scale thickness comparison for 6, 12, 24, and 50 h TAN 5 challenge tests. Graph includes total scale (loose) and adherent scale found at the end of the tests. Number 7 above the sulfidation reference represents the number of sulfidation test replicates. Points are average values while errors bars indicate the highest and lowest value obtained on multiple samples exposed in the same experiment.

The SEM and EDX analysis were done only for the 24 hr challenge test. The SEM surface analysis showed a scale consisting of FeS crystals that were considerably affected by the high TAN challenge. Also under the acidic attack, the scale became looser and much of it spalled off exposing the FeS layer underneath (Figure 33).

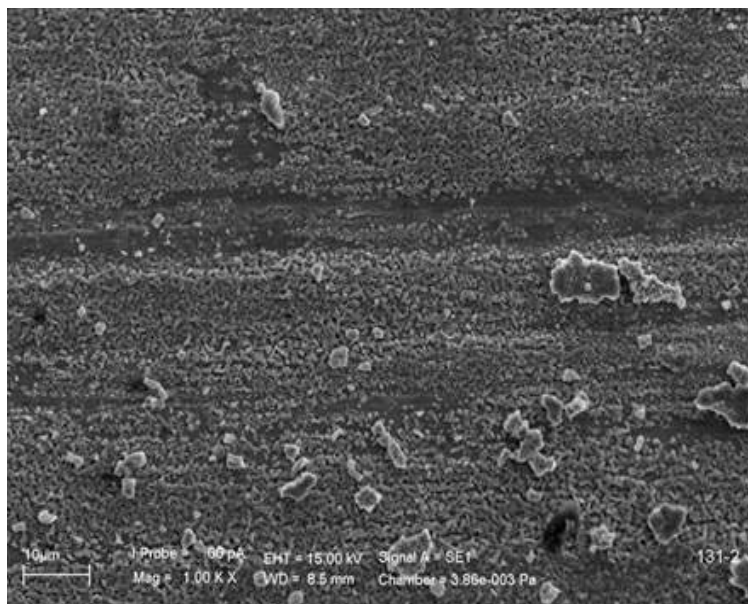


**Figure 33.** SEM surface analysis for CS specimens after 24 h challenge TAN 5 test. FeS crystals have torn and rounded edges and large parts of scale peeled off leaving only fragments from the superficial layer.

The SEM cross-section analysis for CS specimens after 24 h test showed a very irregular, fragmented structure of the scale. It is believed that this porous structure of the scale allowed the transport of reactive species towards the metal surface thus maintaining the corrosion process as well as the scale formation. The EDX analysis of the cross-section of same scale (Figure 34) shows the elemental distribution along the scale. Sulfur and iron are of main interest, being the two main constituents of the scale. As it can be observed, as sulfur concentration increases (“S” line peak), iron concentration decreases (“Fe” line). Silica was introduced during the polishing procedure, carbon was contained in the epoxy and oxygen might correspond to an oxide layer formed on the metal before FeS was formed. The metal under the scale has a very irregular shape with pits created by the acidic attack.

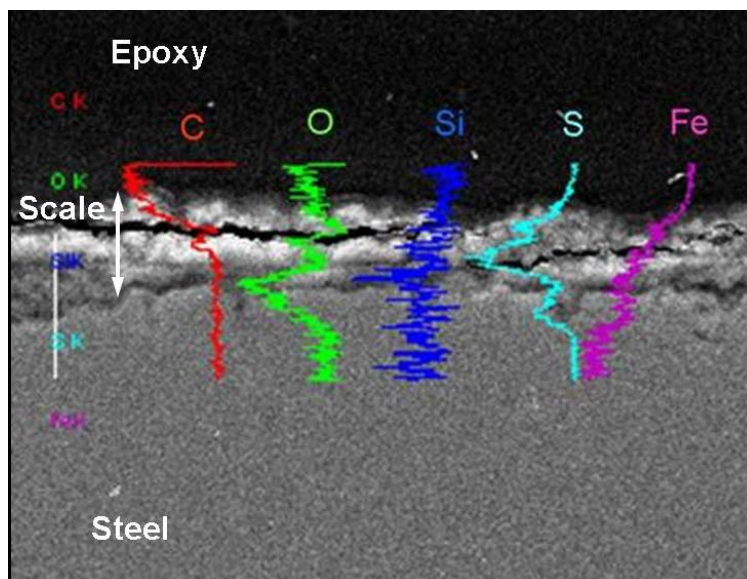


**Figure 34.** EDX analysis along cross-section of the FeS scale on CS specimens after 24 hr challenge TAN 5 test. The analysis compares concentrations of main chemical elements along the cross-section of the FeS layers.

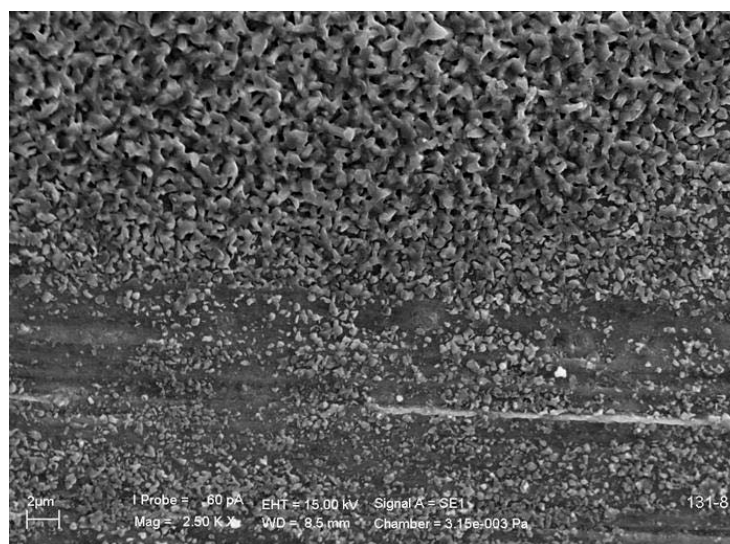


**Figure 35.** SEM surface analysis for 5Cr specimens after 24 h challenge TAN 5 test. FeS crystals have torn and rounded edges and the scale surface has regions where crystals have been removed.

In the case of the 5Cr samples surface analysis using SEM showed a scale consisting of damaged FeS crystals and regions where layers were removed completely (Figure 35).

In spite of this worn aspect of the scale, the corresponding corrosion rates for 5Cr showed that FeS offered a better protection to the metal compared to scale formed on CS.

The SEM cross-section analysis of the FeS scale on the 5Cr specimens presented a very irregular structure (Figure 36) that was confirmed by the EDX analysis included in the SEM image. According to the EDX analysis, the scale was formed from sulfur (“S” line), chromium (“Cr” line), and iron (“Fe” line). As it was already mentioned, Si was introduced during polishing and C corresponds to the epoxy mounting. Although the scale on the 5Cr specimens had a grainy porous structure it offered a better protection compared to CS specimens where deeper attacks could be observed on the metal surfaces.

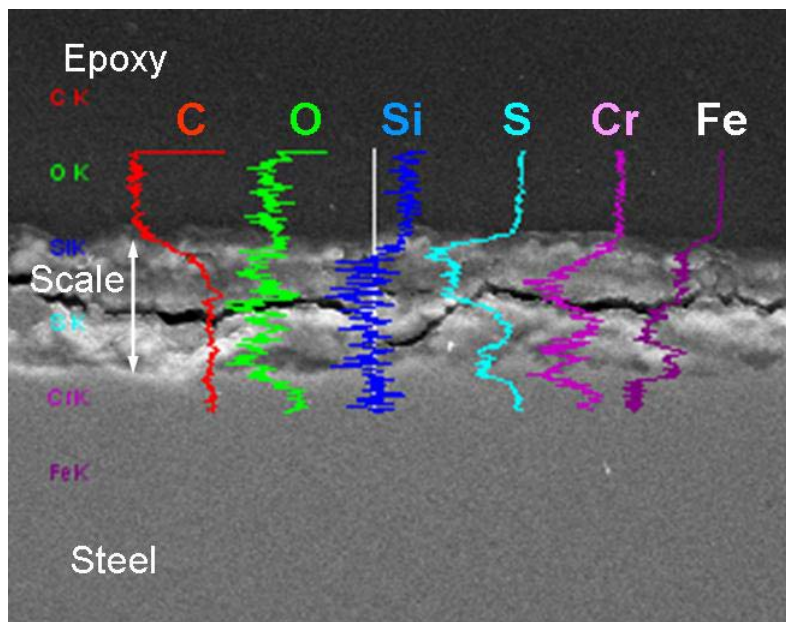


**Figure 36.** EDX analysis for cross-section through FeS scale on 5Cr specimens after 24 h challenge TAN 5 test. Sulfur has two distinct peaks suggesting a multiple layer structure for the scale.

### 5.3.5 TAN 6.5 Results

The TAN 5 was apparently a strong enough challenge for the CS specimens where the FeS scale protection was overpowered and corrosion rates were high especially in long experiments. However the 5Cr steel showed a good resistance to the TAN 5 challenge even when the challenge time was extended to 50 h. Therefore in order to test the protectiveness of the FeS scale, the NAP concentration was increased to TAN 6.5 with two different testing times: 24 h and 50 h. Corresponding corrosion rates for the two types of steel exposed to the TAN 6.5 challenges are presented in Figure 37.

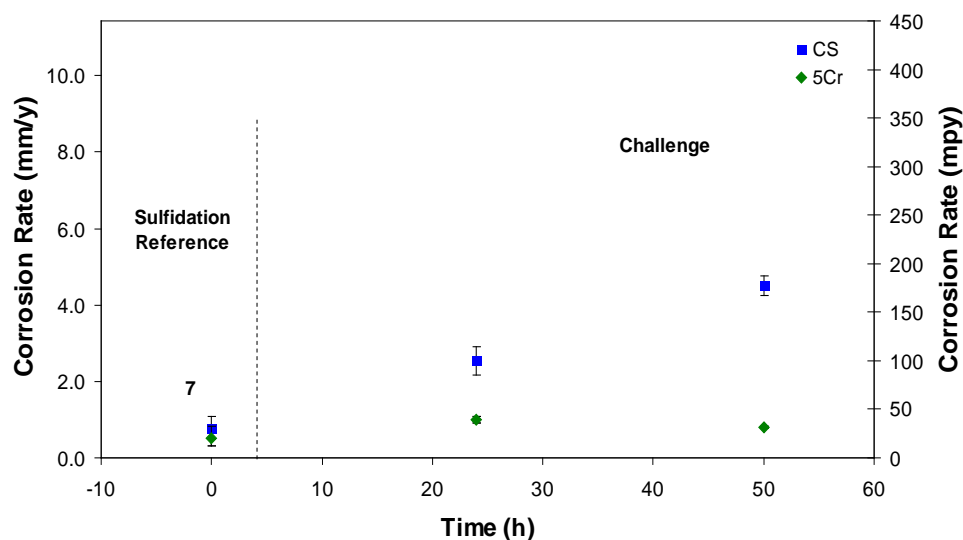


**Figure 37.** Corrosion rates for CS and 5Cr in 24hr and 50hr challenge tests using TAN 6.5. Number 7 above the error bars for sulfidation point represents the number of experiments that were averaged for calculating the respective reference value. Points are average values while errors bars indicate the highest and lowest value obtained on multiple samples exposed in the same experiment.

As Figure 37 shows the corrosion rates for the CS specimens were much higher during the challenge test than those corrosion rates calculated for 5Cr steel. The CS corrosion rate value in the 24 h test was almost double than that of the reference

sulfidation test, proving that the FeS scale lost the protective effect on the CS surface. The 50 h challenge results were more proof that the FeS scale on the CS had a poor resistance against the high TAN attack. The 5Cr steel had a better resistance to the high NAP attack compared to the CS. Corrosion rates for 5Cr increase slightly in the 24 h challenge test remaining constant after 50 h exposure to TAN 6.5 (Figure 37). Similar to previous TAN series, the scale on the 5Cr steel “won” the battle against corrosion again. Therefore the TAN value that was used in further tests was TAN 8, and the results will be discussed in the following subsection chapter.

The scale thickness values for the two steel were plotted on the same graph presented in Figure 38.

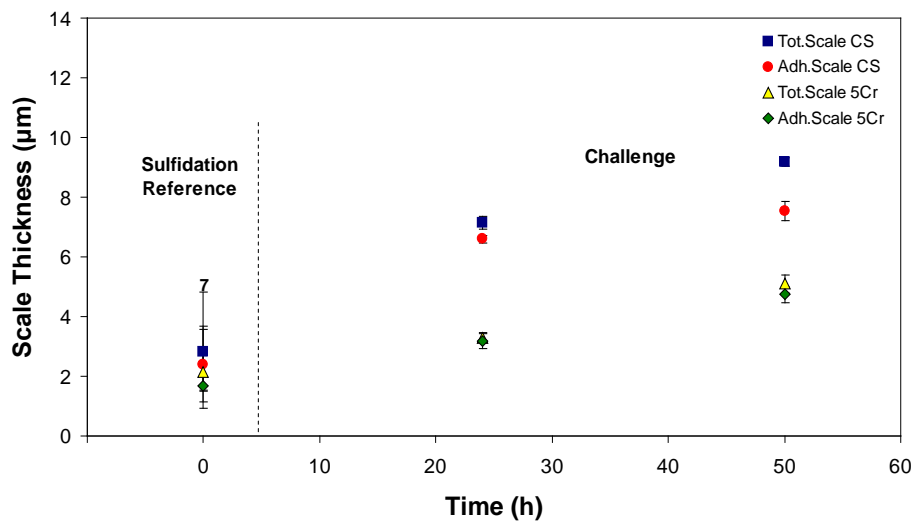


**Figure 38.** CS vs. 5Cr steel. Scale thickness comparison for 24 and 50 h TAN 6.5 challenge tests. Graph includes total scale (loose) and adherent scale found at the end of the tests. Number 7 above the sulfidation reference represents the number of sulfidation test replicates. Points are average values while errors bars indicate the highest and lowest value obtained on multiple samples exposed in the same experiment.

In spite of the high acidity, sulfur residues were still able to generate more FeS scale on both metals after sulfidation as the above figure shows. However the ratio of new FeS scale generated on CS was higher (thick scale) than on 5Cr where only small quantities of scale were measured at the end of the tests. Thinner FeS scale on 5Cr specimens was more adherent and protective and might explain 5Cr lower corrosion rates compared to CS. For both CS and 5Cr, a mole analysis was done and the graphs are included in Appendix C.

The SEM and EDX analysis were done only for the 24 h challenge test and they provided new evidence in favor of the aggressive attack of high TAN acids on the FeS scale which resulting in high corrosion rates (Figure 39).

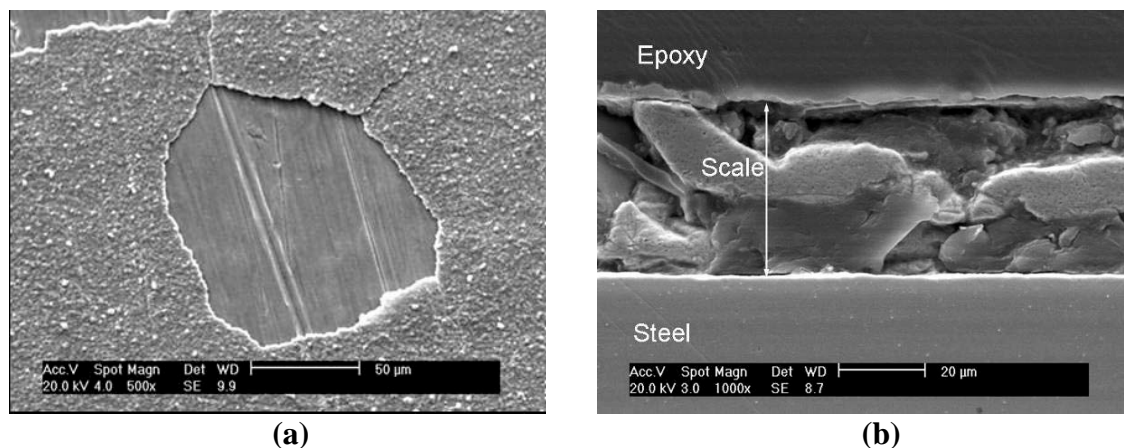


**Figure 39.** (a) SEM surface analysis for CS specimens after 24 h challenge TAN 6.5 test. FeS crystals have torn and rounded edges and large parts of scale peeled off from metal surface. (b) Cross-section through FeS scale on CS specimens after 24 h challenge TAN 6.5 test. FeS scale presents large empty spaces between scale fragments (high porosity).

The SEM surface analysis for CS showed a scale consisting of FeS crystals that were considerably damaged by the high TAN challenge. Under acidic attack, the scale became

loose and part of it spalled off exposing the underlying FeS (Figure 39 - *a*). The SEM cross-section analysis for the CS specimens after the 24 h test showed not only a very irregular structure for the scale but also some large fragments of separated scale. (Figure 39 - *b*) This porous structure of the scale allowed the transport of reactive species towards the metal thus increasing the corrosion rate and scale formation. The EDX analysis of the FeS scales is included in Appendix B and reveals the scale composition and elemental distribution across it.

The SEM analysis for the 5Cr specimens exposed to the 24 h challenge with TAN 6.5 provided very similar results to those of the CS (see Figure 40). The combined effect of flow velocity and high naphthenic attack removed some of the FeS scale from the 5Cr specimens as seen in Figure 40-*a*. The same aggressive testing conditions even affected the “inner” structure of the scale fragmenting it and leaving voids where the corrosive fluid could reach the metal surface (Figure 40-*b*). In spite of these observations, the FeS scale on the 5Cr steel was still able to resist corrosive attack better than CS under similar testing conditions. It should be noted that by looking at the SEM images alone, one would get the false impression about the actual situation of the scale protectiveness as function of its structure.

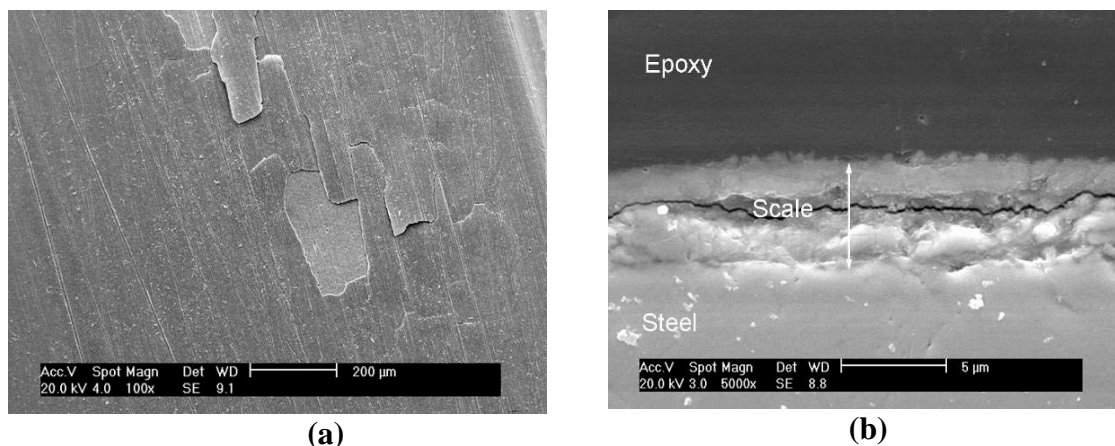


**Figure 40.** (a) SEM surface analysis for 5Cr specimens after 24 h challenge TAN 6.5 test. SEM surface image shows large parts of scale peeled off from metal surface. (b) Cross-section through FeS scale on 5Cr specimens after 24 h challenge TAN 6.5 test. FeS scale presents large empty spaces between scale fragments (high porosity).

### 5.3.6 TAN 8 Results

TAN 8 was the last and highest TAN concentration used in the sulfidation–challenge tests. Considering the high acidity of TAN 8 as well as the previous test results, it was decided to run only short time experiments ranging from 6 to 24 h. The 6 h and 12 h tests were relatively short time tests for challenging the FeS scales. However, corrosion rates of these two tests shown in Figure 41 proved that TAN 8 was very aggressive and both metals (CS and 5Cr) had much higher corrosion rates than in the reference sulfidation tests. The CS corrosion rates remained constant after the 6 and 12 h challenges, but the 5Cr steel showed a decrease of CR in the 12 h test. When the challenge time was doubled in the 24 h test, the CS corrosion rate increased sharply whereas for the 5Cr steel the corrosion rate was constant and similar to the 12 h test value. Again 5Cr steel had the best resistance to NAP attack as compared to CS.

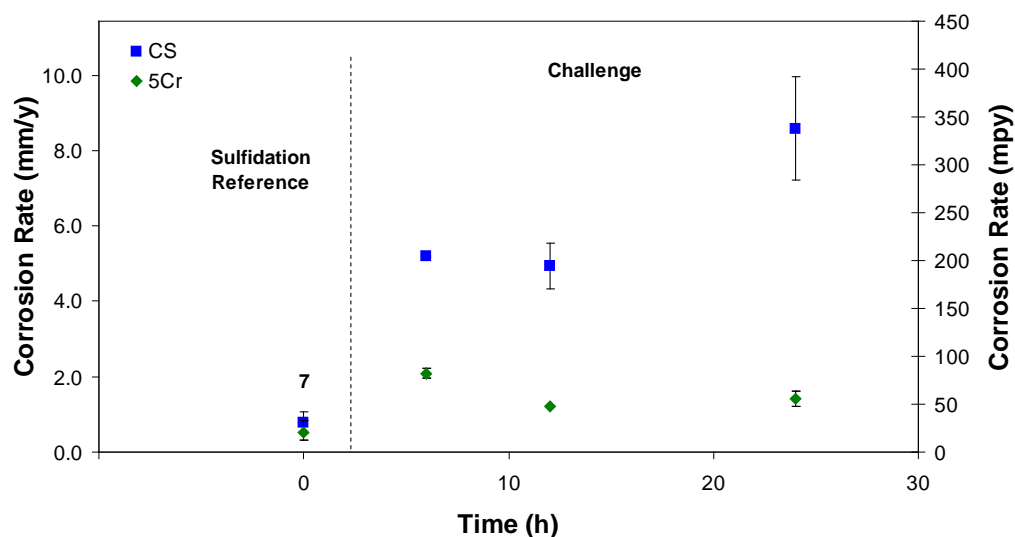


**Figure 41.** Corrosion rates for CS and 5Cr in 6, 12, and 24h challenge tests using TAN 8. Number 7 above the error bars for sulfidation point represents the number of experiments that were averaged for calculating the respective reference value. Points are average values while errors bars indicate the highest and lowest value obtained on multiple samples exposed in the same experiment.

The scale thickness plot (Figure 42) showed that the scale continued to grow in the TAN 8 challenge tests, the scale growing source being sulfur residues remaining in the system from sulfidation. More scale was formed on both types of specimens (CS vs. 5Cr) as Figure 42 presents but the scale formation rate was much lower for 5Cr steel than for CS.

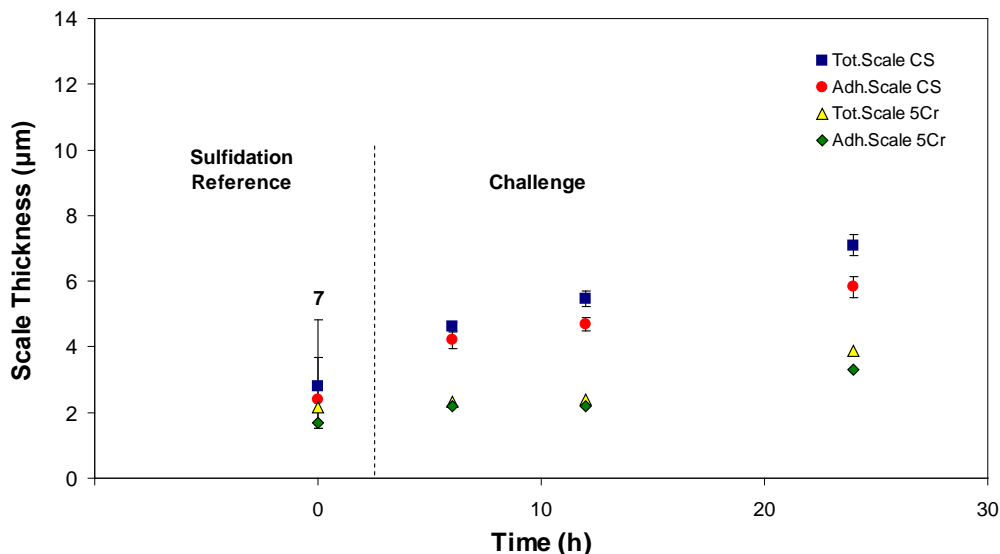


**Figure 42.** CS vs. 5Cr steel. Scale thickness comparison for 6, 12, and 24 h TAN 8 challenge tests. Graph includes total scale (loose) and adherent scale found at the end of the tests. Number 7 above the sulfidation reference represents the number of sulfidation test replicates. Points are average values while errors bars indicate the highest and lowest value obtained on multiple samples exposed in the same experiment.

Corrosion rates and FeS scale were also analyzed in terms of mole formation rates as in each of the previous TAN series. These moles analyses are included in Appendix C for both steel types.

The SEM surface analysis for the scales formed on CS revealed similar surface characteristics in every test (6, 12, and 24h). Thus the scale had a surface consisting of crystals with rounded edges with large, deep cracks. Only the SEM surface image for 24 hr test is presented below. (Figure 43) Others can be found in Appendix C. The SEM cross-section of the FeS scale formed on CS specimens shows a fragmented structure as a consequence of TAN 8 acidic attack (Figure 44). In addition the EDX analysis included in the same SEM image shows the distribution of main components along the scale cross-section. The scale layers were separated during the curing process of the sample. In spite

of this artifact, the EDX analysis reveals the sulfur and iron presence in both separated layers.

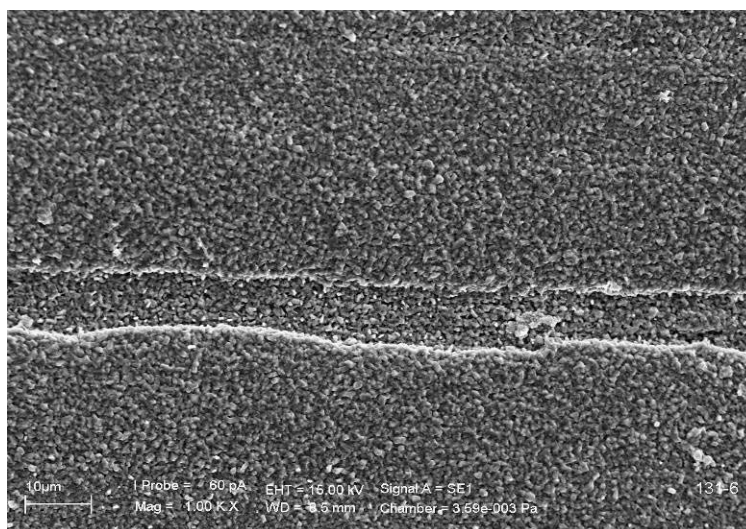


**Figure 43.** SEM surface analysis for CS specimens after 24 h challenge TAN 8 test. FeS crystals have torn rounded edges and large cracks in the scale revealed its multiple layer structure.

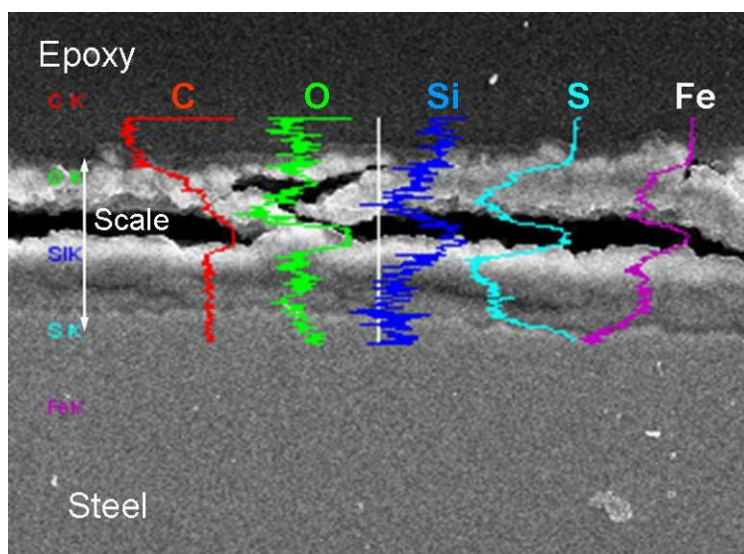


**Figure 44.** SEM cross-section for FeS scale formed CS specimens after 24 h challenge TAN 8 test. SEM analysis shows distribution of main scale components across the FeS scale.

Similar to the FeS scale formed on the CS, the scale surface on the 5Cr specimens had cracks and crystals with a worn look, with rounded corners and edges, as shown in Figure 45.

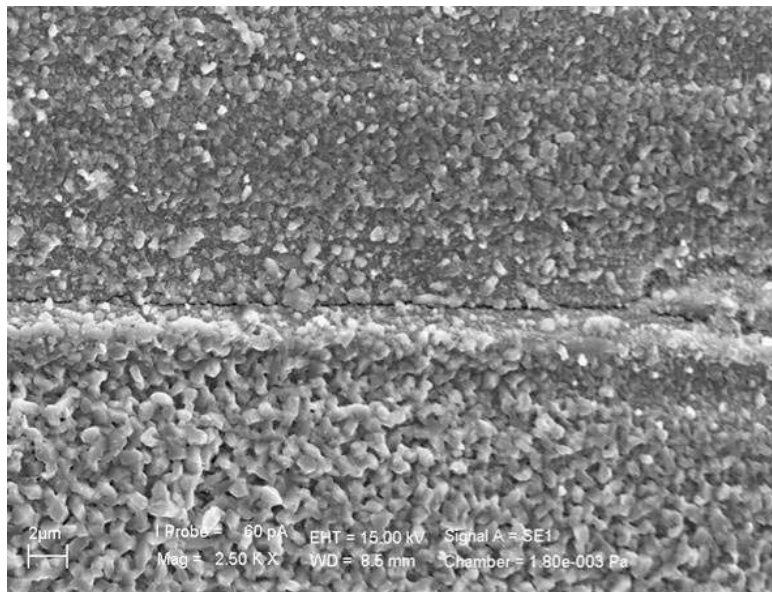


**Figure 45.** SEM surface analysis for 5Cr specimens after 24 h challenge TAN 8 test. FeS crystals have torn rounded edges and large cracks in the scale revealed its multiple layer structure.

The 5Cr corrosion rates were lower than the CS corrosion rates during 24 h challenge test of TAN 8. However the FeS scale formed on 5Cr had a similar fragmented appearance as is shown in the SEM cross-section image (Figure 46). The EDX analysis presented in same Figure 46 shows the components of the FeS scale on 5Cr steel, indicating that this scale had different composition than the scale formed on CS. Calcium and silica as well were introduced during the polishing procedure of the epoxy embedded sample before the SEM analysis.

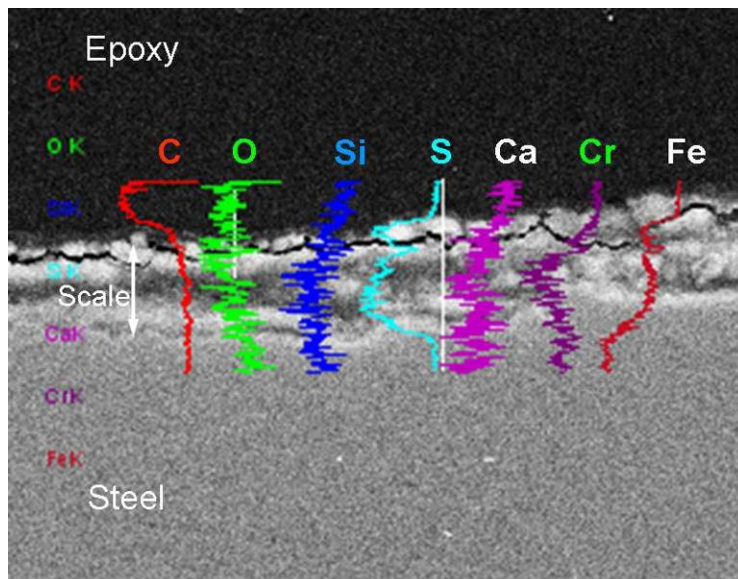


**Figure 46.** Cross-section through FeS scale on 5Cr specimens after 24 h challenge TAN 8 test. Picture shows a grainy characteristic structure of FeS scale. The EDX analysis was run across the white line and shows main components detected in that region of the FeS scale.

### 5.3.7 Comparison of 24 hr Test Results

The 24 h challenge test was common for every TAN series described previously. Therefore these 24 h test data were used for presenting a different perspective of sulfidation – challenge tests: corrosion rate as a function of different TAN's (0.1 - 8)

Comparison of the corrosion rates of CS vs. 5Cr is presented in Figure 47. The CS corrosion rates increased slowly from TAN 2 to TAN 5. The corrosion rate of the TAN 6.5 challenge is almost double than the TAN 5 and the corrosion of CS becomes very high in the TAN 8 challenge test proving that FeS scale protection for CS failed completely. The 5Cr steel presented a very good resistance against NAP attack which was different from the CS results. Thus the 5Cr corrosion rates increased slowly, reached a plateau for TAN 5 and 6.5 and then slightly increased for the TAN 8 challenge.

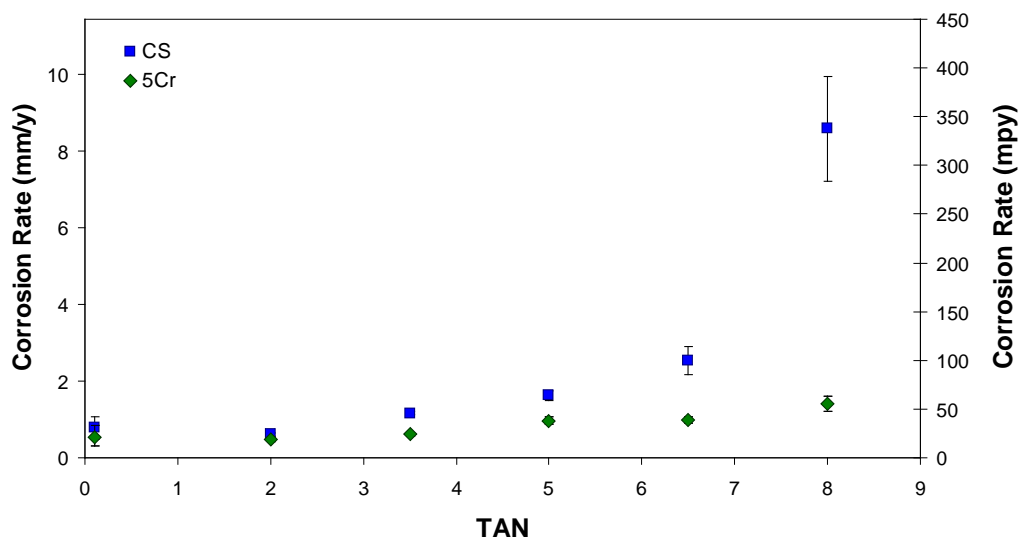


**Figure 47.** Comparison for corrosion rates of CS and 5Cr specimens in 24 h challenge tests with different NAP concentrations (TAN 2 to TAN 8). Points are average values while errors bars indicate the highest and lowest value obtained on multiple samples exposed in the same experiment.

The FeS scale formed on the CS specimens in all 24 h tests as summarized in Figure 48, where both total and adherent scale thicknesses were plotted. For TAN 2, 3.5 and 5 test the amount of scale was formed almost constant and corresponding corrosion rates for these tests showed only a slight increase. Therefore it can be said that scale preserved its protective properties during the tests. However, when the challenging TAN was increased to 6.5 and 8 although more scale was produced, it was of lesser quality and the corresponding corrosion rates increase significantly.

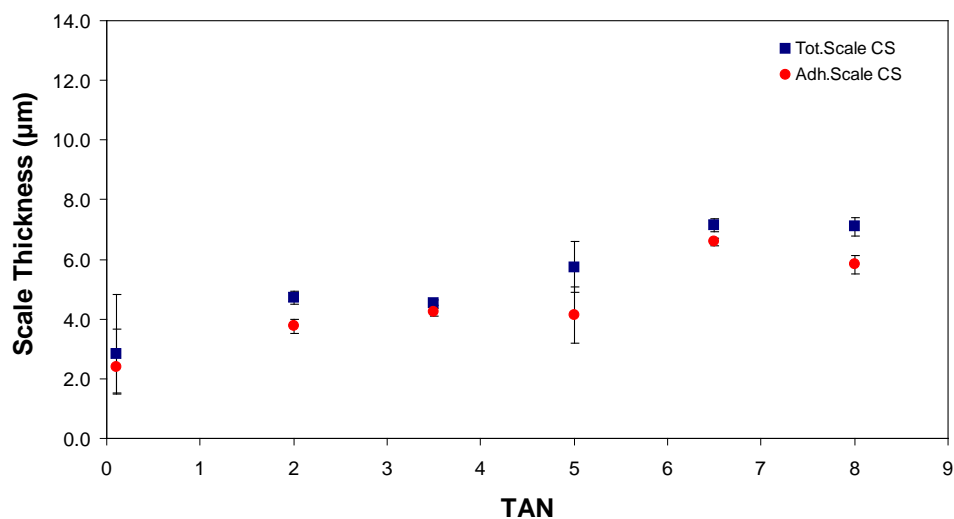


**Figure 48.** Total and adherent scale thickness formed on CS specimens during 24 h challenge tests with different NAP concentrations (TAN 2 to TAN 8). Points are average values while errors bars indicate the highest and lowest value obtained on multiple samples exposed in the same experiment.

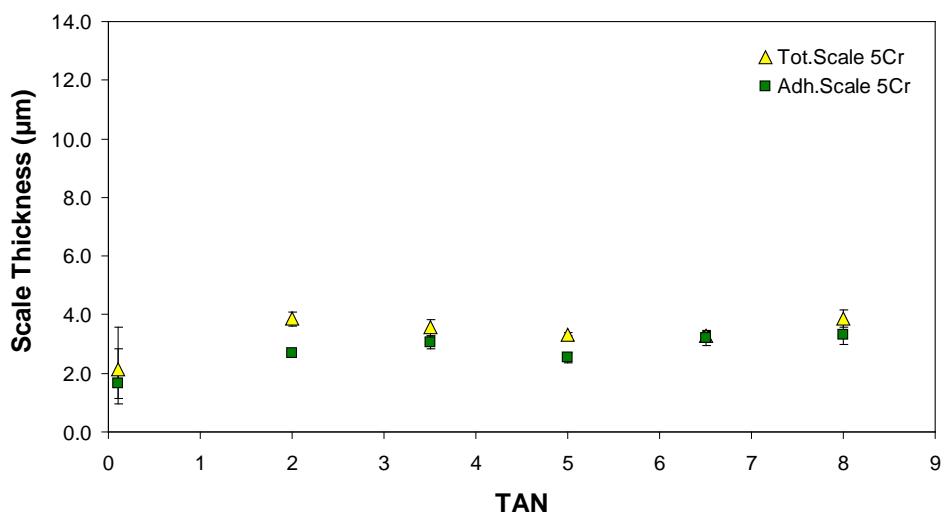


**Figure 49.** Total and adherent scale thickness formed on 5Cr specimens during 24 h challenge tests with different NAP concentrations (TAN 2 to TAN 8). Points are average values while errors bars indicate the highest and lowest value obtained on multiple samples exposed in the same experiment.

The FeS scale formed on the 5Cr specimens had almost a constant thickness in every 24 hr test as shown in Figure 49. If these scale thicknesses are compared to their

corresponding test corrosion rates it becomes clear how protective the scales were for the 5Cr against NAP corrosive effects.

### ***5.3.8 Low Velocity Experiment Results***

Shear stress is one of the factors that influenced corrosion rate as well as scale formation under high velocity and continuous flow testing conditions. Typically, the experimental conditions in the HVR were set so that the specimens were rotated with 2000 rpm and fluid was constantly circulated through the rig at 7ccm (cubic centimeters/minute) In order to verify how shear stress created by rotating of the specimens could influence corrosion rates, it was decided to do an experiment with little rotation. It was not possible to entirely stop the rotation of the specimens during the tests due to limitations of the equipment and the controllers. Therefore a very low rotation speed was selected (500 rpm) in order to meet the goals of this special test. The test consisted of the usual specimens sulfidation phase, followed by a 24 h challenge with TAN 5. The sulfidation part of this test was done under 2000 rpm rotation the same as the other reference sulfidation tests, whereas the challenge part was done at 500 rpm (low velocity conditions).

The low velocity test results showed that the corrosion rate for CS at 500 rpm was very close to that rate corresponding to 2000 rpm test and in the same range with previous TAN 5 tests (Figure 50). Therefore it was concluded that for CS the shear stress did not play an important role in the scale challenge processes.

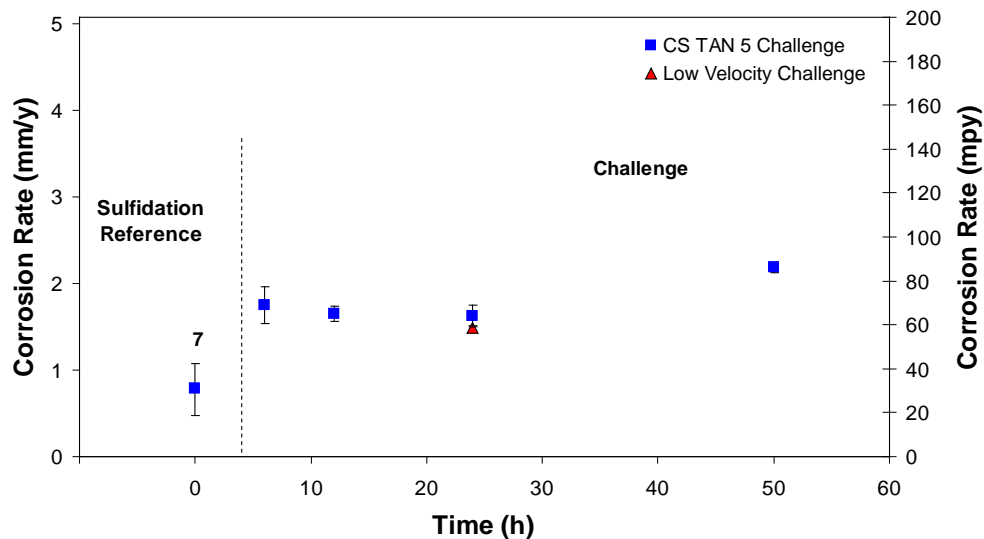


**Figure 50.** Comparison of corrosion rates on CS under different rotation conditions. Lower point represents the corrosion rate corresponding to low velocity test (500 rpm). Points are average values while errors bars indicate the highest and lowest value obtained on multiple samples exposed in the same experiment. Number 7 above the sulfidation reference represents the number of sulfidation test replicates.

A similar trend to CS was found for 5Cr specimens (Figure 51), low velocity (500 rpm) corrosion results being very close to those produced in a test where rotating speed was much higher (2000 rpm).

The scale thickness values in the low velocity test were almost the same with the values of high velocity tests both for CS and for 5Cr specimens and their corresponding plots are included in Appendix C.

All of these results suggested that the rotation velocity does not significantly influence the corrosion and scale formation processes during sulfidation – challenge tests.

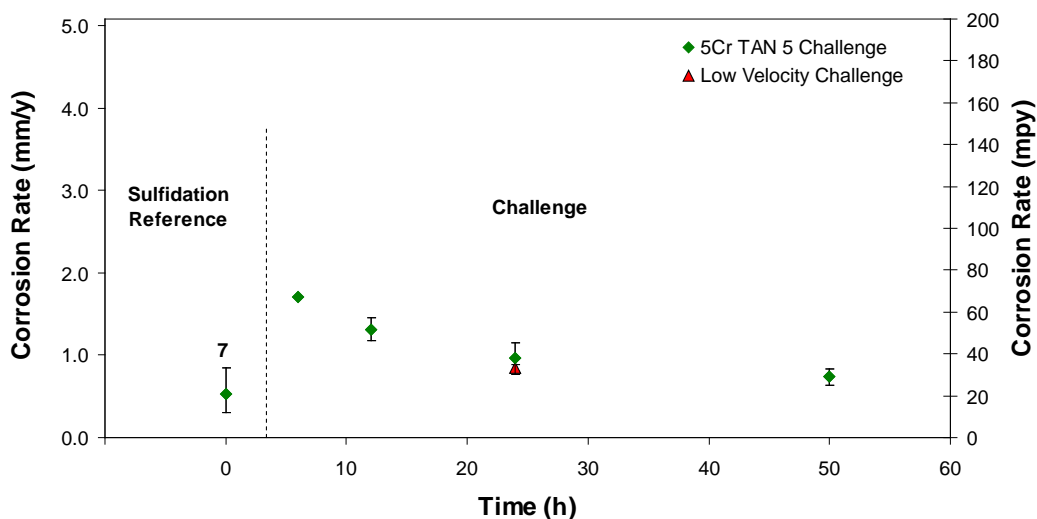


**Figure 51.** Comparison of corrosion rates on 5Cr under different rotation conditions. Lower point represents the corrosion rate corresponding to low velocity test (500 rpm). Points are average values while errors bars indicate the highest and lowest value obtained on multiple samples exposed in the same experiment. Number 7 above the sulfidation reference represents the number of sulfidation test replicates.

### 5.3.9 Sulfidation at Lower Temperature - 287°C (550°F)

All FeS scales discussed previously were formed and challenged at 343°C (650°F). The scales were able to preserve their protective properties to some extent for CS and almost over the whole TAN range for 5Cr steel. This temperature was selected because it was said to be favorable to give the highest “yield” of NAP corrosion and sulfidation reactions, according to anecdotal field experience. The temperature influence on FeS protective properties was investigated in one experiment during the sulfidation-challenge test series. It was decided to form the FeS scale at a lower temperature - 287°C (550°F) during sulfidation part and then to challenge the preformed scale under one of the previously used conditions - with TAN 3.5 for 24 h at 343°C (650°F). In order to calculate accurately the corrosion and scale formation rates for the “287°C scale”, a special sulfidation reference test was also done at 287°C (550°F). The new results were

compared to complete the TAN 3.5 sulfidation-challenge set. The CS corrosion rate of specimens presulfidized at 287°C and then challenged at 343°C were significantly lower than those where specimens presulfidized at 343°C, as shown in Figure 52. The same trend of corrosion rates was noticed for the 5Cr steel specimens that were presulfidized at 287°C and then challenged with TAN 3.5 (Figure 53) at 343°C.

The final conclusion regarding this test was that the temperature has a significant importance on scale properties with somewhat lower temperatures increasing its protectiveness against corrosive attack. However this newly formed scale was only challenged with TAN 3.5 which is a low value. It is believed that a higher TAN challenge would overcome scale protectiveness leading to high corrosion rates.

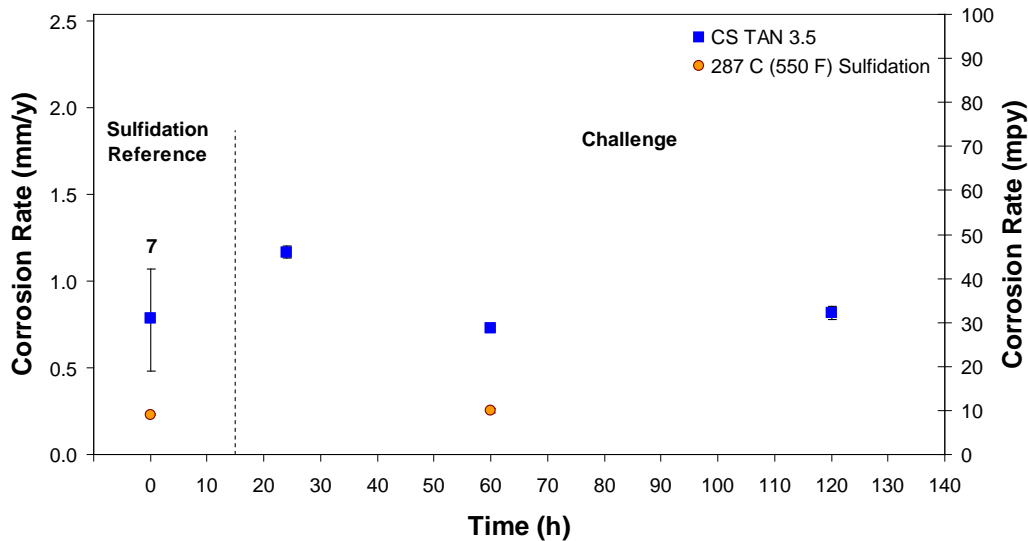


**Figure 52.** Comparison of corrosion rates for CS specimens presulfidized at 650°F with corrosion rates for CS specimens presulfidized at (287°C) 550°F – lower points. Points are average values while errors bars indicate the highest and lowest value obtained on multiple samples exposed in the same experiment.

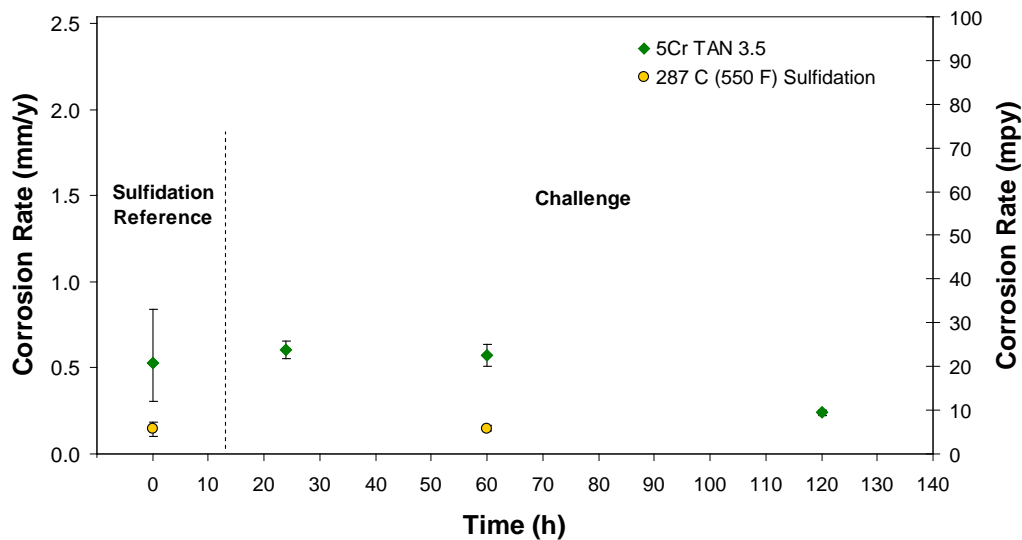


**Figure 53.** Comparison of corrosion rates for 5Cr specimens presulfided at 343°C (650°F) with corrosion rates for 5Cr specimens presulfided at 287°C (550°F) – lower points. Number 7 above the sulfidation reference represents the number of sulfidation test replicates. Points are average values while errors bars indicate the highest and lowest value obtained on multiple samples exposed in the same experiment.

### 5.3.10 Summary

Corrosion rates for CS specimens are presented in Figure 54 and for 5Cr steel in Figure 55 and Figure 56. The results show that TAN 2 and TAN 3.5 were mild challenges for FeS scale formed on CS and this scale was able to preserve the protectiveness even after long exposure testing times (Figure 54). The turning point was reached in the TAN 5 challenge for CS when the protectiveness of the FeS scale began to fail.

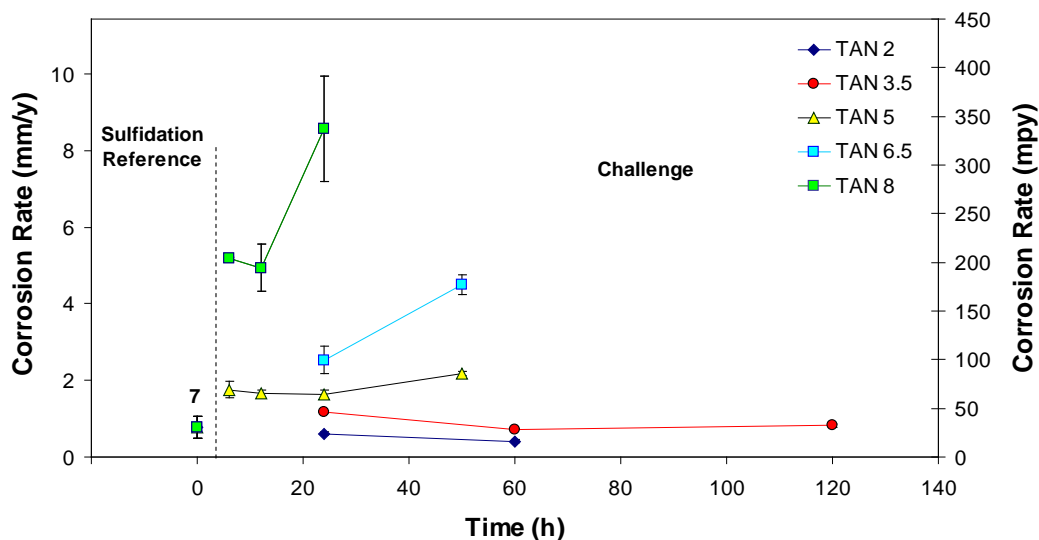


**Figure 54.** Comparison of corrosion rates for CS generated during sulfidation-challenge tests. TAN challenge series are plotted as function of time. All TAN challenge series were done at the same temperature 343°C (650°F). Number 7 above the sulfidation reference represents the number of sulfidation test replicates. Points are average values while errors bars indicate the highest and lowest value obtained on multiple samples exposed in the same experiment.

The 5Cr corrosion rates were plotted on the same scale as the CS corrosion rates.

Figure 55 presents corrosion rates of 5Cr and as it shows that most of the rates were much lower in comparison. To show these results more clearly, the 5Cr corrosion data were expanded (see Figure 56) on a finer scale and thus it was possible to analyze the observed trends. In the expanded view of the 5Cr corrosion rates it is easy to separate the low TAN challenges (TAN 2 and TAN 3.5) and the high TAN challenges (TAN 5, TAN 6.5, and TAN 8). No threshold TAN value for 5Cr steel was found that led to permanent failure of the protective scale as all the corrosion rates decreased with time.

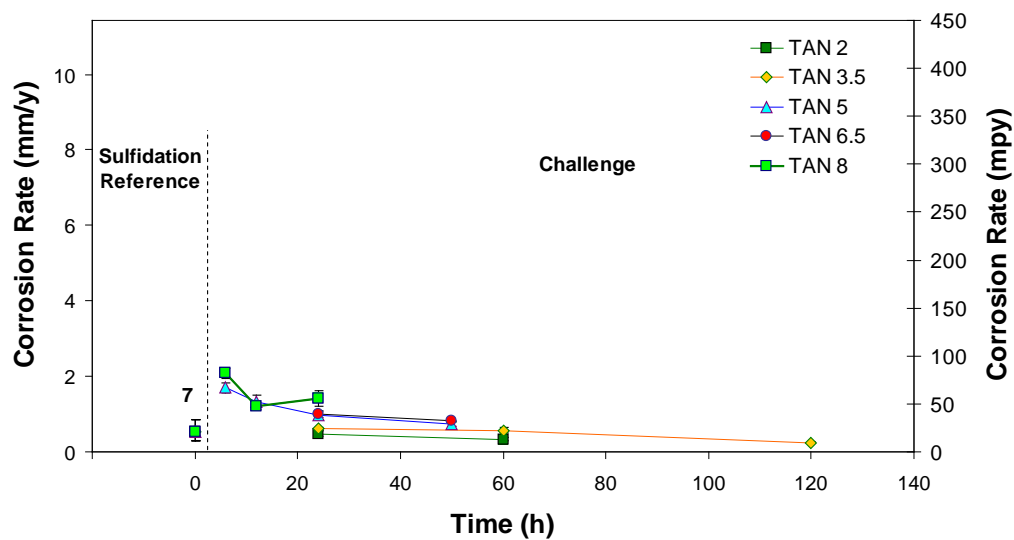


**Figure 55.** Comparison of corrosion rates for 5Cr generated during sulfidation-challenge tests. All TAN challenge series were done at the same temperature 343°C (650°F). Number 7 above the sulfidation reference series represents the number of sulfidation test replicates. Points are average values while errors bars indicate the highest and lowest value obtained on multiple samples exposed in the same experiment.

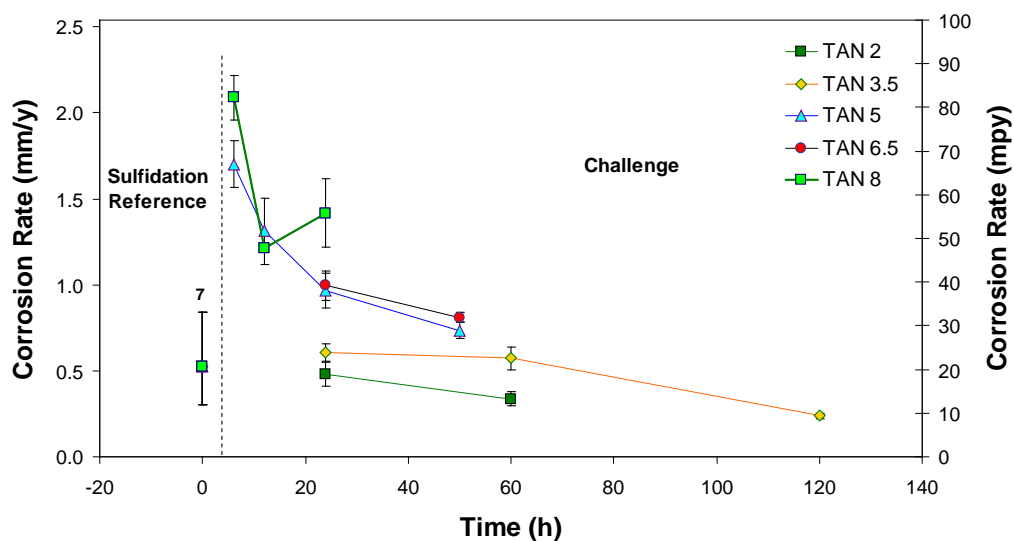


**Figure 56.** Expanded view for comparison of corrosion rates for 5Cr generated during sulfidation-challenge tests. All TAN challenge series were done at the same temperature 343°C (650°F). Number 7 above the sulfidation reference series represents the number of sulfidation test replicates. Points are average values while errors bars indicate the highest and lowest value obtained on multiple samples exposed in the same experiment.

Based on this summary of corrosion rate experiments it was decided that further sulfidation tests will include challenges only with a low TAN value (TAN 3.5) and a high TAN value (TAN 6.5). It was considered that these values: TAN 3.5 and TAN 6.5 were adequate to characterize the protectiveness of FeS scales generated in different sulfidation testing conditions.

It was also decided to change the procedure slightly for further tests and conduct the sulfidation part separately in autoclaves, followed by a challenge done in the HVR.

This was done in order to:

- eliminate the sulfur “contamination” that influenced the challenge results when both phases of the test (sulfidation and challenge) were done in the same testing rig, and
- make it easier to use (and clean) different real crude oil fractions used to build FeS scales that will be challenged.

## CHAPTER 6: SULFIDATION-CHALLENGE EXPERIMENTS USING REAL CRUDE OIL FRACTIONS

### 6.1 Introduction

The previous two parts of the project generated a consistent amount of experimental results which made possible the modeling of naphthenic acid corrosion and the interaction with the sulfidation processes. However, as the model is being developed ultimately for practical applications in industry, it had to cover experimental conditions involving real crude oil fractions tests. Thus, the third part of this project was focused mainly on testing the protectiveness of FeS scales formed in real crude oil fractions. The experimental details and results will be described in following chapter.

### 6.2 Crude Oil Fractions

Crude oil components are separated mainly by distillation as a function of their different boiling points. Most of the oil fractions obtained in distilling towers are complex mixtures with different volatilities and molecular weights. Based on these two properties crude oil fractions are generally separated into lighter and heavier fractions in distinct distilling units. Thus

- atmospheric distillation units separate lighter oil fractions and
- vacuum distillation units are used to separate heavy oil fractions.

An *atmospheric distilling unit* separates oil fractions by boiling point i.e. molecular weight. Thus oil is vaporized almost completely in a furnace and then sent to the distilling tower where lower molecular weight fractions with high volatility are separated at the top of the tower and higher molecular weight molecular fractions which

are less volatile are collected at the bottom of it. Table 8 presents most typical fractions separated in an atmospheric distilling tower:<sup>45</sup>

**Table 8.** *Oil Fractions Separated in Atmospheric Distilling Units*<sup>45</sup>

<b>Atmospheric Distillation Fractions</b>	<b>Temperature</b>
Kerosene	160-232°C (320-450°F)
Light gas oil	232-304°C (450-580°F)
Heavy gas oil	260-343°C (500-650°F)
Fuel oil (residue)	+343°C (+650°F)

The residue from atmospheric distillation is rich in higher boiling constituents that can be separated by *distillation in vacuum units*. These higher boiling constituents cannot be separated at normal atmospheric pressure because they will decompose at temperatures above 350°C (660°F). Therefore they are processed under reduced pressure in vacuum distilling towers. The main fractions that are separated in vacuum towers are presented in Table 9:<sup>45</sup>

**Table 9.** *Oil Fractions Separated in Vacuum Distilling Units*<sup>45</sup>

<b>Vacuum Distillation Fractions</b>	<b>Temperature</b>
Light vacuum gas oil (LVGO)	343-471°C (650-880°F)
Heavy vacuum gas oil (HVGO)	471-565°C (880-1050°F)
Bitumen (residue)	565°C (+1050°F)

For the third part of this research project, protective FeS scales were built using VGO's with different TAN and sulfur concentrations. All VGO samples were provided by EMRE and were handled according to company requirements. Corresponding TAN and sulfur concentrations of tested VGO's are presented in Table 10 which is included in the next chapter.

## **6.3 Experimental**

### ***6.3.1 Experimental Considerations***

Building the iron sulfide scales *ex-situ* and then attacking them with NAP was a difficult experimental task due to the interfering factors (i.e. thermal stresses, reaction with oxygen in air). It was assumed that thermal stresses and oxygen contact could affect scale properties and integrity. As a consequence it was attempted to eliminate or mitigate the effects of these disturbing factors whenever it was possible. This was the reason that the FeS scales were initially formed *in-situ* and then challenged with naphthenic acids in the same rig. These tests were described in previous chapter.

As already discussed, the major drawback of this experimental setup was contamination of the challenge experimental phase with sulfur residues remaining from the previous sulfidation phase. It was believed that the sulfur containing residues left in the equipment were lowering corrosion rates during the challenge phase by helping in “healing” of the iron sulfide scales attacked by the naphthenic acids.

Therefore the test matrix for this third part of the project was designed so that any sulfur contamination possibility was to be eliminated. Sulfidation tests with real crude oil

fractions were run separately in autoclaves and then presulfided specimens were transferred into the HVR unit and challenged with different TAN solutions. Of course this brought other concerns such as oxygen contamination and thermal stresses for example.

### **6.3.2 Instrumentation**

#### **6.3.2.1 Sulfidation**

The sulfidation part of the test was done in an autoclave at high temperature 343°C (650°F) and under continuous stirring conditions. The autoclave consisted of a cylindrical type of reactor with an internal stirring device. The reactor was enclosed by an electric heater which kept the high temperature constant during the test. The autoclave was also equipped with a venting system used for purging the system with nitrogen before and after the test. The specimens were stacked on a specimen holder that was introduced in the autoclave and then testing fluid (crude oil fraction) was added.

#### **6.3.2.2 Challenge**

Presulfided specimens were challenged in the High Velocity Rig (HVR) with naphthenic acid white oil solutions. The HVR testing unit was already described and schematically presented in Chapter 5. Therefore this chapter does not include any details regarding the challenge testing unit.

### **6.3.3 Materials**

#### **6.3.3.1 Metal Specimens**

All specimens tested in this series of “sulfidation-challenge” tests were made of the same two types of steels: carbon steel (CS A106) and 5-Cr steel (F5-A182) that were

used in previously described tests. Specimens had identical shape and dimensions. The dimensions of each ring were: outer diameter OD = 81.76 mm, inner diameter ID = 70.43 mm, and height = 5 mm, made of carbon steel (CS A106) and 5-Cr steel (F5-A182) respectively.

### 6.3.3.2 Test Fluids

The two different experimental phases: sulfidation and challenge used different testing fluids. Thus real crude oil fractions were used during the sulfidation phase for building the iron sulfide scales on the metal specimens. Corresponding sulfur content and TAN concentrations of the tested real crudes are summarized in Table 10. For the challenge phase it was decided to use only the white oil with TAN 3.5 and TAN 6.5. From previous experience, TAN 3.5 was considered high enough to damage the scale on CS but possibly not on 5Cr, while TAN 6.5 was considered a very aggressive challenge that could damage any preformed FeS scale. Both solutions were prepared by spiking the white oil with commercial NAP. Physical properties of white oil were already presented in Chapter 5.

**Table 10.** *NAP Acids and Sulfur Concentrations of Main Model Oils and Crude oil fractions Used for Generating and Challenging FeS Scales*

	Tested Fluid	Total Acid Number (mg KOH/g oil)	Corrosive Sulfur (%wt)
1.	White Oil	0	0
2.	Yellow Oil	0	0.25
3	Naphthenic acids	~ 230	0
4.	AAA VGO	1.75	0.18
5.	BBB VGO	<0.1	0.6
6.	CCC 650+	1	1.51
7.	DDD VGO	0.2	0.7
8.	HH1 VGO	0.2	0.92

### ***6.3.4 Test Conditions***

#### ***6.3.4.1 Sulfidation Test Conditions***

The sulfidation condition for the autoclave tests were almost identical to those of previous sulfidation tests run, in the HVR and described in Chapter 5. Thus the test temperature in the autoclave was set to 343°C (650°F), pressure was 200 psig and duration of each sulfidation test was 24 h. The only difference between the HVR and autoclave sulfidation tests was that the rings were rotated during sulfidation in the HVR while in the autoclave tests rings were stacked on a holder and only the testing fluid was stirred continuously.

#### ***6.3.4.2 Challenge Test Conditions***

After autoclave sulfidation, the steel specimen rings were transferred into the HVR to challenge the FeS scale they formed, with white oil containing naphthenic acids. During the challenge tests, the temperature was 343°C (650°F), identical to the one used in the sulfidation tests and the pressure was 150 psig. Exposure time was the same 24hr for each challenge test. Rings were rotated during tests with 2000 rpm corresponding to a calculated peripheral velocity of  $8.56 \text{ m}\cdot\text{s}^{-1}$ .

Testing conditions are summarized in Table 11 for both the sulfidation and challenge experiments.

**Table 11.** *General Test Conditions Used in Sulfidation and Challenge Tests Done with Real Crude oil fractions*

Test phase	Sulfur content (%w/w)	TAN	Temp. (°C)	Time (h)	Pressure (psig)	Peripheral Velocity (m/s)
Sulfidation (Autoclave)	0.25-1.51	0.1–1.75	343 (650°F)	24	200	0
Challenge (HVR)	0	3.5	343 (650°F)	24	150	8.5
	0	6.5	343 (650°F)	24	150	8.5

## 6.4 Results and Discussion

Compared to model oils the real crude oil fractions represent very complex mixtures containing hydrocarbons and organic compounds such as acids, phenols, sulfides, etc. Interactions between these different compounds influence their reactivity and corrosivity.

In previous chapters, experiments were run exclusively with model oils which offer certain reproducibility and predictability of results. When the experiments were done with crude oil fractions, the final results varied much more due to complex interaction between various fraction components during the scale formation processes. Thus the FeS scales generated from different crudes offered a different protection against NAP attack. Therefore in many cases the same experiments had to be repeated as many as three times in order to find the real trend for a given tested fraction. Also, due to the same complex compositions, the final results have a much higher margin of error for some of the crude oil fractions. In spite of all these variations it was decided to present here all the test results for every fraction used, even for cases when the variability of the

results was high. Thus it was possible to paint a more thorough image of protectiveness (or the lack of it) offered by the different FeS scales formed in crude oil fractions.

#### **6.4.1 Real Crude Oil Fractions Testing Matrix**

A complete testing matrix for experiments done with real crude oil fractions is presented in Appendix D. Due to a change in the test procedure (*ex-situ* sulfidation) the first tests in this series were designed to verify the correlation with previous experimental work with model oils. Thus the baseline experiments were done with sulfidation in yellow oil in the same way and using the same conditions as in the previous sulfidation–challenge test (presented in Chapter 5). In subsequent tests two different oil fractions were diluted to identical TAN and sulfur concentrations as those of yellow oil. Diluting the crude oil fractions was done in order to try and insulate the effect of any additional components of the crude oil fraction. Scale protectiveness formed with diluted fractions was later challenged with a low and a high NAP acidic level: TAN 3.5 vs. TAN 6.5, as was already mentioned.

The next experimental set tested the corrosion behavior in undiluted crude oil fractions as they were delivered from refineries – so called “neat” fractions.

The presence of higher concentration of NAP acids effect during the FeS scale formation was tested in the last experimental series involving real fractions. This was done so that some of the oil fractions as well as the yellow model oil were spiked with naphthenic acids to a TAN 1.75 which was higher than their original TAN level used in the sulfidation experiments. The value of TAN = 1.75 was selected as a reference because

it was the highest TAN of a crude oil fraction used for the FeS scale formation in the previous experiments and the results could be compared to that of a crude oil fraction.

A final group of six tests was done for reference purposes and focused exclusively on pure NAP corrosion of the two steel types and covered the whole TAN range used previously.

#### ***6.4.2 Sulfidation Reference Test***

A sulfidation reference test was run in the autoclave for every model oil or crude oil fraction that was tested in this project section. Data were collected at the end of every reference test i.e. the weight losses and weight gains corresponding to corrosion and scale formation rates during sulfidation. These data were later used to evaluate the effects of NAP attacks on preformed FeS scales as described earlier. Graphically, every plot included in this chapter will present and compare both the sulfidation and the challenge data offering the complete picture for every model or crude oil fraction used.

Figure 57 presents the reference corrosion rates (CR) for CS and Figure 58 shows the FeS scale thickness formed on the steel specimens in yellow oil. Both these plots and as well as all the plots presented later in this chapter include results corresponding to sulfidation (i.e. corrosion rates, scale thickness) as well as the corresponding results of the challenge phases.

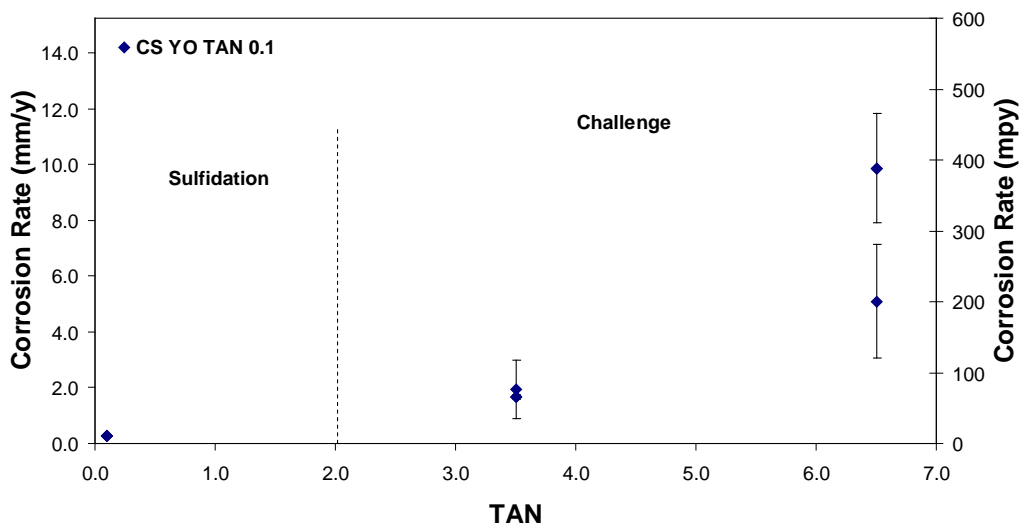


**Figure 57.** Corrosion rates for CS specimens presulfidated with Yellow oil and then challenged with NAP at TAN = 3.5 and TAN = 6.5. Points are average values while errors bars indicate the highest and lowest value obtained on multiple samples exposed in the same experiment.

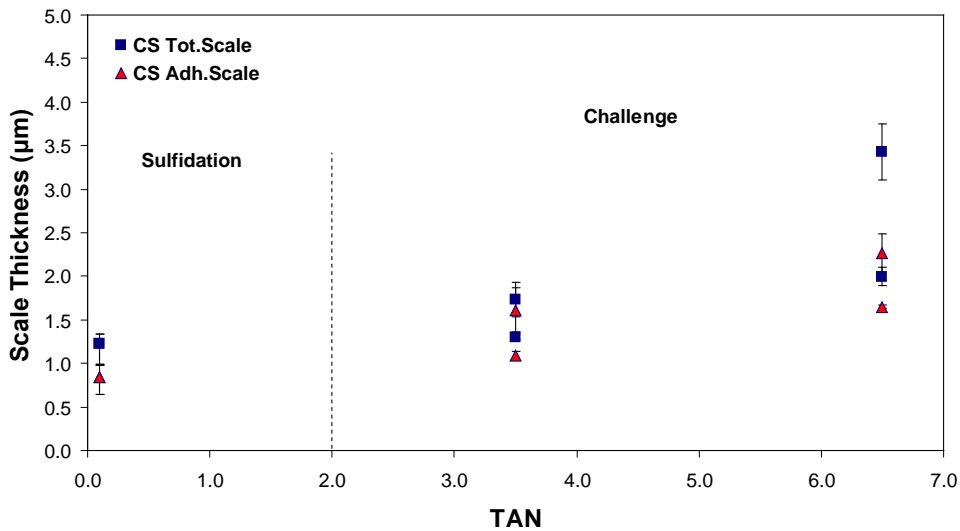


**Figure 58.** Scale thickness formed on CS specimens presulfidated with Yellow oil and then challenged with NAP at TAN = 3.5 and TAN = 6.5. Points are average values while errors bars indicate the highest and lowest value obtained on multiple samples exposed in the same experiment.

It is obvious that the FeS scales formed with yellow oil offered a better protection for CS when challenged with TAN 3.5 than challenged with TAN 6.5. CR results of TAN

3.5 challenge were almost identical whereas TAN 6.5 generated two different results but both are much higher than the low challenge. This demonstrates that the FeS scale from Yellow oil completely lost its protectiveness when challenged with high NAP acidic concentrations.

The scale thickness presented in Figure 58 includes two sets of data, one set presents data regarding the scale that was measured at the end of every test (total scale) and other data set corresponds to the scale that was strongly adherent to metal surface (adherent scale). The adherent scale could only be removed by aggressive chemical means (Clarke solution).

In terms of scale thicknesses there were differences between scales formed in every test. However when these different scales presented in Figure 58 are analyzed it is clear that even if more scale was generated and “survived” to the TAN 6.5 challenge, it did not offer any significant protection against NAP acids attack and CRs were high. For the TAN 3.5 challenge tests both total and adherent scale were in the same range and offered a good protection as showed by low CS corrosion rates.

The extent of damage of NAP attack against both FeS scale and CS can be easily noticed in the SEM backscattered images of Figure 59. The challenge by TAN 3.5 appears to have penetrated the FeS scale and corroded the metal beneath the scale (Figure 59 – *a*). In spite of the scale porous structure revealed by SEM image, in the case of TAN 3.5 challenge the NAP attack was moderate and the metal surface had no pits. Compared to TAN 3.5, the higher challenge TAN 6.5 creates deep pits in the metal (Figure 59 – *b*) and scale structure is very fragmented with the top layer separated from the bottom ones.

All the scale and metal damages are reflected in high corrosion rates measured at the end of the TAN 6.5 challenge tests.

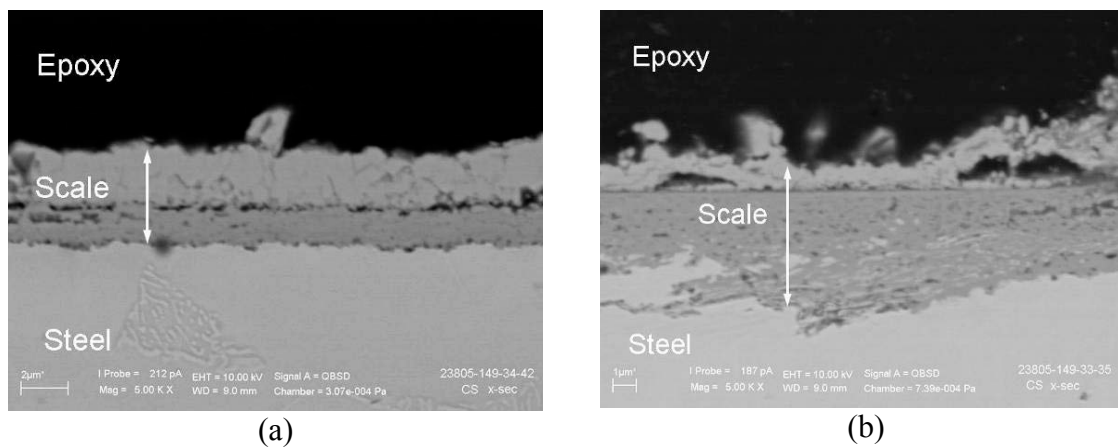


**Figure 59.** SEM backscattered images represent cross-sections on CS specimens presulfided with Yellow oil and then challenged with NAP acids. FeS scale was challenged with TAN 3.5 (image *a*) and with TAN 6.5 (image *b*). In both images the metal is on the bottom side.

The FeS scales formed on 5Cr steel from Yellow oil and then challenged with TAN 3.5 and 6.5 respectively are shown in Figure 60 which presents the corrosion rates of 5Cr corresponding to low and high TAN challenges. The FeS scale preserved its protectiveness against TAN 3.5 attack but lost it when challenged with TAN 6.5 therefore corrosion rates were lower in the former than in the latter case.

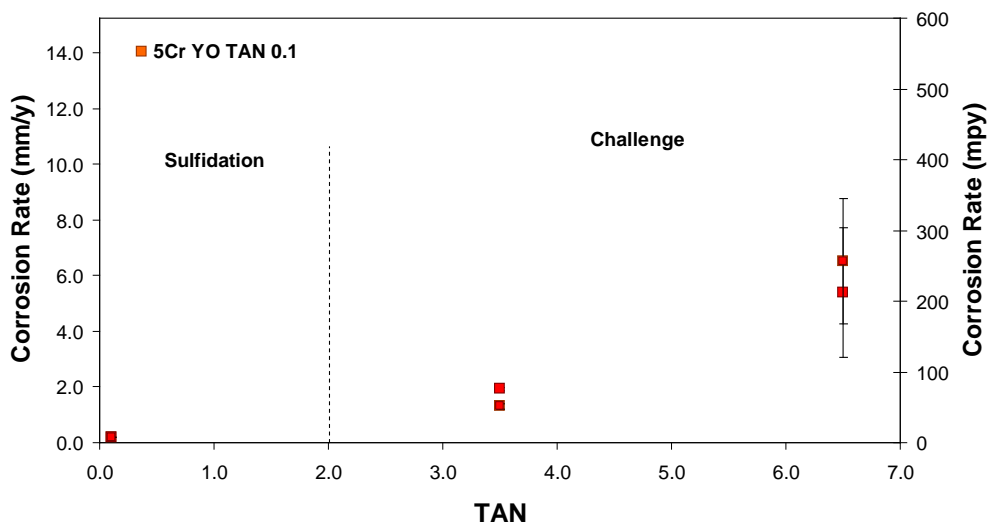


**Figure 60.** Corrosion rates for 5Cr specimens presulfidated with Yellow oil and then challenged with NAP at TAN = 3.5 and TAN = 6.5. Points are average values while errors bars indicate the highest and lowest value obtained on multiple samples exposed in the same experiment.

The thickness of scales formed on the 5Cr steel was almost the same for sulfidation and TAN 3.5 challenge as shown in Figure 61. If this scale thickness is related to the corresponding low corrosion rate, then the protective effect of the scale is self-evident in the TAN 3.5 challenge. However the FeS scale was not that protective when challenged with TAN 6.5 in spite of its higher thickness and corrosion rates become high for 5Cr steel as high as they were for the CS.

For 5Cr steel the SEM images of scale cross-sections were very similar to those of CS presenting a very porous scale structure covering the pitted metal surface. All SEM pictures corresponding to 5Cr steel are included in Appendix E. Overall it can be summarized that the sulfidation-challenge results using the Yellow oil and the new *ex-situ* sulfidation procedure were successful in reproducing the same results as those obtained in the *in-situ* sulfidation.

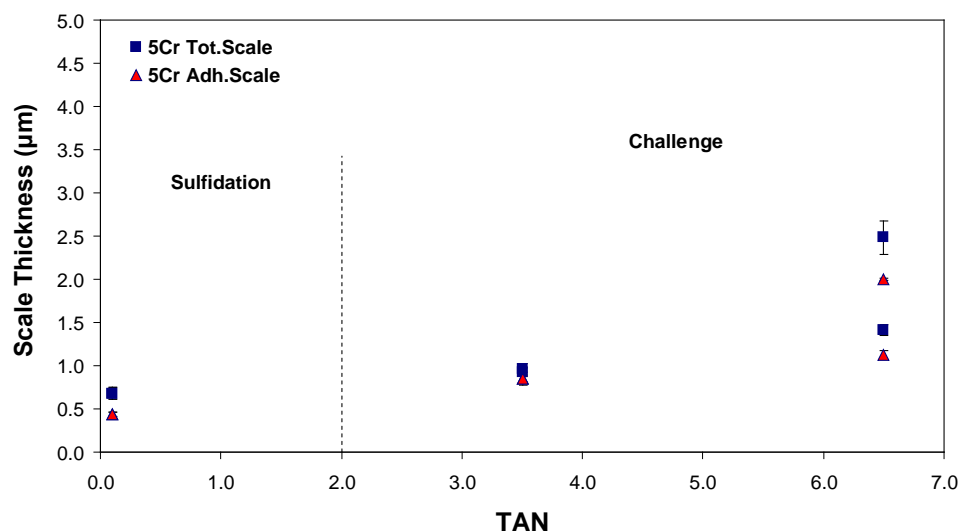


**Figure 61.** Scale thickness formed on 5Cr specimens presulfided with Yellow oil and then challenged with NAP at TAN = 3.5 and TAN = 6.5. Points are average values while errors bars indicate the highest and lowest value obtained on multiple samples exposed in the same experiment.

#### 6.4.3 Diluted Fractions Tests Results

The first experimental set with crude oil fractions was done using the diluted real crude oil fractions for building up the FeS scales. It was decided to dilute the crude oil fractions to the same TAN = 0.1 and sulfur content (0.25%wt) of the Yellow oil which was used in all the previous experiments. In this way it became possible to compare the protectiveness of the FeS scale formed in diluted fractions to those from the Yellow oil tests and draw some tentative conclusions about the effect of real crude oil fractions.

DDD VGO was the first of the crude oil fractions tested in diluted form similar to that of Yellow oil (TAN = 0.1, S = 0.25% wt). Originally DDD VGO had TAN = 0.2 and S = 0.7 % wt. DDD VGO had a different effect on CS and 5Cr corrosion rates therefore they will be presented on the same plot for a better comparison (Figure 62). In the TAN

3.5 challenge test, the corrosion rates for CS were slightly higher than in sulfidation test whereas for 5Cr steel the two corrosion rates were identical. These very low corrosion rates showed how effective the protection offered by FeS scales was when formed from DDD VGO - on both steel types. The FeS scale protectiveness for 5Cr was preserved even during the TAN 6.5 challenge where corrosion rates were constant and equal to the TAN 3.5 challenge. However scale formed from DDD VGO was not able to protect CS against NAP attack in case of TAN 6.5 when corrosion rates were much higher than for 5Cr under similar challenge conditions.

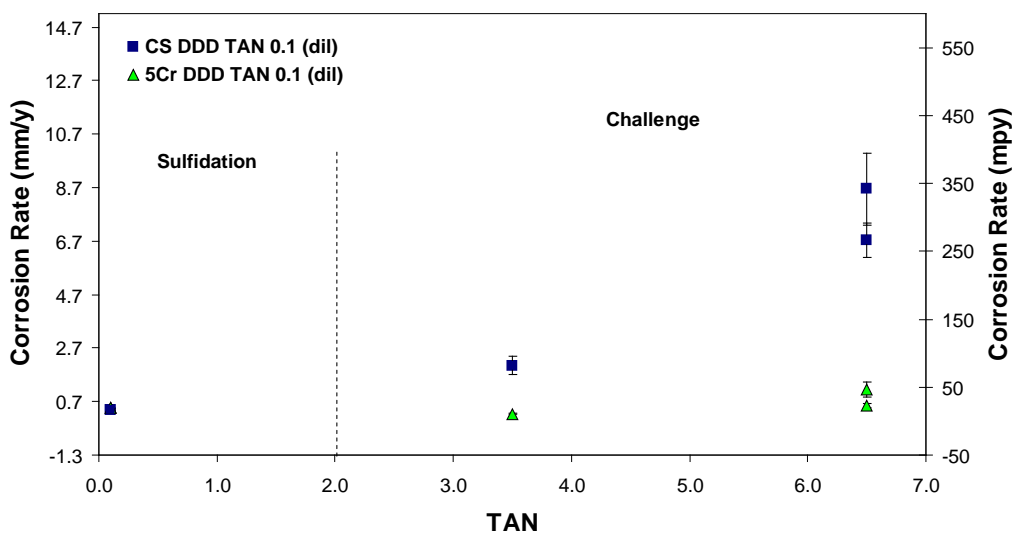


**Figure 62.** Corrosion rates for CS and 5Cr steel specimens presulfided with *diluted* DDD VGO and then challenged with NAP at TAN = 3.5 and TAN = 6.5. Points are average values while errors bars indicate the highest and lowest value obtained on multiple samples exposed in the same experiment.

The thickness of adherent scale on CS remains the same after both TAN 3.5 and TAN 6.5 challenges (Figure 63). The total scale values almost overlap with the adherent scale thickness in the TAN 3.5 experiment but become very different in the TAN 6.5

challenge, which made it more porous and fragile (Figure 63). These scale changes are best revealed by the SEM backscattered images included in Figure 95 for the two analyzed scales (TAN 3.5 vs. TAN 6.5).

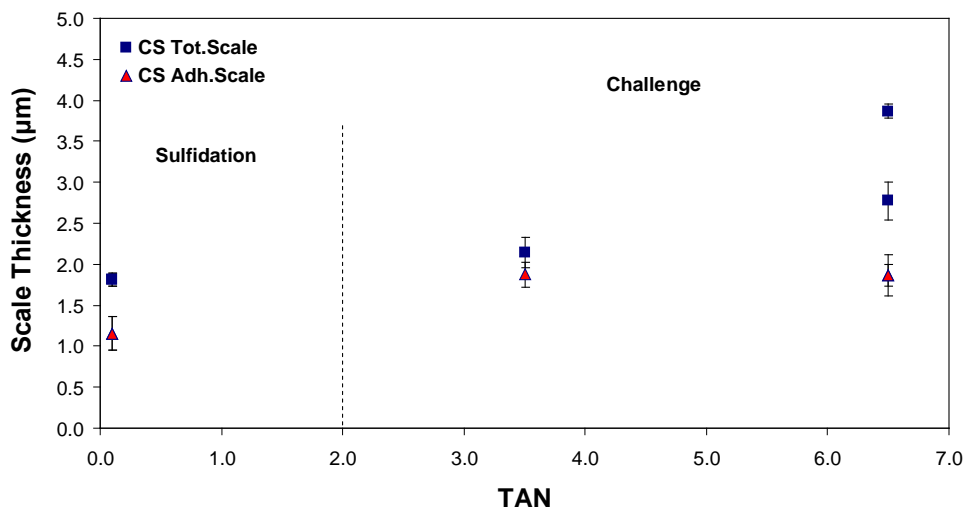


**Figure 63.** Scale thickness formed on CS specimens presulfided with *diluted* DDD VGO and then challenged with NAP at TAN = 3.5 and TAN = 6.5. Points are average values while errors bars indicate the highest and lowest value obtained on multiple samples exposed in the same experiment.

The end effect of NAP attack is very clear in the two SEM images below. Thus Figure 64 – *a* shows the FeS scale which survived the TAN 3.5 challenge. Although the scale was fragmented (porous structure) it was able to protect the CS that had a relatively low CR. TAN 6.5 challenge caused major damage both to the scale and the metal (high CR for CS) making it very difficult to make a clear separation between the metal and scale surfaces at their common interface (Figure 64 - *b*).

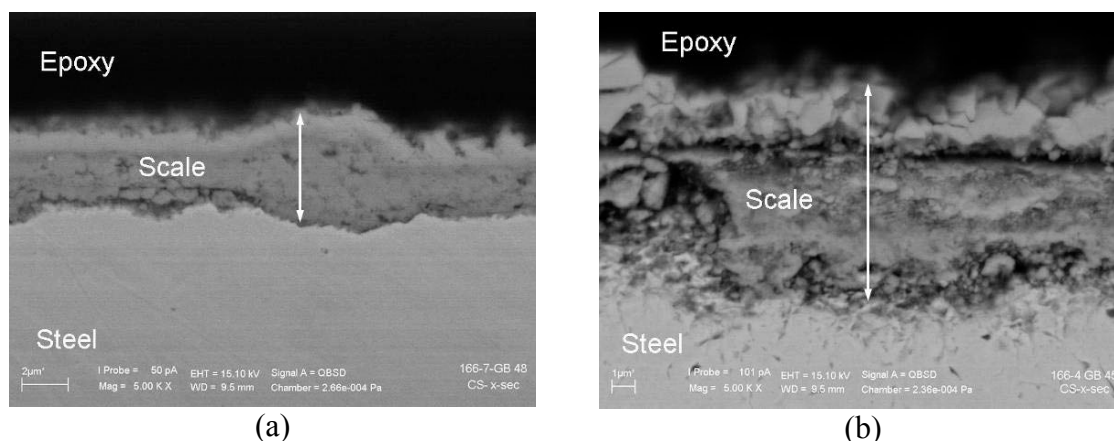


**Figure 64.** SEM backscattered images represent cross-sections on CS specimens presulfided with *diluted* DDD VGO and then challenged with NAP. FeS scale was challenged with TAN 3.5 (image *a*) and with TAN 6.5 (image *b*). In both images the metal is on the bottom side.

For the 5Cr steel specimens both total and adherent scale thicknesses remain in the same range starting from the sulfidation reference test to the highest challenge test (Figure 65). This scale corroborated the corrosion rates obtained in these tests. Thus both SEM pictures corresponding to the TAN 3.5 challenge test (Figure 66 – *a*) and the TAN 6.5 challenge (Figure 66 – *b*) present a relatively dense and consistent scale layer covering the metal. This FeS scale protected the 5Cr steel against NAP attack even though its outer layer was delaminated or partially removed.

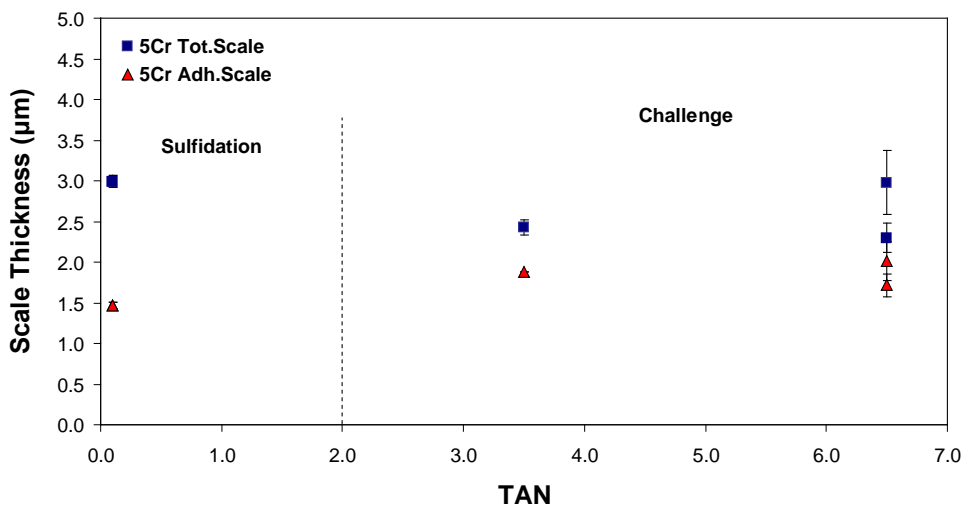


**Figure 65.** Scale thickness formed on 5Cr specimens presulfidated with *diluted* DDD VGO and then challenged with NAP at TAN = 3.5 and TAN = 6.5. Points are average values while errors bars indicate the highest and lowest value obtained on multiple samples exposed in the same experiment.

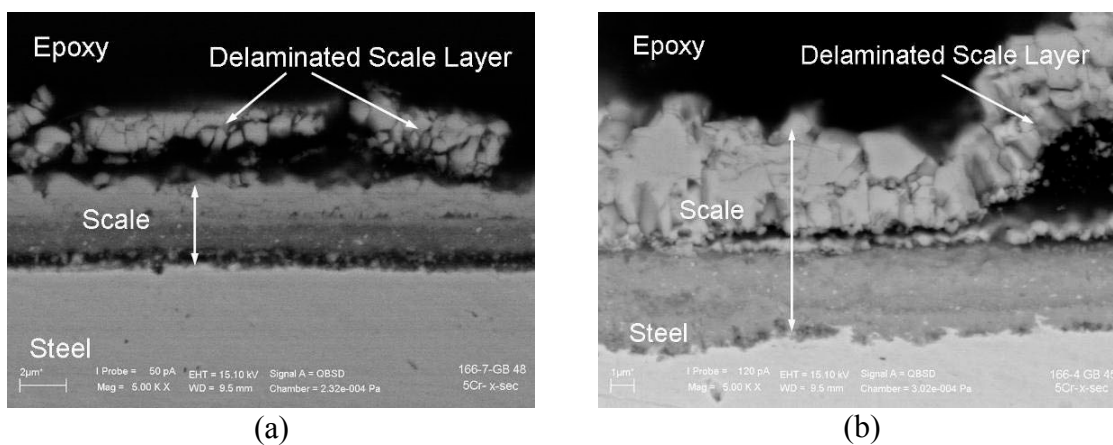


**Figure 66.** SEM backscattered images represent cross-sections on 5Cr specimens presulfidated with *diluted* DDD VGO and then challenged with NAP. FeS scale was challenged with TAN 3.5 (image *a*) and with TAN 6.5 (image *b*). In both images the metal is on the bottom side.

The last crude oil fraction that was tested in diluted form and compared to model oils was HH1 VGO. The fraction HH1 VGO had initial TAN = 0.2 and S = 0.92% wt. Diluted to TAN = 0.1 and S = 0.25%wt the HH1 VGO offered a poor protection for both

steel types and each challenge test had to be repeated at least once. Thus, the graphical representation of the corrosion rates (Figure 67) showed that it was not really possible to make a distinction between the two metals (CS and 5Cr) when they were challenged with either low or high TAN solutions. As Figure 67 plot shows, the CS corrosion rates overlap those of 5Cr steel when the scales were challenged with TAN 3.5. A similar situation with overlapping corrosion rates for CS and 5Cr is generated in the TAN 6.5 challenge as well. The CS corrosion rate had a much higher value in one TAN 6.5 challenge that can be considered an outlier. If the outlier of the CS corrosion rate is ignored then all other results for TAN 6.5 are in the same range and similar to TAN 3.5. The final conclusion of the CR analysis was that the scales formed from HH1 VGO did not protect CS and 5Cr against NAP attack regardless of the challenge level.

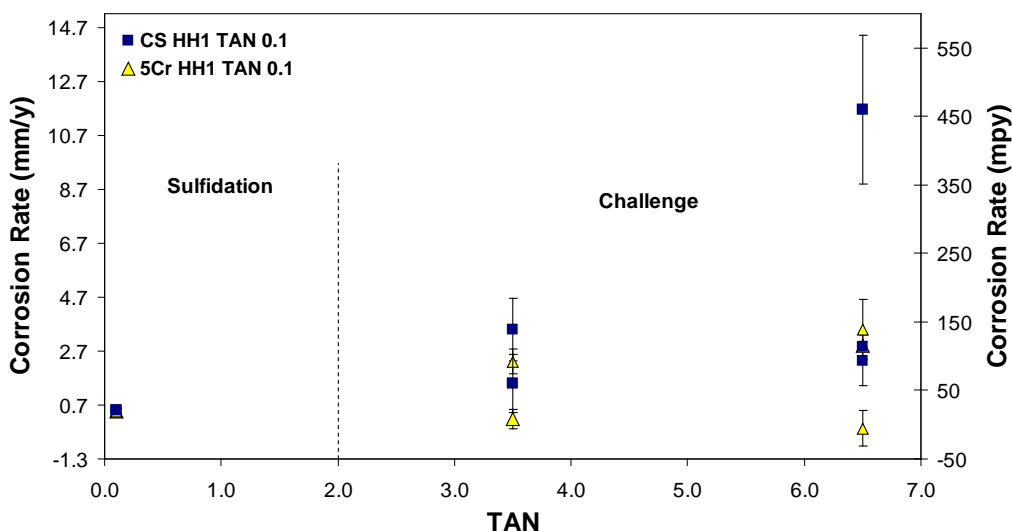


**Figure 67.** Corrosion rates for CS and 5Cr steel specimens that were presulfidated with *diluted* HH1 VGO and then challenged with NAP at TAN = 3.5 and TAN = 6.5. Points are average values while errors bars indicate the highest and lowest value obtained on multiple samples exposed in the same experiment.

The total and adherent scales were measured and graphically represented for both steel types i.e. Figure 68 scale on CS and Figure 69 scale on 5Cr respectively. For both CS and 5Cr the scale results overlapped making it difficult to make a clear separation between the total and adherent scale thicknesses. The analysis of the two plots corresponding to the scales formed on CS and 5Cr indicate that the scale thickness ranges were almost the same for both steel types in both challenge tests. All other plots referring to the tests done with diluted HH1 are included in Appendix E.

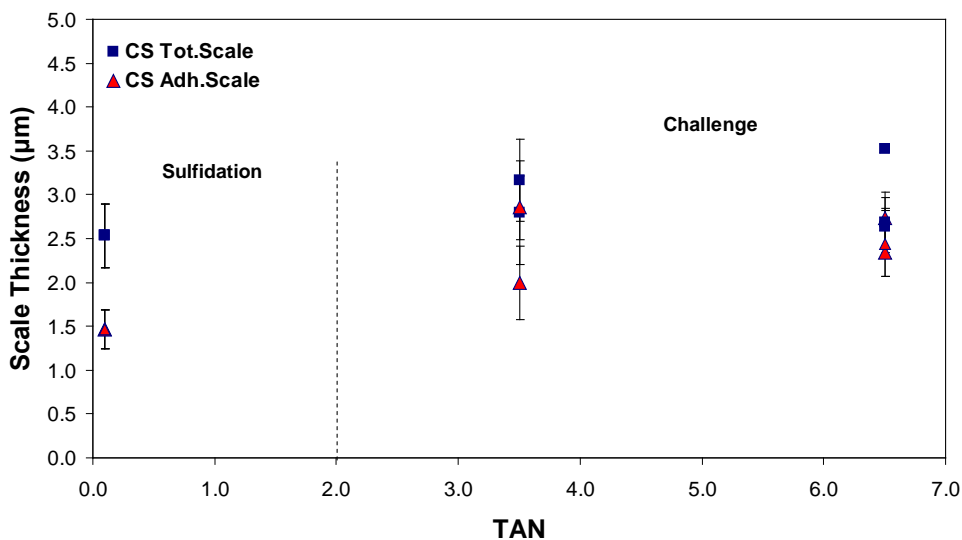


**Figure 68.** Total and adherent scale measured on CS specimens presulfided with *diluted* HH1 VGO. Scale values cover similar ranges in TAN 3.5 as in TAN 6.5 challenges. Points are average values while error bars indicate the highest and lowest value obtained on multiple samples exposed in the same experiment.

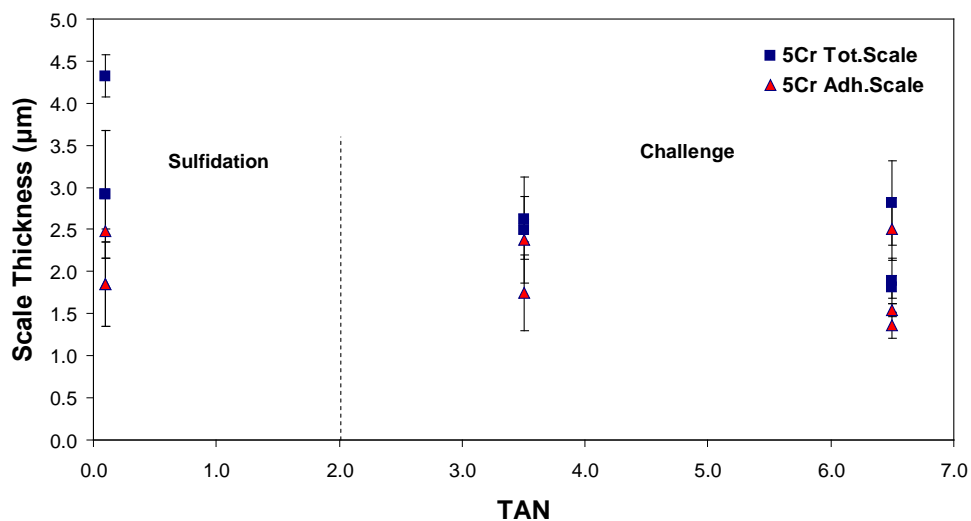


**Figure 69.** Total and adherent scale measured on 5Cr specimens presulfidized with *diluted* HH1 VGO. Scale values cover similar ranges in TAN 3.5 as in TAN 6.5 challenges. Points are average values while error bars indicate the highest and lowest value obtained on multiple samples exposed in the same experiment.

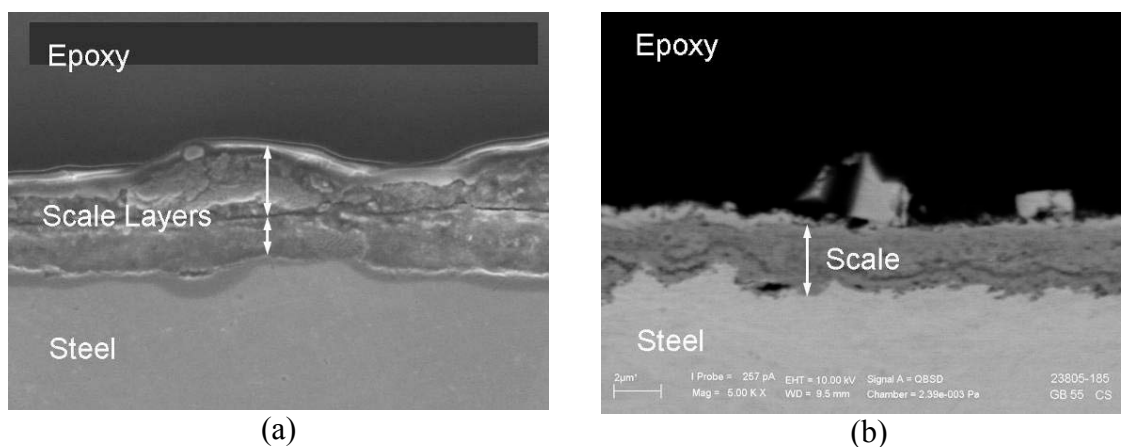


**Figure 70.** SEM images of cross-sections on CS specimens sulfidized with *diluted* HH1 VGO. SEM image *a* represents the scale that was found at the end of TAN 3.5 challenge and image *b* the scale at the end of TAN 6.5 challenge. In image *b* the scale had only one layer compared to image *a* where two layer are visible.

The SEM analysis indicated the fragmented and damaged FeS scale on both CS and 5Cr steel. On the CS specimens the scale was considerably thinned in the TAN 6.5

challenge leaving only one layer whereas in the TAN 3.5 challenge the two scale layers survived (Figure 70 *a* and *b*).

On the 5Cr specimens the scale had a fragmented structure as it is show in the SEM images included in Figure 71. The scale layers are very fragmented and in the image Figure 71 *b* corresponding to TAN 6.5 challenge. The FeS scale has large voids at the interface with the metal. This was the result of strong NAP attack. All other SEM images for FeS scales formed with the HH1 VGO fraction are included in Appendix E.

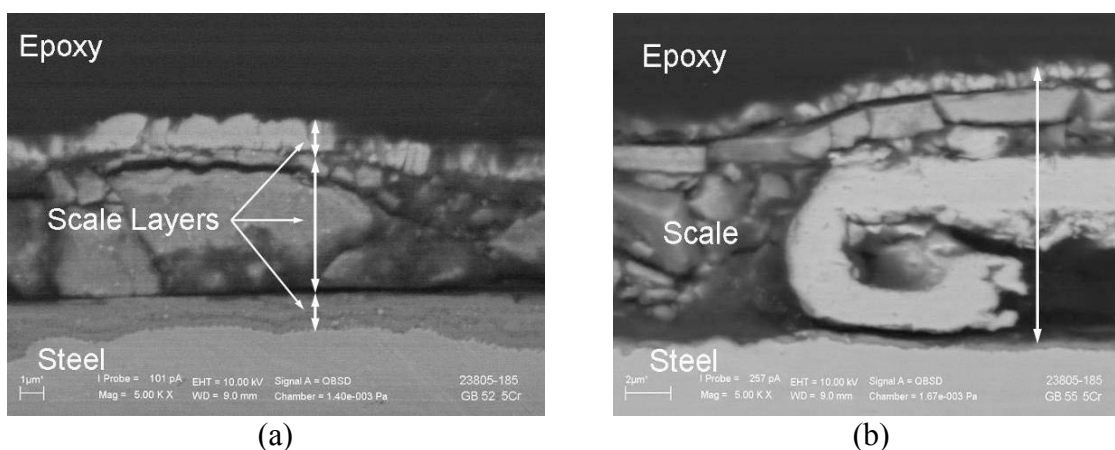


**Figure 71.** SEM images of scales formed with *diluted* HH1 VGO on 5Cr specimens. Image *a* presents the scale challenged with TAN 3.5 and image *b* corresponds to TAN 6.5 challenged scale. In Both images scales had multiple layers with porous structures.

#### 6.4.3.1 Summary

In conclusion: the results obtained for the diluted real crude oil fraction tests suggest that some crude oil fraction presented very different results when compared to those obtained in model Yellow oil tests even if the NAP and sulfur levels were the same. The reasons for this behavior are not understood at this time.

#### ***6.4.4 “Neat” Fractions Experimental Results***

Based on the diluted fraction results, the next experiments investigated the protectiveness of the FeS scales formed from the so called “neat” crude oil fractions. The crude oil fractions were called “neat” when they were used for experiments in their original undiluted form provided by refineries (i.e. original TAN and sulfur concentrations).

Diluted DDD VGO formed the most protective FeS scale therefore it was the first fraction tested in the “neat” form. Originally DDD VGO had TAN = 0.2 and S= 0.7 % wt and in this form it was used in the autoclaves to generate the FeS scales on CS and 5Cr specimens. Challenged with TAN 3.5 the FeS scales resisted NAP attack, protected the steels and corrosion rates were low and similar to those of sulfidation as shown in Figure 72. Later when the same scale formed by DDD VGO was challenged with TAN 6.5 it protected only the 5Cr steel which had low corrosion rates. CS was less protected by the same FeS scale and had high corrosion rates in TAN 6.5 challenge tests (Figure 72).

The FeS scale formed on both CS and 5Cr specimens preserved its initial thickness from sulfidation tests during challenges with TAN 3.5 and 6.5. Figure 73 compares the scale thickness found on the CS specimen at the end of the TAN 3.5 and 6.5 challenges. In the TAN 6.5 challenge, the scale thickness has higher values than in TAN 3.5. In spite of a thicker scale NAP were able to diffuse to the metal surface causing higher corrosion rates on CS than on 5Cr steel specimens.

Figure 74 compares the scales on 5Cr specimens which were in the same thickness range both in the TAN 3.5 and TAN 6.5 tests. All other plots regarding the scale thickness and scale formation are included in Appendix E.

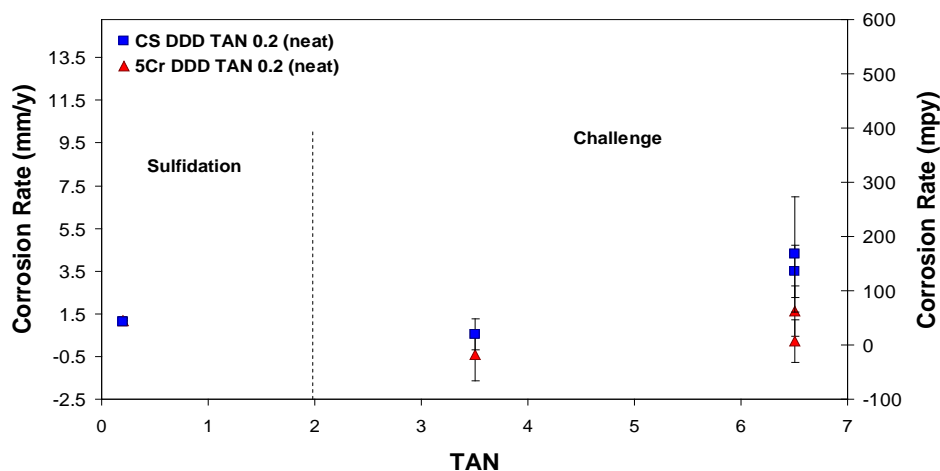


**Figure 72.** Corrosion rates for CS and 5Cr steel specimens that were presulfided with DDD VGO (*neat*) and then challenged with naphthenic acids at TAN = 3.5 and TAN = 6.5. Points are average values while errors bars indicate the highest and lowest value obtained on multiple samples exposed in the same experiment.

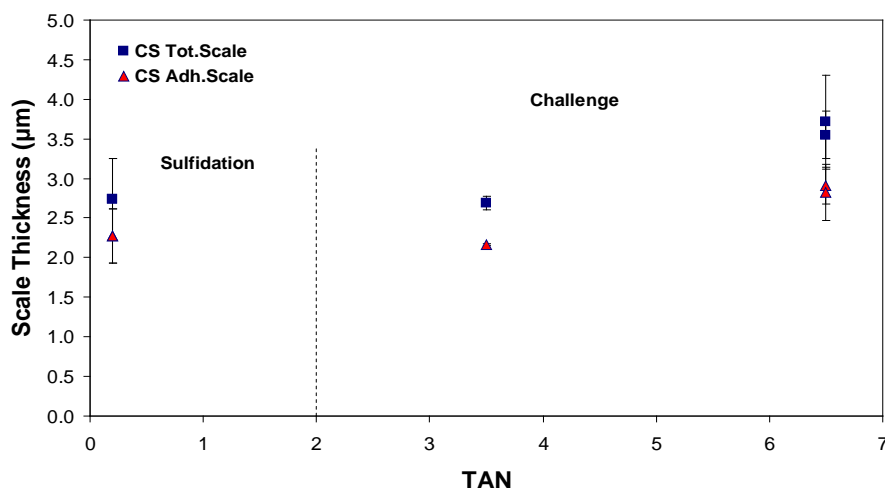


**Figure 73.** FeS scale thickness on CS specimens that were presulfided with DDD VGO (*neat*) and then challenged with NAP at TAN = 3.5 and TAN = 6.5. Points are average values while errors bars indicate the highest and lowest value obtained on multiple samples exposed in the same experiment.

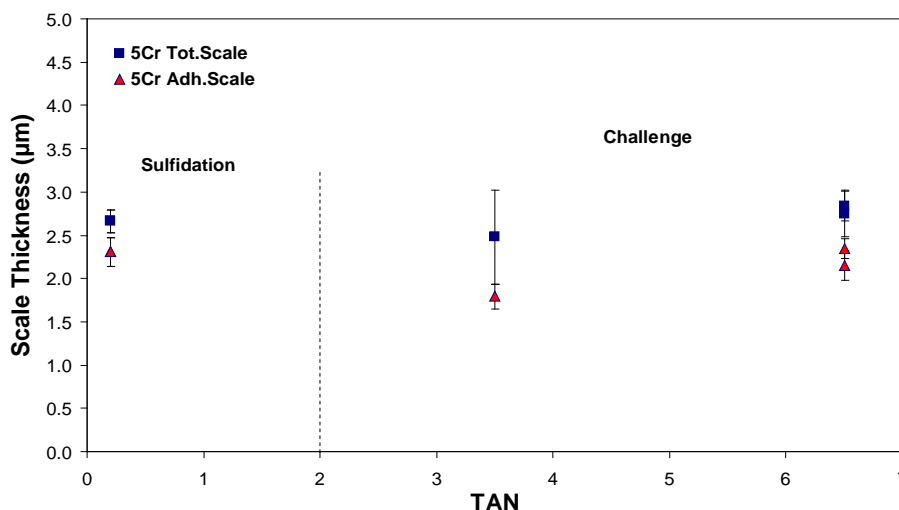


**Figure 74.** FeS scale thickness on 5Cr steel specimens that were presulfided with DDD VGO (*neat*) and then challenged with NAP at TAN = 3.5 and TAN = 6.5. Points are average values while errors bars indicate the highest and lowest value obtained on multiple samples exposed in the same experiment.

An interesting aspect of the FeS scale structure was revealed by the SEM images for scale cross-sections. The most representative SEM images are included in Figure 75 (*a* and *b*) and they correspond to scales formed on CS and 5Cr respectively and challenged with TAN 6.5. The 5Cr steel had a lower corrosion rate than CS in TAN 6.5 challenge tests. The SEM image *b* shows the FeS scale consisting of multiple layers and different consistencies that was formed on 5Cr steel. In contrast, the FeS scale formed on the CS (image *a*) has fewer layers with a porous structure that allowed NAP to reach the metal surface and create large pits. In summary the performance of the neat crude oil fraction DDD VGO was similar to that when it was diluted to the lower NAP and sulfur content as described in the section above.

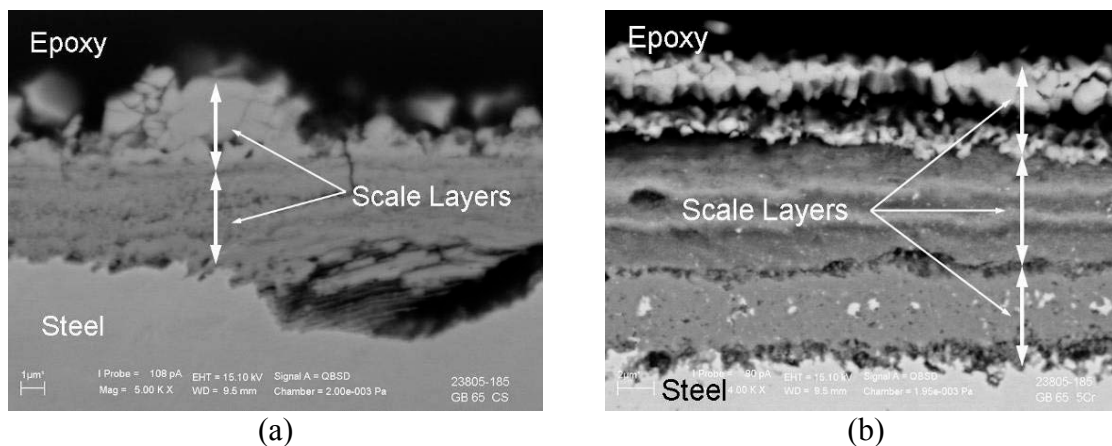


**Figure 75.** SEM backscattered images represent cross-sections on CS and 5Cr specimens presulfidated with DDD VGO (*neat*) and then challenged with NAP. FeS scale was challenged with TAN 6.5. Image *a* shows scale formed on CS and image *b* scale formed on 5Cr steel. In both images the metal is on the bottom side.

HH1 VGO was the next crude oil fraction tested in its original form TAN = 0.2 and S = 0.92% wt. From the previous results it was expected that the higher sulfur content of HH1 VGO would build a very protective FeS scale on the CS and 5Cr specimens. The challenge tests results presented in Figure 76 demonstrated that the FeS scales were protective on both steels only at low TAN 3.5 when corrosion rates were similar to those in sulfidation results. In higher challenges (TAN 6.5) the FeS scales formed with HH1 VGO could not protect the metal surface and corrosion rates were high both for CS and for 5Cr. With this crude oil fraction, the scale thickness was relatively constant in all tests on 5Cr specimens (Figure 78) whereas on CS the scale thickness varied from one test to another (Figure 77). On the CS specimens there was more scale surviving at the end of the TAN 6.5 challenge but it was more porous than the scale found at the end of the TAN 3.5 test. This scale variability on CS specimens might have been caused by NAP attack combined with flow conditions.

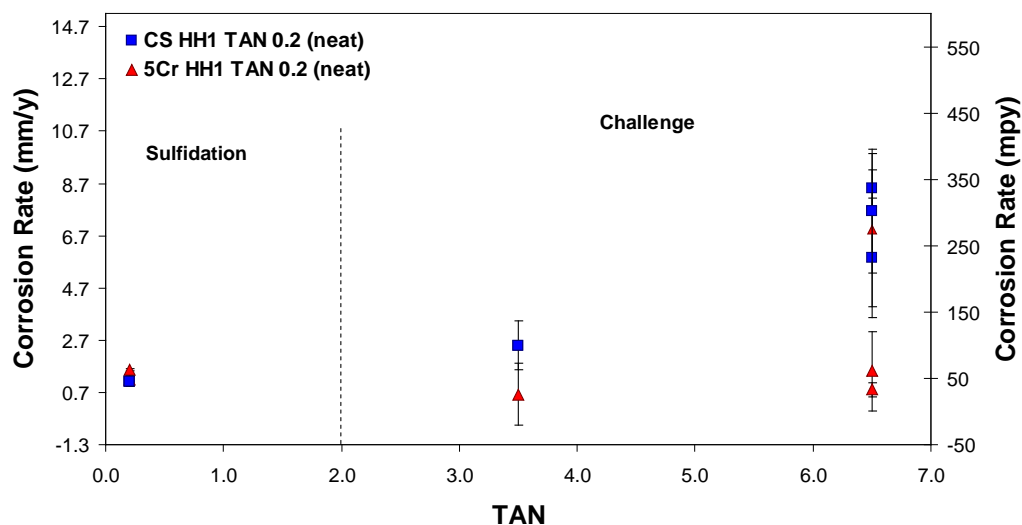


**Figure 76.** Corrosion rates for CS and 5Cr steel specimens that were presulfided with HH1 VGO (*neat*) and then challenged with NAP at TAN = 3.5 and TAN = 6.5. Points are average values while errors bars indicate the highest and lowest value obtained on multiple samples exposed in the same experiment.

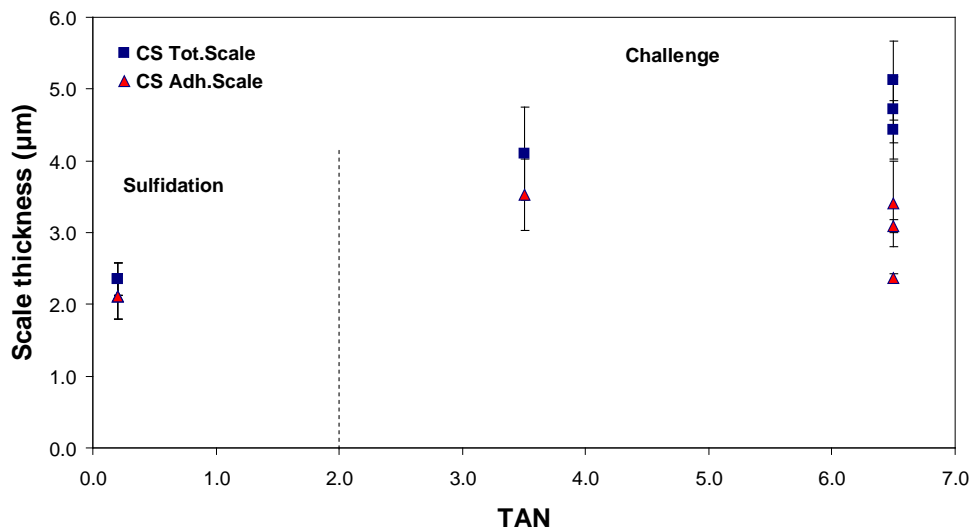


**Figure 77.** Scale thickness measured on CS at the end of TAN 3.5 and TAN 6.5 challenge tests. The scale was formed with HH1 VGO undiluted (*neat*). Points are average values while errors bars indicate the highest and lowest value obtained on multiple samples exposed in the same experiment.

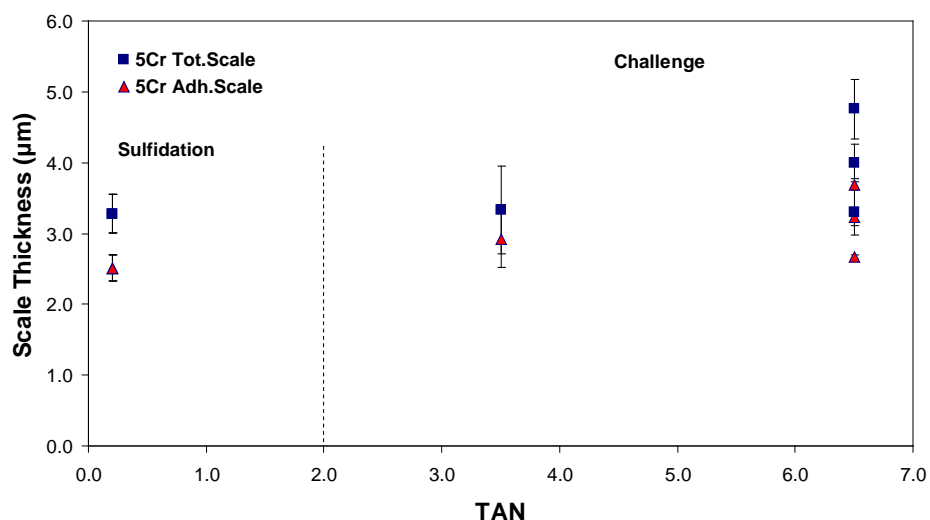


**Figure 78.** Scale thickness measured on CS at the end of TAN 3.5 and TAN 6.5 challenge tests. The scale was formed with HH1 VGO undiluted (*neat*). Points are average values while errors bars indicate the highest and lowest value obtained on multiple samples exposed in the same experiment.

The SEM pictures supported this hypothesis of the FeS scale damaged under the NAP attack by showing a very fragmented scale on CS. Thus Figure 79 compares the FeS scales formed on CS and challenged with TAN 3.5 (*a*) and TAN 6.5 (*b*). Although there are some similarities of the scale structures in both images Figure 79 - *a* and *b*, the aggressive NAP attack is very obvious for the TAN 6.5 case. It damaged the scale, penetrated to the metal and caused large pits on the metal surface (image *b*). All plots regarding FeS scale data and SEM images for this series of tests are included in Appendix E.

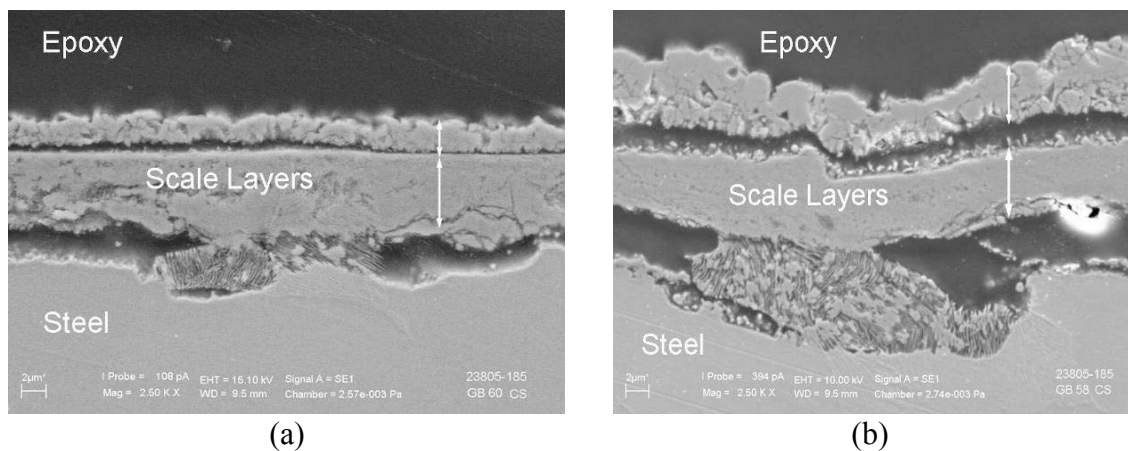


**Figure 79.** SEM images represent cross-sections on CS specimens presulfided with HH1 VGO (*neat*) and then challenged with NAP. FeS scale was challenged with TAN 3.5 (image *a*) and with TAN 6.5 (image *b*). In both images the metal is on the bottom side.

As mentioned above, naphthenic acids in small concentrations were thought to stimulate formation of FeS scales by high sulfur containing crude oil fractions. Both DDD and HH1 had identical TAN = 0.2 values and high sulfur content: 0.7 and 0.92 % wt respectively, however they generated FeS scales with different protectiveness. The scale from HH1 was less protective than the scale generated from DDD in spite of higher sulfur content. Based on these experimental observations it was decided to select and test a fraction that had a lower TAN and sulfur content than DDD and HH1. This crude oil fraction was BBB VGO that had TAN < 0.1 and S = 0.6 % wt and was tested using identical conditions as DDD and HH1. The FeS scales generated from BBB VGO had a very different effect compared to the scales formed with DDD and HH1 VGO on CS and 5Cr. The scales from BBB VGO were more protective for CS than for 5Cr in TAN 6.5 challenges and is presented in Figure 80. For low challenge (TAN 3.5) 5Cr steel was more protected by the FeS scale than CS as in previous tests done with other fractions.

The corresponding corrosion rates for CS and 5Cr steel were very similar to all other TAN 3.5 challenge results.

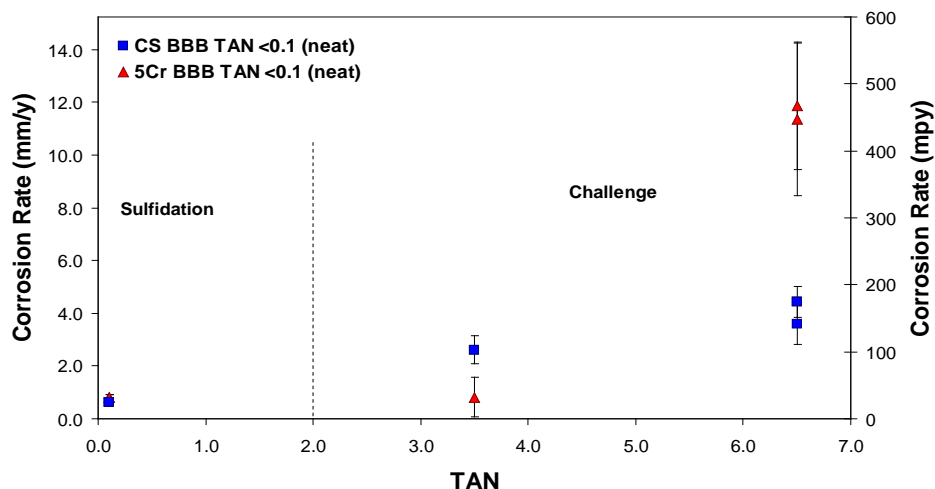


**Figure 80.** Corrosion rates for CS and 5Cr steel specimens that were presulfided with BBB VGO (*neat*) and then challenged with NAP at TAN = 3.5 and TAN = 6.5. Points are average values while errors bars indicate the highest and lowest value obtained on multiple samples exposed in the same experiment.

The 5Cr high corrosion rate demonstrated that the FeS scale formed with BB VGO was less protective for 5Cr than for CS. This statement was supported by the scale thickness measured on 5Cr specimens at the end of the tests. As shown in Figure 82, less scale was found at the end of the TAN 6.5 challenge than it was found in the TAN 3.5 experiment. This scale decrease on 5Cr steel was also revealed in the SEM images. Figure 81 presents scale results corresponding to CS specimens.

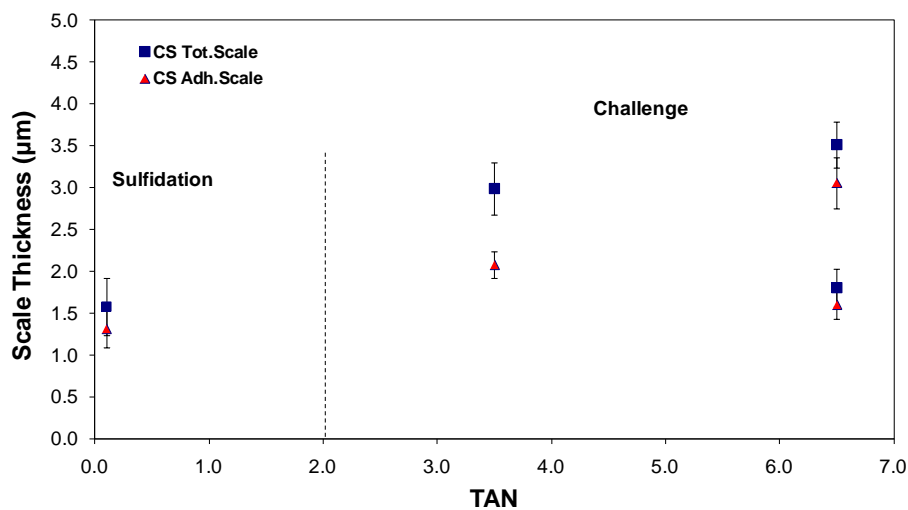


**Figure 81.** Scale thickness on CS specimens that were presulfided with BBB VGO (*neat*) and then challenged with NAP at TAN = 3.5 and TAN = 6.5. Points are average values while errors bars indicate the highest and lowest value obtained on multiple samples exposed in the same experiment.

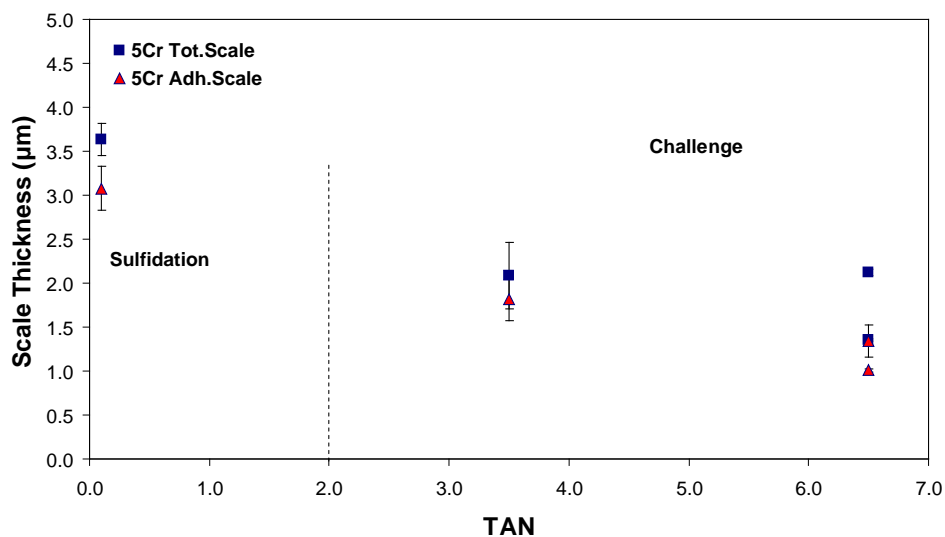


**Figure 82.** Scale thickness on 5Cr steel specimens that were presulfided with BBB VGO (*neat*) and then challenged with NAP at TAN = 3.5 and TAN = 6.5. Points are average values while errors bars indicate the highest and lowest value obtained on multiple samples exposed in the same experiment.

The higher corrosion rates for 5Cr than for CS can be explained by a different scale structure that was found on the specimens at the end of the tests. On 5Cr the scale was

almost completely removed after the TAN 6.5 challenge, whereas on CS most of the scale survived the high challenge. The scale thickness on CS was 4-5 times thicker than on 5Cr as it can be noticed in the SEM images (Figure 83 *a* and *b*) of scales cross-sections on the two metals.

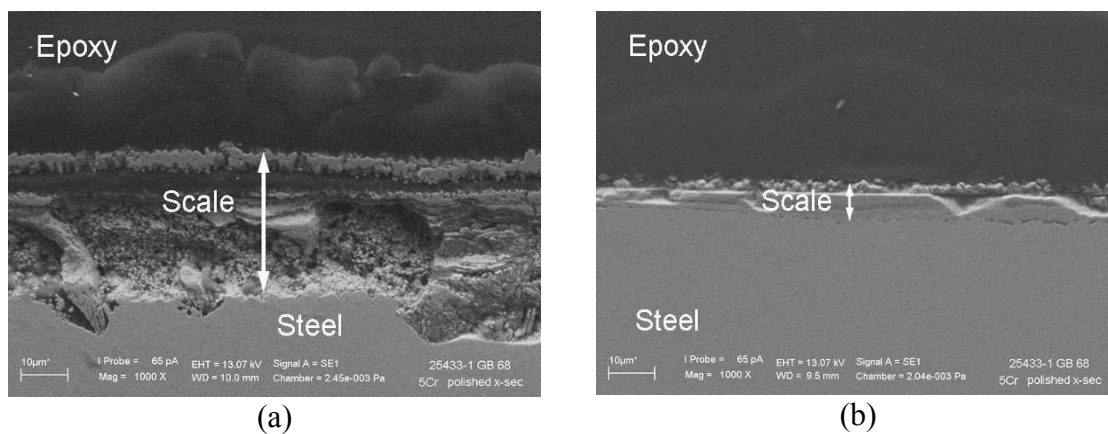


**Figure 83.** SEM images represent cross-sections on CS and 5Cr presulfided with BBB VGO (*neat*) and then challenged with NAP. FeS scale was challenged with TAN 6.5 Image *a* represents the scale formed on CS and image *b* the scale formed on 5Cr. In both images the metal is on the bottom side. Magnification in both images was 1000 X.

Another crude oil fraction, AAA VGO, was then tested in the “neat crude oil fraction” series. In contrast to the BBB VGO having the lowest TAN (<0.1), the AAA VGO had the highest acidity of all fractions: TAN = 1.75 and a rather low sulfur content S= 0.18 % w/w. In spite of its high TAN and low sulfur content the AAA VGO formed a very protective scale in case of 5Cr specimens where the scale resisted both TAN 3.5 and TAN 6.5 challenges and corrosion rates were low and almost the same as shown in Figure 84. The FeS scale formed on CS resisted only to the TAN 3.5 challenge and provided a limited protection for the metal. Further challenge with TAN 6.5 damaged the scale on CS and the corrosion rate was very high (Figure 84).

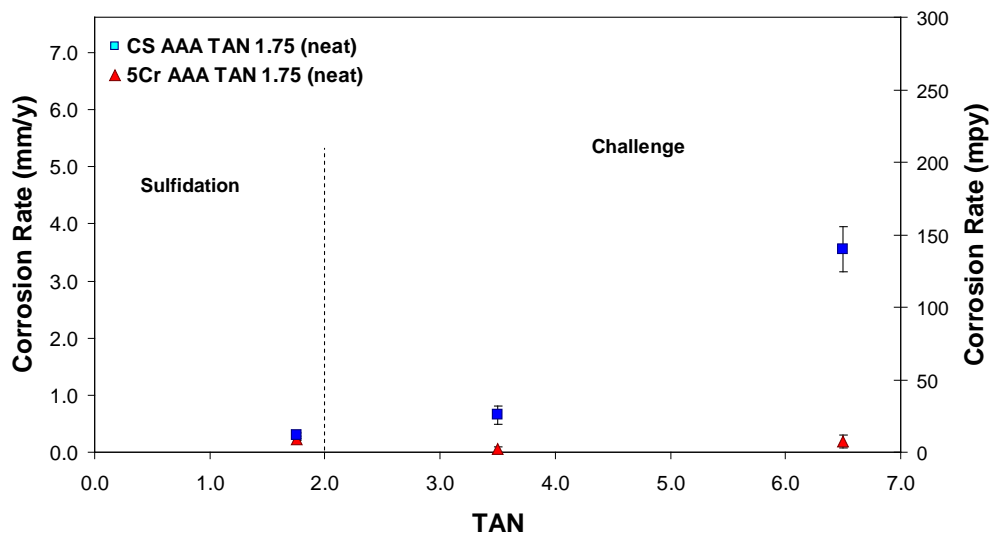


**Figure 84.** Corrosion rates for CS and 5Cr steel specimens that were presulfided with AAA VGO (*neat*) and then challenged with NAP at TAN = 3.5 and TAN = 6.5. Points are average values while errors bars indicate the highest and lowest value obtained on multiple samples exposed in the same experiment.

The scale thickness was constant and lower on 5Cr than on CS specimens where the thickness did not represent a barrier for NAP which diffused through and attacked the metal. Figure 85 presents the scale thicknesses measured on the CS specimens at the end of two challenges, whereas Figure 86 summarizes the scale thickness results for the 5Cr specimens. Appendix E includes all the scale plots as well as SEM images for these tests done with AAA VGO (*neat*).

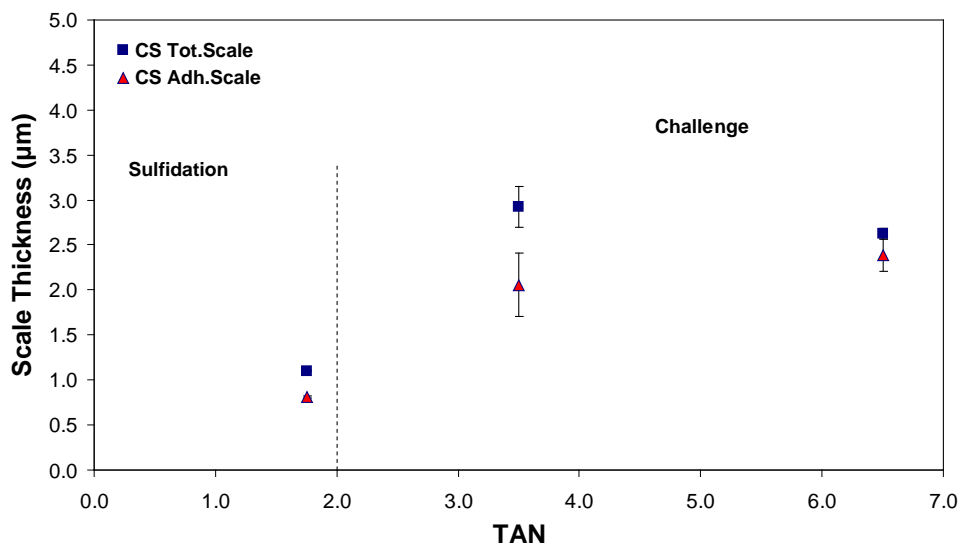


**Figure 85.** Scale thickness on CS specimens that were presulfided with AAA VGO (*neat*) and then challenged with NAP at TAN = 3.5 and TAN = 6.5. Points are average values while errors bars indicate the highest and lowest value obtained on multiple samples exposed in the same experiment.

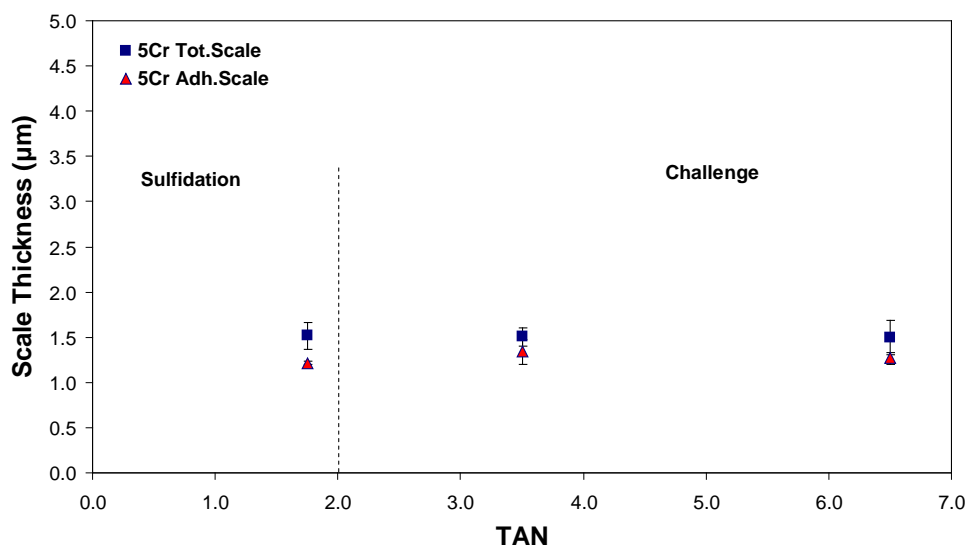


**Figure 86.** Corrosion rates for CS and 5Cr steel specimens that were presulfided with AAA VGO (*neat*) and then challenged with NAP at TAN = 3.5 and TAN = 6.5. Points are average values while errors bars indicate the highest and lowest value obtained on multiple samples exposed in the same experiment.

The SEM images for the FeS scales challenged with TAN 6.5 are included in Figure 87. Thus Figure 87 *a* represents the cross-section on the CS specimen. The scale was

fragmented by the NAP acid attack which diffused through, reaching the metal surface and producing deep pits. This massive NAP attack in the case of TAN 6.5 challenge was also demonstrated by the high CS corrosion rates. The 5Cr specimens had a constant and low corrosion rate in both challenge tests. As Figure 87 *b* shows, the scale formed on the 5Cr steel was relatively thin compared to the CS case but offered a better protection against corrosive NAP acids.

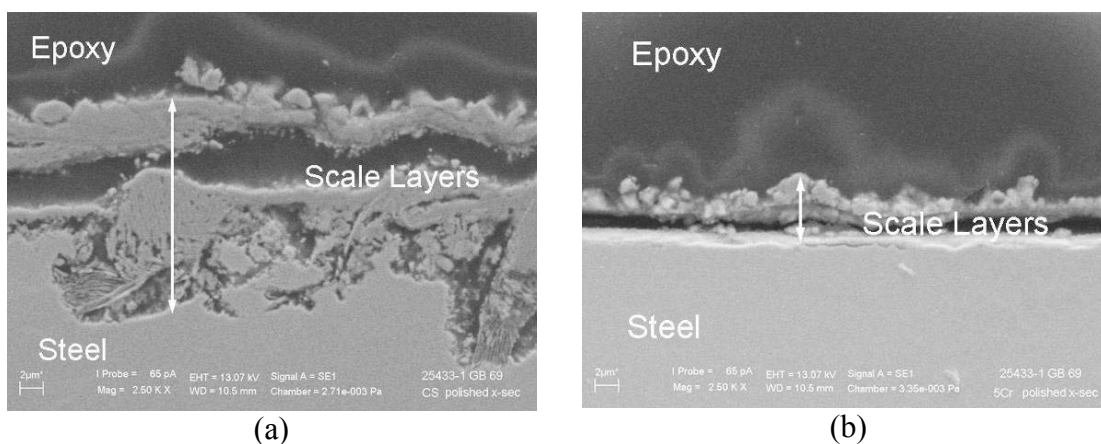


**Figure 87.** SEM images represent cross-sections on CS and 5Cr presulfided with AAA VGO (*neat*) and then challenged with NAP (TAN 6.5). Image *a* represents the scale formed on CS and image *b* the scale formed on 5Cr. In both images metal is on the bottom side.

The last crude oil fraction that was tested besides in the “neat crude oil fractions” series was the CCC 650+ which had both high acids: TAN = 1 and sulfur: S = 1.51. As Figure 88 shows the corrosion rates for the TAN 6.5 challenge were very high especially in the 5Cr case. This means that the scale formed from CCC could not protect the metals against a high TAN attack. The FeS scale was only protective against the TAN 3.5 challenge where both CS and 5Cr had similar low corrosion rates.

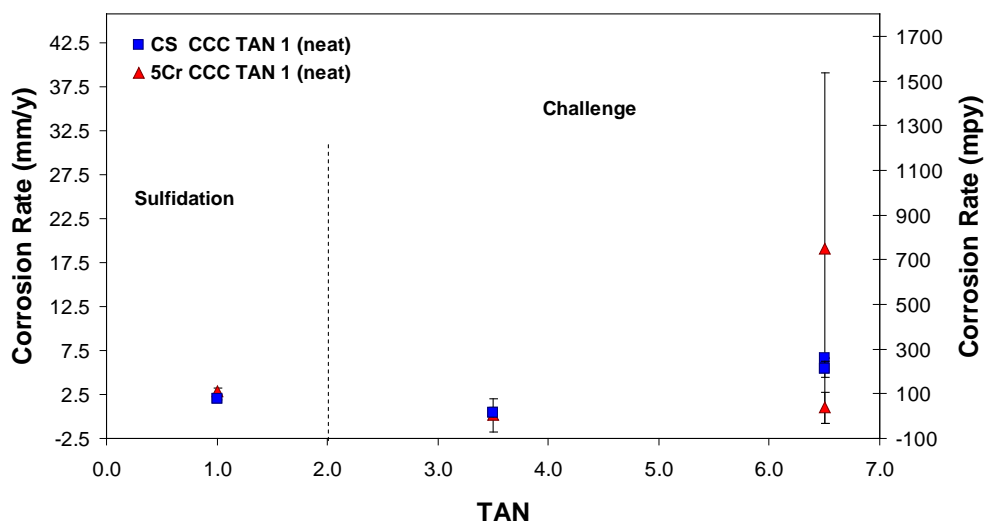


**Figure 88.** Corrosion rates for CS and 5Cr steel specimens that were with CCC 650+ (*neat*) and then challenged with NAP at TAN = 3.5 and TAN = 6.5. Points are average values while errors bars indicate the highest and lowest value obtained on multiple samples exposed in the same experiment.

The CCC fraction was very viscous with a consistency like peanut butter. This caused difficulties in evaluating scale thickness by weight measurements at the end of the tests when some of the CCC fraction remained on the specimens covering the scale. However it was possible to measure the scale thicknesses at the end of the challenge test and the corresponding results are included in Figure 89 for CS and in Figure 90 for 5Cr. The CS scale had two very different thicknesses in the two TAN 6.5 tests. However these could be the consequence of the viscous properties of the CCC which made it difficult to get reproducible results. In the 5Cr case, the scale found on specimens was almost the same in two tests done at TAN 6.5 challenge and very close to those of the TAN 3.5 challenge. These results were not in agreement with the measured 5Cr corrosion rates which were very high for the 5Cr steel.

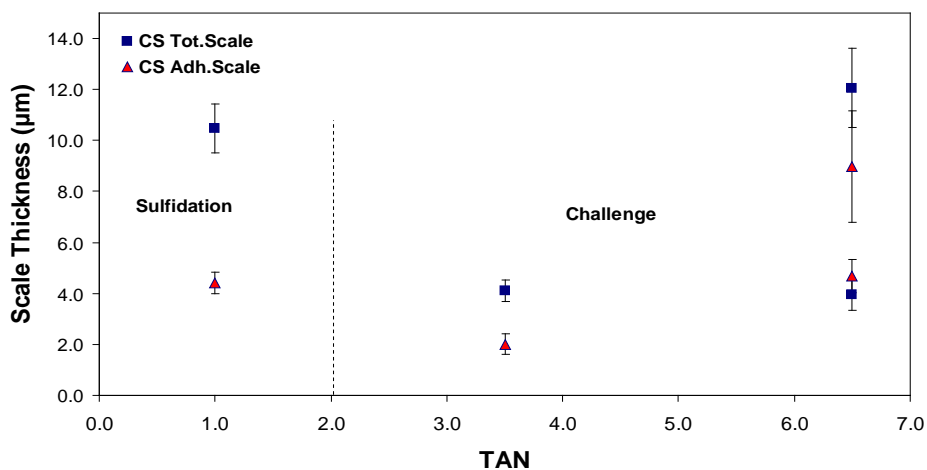


**Figure 89.** Scale thickness for CS specimens that were presulfided with CCC 650+ (*neat*) and then challenged with NAP at TAN = 3.5 and TAN = 6.5. Points are average values while errors bars indicate the highest and lowest value obtained on multiple samples exposed in the same experiment.

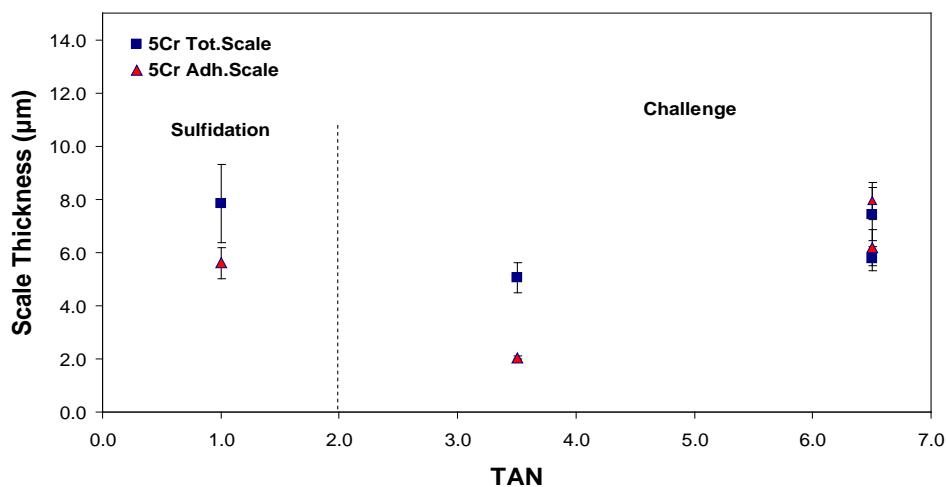


**Figure 90.** Corrosion rates for CS and 5Cr steel specimens that were presulfided with CCC 650+ (*neat*) and then challenged with NAP at TAN = 3.5 and TAN = 6.5. Points are average values while errors bars indicate the highest and lowest value obtained on multiple samples exposed in the same experiment.

The SEM analysis compares the two specimens pretreated with CCC 650+ and then challenged with NAP (Figure 91). The scale shows similar multilayer structures on both

steel types. However, apparently the NAP diffused through these scales and attacked the metal surface causing pits that can be noticed both on the CS (Figure 91 - *a*) and on 5Cr steel (Figure 91 - *b*).

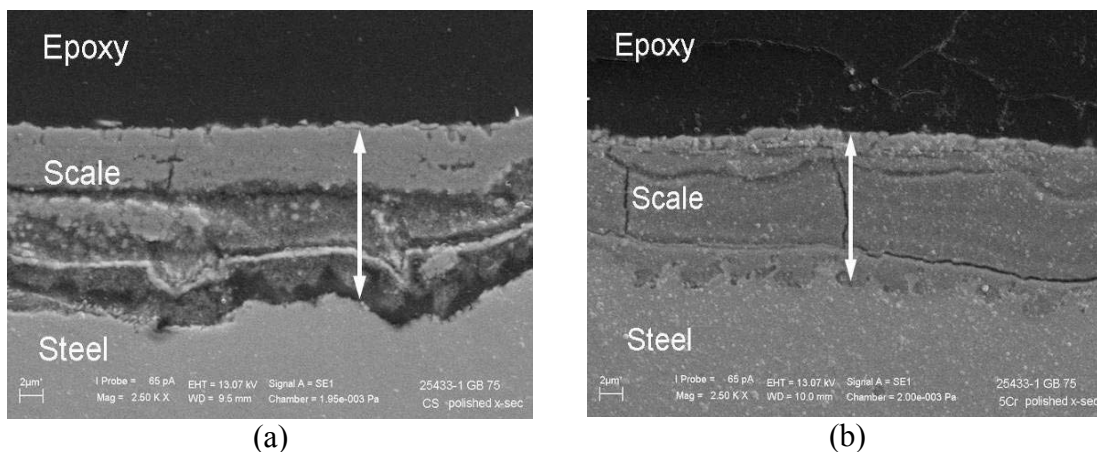


**Figure 91.** SEM images represent cross-sections on CS and 5Cr presulfided with CCC 650+ (*neat*) and then challenged with NAP (TAN 6.5). Image *a* represents the scale formed on CS and image *b* the scale formed on 5Cr. In both images metal is on the bottom side.

#### 6.4.4.1 Summary

The test results of crude oil fractions demonstrated that it is not possible to predict the protectiveness of the FeS scale based only on sulfur content of fractions generating the scales. However based on the same neat fractions results it was possible to formulate a procedure that can be used in testing crude oil fractions.

#### 6.4.5 High TAN Spiked Crude Oil Fractions Tests

The last set of experiments using real crude oil fractions investigated if the scale protectiveness improves when a high NAP concentration is used during its formation. This assumption was inspired by results of the AAA VGO testing when, in spite of its high TAN level, the fraction proved to be very protective against acidic challenges.

Because the AAA VGO results were considered as references for this part it was decided to spike some other fractions to TAN = 1.75 which is the original AAA TAN value and then build up scales with them. The HH1 VGO, BBB VGO, CCC 650+, and Yellow oil were selected for these experiments. Each one of them was spiked with NAP to TAN = 1.75 and then used to generate FeS scales.

The spiked Yellow oil formed scales that were able to protect both CS and 5Cr during the TAN 3.5 challenge but for TAN 6.5 challenge the scales protected only the 5Cr and failed in the case of CS. These differences in FeS scale protectiveness are reflected in corrosion rates evaluated for both steel types and plotted in Figure 92. As in most of the previous tests, the 5Cr steel had low corrosion rates after both challenges whereas in the CS case corrosion rates were increasing slowly for TAN 3.5 and faster for TAN 6.5 challenge. Spiked Yellow oil (TAN 1.75) formed more scale on CS (Figure 93) than on 5Cr (Figure 94). In spite of the thicker layer on CS, the corresponding corrosion rates were very high demonstrating the lesser quality of the FeS scale generated at higher TAN. The 5Cr steel as in most of previous tests “won” the corrosion “battle” over CS. Covered by a thinner scale than CS, the 5Cr steel had lower corrosion rates, all these results being similar to what was seen before with the neat Yellow oil.

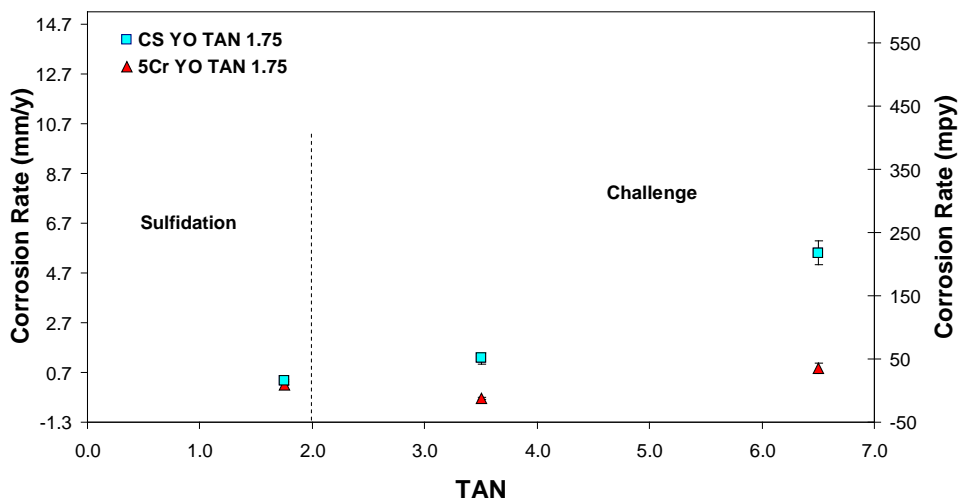


**Figure 92.** Corrosion rates for CS and 5Cr steel specimens that were presulfided with Yellow oil spiked to TAN 1.75 and then challenged with NAP at TAN = 3.5 and TAN = 6.5. Points are average values while errors bars indicate the highest and lowest value obtained on multiple samples exposed in the same experiment.

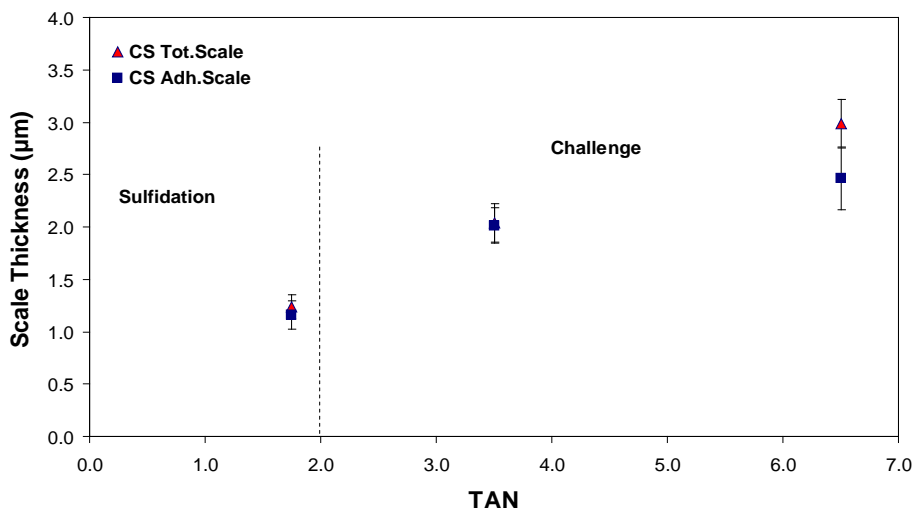


**Figure 93.** Scale thickness measured on CS specimens presulfided with Yellow oil spiked to TAN 1.75 and then challenged with NAP at TAN = 3.5 and TAN = 6.5. Points are average values while errors bars indicate the highest and lowest value obtained on multiple samples exposed in the same experiment.

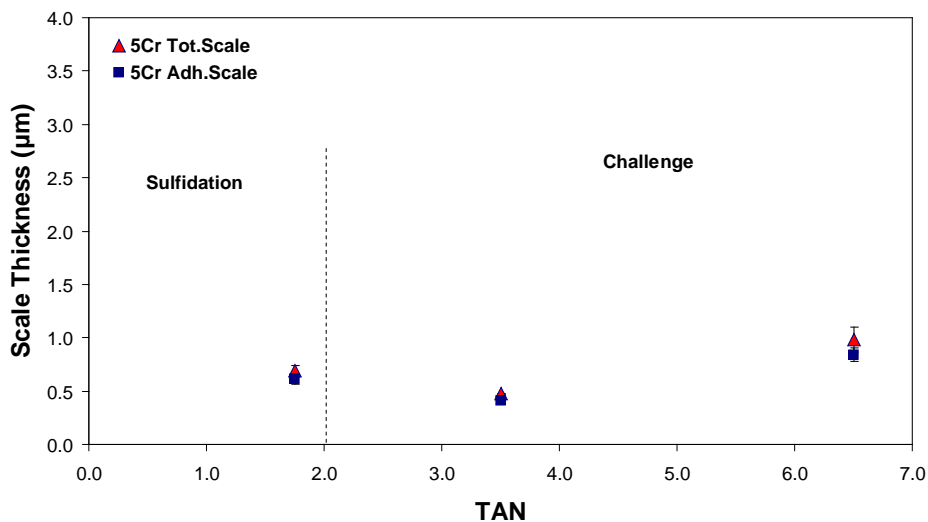


**Figure 94.** Scale thickness measured on 5Cr specimens that were presulfided with Yellow oil spiked to TAN 1.75 and then challenged with NAP at TAN = 3.5 and TAN = 6.5. Points are average values while errors bars indicate the highest and lowest value obtained on multiple samples exposed in the same experiment.

The SEM images (Figure 95) reveal the differences in scale structure formed on the CS and 5Cr steel with spiked Yellow oil. The FeS scale formed on CS was thick but with a very fragmented structure (Figure 95 - *a*). It is certain that the NAP diffused easily across this scale and caused the deep attack. The scale formed on 5Cr steel was thinner and adherent, protecting the metal surface very well (Figure 95 - *b*). No pits could be identified on the cross section of the 5Cr steel specimen surface.

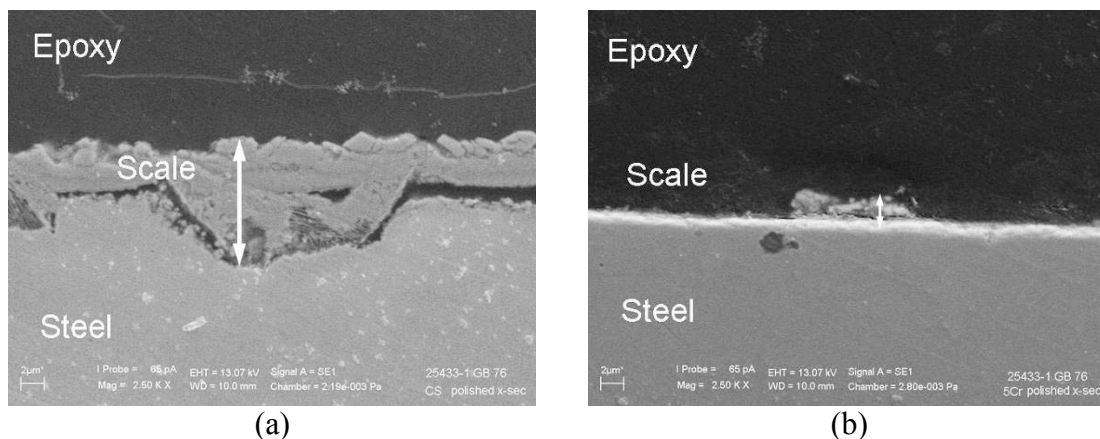


**Figure 95.** SEM images represent cross-sections on CS and 5Cr presulfidated with Yellow oil spiked to TAN 1.75 and then challenged with NAP (TAN 6.5). Image *a* represents the scale formed on CS and image *b* the scale formed on 5Cr. In both images metal is on the bottom side.

As it was previously shown, the HH1 VGO formed FeS scales with reduced protectiveness for CS and 5Cr regardless the whether it was used for sulfidation (diluted or undiluted). When spiked to TAN 1.75, the HH1 produced a scale that protected very well on 5Cr, but failed again to protect in the CS case. Thus Figure 96 presents the comparison of corrosion rates evaluated for CS and 5Cr after they have been presulfidated with spiked HH1 and then challenged with low and high TAN. Although CS corrosion rates for sulfidation and TAN 3.5 challenge were close, both rates were located in the high range (1-1.5 mm/y). Thus the spiked HH1 was not efficient in protecting CS but worked for 5Cr which had very low corrosion rates. Both plots for scale thickness formed on CS and 5Cr steel showed a very thin layer that survived the challenge. The scale thickness on CS was almost the same at the end of each test (Figure 97) but the TAN 6.5 succeeded to impair its protectiveness and generated a high corrosion rate. Figure 98 presents a thin scale formed 5Cr specimens that protected efficiently.

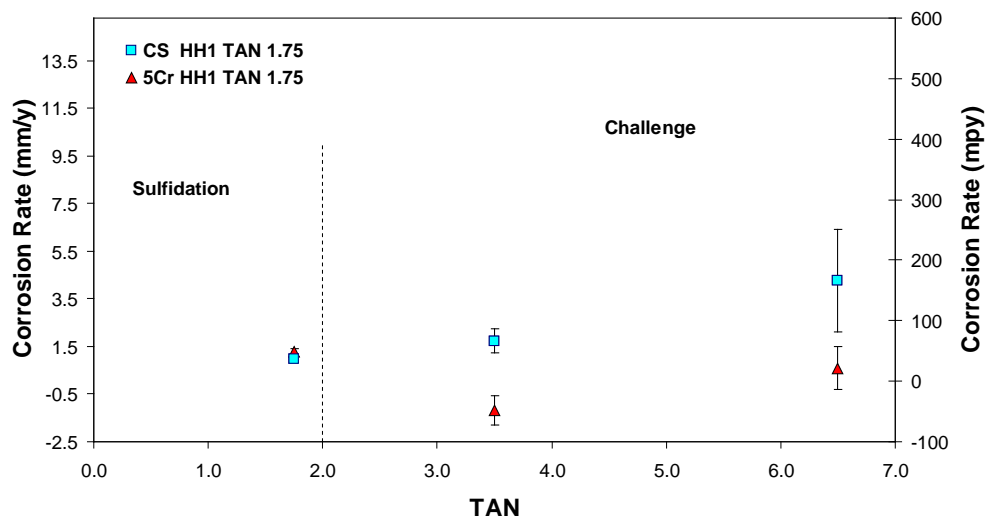


**Figure 96.** Corrosion rates for CS and 5Cr steel specimens that were presulfided with HH1 VGO spiked to TAN 1.75 and then challenged with NAP at TAN = 3.5 and TAN = 6.5. Points are average values while errors bars indicate the highest and lowest value obtained on multiple samples exposed in the same experiment.

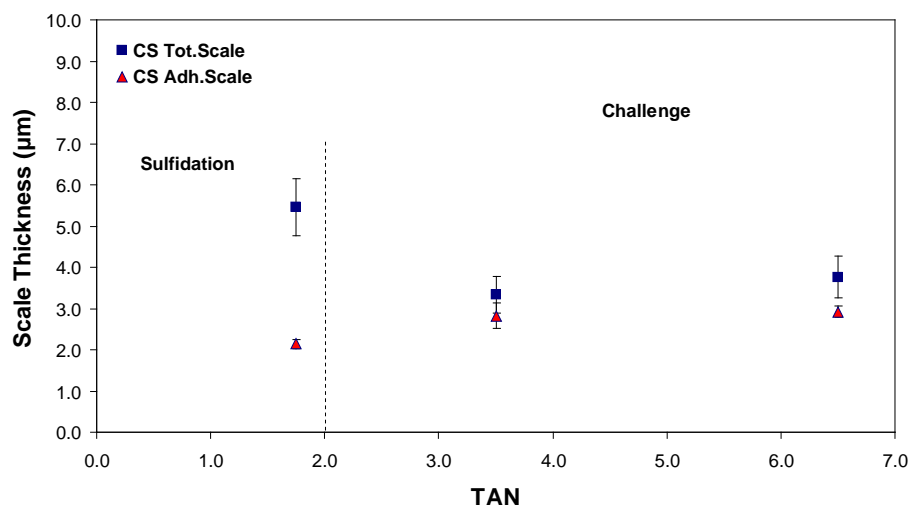


**Figure 97.** Scale thickness on CS specimens presulfided with HH1 VGO spiked to TAN 1.75 and then challenged with NAP at TAN = 3.5 and TAN = 6.5. Points are average values while errors bars indicate the highest and lowest value obtained on multiple samples exposed in the same experiment.

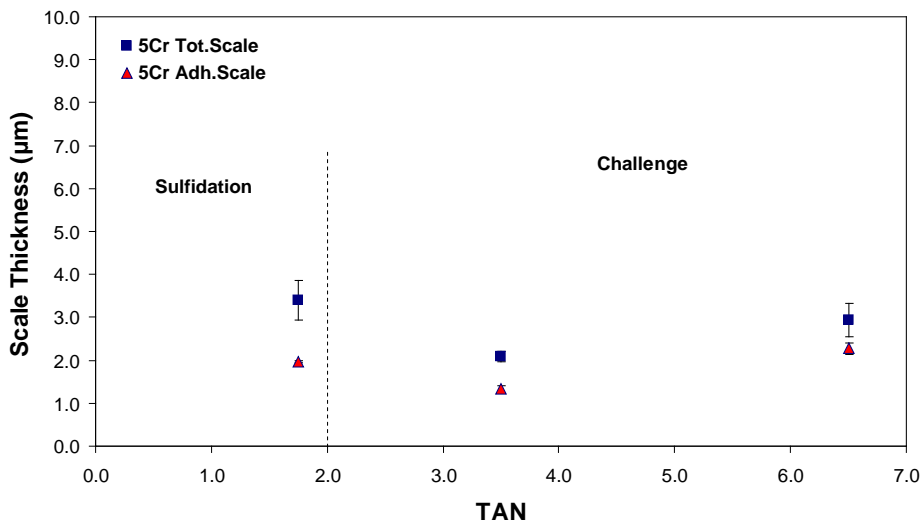


**Figure 98.** Scale thickness on 5Cr steel specimens that were presulfided with HH1 VGO spiked to TAN 1.75 and then challenged with NAP at TAN = 3.5 and TAN = 6.5. Points are average values while errors bars indicate the highest and lowest value obtained on multiple samples exposed in the same experiment.

The scales formed on the two different steel surfaces both had multiple layers as presented in the SEM images in Figure 99. The scale layers were damaged by the acidic attack which created voids between the FeS layers and the metal surface (Figure 99 - *a*). In Figure 99 - *b* it is thought that the scale was detached from the metal surface during sample preparation for the SEM analysis. In spite of this artifact caused by epoxy curing it is obvious that the FeS scale formed on 5Cr had a more compact structure than the scale on CS i.e. the “bottom” layers were not damaged by the acidic attack. These arguments are supported by the low corrosion rate of 5Cr covered by this protective scale.

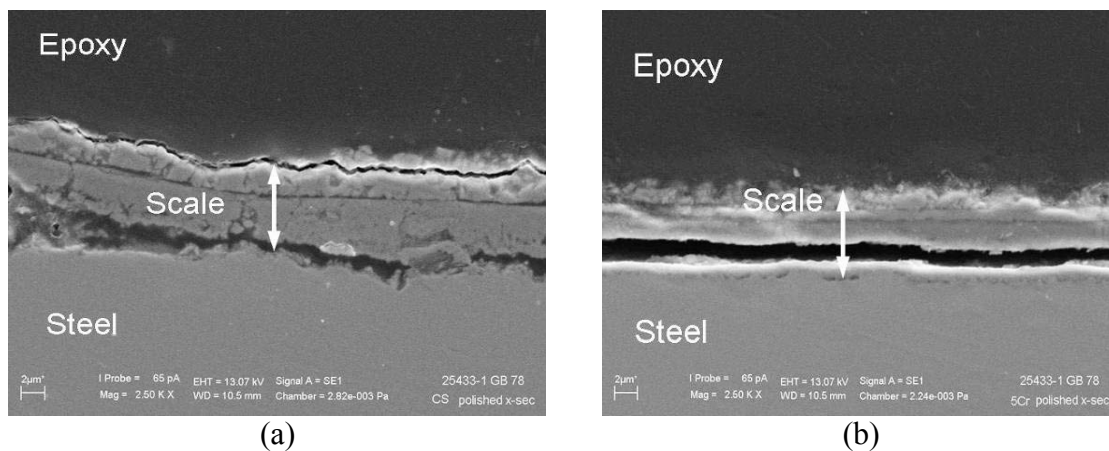


**Figure 99.** SEM images represent cross-sections on CS and 5Cr presulfidized with HH1 VGO spiked to TAN 1.75 and then challenged with NAP acids (TAN 6.5). Image *a* represents the scale formed on CS and image *b* the scale formed on 5Cr. In both images the metal is on the bottom side.

As a neat fraction, BBB VGO had the lowest TAN value ( $<0.1$ ) and sulfur content (0.6% w/w). Spiked to TAN = 1.75 BBB VGO failed in generating a more protective FeS scale. Thus in both the TAN 3.5 and TAN 6.5 challenges, the final corrosion rates of CS and 5Cr spread over a very large region with very high maximum values (Figure 100). The TAN 3.5 challenge test was repeated twice, but in both cases the corrosion rates were high and overlapped for the two steels. The conclusion was that the spiking – i.e. increased TAN value during sulfidation – did not improve the scale generated by BBB VGO.

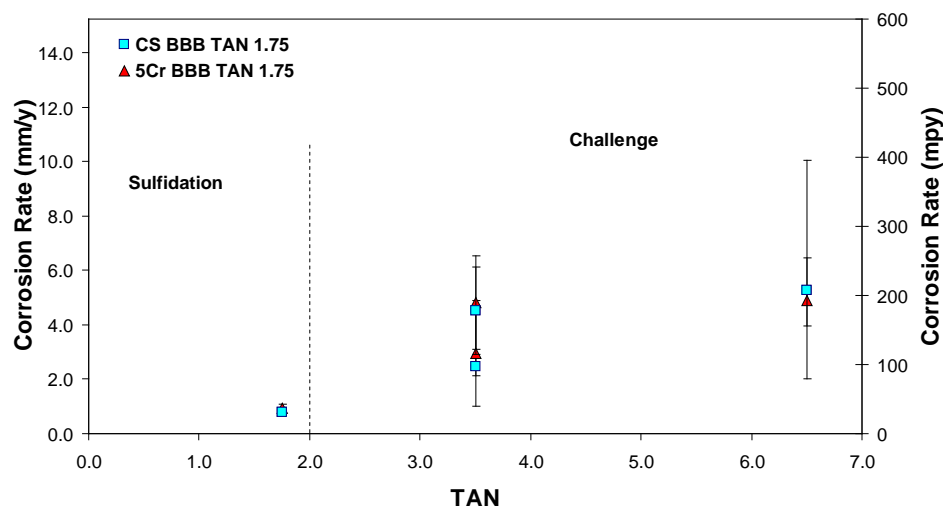


**Figure 100.** Corrosion rates for CS and 5Cr steel specimens that were presulfided with BBB VGO spiked to TAN 1.75 and then challenged with NAP at TAN = 3.5 and TAN = 6.5. Points are average values while errors bars indicate the highest and lowest value obtained on multiple samples exposed in the same experiment.

Although less scale was formed on 5Cr specimens (Figure 102) than on CS (Figure 101) the quality of both scales was similar because the corrosion rates were almost identical for both steel types when they were challenged with TAN 3.5. These TAN 3.5 challenge results overlapped within the error range of the TAN 6.5 challenge results demonstrating that spiking BBB VGO to a higher TAN did not improve the scale protective qualities.

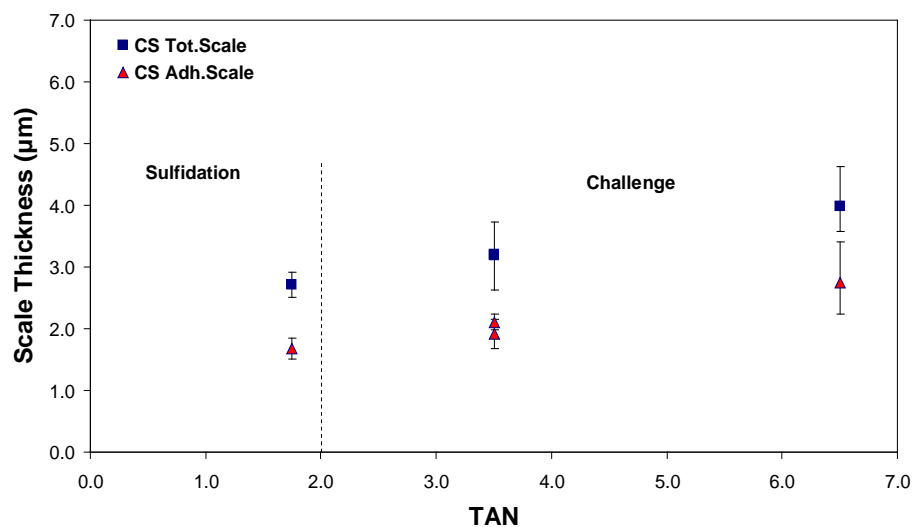


**Figure 101.** Scale thickness measured on CS specimens that were presulfided with BBB VGO spiked to TAN 1.75 and then challenged with NAP at TAN = 3.5 and TAN = 6.5. Points are average values while errors bars indicate the highest and lowest value obtained on multiple samples exposed in the same experiment.

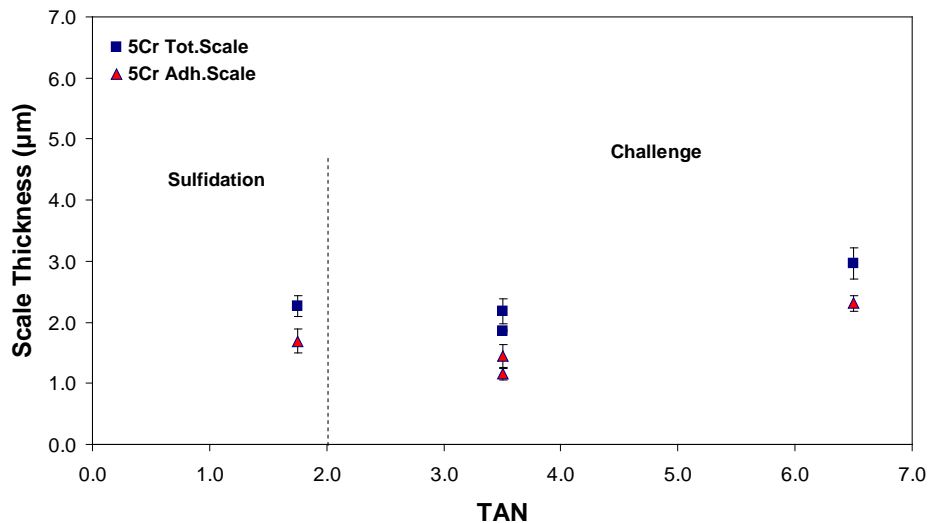


**Figure 102.** Scale thickness measured 5Cr steel specimens that were presulfided with BBB VGO spiked to TAN 1.75 and then challenged with NAP at TAN = 3.5 and TAN = 6.5. Points are average values while errors bars indicate the highest and lowest value obtained on multiple samples exposed in the same experiment.

The SEM cross-sections of the FeS scales formed with spiked BBB VGO are presented in Figure 103. The bottom layer of the scale formed on CS was almost completely destroyed by the NAP attack leaving an empty space where acids created pits on the metal surface (Figure 103 - *a*). Compared to CS, the scale generated on 5Cr was more compact and less prone to acidic attack. However NAP diffused through the consecutive layers of the scale creating pits on the 5Cr steel surface as well.

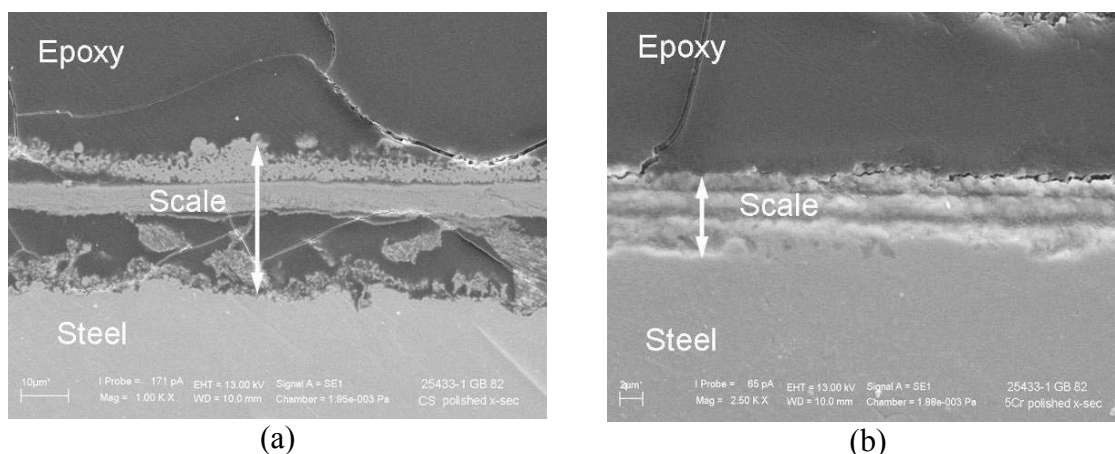


**Figure 103.** SEM images represent cross-sections on CS and 5Cr presulfided with BBB VGO spiked to TAN 1.75 and then challenged with NAP acids (TAN 6.5). Image *a* represents the scale formed on CS and image *b* the scale formed on 5Cr. In both images the metal is on the bottom side.

Testing of the crude oil fraction CCC 650+ concluded the “spiked fractions” test series. The CCC already had a high TAN = 1 value and the highest sulfur content (1.51 % wt) of all the tested crude oil fractions. The FeS scales formed from CCC 650+ spiked to TAN 1.75 did not show better qualities against NAP challenge tests. Figure 104 presents a comparison of the corrosion rates which were measured on CS and 5Cr specimens presulfided in spiked CCC. With the exception of one result for 5Cr in TAN 6.5 challenge, all the other corrosion rates were high including those of the sulfidation test.

These high corrosion rates proved that poor protectiveness was offered by the FeS scale generated from the CCC crude oil fraction spiked to TAN 1.75.

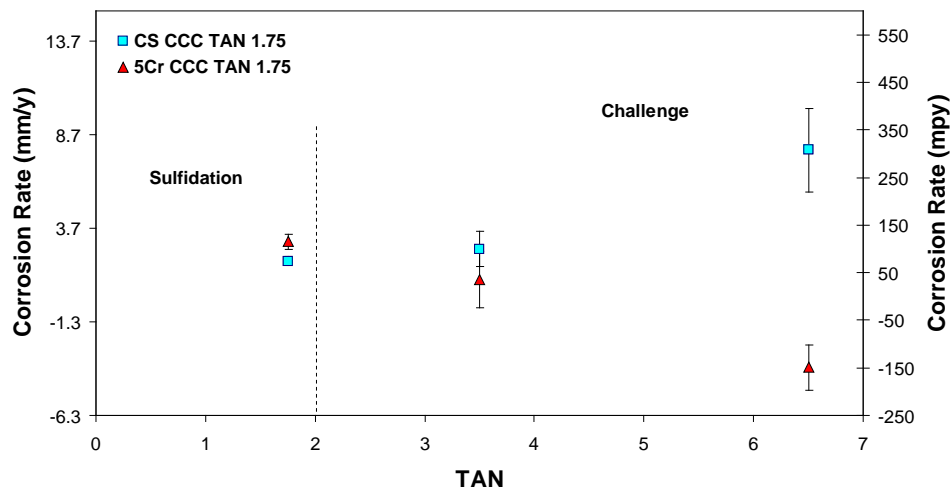


**Figure 104.** Corrosion rates for CS and 5Cr steel specimens that were presulfided with CCC 650+ spiked to TAN 1.75 and then challenged with NAP at TAN = 3.5 and TAN = 6.5. Points are average values while errors bars indicate the highest and lowest value obtained on multiple samples exposed in the same experiment.

The scale that was formed with spiked CCC 650+ at the end of TAN 3.5 and TAN 6.5 challenge tests is shown for CS (Figure 105) and 5Cr (Figure 106). On both steels, the scale thickness was low and, as it was already presented above, the corresponding corrosion rates were high in both cases. Correlating these two results sets it becomes clear that scales formed with CCC crude oil fraction offered poor protection against the TAN challenge.

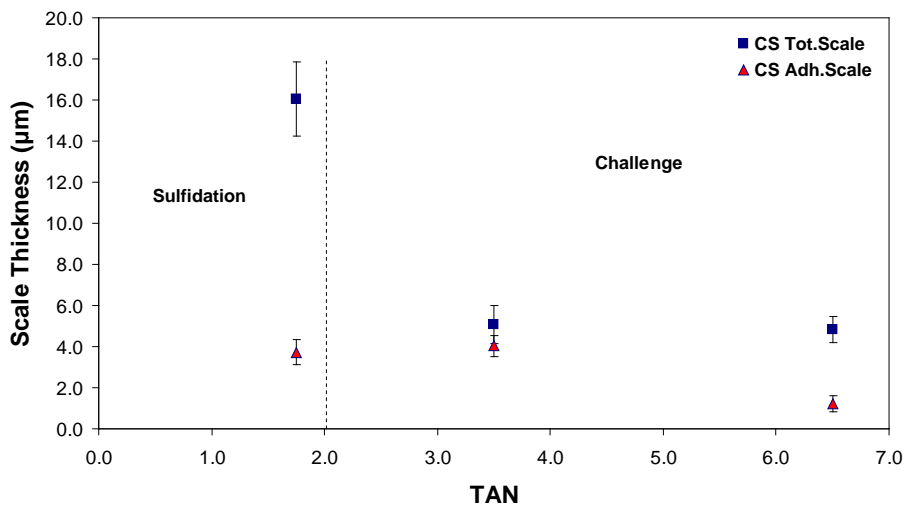


**Figure 105.** Scale thickness on CS specimens that were with CCC 650+ spiked to TAN 1.75 and then challenged with NAP at TAN = 3.5 and TAN = 6.5. Points are average values while errors bars indicate the highest and lowest value obtained on multiple samples exposed in the same experiment.

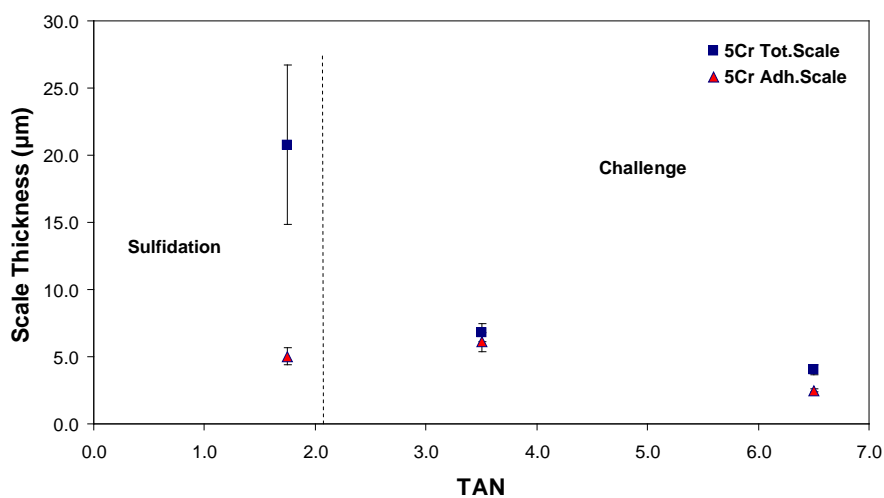


**Figure 106.** Scale thickness on 5Cr steel specimens that were presulfided with CCC 650+ spiked to TAN 1.75 and then challenged with NAP at TAN = 3.5 and TAN = 6.5. Points are average values while errors bars indicate the highest and lowest value obtained on multiple samples exposed in the same experiment.

On the SEM images (Figure 107), the scales from spiked CCC display similar multilayered structure. On CS and on 5Cr, the top scale layers delaminated under the

combined effect of NAP acids and high velocities. The differences between the two scales are found in the fine scale structure, fragmented in the case of CS and more compact for 5Cr steel. These differences were confirmed by the corresponding variation in the corrosion rates.

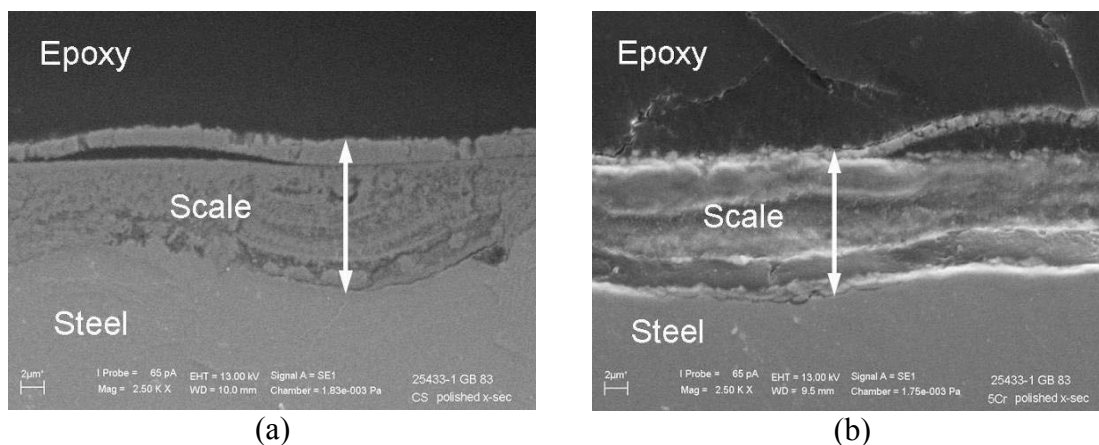


**Figure 107.** SEM images represent cross-sections on CS and 5Cr presulfided with BBB VGO spiked to TAN 1.75 and then challenged with NAP acids (TAN 6.5). Image *a* represents the scale formed on CS and image *b* the scale formed on 5Cr. In both images the metal is on the bottom side.

The conclusion based on this series of experiments was that NAP concentration increase did not improve the qualities of FeS scales generated by real crude oil fraction. A high TAN had an opposite effect on the newly formed scales making them less protective against further acidic attack.

#### 6.4.5.1 Summary

Real crude oil fractions with low TAN and reactive sulfur concentrations were used to form FeS scales on CS and 5Cr specimens. Presulfided CS and 5Cr specimens were later challenged with NAP to estimate the FeS scale protectiveness. The protectiveness of the scales were evaluated by comparing corrosion rates measured at the

end of high and low TAN challenges on both steel types. Scale evaluation tests were run with real crude oil fractions in their original form (neat), diluted to a low TAN, and spiked to a higher TAN.

The FeS scales formed with diluted fractions had a very low protectiveness and corresponding corrosion rates were high for both CS and 5Cr, regardless of the challenge levels. Only one crude oil fraction, DDD, was able to build up protective scales that lowered the CRs for both steel types.

In the case of TAN 3.5 challenges all scales protected both steel types very efficiently. The corrosion rates of the TAN 6.5 challenges showed that some scales like those from AAA, CCC, and DDD crude fractions were protective only for 5Cr and failed for CS.

Increasing the NAP acid content of fractions to TAN 1.75 did not improve scale protectiveness. All corrosion rates for CS and 5Cr were higher for spiked fractions or were in the same range.

#### ***6.4.6 Special Corrosion Tests Using Only Naphthenic Acids***

A few special NAP corrosion tests were run at the end of this research project. These tests were not strictly related to crude oil fractions, but their final results were needed for the modeling part. Therefore it was decided to include them at the end of the description of the experimental part of this project.

All previous experiments investigated the NAP corrosive effect in environments with oils having different sulfur content. It was already described and experimentally proven that reactive sulfur mitigates NAP corrosive effects by building FeS scales on

metal surfaces. The question was raised about how high would the corrosion rates be when steel was attacked by NAP in the absence of any sulfur? The answer to this question was given by results of several tests done with acidic white oil. The white oil was spiked with naphthenic acids and was then allowed to attack the CS and 5Cr specimens in the HVR under high temperature and high velocity conditions identical to those in previous tests. Time exposure was limited to 24 h and the TAN concentrations were those used in all previous challenge tests i.e. TAN: 0.1, 2, 3.5, 5, 6.5 and 8. Final corrosion rates evaluated in NAP acids corrosion tests are presented in Figure 108. Comparing the results presented in Figure 108, it is clear that at relatively low TAN values (TAN 1 - 5), the 5Cr steel showed a better resistance to NAP attack than CS under identical conditions. However the turning point in corrosive attack was represented by TAN 6.5 when both steel types had almost identical and high corrosion rates. TAN 8 also generated very high CRs for both steels.

Protective effect of the sulfide scales against NAP corrosion is very well illustrated in the two comparisons presented bellow in Figure 109 and Figure 110. Figure 109 compares corrosion rates for CS generated by NAP in the absence of sulfur to corrosion rates of CS that have been presulfided in Yellow oil before the challenge tests. For CS specimens significant differences of CRs appeared even at low TAN = 2 and they became bigger as the TAN level is increased.

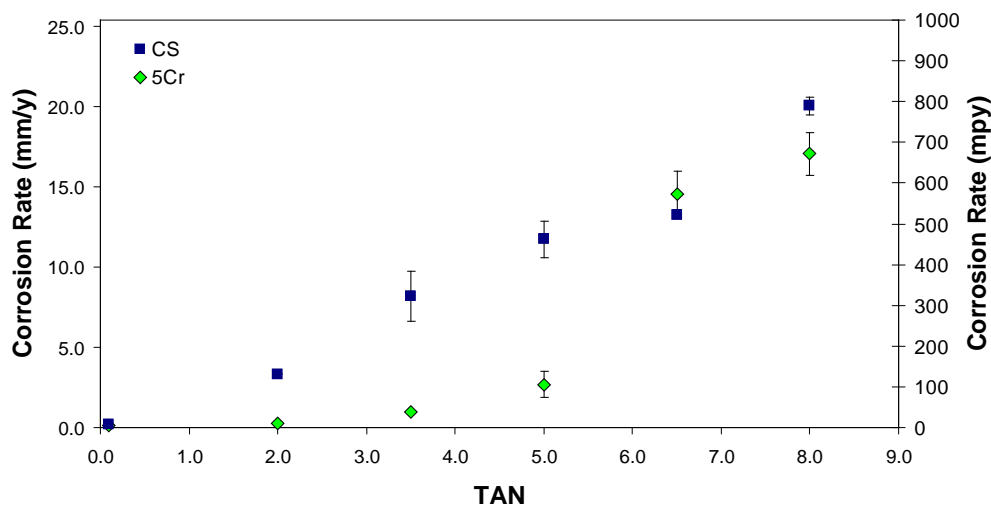


**Figure 108.** Comparison of corrosion rates for CS and 5Cr steel specimens challenged with different TAN concentrations in the absence of sulfur compounds. Tests were run for 24 h at 343°C (650°F). Points are average values while errors bars indicate the highest and lowest value obtained on multiple samples exposed in the same experiment.

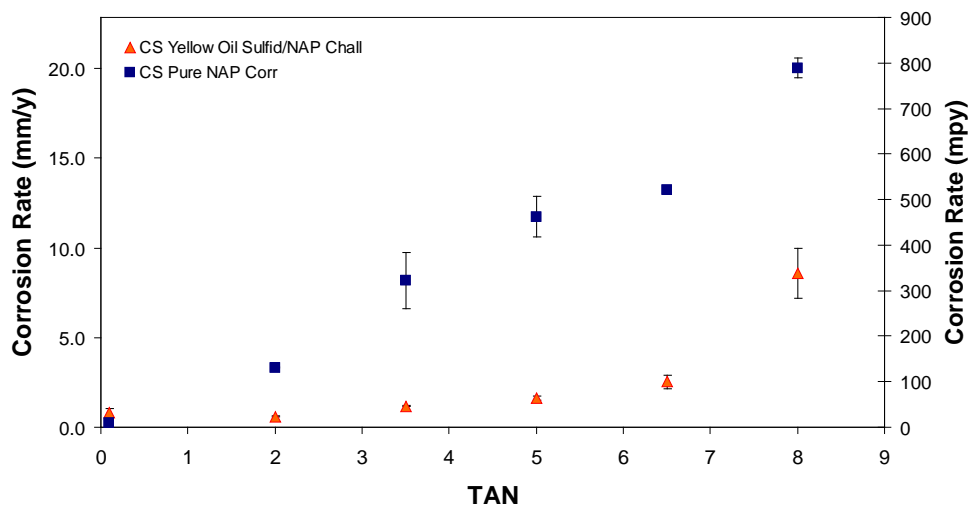


**Figure 109.** NAP corrosion of presulfided CS specimens vs. NAP corrosion of CS specimens in the absence of sulfur. Tests were run for 24 hr at 343°C (650°F). Points are average values while errors bars indicate the highest and lowest value obtained on multiple samples exposed in the same experiment.

In the case of 5Cr specimens (Figure 110) the FeS scale was able to protect the metal surfaces and to keep the corrosion rates low all along the TAN series. However the

5Cr steel resisted to pure NAP attack at low TAN concentrations even in the absence of a protective FeS scale. Only higher TAN levels starting from TAN = 5 broke the corrosion resistance of 5Cr in the absence of a protective scale and brought it to similar corrosion rates as for the CS.

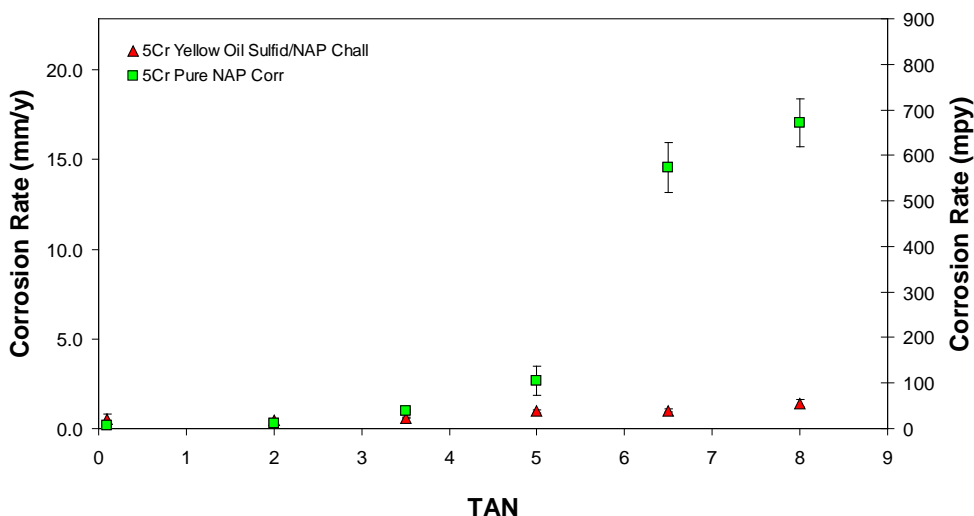


**Figure 110.** NAP corrosion of presulfided 5Cr specimens vs. NAP corrosion of 5Cr specimens in the absence of sulfur. Tests were run for 24 hr at 343°C (650°F). Points are average values while errors bars indicate the highest and lowest value obtained on multiple samples exposed in the same experiment.

The final conclusion of these results is that 5Cr steel showed a better resistance than CS against NAP acids corrosion especially when the environment contained reactive sulfur compounds. In the absence of sulfur, the 5Cr steel resistance was limited and efficient only at low TAN values. Beyond TAN = 5 both CS and 5Cr were strongly corroded and had similar corrosion rates. Considering that in real refinery cases sulfur compounds cannot be eliminated, the pure NAP acids corrosion becomes important only

in those specific locations where sulfide scales are removed or do not form such as in transfer lines.<sup>5,6,72</sup>

## CHAPTER 7: MECHANISTIC MODEL OF NAPHTHENIC ACID CORROSION

### 7.1 Introduction

There is no work in the current literature where a comprehensive mechanism or a model for naphthenic acid corrosion is proposed. Some papers mentioned the models of NAP corrosion are developed but did not give any details whether they were finished and validated.<sup>69</sup> Thus this work is the first attempt to propose a detailed model for naphthenic corrosion at high temperature and high velocity conditions. The model consists of two main parts: a *corrosion model* that covers both sulfidation attack and naphthenic acid attack on the metal surface and the *scaling model* which focuses on scale formation and scale damage under the combined action of mechanical and chemical factors. The following paragraphs will describe briefly the way in which the basic concepts of corrosion and mass transfer were used and assembled together to build the model of naphthenic corrosion.

Experimental data proved that, in oil environments containing both sulfur and naphthenic acids, iron sulfide scale forms fast. The sulfur compounds from the oil, attack the metal and generate iron sulfide through a solid state chemical reaction, which is deposited as a thin but strongly adherent film on metal surface. This FeS solid state film reduces the corrosion rate (Figure 111). Reactive species are depleted at the metal surface while corrosion products accumulate on the steel surface. Thus a concentration gradient is established on both sides of the thin film. As a result of further corrosion, more FeS is generated on the outer side of the thin film, via  $\text{Fe}^{2+}$  solid state diffusion through the thin film, leading to film undermining or/and at the inner side of the thin film via  $\text{S}^{2-}$  solid

state counter-diffusion, leading to internal stresses. Regardless of which of these is more intense, film cracking will occur either due to loss of support at the steel surface, internal stresses or both. Cracks produced in the film structure will allow more sulfur species to reach the metal surface, react and generate FeS. Newly generated FeS under the old film will increase the stresses inducing not only cracks but also film detachment. In this way more metal surface is exposed to corrosive sulfur and the process is restarted (Figure 112). The process of continuous film regeneration by forming new FeS layers followed by film spalling will transform the thin, dense, and strongly adherent film into a thick, loose and porous FeS film that is easier to detach. However, the portion of this thick porous film structure that survives will further slow down the transport of species and reduce the sulfidation corrosion rate (Figure 113).

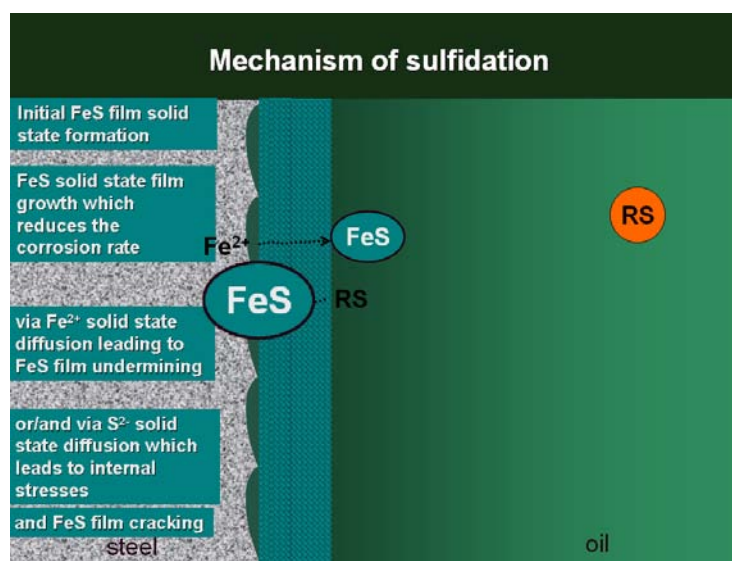


**Figure 111.** Mechanism of sulfidation at the metal-oil interface. Initial attack of sulfur species (RS) on the metal surface causing formation of successive layers of iron sulfide scale (FeS).

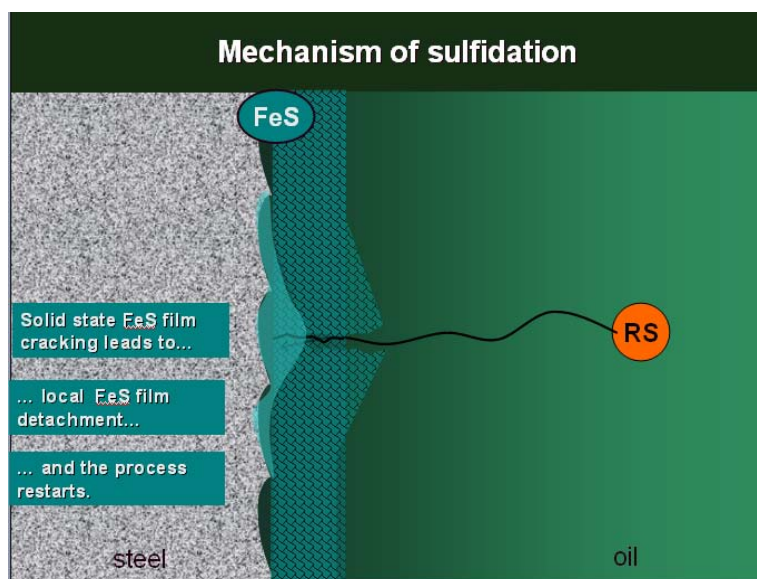


**Figure 112.** Mechanism of sulfidation at the metal-oil interface. Formation of cracks and new scale. FeS scale cracking is caused by internal stresses. Cracks in the scale allow new attacks of sulfur species on the metal exposed surface. As a result of these attacks new FeS scale is formed.

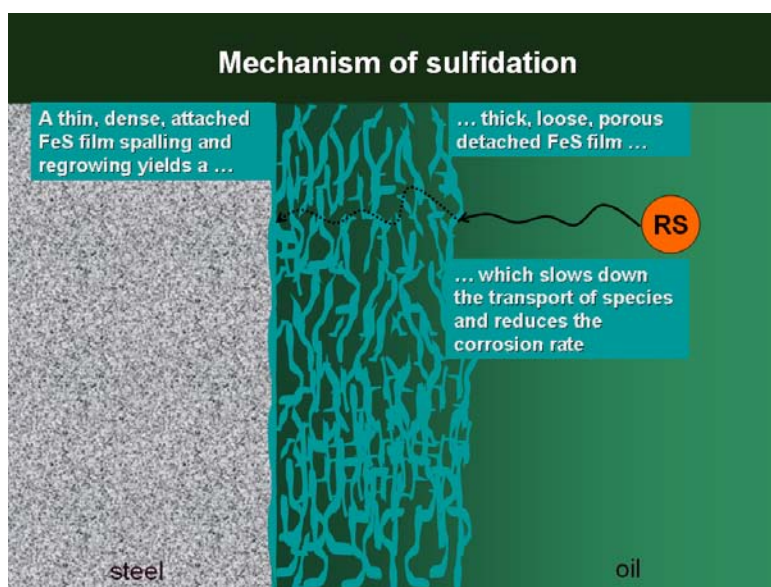


**Figure 113.** Mechanism of sulfidation at the metal-oil interface. FeS scale becomes thick and porous due to repeated forming, cracking and peeling off processes. The thick scale reduces the corrosion rate by slowing down the transport of species.

The combined actions of high flow conditions and naphthenic acid must be taken into consideration next to complete the sulfidation mechanism. The turbulent flow increases the shear stress causing the removal of the outer looser film. It also increases the convection and thus enhances the mass transfer and the corrosion caused by the presence of NAP acids (Figure 114).

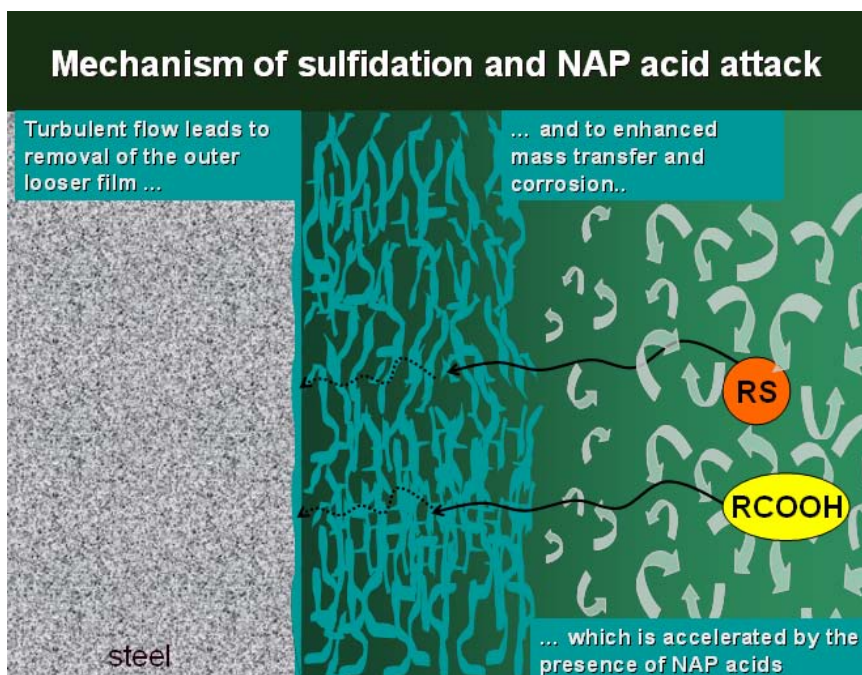


**Figure 114.** Mechanism of sulfidation at the metal-oil interface. Combined mechanism of sulfidation and acid attack. Turbulent flow removes layers of porous scale enabling naphthenic acids to attack the metal increasing the corrosion rate.

As the overall corrosion process consists of the combined effects of sulfur and naphthenic acids, it can be expressed qualitatively by Equation 12 where  $CR$  is total corrosion rate,  $SR$  represents the sulfidation rate and  $NAP$  refers strictly to naphthenic acids corrosion rate.

$$CR = SR + NAP \quad (12)$$

The above described process is more complex than adding the contributions of two major effects because other important factors interfere (i.e. temperature, velocity). Therefore the corrosive process has to be evaluated as a function of all major contributions as in Equation 13:

$$CR = f(TS, T, \delta_{os}, \dots) + f(TAN, \delta_{os}, V, T, \dots) \quad (13)$$

where:

$TS$  is the total sulfur compounds [wt %],

$T$  - temperature [ $^{\circ}K$ ],

$\delta_{os}$  - thickness of the outer sulfide scale [m],

$TAN$  - total acid number [ $mg_{KOH}/g_{oil}$ ],

$V$  - velocity [m/s].

The FeS scale offers limited protection against corrosion because it is continuously formed and removed from the metal surface and only a small part of it remains adherent. This adherent scale can be calculated from a scale formation rate equation accounting for the scale damage produced by mechanical and chemical factors that affect scale integrity. Thus the so called scale retention rate ( $SRR$ ) calculated according to Equation 14 is a difference between the sulfidation rate ( $SR$ ) and the scale damaged rate ( $SDR$ ) where  $SDR$  is represented in Equation 14 as the sum of mechanically and chemically damage scale rates ( $SDR_{mech}$  and  $SDR_{chem}$ , respectively).

$$SRR = SR - [SDR_{mech} + SDR_{chem}] \quad (14)$$

The FeS scale formation, growth, and removal are strongly dependent on total sulfur concentration in oils, TAN, temperature, velocity, thickness of scale itself.

Equation 15 expresses the scale thickness variation in time as a function of all these factors.

$$d\delta_{os}/dt = f(TS, T, \delta_{os}, \dots) - [f(V, \delta_{os}, \dots) + f(V, T, TAN, \dots)] \quad (15)$$

The following sections in this chapter will present in detail the naphthenic acid corrosion model with its main components: sulfidation rate and NAP corrosion rate.

## 7.2 Corrosion model

### 7.2.1 Sulfidation Rate (SR)

Scale formation is one of the mechanisms that govern the naphthenic acid corrosion in oil environments. The rate of scale formation is dependent of sulfur concentration in oil (TS), temperature, and thickness of the outer scale as was presented in Equation 15. Qualitatively the process is described by the following in the physico-chemical model.

### 7.2.2 Sulfidation Rate – Physico-Chemical Model

Iron sulfide (FeS) is the final product of the sulfur compounds reaction with the  $Fe^{2+}$  in the steel and is deposited on metal surfaces as a strongly adherent film. As it was mentioned before, the sulfur compounds in oil cover a large variety from simple hydrogen sulfide ( $H_2S$ ) to aliphatic and aromatic structures. The most reactive of these sulfur species is  $H_2S$  but there are also aliphatic compounds that attack the metal and aromatic structures though they have the lowest reactivity in sulfidation processes. Generally the sulfidation reaction that forms FeS on metal surface is believed to be according to Equation 16:



This reaction happened predominately via a direct heterogeneous solid state reaction at the steel surface. It is assumed that there is always a very thin ( $\ll 1\ \mu\text{m}$ ) dense film of FeS at the steel surface which acts as a solid state diffusion barrier for the sulfide species involved in the corrosion reaction. This FeS film continuously goes through a cyclic process of growth, cracking, and delamination generating the outer sulfide scale. This outer scale grows in thickness (typically  $>1\ \mu\text{m}$ ) over time and also represents a diffusion barrier for naphthenic acids and sulfur species. The outer scale is layered, very porous and rather loosely attached. The outer scale peels and spalls over the time - a process aggravated by fluid flow and naphthenic acids.

### ***7.2.3 Sulfidation Rate – Mathematical Model***

The mathematical model of sulfidation will apply the physico-chemical laws and their corresponding equations to describe formation and regeneration processes of the FeS scale.

In order to build up an appropriate mathematical model it is necessary to define the domain describing the sulfidation processes. Starting from the metal surface the domain stretches through the FeS scale layers to the bulk solution where the turbulent flow is dominant. The transport of reactive species in this domain is governed by different mechanisms influenced by local concentrations of species and different domain structures. Thus the transport of species in the superficial oil layer close to the scale surface is dominated by turbulent flow. Therefore the species transport through this boundary layer is done by convective diffusion. The flux of the species transported through convective diffusion is expressed by Equation 17.

$$Flux_{RS} = k_{m,RS} (c_{b,RS} - c_{o,RS}) \quad (17)$$

The FeS scale formed on the metal surface has a multilayer structure with different porosities and densities along its successive layers. The transport of the reactive species through the pores of scale layers is governed by molecular diffusion. The expression of the reactive species flux is given in Equation 18:

$$Flux_{RS} = \frac{D_{R-S} \epsilon \Psi}{\delta_{os}} (c_{o,RS} - c_{i,RS}) \quad (18)$$

The inner FeS film which is attached to metal surface has a very compact structure and in this region the reactive species transport is made through solid state diffusion. Thus the flux corresponding to solid state diffusion of reactive species is according to Equation 19:

$$Flux_{RS} = A_{RS} e^{-\frac{E_{RS}}{RT}} \ln \left( \frac{c_{i,RS}}{c_{s,RS}} \right) \quad (19)$$

The significance of each term in the three above mentioned equations (9-11) is as it follows:

$Flux_{RS}$  - flux of  $RS$  [ $\text{mol}/(\text{m}^2\text{s})$ ],

$k_{m,RS}$  – mass transfer coefficient for  $RS$  in the boundary layer [ $\text{m}/\text{s}$ ],

$D_{RS}$  - diffusion coefficient for dissolved  $RS$  in the oil phase [ $\text{mol}/\text{m}^3$ ],

$c_{b,RS}$  - bulk concentration of  $RS$  in the oil phase [ $\text{mol}/\text{m}^3$ ],

$c_{o,RS}$  - interfacial concentration of  $RS$  at the outer scale/oil interface, [ $\text{mol}/\text{m}^3$ ],

$c_{i,RS}$  - interfacial concentration of  $RS$  at the inner scale/film interface,  
[ $\text{mol}/\text{m}^3$ ],

$c_{s,RS}$  - concentration of  $RS$  at the steel surface [ $\text{mol}/\text{m}^3$ ],

$\delta_{os}$  - thickness of the outer scale [m],

$\epsilon, \Psi$  - outer scale porosity and tortuosity,

$R$  - universal gas constant [ $\text{J}/(\text{mol} \cdot \text{K})$ ],

$T$  - temperature [K],

$A_{RS}$  - kinetic constant [ $\text{mol}/\text{m}^2 \cdot \text{s}$ ], for reaction  $\text{Fe}_{(s)} + \text{H}_2\text{S} \rightleftharpoons \text{FeS}_{(s)} + \text{H}_2$

$E_{RS}$  - activation energy [ $\text{J}/\text{mol}$ ], for reaction  $\text{Fe}_{(s)} + \text{H}_2\text{S} \rightleftharpoons \text{FeS}_{(s)} + \text{H}_2$ .

For the steady state conditions all three diffusion fluxes  $Flux_{RS}$  are equal to each other and equal to sulfidation rate  $SR$  which has the expression as in Equation20:

$$SR = A_{RS} e^{-\frac{E_{RS}}{RT}} \ln \frac{c_{b,RS} - SR \left( \frac{\delta_{os}}{D_{RS} \epsilon \Psi} + \frac{1}{k_{m,RS}} \right)}{c_{s,RS}} \quad (20)$$

Once the expression for sulfidation rate was obtained, the next step is identifying the equation variables that are known or must be determined experimentally so that the model can calculate the sulfidation rates. Bulk concentration of  $RS$  -  $c_{b,RS}$  - is known from the sulfur content (%wt) of oil and so is the temperature -  $T$ . Variables that had to be determine experimentally are outer scale porosity  $\epsilon$ , and tortuosity  $\psi$ , kinetic constant of sulfidation  $A_{RS}$  and activation energy of sulfidation  $E_{RS}$ . Both activation energy and kinetic constant of sulfidation have been published previously. Figure 115 presents sulfidation kinetic constant  $A_{RS}$  and activation energy  $E_{RS}$ . as a function of metallurgy<sup>70</sup>.

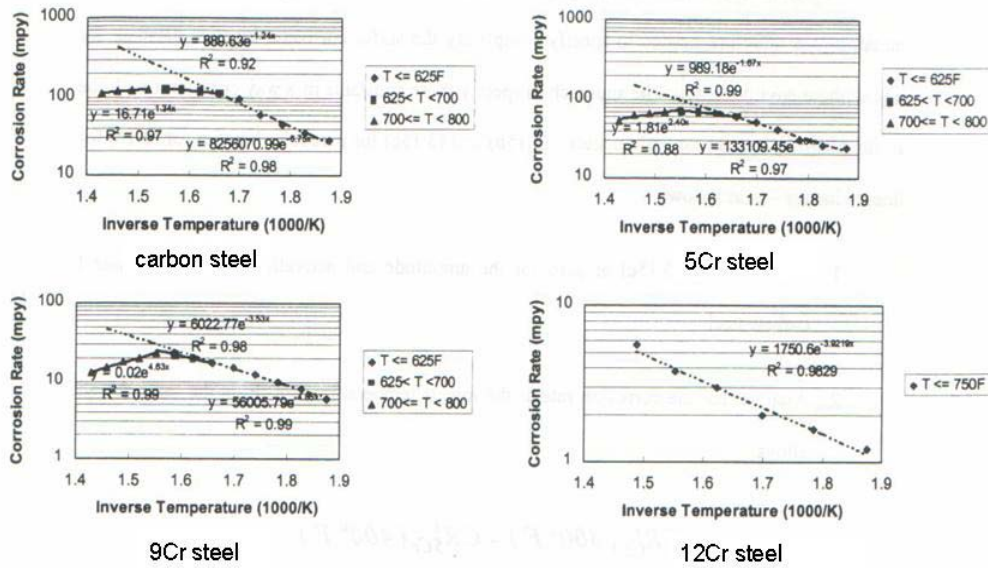


**Figure 115.** Kinetic constant  $A_{RS}$  and activation energy  $E_{RS}$  as function of metallurgy. For different steel types were included as most used as construction materials in refineries<sup>70</sup>.

The mass transfer coefficient for sulfur species  $k_{m,RS}$  at the boundary layer and the thickness  $\delta_{os}$  of the sulfur outer scale are the variables that have to be determined by the model.

The turbulent mixing is dominant in the boundary layer (flowing oil phase) influencing the mass transfer of species. Thus the mass transfer coefficient  $k_{m,RS}$  in the boundary layer is primarily dependent on the level of turbulence i.e. Reynolds and Schmidt numbers as in Equation 21:

$$k_{m,RS} = a \cdot Re^b \cdot Sc^c \tag{21}$$

where:

$$Re = \rho V d / \mu$$

$$Sc = \mu / (\rho D_{RS})$$

and for straight pipe single-phase flow according to literature:  $a = 0.0165$ ,  $b = 0.86$ , and  $c = 0.33$ .<sup>71,72</sup>

The mass transfer coefficient has also to be adjusted accordingly to the flow regime (annular-mist, bubble, bubbly, slug, etc) and to flow geometry. When flow geometry is taken into account, then Equation 21 for the mass transfer coefficient includes a geometry factor  $\xi_{geo}$  and becomes Equation 22:

$$k_{m,RS} = \xi_{geo} \cdot a \cdot Re^b \cdot Sc^c \quad (22)$$

Geometry factor  $\xi_{geo}$  had different values as function of pipe configuration, some of these values being presented in Table 12<sup>71</sup>

**Table 12.** Dimensionless factor  $\xi_{geo}$  for various piping configuration<sup>71</sup>

Pipe configuration	$\xi_{geo}$
Reducer	3.2
Expansion	3.6
Orifice	2.9
Valve/Nozzle	2
Elbow	2.1
Elbow followed by expansion	3.6
Elbow followed by reduction	3.2
Tee	5.7

#### 7.2.4 Naphthenic Acid Corrosion Rate (NAP)

As was mentioned at the beginning of this chapter the total corrosion rate  $CR$ , is the final combined result of the sulfidation  $SR$  and NAP corrosion rates (Equation 23).

$$CR = SR + NAP \quad (23)$$

Sulfidation effects on total corrosion were already described above. The NAP contribution is described by the second term of Equation 24.

$$CR = f(TS, T, \delta_{os}, \dots) + f(TAN, \delta_{os}, V, T, \dots) \quad (24)$$

where:

$TS$  - the total sulfur compounds [wt %],

$T$  - temperature [ $^{\circ}K$ ],

$\delta_{os}$  - thickness of the outer sulfide scale [m],

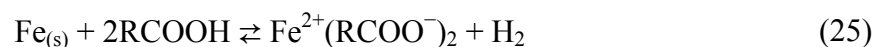
$TAN$  - total acid number [ $mg_{KOH}/g_{oil}$ ],

$V$  - velocity [m/s].

The modeling of the naphthenic acid corrosion starts with a physico-chemical model followed by a mathematical model of the process. The naphthenic acid corrosion model will be presented in a similar manner as was previously done for the sulfidation rate because the two processes evolved simultaneously under the same conditions as they are interconnected.

#### 7.2.5 Naphthenic Acid Corrosion – Physico-Chemical Model

As it was stated in current literature<sup>6,7</sup> and based on the abovementioned experimental observations, naphthenic acids attack the metal forming iron naphthenates and hydrogen (Equation 25).



This reaction happens at the metal surface where there is always a very thin ( $\ll 1\mu\text{m}$ ) and dense layer of iron sulfide. The thin film acts like a solid state diffusion barrier for all species involved in the corrosion reaction, including RCOOH. The ongoing sulfidation processes will generate more and more scale that becomes porous under the combined action of fluid turbulent flow and NAP attack. The outer layer of FeS scale represents a diffusion barrier for NAP. Therefore it is assumed that the NAP attack rate is limited by the diffusion of RCOOH through the thick and porous outer scale as well as the thin inner FeS film. The mechanism of NAP acid corrosion is presented schematically in Figure 116.

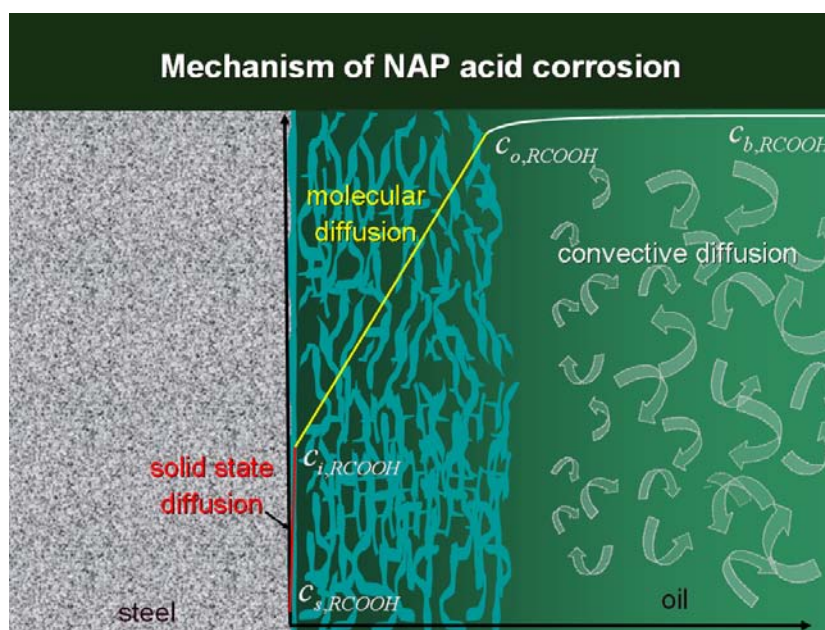


**Figure 116.** Mechanism of naphthenic acid corrosion. Naphthenic acid attack rate is limited by diffusion mechanism (convective, molecular, and solid state) as acids are transported from bulk solution towards steel surface.

In the bulk solution where turbulent flow is dominant, the NAP concentration will always be higher than at metal surface which is covered by the FeS scale. In the region outside the scale, transport of NAP is governed by convective diffusion. The fluid flow continuously refreshes NAP concentrations at the scale surface, keeping it almost constant and higher than on the other side of the scale towards the steel surface, where NAP are consumed. Therefore concentration gradients will be established across the sulfide layers which generate molecular diffusion of species through the porous sulfide layer. The thin solid state sulfide layer attached to the steel surface is very dense and NAP are transported across it through solid state diffusion reaching the steel surface and attacking it.

#### ***7.2.6 Naphthenic Acid Corrosion – Mathematical Model***

The mathematical model below describes these processes by focusing on the transport of species by convection and diffusion fluxes from the bulk solution to the metal surface. The boundary layer is situated at the interface of the porous scale and is mainly dominated by the turbulent flow. Therefore the flux of RCOOH, done via convective diffusion is described by Equation 26:

$$Flux_{RCOOH} = k_{m,RCOOH} (c_{b,RCOOH} - c_{o,RCOOH}) \quad (26)$$

The molecular diffusion represents the transport mechanism of RCOOH through the porous sulfide scale. The flux of RCOOH by molecular diffusion is described according to Equation 27:

$$Flux_{RCOOH} = \frac{D_{RCOOH} \varepsilon \Psi}{\delta_{os}} (c_{o,RCOOH} - c_{i,RCOOH}) \quad (27)$$

The mass transport through the inner thin and dense layer is done by solid state diffusion. Thus the flux of RCOOH through the dense film is described by Equation 28:

$$Flux_{RCOOH} = A_{RCOOH} e^{-\frac{E_{RCOOH}}{RT}} \ln \left( \frac{c_{i,RCOOH}}{c_{s,RCOOH}} \right) \quad (28)$$

where:

$Flux_{RCOOH}$  - flux of RCOOH species [mol/(m<sup>2</sup>s)],

$k_{m,RCOOH}$  – mass transfer coefficient for RCOOH in the boundary layer [m/s].

$D_{RCOOH}$  - diffusion coefficient for dissolved RCOOH in the oil phase [mol/m<sup>3</sup>],

$c_{b,RCOOH}$  - bulk concentration of RCOOH in the oil phase [mol/m<sup>3</sup>],

$c_{o,RCOOH}$  - interfacial concentration of RCOOH at the outer scale interface, [mol/m<sup>3</sup>],

$c_{i,RCOOH}$  - interfacial concentration of RCOOH at the inner scale interface, [mol/m<sup>3</sup>],

$c_{s,RCOOH}$  - concentration of RCOOH at the steel surface [mol/m<sup>3</sup>],

$\delta_{os}$  – thickness of the outer scale [m],

$\varepsilon, \Psi$  – outer scale porosity and tortuosity,

$R$  - universal gas constant [J/(mol·K)],

$T$  – temperature [K],

$A_{RCOOH}$  - kinetic constant [mol/m<sup>2</sup>·s] for  $Fe_{(s)} + 2RCOOH \rightleftharpoons Fe^{2+}(RCOO^-)_2 + H_2$ ,

$E_{RCOOH}$  - activation energy [J/mol] for  $Fe_{(s)} + 2RCOOH \rightleftharpoons Fe^{2+}(RCOO^-)_2 + H_2$

Assuming that the mass transport of species is done under steady state conditions, all fluxes  $Flux_{RCOOH}$  are equal to each other and are equal to the NAP attack rate giving Equation 29:

$$NAP = A_{RCOOH} e^{-\frac{E_{RCOOH}}{RT}} \ln \frac{c_{b,RCOOH} - NAP \left( \frac{\delta_{os}}{D_{RCOOH} \varepsilon \Psi} + \frac{1}{k_{m,RCOOH}} \right)}{c_{s,RCOOH}} \quad (29)$$

Bulk concentration of RCOOH in the oil phase -  $c_{b,RCOOH}$  is known from TAN and so is the temperature  $T$ . The variables that had to be determined experimentally are the outer scale porosity  $\varepsilon$  and tortuosity  $\Psi$ , the kinetic constant and the activation energy for NAP corrosion attack  $A_{RCOOH}$  and  $E_{RCOOH}$  respectively. The model will calculate  $k_{m,RCOOH}$  – mass transfer coefficient for RCOOH in the boundary layer and  $\delta_{os}$  – thickness of the outer scale. Both variables  $k_{m,RCOOH}$  and  $\delta_{os}$  will be calculated in an analogous manner as it was done in the sulfidation rate model, by taking into account all possible influences induced by the level of turbulence, the flow regimes (annular- mist, bubble, slug, etc.), and the different flow geometries (bends, obstacles, constrictions, etc.).

The literature data were used again to calculate the values of activation energy and kinetic constant for NAP attack rate. Table 13 presents activation energy and kinetic constant values as function of metallurgy for most commonly used steel types.<sup>70</sup>

**Table 13.** Kinetic constant  $A_{RCOOH}$  and activation energy  $E_{RCOOH}$  for NAP corrosion attack as function of metallurgy<sup>70</sup>

Metallurgy	$A_{RCOOH}$ [mol/m <sup>2</sup> ·s]	$E_{RCOOH}$ [J/mol]
Carbon Steel	198.47	19,000
5Cr	198.47	19,000
9Cr	198.47	19,000
12Cr	168.70	19,000
304	49.62	19,000
306	0.99	19,000

### 7.3 Verification of the Model

In order to verify and fine tune the model for NAP corrosion it was decided to compare the sulfidation-challenge tests results against model predictions. The sulfidation-challenge experiments have already been described in Chapter 5 but they will be explained briefly below for a better understanding of comparisons with model predictions. The sulfidation-challenge tests were done in the HVR where specimens were presulfided *in-situ* and then challenged with NAP acids of different TAN levels. During sulfidation FeS scales were formed on CS and 5Cr specimens using Yellow oil with TAN = 0.1 and S = 0.25 % wt. In the challenges, the steel specimens were attacked with NAP contained in white oil. NAP concentrations in white oil covered a range of TAN 2 – 8. NAP effects against FeS scales and metals were evaluated by measuring final corrosion rates of specimens.

### 7.3.1 CS Corrosion Rate Comparison

Figure 117 presents the comparison of CS corrosion rates against model predictions. Model predictions represented by continuous thick lines were generated for each TAN challenging level used in experiments. Although these predictions are lower than their corresponding experimental data it is very clear that the model was able to reproduce the trends of corrosion rates for each TAN case. These predictions can be corrected as the kinetics of scale formation and damage and the factors that influence them are further investigated and better understood.

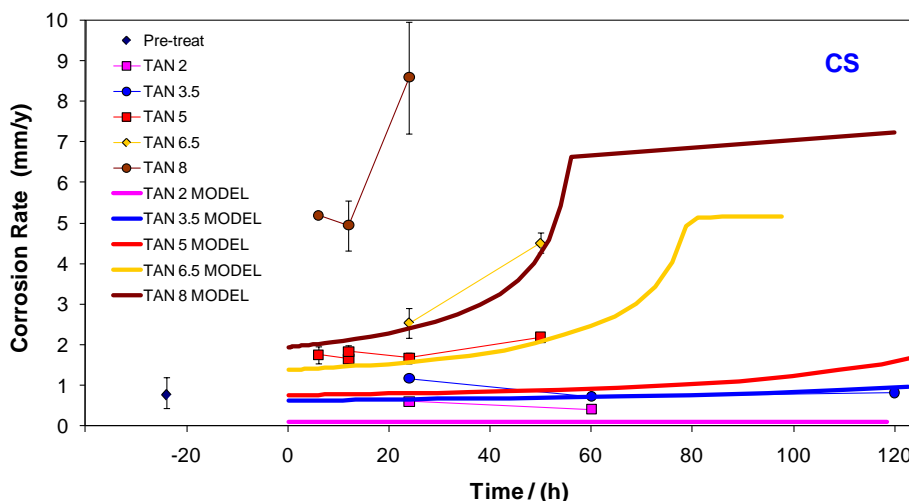


**Figure 117.** Comparison between model prediction and measured corrosion rates on CS during sulfidation-challenge experiments. Model predictions are plotted as continuous thick lines whereas experimental data are points connected by lines.

### 7.3.2 5Cr Corrosion Rate Comparison

The comparison of 5Cr corrosion rates to model predictions is shown in Figure 118. As in the case of CS, the model generated lower predicted values than real experimental data.

For 5 Cr steel the model predicts an increase of CRs over longer exposures, something that has to be confirmed in longer experiments. Similarly to the case of CS the predictions for 5Cr will be corrected as the influencing factors of these processes will be thoroughly investigated and understood during the future work of this current project.

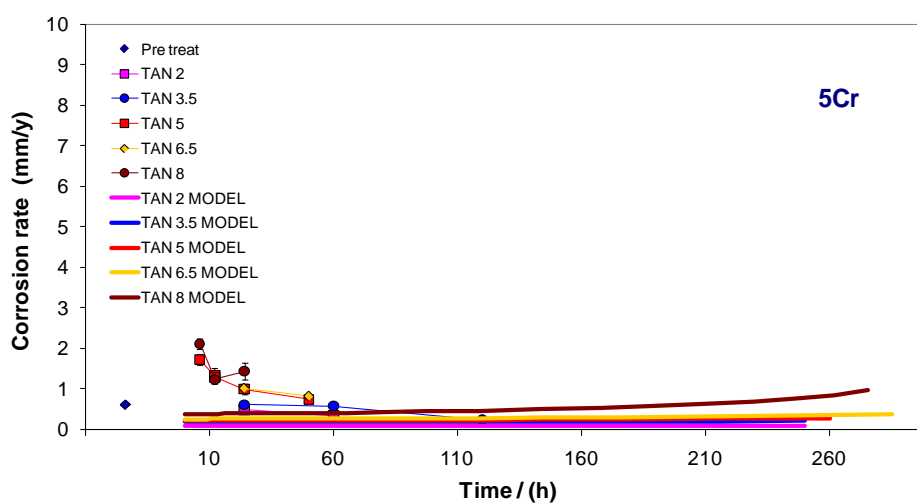


**Figure 118.** Comparison between model prediction and measured corrosion rates on 5Cr during sulfidation-challenge experiments. Model predictions are plotted as continuous thick lines whereas experimental data are points connected by lines.

## CHAPTER 8: CONCLUSIONS

A physico-chemical model of naphthenic acid corrosion in the presence of reactive sulfur compounds was built. This model consists of two interconnected parts: sulfidation model that predicts the growth of FeS scales on metal surfaces and naphthenic acid corrosion predicting model. Both parts of the model are a function of reactive species concentrations (i.e. sulfur %, TAN) at metal surfaces and the testing conditions such as high temperatures and high velocities. The sulfidation part includes a mechanism that takes into consideration the kinetics of FeS scale growth and damage under NAP acids corrosive attack. Similarly the NAP corrosion part of the model is based on a mechanism taking into consideration NAP diffusion processes through FeS scales.

The model was able only partially to predict NAP corrosion rates on the two types of steel in sulfur containing oils. While the model predictions reproduced the trend of the corrosion rates, the predicted levels of attack were lower than observed. These differences between predictions and experimental data require additional experimental work in order to fine tune the model.

The model was calibrated against two large sets of experimental data generated using model oils. The first set of data referred mainly to the sulfidation processes that were run under low NAP acid concentrations. The second set of experimental data was related to NAP attacks on both CS and 5Cr surfaces and to the FeS scales covering them. A third set of experimental data were generated by challenging with NAP the FeS scales formed with real crude oil fractions. This third data set will be used when the model is evolved to account for the effects seen in real crude oil fraction corrosion. These are not properly understood yet.

Finally it can be concluded that the main goals of the project were accomplished by building a NAP acid corrosion model based on experimental data generated with both model oils and crude oil fractions.

## CHAPTER 9: RECOMMENDATION AND FUTURE WORK

As it was mentioned in previous Chapter 8, the model for NAP corrosion was able to predict the trend in corrosion but at a lower level than experimental data. Therefore further adjustments have to be done to improve model accuracy and corrosion rates predictions. It was suggested that asphaltene oil content might influence formation of FeS scales on metals as well as the scale protectiveness against NAP attack. Future experiments have to investigate if asphaltene play an important role in FeS scale formation and resistance.

New literature data <sup>43,73</sup> suggested the existence of differences in NAP reactivity as function of their structure and corresponding molecular weight. Future experimental studies might take into consideration the corrosion rates as function of NAP acids molecular weight distribution. Whether or not these factors are important in NAP acids corrosion remains to be determined in further experimental work.

## REFERENCES

1. Bota, G.M.; HVR Progress Report, Institute for Corrosion & Multiphase Technology, Ohio University, Confidential Report, **2005**.
2. Bota, G.M.; HVR Progress Report - Presulfidation Challenge, Institute for Corrosion & Multiphase Technology, Ohio University, Confidential Report, **2006**.
3. Bota, G.M.; HVR Progress Report, Institute for Corrosion & Multiphase Technology, Ohio University, Confidential Report, **2008**.
4. Derungs, W.A.; Naphthenic Acid Corrosion – An Old Enemy of the Petroleum Industry. *Corr.* **1956**, *12*, 617-622.
5. Gutzeit, J.; Naphthenic Acid Corrosion in Oil Refineries. *Mater. Perform.* **1977**, *16*, 24-35.
6. Piehl, R.L.; Naphthenic Acid Corrosion in Crude Distillation Units. *Mater. Perform.* **1988**, *27* (1), 37-43.
7. Slavcheva, E.; Shone, B.; Turnbull, A.; Review of Naphthenic Acid Corrosion in Oil Refining. *Br. Corr. J.* **1999**, *34* (2), 125-131.
8. Kane, R.D.; Cayard, M.S.; Understanding Critical Factors that Influence Refinery Crude Corrosiveness. *Mater. Perform.* **1999**, July, 48-54.
9. Yépez, O.; Influence of Different Sulfur Compounds on Corrosion due to Naphthenic Acid. *Fuel*, **2005**, *84*, 97-104.
10. Hau, J.L.; Yépez, O.; Specht, M.I.; Lorenzo, R.; The Iron Powder Test for Naphthenic Acid Corrosion Studies. *Corr. Paper No.379.*, **1999**, 1-16.
11. Hau, J.L.; Yépez, O.; Torres, L.; Specht, M.I.; Classifying Crude Oils According to Corrosivity Using The Fe Powder Test. *Corr. Paper No.00699*, **2000**, 1-9.
12. Kapusta, S.D.; Ooms, A.; Smith, A.; Van den Berg, F.; Fort, W.; Safe Processing of Acid Crudes. *Corr. Paper 04637*, **2004**, 1-19.
13. Hsu, C.S.; Dechert, G.J.; Robbins, W.K.; Fukuda, E.K.; Naphthenic Acids in Crude Oils Characterized by Mass Spectrometry. *Energy & Fuels*, **2000**, *14*, 217-223.
14. Marshall, A.G.; Rodgers, R.P.; Petroleomics: Chemistry of the Underworld. *Proc. Natl. Acad. Sci. U.S.A.* **2008**, *105* (47), 18090-18095.

15. Fan, T.P.; Characterization of Naphthenic Acids in Petroleum by Fast Atom Bombardment Mass Spectrometry. *Energy & Fuels*, **1991**, *5*, 371-375.
16. Dzidic, I.; Somerville, A.C.; Raia, J.C.; Hart, H.V.; Determination of Naphthenic Acids in California Crudes and Refinery Waste Waters by Fluoride Ion Chemical Ionization Mass Spectrometry, *Anal. Chem.* **1988**, *60*, 1318-1323.
17. St. John, W.P.; Rughani, J.; Green, S.A.; McGinnis, G.D.; Analysis and Characterization of Naphthenic Acids by Gas Chromatography-Electron Impact Mass Spectrometry of *tert.*-Buthyldimethylsilyl Derivatives. *J.Chromatogr., A.* **1998**, *807*, 241-251.
18. Clemente, J.S.; Fedorak, P.M.; Evaluation of the Analyses of *tert.*-Buthyldimethylsilyl Derivatives of Naphthenic Acids by Gas Chromatography-Electron Impact Mass Spectrometry. *J.Chromatogr., A.* **2004**, *1047*, 117-128.
19. Barrow, M.P.; McDonnell, L.A.; Feng, X.; Walker, J.; Derrick, P.J.; Determination of the Nature of Naphthenic Acids Present in Crude Oils Using Nanospray Fourier Transform Ion Cyclotron Resonance Mass Spectrometry: The Continued Battle Against Corrosion. *Anal. Chem.* **2003**, *75* (4), 860-866.
20. Tomczyk, N.A.; Winans, R.E.; Shinn, J. H.; Robinson, R.C.; On the Nature and Origin of Acidic Species in Petroleum. 1 Detailed Acid Type Distribution in a California Crude Oil. *Energy & Fuels*, **2001**, *15*, 1498-1504.
21. Rudzinski, W.E.; Oehlers, L.; Zhang, Y.; Tandem Mass Spectrometric Characterization of Commercial Naphthenic Acids and a Maya Crude Oil. *Energy & Fuels*, **2002**, *16*, 1178-1185.
22. Clemente, J.S.; Prasad, N.G.N.; MacKinnon, M.D.; Fedorak, P.M.; A Statistical Comparison of Naphthenic Acids Characterized by Gas Chromatography-Mass Spectrometry. *Chemosphere.* **2003**, *50*, 1265-1274.
23. Laredo, G.C.; Lopez, C.R.; Alvarez, R.E.; Cano, J.L.; Naphthenic Acids Total Acid Number and Sulfur Content Profile Characterization in Isthmus and Maya Crude Oils. *Fuel*, **2004**, *83*, 1689-1695.
24. Laredo, G.C.; Lopez, C.R.; Alvarez, R.E.; Castillo, J.J.; Cano, J.L.; Identification of Naphthenic Acids and Other Corrosivity-Related Characteristics in Crude Oil and Vacuum Gas Oils from a Mexican Refinery. *Energy & Fuels*, **2004**, *18*, 1687-1694.

25. Rogers, V.V.; Liber, K.; MacKinnon, M.D.; Isolation and Characterization of Naphthenic Acids from Athabasca oil Sands Tailings Pond Water. *Chemosphere*. **2002**, *48*, 519-527.
26. Holowenko, F.M.; MacKinnon, M.D.; Fedorak, P.M.; Characterization of Naphthenic Acids in Oil Sands Wastewaters by Gas Chromatography-Mass Spectrometry. *Water Res.* **2002**, *36*, 2843-2855.
27. Saab, J.; Mokbel, I.; Razzouk, A.C.; Ainous, N.; Zydowicz, N.; Jose, J.; Quantitative Extraction Procedure of Naphthenic Acids Contained in Crude Oils. Characterization with Different Spectroscopic Methods. *Energy & Fuels*, **2005**, *19*, 525-531.
28. Babaian-Kibala, E.; Craig H.L.; Rusk, G.L.; Quinter R.C.; Summers M.A.; Naphthenic Acid Corrosion in Refinery Settings. *Mater. Perform.* **1993**, 50-55.
29. Jayaraman, A.; Singh, H.; Naphthenic Acid Corrosion in Petroleum Refineries – A Review. *Revue de l'Institute Français du Pétrole*, **1986**, *41* (2), 265-274.
30. Hopkinson, B.E.; Penuela, L.E.; Lagoven, L.P.; Naphthenic Acid Corrosion by Venezuelan Crudes. *Corr. Paper No.502*, **1997**, 1-15.
31. Nugent, M.J.; Dobis, J.D.; Experience with Naphthenic Acid Corrosion in Low TAN Crudes. *Corr. Paper No.577*, **1998**, 1-8.
32. Lewis, K.R.; Daane, M.L.; Scheling, R.; Processing Corrosive Crude Oils. *Corr. Paper No.377*, **1999**, 1-10.
33. Groysman, A.; Brodsky, N.; Penner, J.; Goldis, A.; Savchenko, N.; Study of corrosiveness of acidic crude oil and its fractions. *Corr. Paper No.05568*, **2005**, 1-13.
34. ASTM D664: Standard Test Method for Acid Number of Petroleum Products by Potentiometric Titration. (West Conshohocken, PA, Annual Book of ASTM Standards Vol. 05.01 1990).
35. ASTM D974: Standard Test Method for Acid Number and Base Number by Color-Indicator Titration. (West Conshohocken, PA, Annual Book of ASTM Standards Vol. 05.01, 1990).
36. Schulz, H.; Böhringer, W.; Waller, P.; Ousmanov, F.; Gas Oil Deep Hydrodesulfurization: Refractory Compounds and Retarded Kinetics. *Catal. Today*. **1999**, *49*, 87-97.
37. Schulz, H.; Böhringer W.; Ousmanov, F.; W.; Waller, P.; Refractory Sulfur Compounds in Gas Oils, *Fuel Process. Technol.* **1999**, *61*, 5-41.

38. Nihioka, M.; Aromatic Sulfur Compounds Other Than Condensed Thiophenes in Fossil Fuels: Enrichment and Identification. *Energy & Fuels*, **1988**, 2, 214-219.
39. Murillo, M.; Carrión, N.; Chirinos, J.; Determination of Sulfur in Crude Oils and Related Materials With a Parr Bomb Digestion Method and Inductively Coupled Plasma Atomic Emission Spectrometry. *J. Anal. At. Spectrom.* **1993**, 8, 493-495.
40. Hua, R.; Wang, J.; Kong, H.; Liu, J.; Lu, X.; Xu, G.; Analysis of Sulfur-Containing Compounds in Crude Oils by Comprehensive Two-Dimensional Gas Chromatography with Sulfur Chemiluminescence Detection. *J. Sep. Sci.* **2004**, 27, 691-698.
41. Okuno, I.; Latham, D.R.; Haines, W.E.; Separation of Sulfoxides from Petroleum Fractions by Cation Exchange Resin Chromatography. *Anal. Chem.* **1967**, 39,(14), 1830-1833.
42. Hegazi, A.H.; Anderson, J.T.; El-Gayar, M.S.; Application of Gas Chromatography with Atomic Emission Detection to the Geochemical Investigation of Polycyclic Aromatic Sulfur Heterocycles in Egyptian Crude Oils. *Fuel Process. Technol.* **2003**, 85, 1-19.
43. Messer, B.; Tarleton B.; Beaton M.; Phillips, T.; New Theory for Naphthenic Acid Corrosivity of Athabasca Oilsandes Crudes. *Corr. Paper No.04634*, **2004**, 1-11.
44. Speight, J.G.; *The Chemistry and Technology of Petroleum* 3<sup>rd</sup> Ed. Marcel Dekker, New York 1999, pp 244f.
45. Jones, D.S.J.; *Elements of Petroleum Processing* Ed. Wiley & Sons New York **1995**.
46. Jayaraman, A.; Saxena, R.C.; Corrosion and its Control in Petroleum Refineries – A Review. *Corr. Prevent. & Contr.* **1995**, 123-131.
47. Zeianov, E.B.; Abbasov, V.M.; Alieva, L.I.; Petroleum Acids and Corrosion, *Petroleum Chem.*, **2009**, 49, (3), 185-192.
48. Tebbal, S.; Kane, R.D.; Yamada, K.; Assessment of the Corrosivity of Crude oil fraction s from Varying Feedstock. *Corr. Paper No.498*, **1997**, 1-13.
49. Tebbal, S.; Schutt, H.; Podlecki, R.; Sudhakar, C.; Analysis and Corrosivity Testing of Eight Crude Oils. *Corr. Paper No. 04636*, **2004**, 1-13.
50. Kane, R.D.; Cayard, M.S.; A Comprehensive Study on Naphthenic Acid Corrosion. *Corr. Paper No.02555*, **2002**, 1-16.

51. Craig H.L.; Temperature and Velocity Effects in Naphthenic Acid Corrosion. *Corr. Paper No.603*, **1996**, 1-13.
52. Groysman, A.; Brodsky, N.; Penner, J; Shmulevich,D.; Low Temperature Naphthenic Acid Corrosion Study. *Corr. Paper No.07569*, **2007**, 1-20.
53. Efrid, K.D.; Wright, E.J.; Boros, J.A.; Hailey, T.G.; Experimental Correlation of Steel Corrosion in Pipe Flow with Jet Impingement and Rotating Cylinder Laboratory Tests. *Corr. Paper No 81*, **1993**, 1-21.
54. Craig H.L.; Naphthenic Acid Corrosion in the Refinery. *Corr. Paper No.333*, **1995**, 120-141.
55. Johnson, D.; McAteer, G.; Zuk, H.; The Safe Processing of High Naphthenic Acid Content Crude Oil-Refinery Experience and Mitigation Studies. *Corr. Paper No. 03645*, **2003**, 1-18.
56. Pritchard, A.M.; Graham, A.; Rance, A.; Use of a Rotating Cylinder System to determine the Corrosivities of Acid Crudes. *Corr. Paper No. 01525*, **2001**, 1-8.
57. Smart, N.R.; Rance, A.P.; Pritchard, A.M.; Laboratory Investigation of Naphthenic Acid Corrosion under Flowing Conditions. *Corr. Paper No. 02484*, **2002**, 1-23.
58. Wu, X.Q.; Jing, H.M.; Zheng, Y.G.; Yao, Z.M.; Ke, W.; Resistance of Mo-Bearing Stainless Steels and Mo-Bearing Stainless Steel Coating to Naphthenic Acid Corrosion and Erosion-Corrosion. *Corros. Sci.* **2004**, *46*, 1013-1032.
59. .Wu, X.Q.; Jing, H.M.; Zheng, Y.G.; Yao, Z.M.; Ke, W; Errosion-Corrosion of Various Oil-Refining Materials in Naphthenic Acid. *Wear.* **2004**, *256*, 133-144.
60. Wu, X.Q.; Jing, H.M.; Zheng, Y.G.; Yao, Z.M.; Ke, W; Corrosion and Errosion-Corrosion Behaviors of Carbon Steel in Naphthenic Acid Media. *Mater. Corr.* **2002**, *53*, 833-844.
61. Wu, X.Q.; Jing, H.M.; Zheng, Y.G.; Yao, Z.M.; Ke, W; Study on High Temperature Naphthenic Acid Corrosion and Errosion-Corrosion of Aluminized Carbon Steel. *Journ. Mater. Sci.* **2004**, *39*, 975-983.
62. Tsipas, D.N.; Noguera, H.; Rus, J.; Corrosion Behavior of Boronized Carbon Steel. *Mater.Chem.Physics.* **1987**, *18*, 295-303.
63. Oyekunle, L.O.; Dosunmu, A.J.; High Temperature Corrosion Tests for Kerosene and Gas Oil Samples. *Petr. Sci. Technol.* **2003**, *21* (9-10), 1499-1508.

64. Tebbal, S.; Kane, R.D.; Review of Critical Factors Affecting Crude Corrosivity. *Corr. Paper No.607*, **1996**, 1-10.
65. De Bruin H.J.; Naphthenic Acid Corrosion in Synthetic Fuels Production. *Corr. Paper No.576*, **1998**, 1-14.
66. Tebbal, S.; Kane, R.D.; Assessment of Crude Oil Corrosivity. *Corr. Paper No.578*, **1998**, 1-11.
67. Tebbal, S.; Critical Review of Naphthenic Acid Corrosion. *Corr. Paper No.380*, **1999**, 1-9.
68. ASTM G 1-90 "Standard Practice for Preparing, Cleaning, and Evaluating Corrosion Test Specimens".(West Conshohocken, PA, Annual Book of ASTM Standards, Vol. 03.02, 1990).
69. Gabetta G.; Mancini, N.; Montanari, L.; Oddo, G.; Preliminary Results of a Project on Crude Oil Corrosion. *Corr. Paper No.03644*, **2003**, 1-11.
70. McConomy, H.F.; High Temperature Sulfidic Corrosion in Hydrogen Free Environment. *Proceedings of API*, Washington D.C. Vol 43 (3), 1963.
71. *Flow of Fluids Through Valves, Fittings, and Pipe*, Crane Technical Paper No. 410, Shenandoah, TX, 1988.
72. Berger, F.P.; Hau, K.F., F.L.; Mass Transfer in Turbulent Pipe Flow Measured by the Electrochemical Method. *Int. J. Heat Mass Transfer*. **1977**, *20*, 1185-1194.
73. Östlund, J.A.; Nydén, M.; Auflem, I.H.; Sjöblom, J.; Interactions between Asphaltenes and Naphthenic Acids. *Energy & Fuels*, **2003**, *17*, 113-119.

**APPENDIX A: INITIAL TEST MATRIX FOR SULFIDATION TESTS DONE IN THE HIGH VELOCITY RIG  
(HVR) FALL 2005**

HVR Initial Test Matrix  
Yellow Oil

Test No.	Pre-treatment					Challenge					note
	time	feed*	TAN	S	temp	time	feed	TAN	S	temp	
1	6 h	A	0.1	0.25	600	0					to establish connection with static autoclave pre-treatment
2	24	A	0.1	0.25	600	0					
3	48	A	0.1	0.25	600	0					
4	6	A	0.1	0.25	650	0					to establish quality & kinetics of scale growth in model fluid
5	24	A	0.1	0.25	650	0					
6	48	A	0.1	0.25	650	0					
7	based on #4	A	0.1	0.25	650	12	B	5	0	650	challenge with spiked white oil
8	based on #5	A	0.1	0.25	650	based on #7	B	5	0	650	
9	based on #6	A	0.1	0.25	650	based on #7	B	5	0	650	

Runs 1-3 are to establish that sulfide films formed in the HVR are equivalent to those formed in the static autoclave, which is limited to 600°F maximum temperature.

Runs 4-6 are equivalent to runs 1-3 except that they are done at 650°F, and they will be the basis for all runs to follow.

Runs 7-9 challenge the sulfide films formed in runs 4-6 (grown in a model fluid) using white oil spiked to high TAN.

\*Feeds:

A = yellow oil spiked with TAN (yellow oil S = 0.25)

B = white oil spiked with TAN (white oil TAN = 0)

## APPENDIX B: TEST MATRIX FOR SULFIDATION-CHALLENGE TESTS DONE IN THE HIGH VELOCITY RIG (HVR)

HVR Test Matrix  
Sulfidation-Challenge Tests

Test No.	Sulfidation					Challenge					
	time	feed*	TAN	S	temp	time	feed	TAN	S	temp	note
1	24	Yellow Oil	0.1	0.25	650						
2	24	Yellow Oil	0.1	0.25	650						
3	24	Yellow Oil	0.1	0.25	650						
4	24	Yellow Oil	0.1	0.25	650	24	White Oil+TCI	<b>2</b>	0	650	TAN 2 challneges as function of time
5	24	Yellow Oil	0.1	0.25	650	60	White Oil+TCI	<b>2</b>	0	650	
6	24	Yellow Oil	0.1	0.25	650	24	White Oil+TCI	<b>3.5</b>	0	650	TAN 3.5 challneges as function of time
7	24	Yellow Oil	0.1	0.25	650	60	White Oil+TCI	<b>3.5</b>	0	650	
8	24	Yellow Oil	0.1	0.25	650	120	White Oil+TCI	<b>3.5</b>	0	650	
9	24	Yellow Oil	0.1	0.25	650	6	White Oil+TCI	<b>5</b>	0	650	TAN 5 challneges as function of time
10	24	Yellow Oil	0.1	0.25	650	12	White Oil+TCI	<b>5</b>	0	650	
11	24	Yellow Oil	0.1	0.25	650	24	White Oil+TCI	<b>5</b>	0	650	
12	24	Yellow Oil	0.1	0.25	650	50	White Oil+TCI	<b>5</b>	0	650	
13	24	Yellow Oil	0.1	0.25	650	24	White Oil+TCI	<b>6.5</b>	0	650	TAN 6.5 challneges as function of time
14	24	Yellow Oil	0.1	0.25	650	50	White Oil+TCI	<b>6.5</b>	0	650	
15	24	Yellow Oil	0.1	0.25	650	6	White Oil+TCI	<b>8</b>	0	650	TAN 8 challneges as function of time
16	24	Yellow Oil	0.1	0.25	650	12	White Oil+TCI	<b>8</b>	0	650	
17	24	Yellow Oil	0.1	0.25	650	24	White Oil+TCI	<b>8</b>	0	650	
18	24	Yellow Oil	0.1	0.25	<b>550</b>	60	White Oil+TCI	<b>3.5</b>	0	<b>650</b>	FeS scale was formed at low temperature
19	24	Yellow Oil	0.1	0.25	650	24	White Oil+TCI	<b>5</b>	0	650	FeS scale was formed at low velocity conc

Runs 1-3 are sulfidation reference test. FeS scale is formed. Tests are done to determine weight loss (metal) and gain (scale) needed in challenge calculations.

Runs 4-17 challenge the sulfide scales formed with Yellow Oil under identical conditions. Different TAN challenges as function of time.

Run 18 challenge the sulfide films formed at 550F temperature using Yellow Oil. TAN 3.5 challenge was run at 650F.

Run 19 challenged FeS scale formed under low velocity conditions (500rpm). Challenge was done at 2000 as in every previous test.

## **APPENDIX C: EXPERIMENTAL RESULTS AND SEM IMAGES FOR SULFIDATION-CHALLENGE TESTS DONE IN THE HIGH VELOCITY RIG (HVR)**

All experimental results (graphs, SEM images, EDX analysis results) corresponding to this Appendix C can be accessed on this link:

[Appendix C Presulfidation Challenge Experimental Results](#)

## APPENDIX D: TEST MATRIX FOR NAP ACIDS CHALLENGES AGAINST SCALES FORMED WITH REAL CRUDE OIL FRACTIONS

Autoclave-HVR Test Matrix  
Real Crude Fractions Tests

Test No.	Sulfidation (Autoclaves)					Challenge (HVR)					note	
	time	feed*	TAN	S	temp	time	feed	TAN	S	temp		
1	24	Yellow Oil	0.1	0.25	650							Sulfidation Reference Test
2	24	Yellow Oil	0.1	0.25	650	24	White Oil+TCl	3.5	0	650	FeS scales generated in same conditions (TAN and Sulf	in previous sulfidation tests.
3	24	Yellow Oil	0.1	0.25	650	24	White Oil+TCl	6.5	0	650		
4	24	DDD VGO dilut	0.1	0.25	650						Sulfidation Reference Test	
5	24	DDD VGO dilut	0.1	0.25	650	24	White Oil+TCl	3.5	0	650	FeS scales were challenged with low and high TAN solu	
6	24	DDD VGO dilut	0.1	0.25	650	24	White Oil+TCl	6.5	0	650		
7	24	HH1 VGO dilut	0.1	0.25	650						Sulfidation Reference Test	
8	24	HH1 VGO dilut	0.1	0.25	650	24	White Oil+TCl	3.5	0	650	FeS scales were challenged with low and high TAN solu	
9	24	HH1 VGO dilut	0.1	0.25	650	24	White Oil+TCl	6.5	0	650		
10	24	DDD VGO	0.2	0.7	650						Sulfidation Reference Test	
11	24	DDD VGO	0.2	0.7	650	24	White Oil+TCl	3.5	0	650	FeS scale generated with neat fractions (natural TAN an	Sulfur content)
12	24	DDD VGO	0.2	0.7	650	24	White Oil+TCl	6.5	0	650		
13	24	HH1 VGO	0.2	0.92	650						Sulfidation Reference Test	
14	24	HH1 VGO	0.2	0.92	650	24	White Oil+TCl	3.5	0	650	FeS scales were challenged with low and high TAN solu	
15	24	HH1 VGO	0.2	0.92	650	24	White Oil+TCl	6.5	0	650		
16	24	BBB VGO	<0.1	0.6	650						Sulfidation Reference Test	
17	24	BBB VGO	<0.1	0.6	650	24	White Oil+TCl	3.5	0	650	FeS scales were challenged with low and high TAN solu	
18	24	BBB VGO	<0.1	0.6	650	24	White Oil+TCl	6.5	0	650		
19	24	AAA VGO	1.75	0.18	650						Sulfidation Reference Test	
20	24	AAA VGO	1.75	0.18	650	24	White Oil+TCl	3.5	0	650	FeS scales were challenged with low and high TAN solu	
21	24	AAA VGO	1.75	0.18	650	24	White Oil+TCl	6.5	0	650		
22	24	CCC 650+	1	1.51	650						Sulfidation Reference Test	
23	24	CCC 650+	1	1.51	650	24	White Oil+TCl	3.5	0	650	FeS scales were challenged with low and high TAN solu	
24	24	CCC 650+	1	1.51	650	24	White Oil+TCl	6.5	0	650		
25	24	Yellow Oil	1.75	0.25	650						Sulfidation Reference Test	
26	24	Yellow Oil	1.75	0.25	650	24	White Oil+TCl	3.5	0	650	FeS scale generated under identical high TAN test conc	
27	24	Yellow Oil	1.75	0.25	650	24	White Oil+TCl	6.5	0	650		
28	24	HH1 VGO	1.75	0.92	650						Sulfidation Reference Test	
29	24	HH1 VGO	1.75	0.92	650	24	White Oil+TCl	3.5	0	650	FeS scales were challenged with low and high TAN solu	
30	24	HH1 VGO	1.75	0.92	650	24	White Oil+TCl	6.5	0	650		
31	24	BBB VGO	1.75	0.6	650						Sulfidation Reference Test	
32	24	BBB VGO	1.75	0.6	650	24	White Oil+TCl	3.5	0	650	FeS scales were challenged with low and high TAN solu	
33	24	BBB VGO	1.75	0.6	650	24	White Oil+TCl	6.5	0	650		
34	24	CCC 650+	1.75	1.51	650						Sulfidation Reference Test	
35	24	CCC 650+	1.75	1.51	650	24	White Oil+TCl	3.5	0	650	FeS scales were challenged with low and high TAN solu	
36	24	CCC 650+	1.75	1.51	650	24	White Oil+TCl	6.5	0	650		
37						24	White Oil+TCl	0.1	0	650	Pure Naphthenic Acid Corrosion Tests	
38						24	White Oil+TCl	2	0	650		
39						24	White Oil+TCl	3.5	0	650		
40						24	White Oil+TCl	5	0	650		
41						24	White Oil+TCl	6.5	0	650		
42						24	White Oil+TCl	8	0	650		

Runs 1-9 challenge the sulfide scales formed with Yellow Oil and 2 different crude fractions diluted to same TAN and S concentrations as Yellow Oil (model oil).

Runs 10-24 challenge the sulfide scales formed with 5 different neat crude fractions. Neat fractions had natural TAN and S content as they distilled from oil.

Runs 25-36 challenge the sulfide scales formed with Yellow Oil and 4 different crude fractions spiked to identical high TAN (1.75). Original Sulfur content of each fraction was not changed.

Runs 37-42 were Pure Naphthenic Acid Corrosion Tests that were done in the HVR.

**APPENDIX E: EXPERIMENTAL RESULTS AND SEM IMAGES FOR NAP  
ACIDS CHALLENGES AGAINST SCALES FORMED WITH REAL CRUDE OIL  
FRACTIONS**

All experimental results (graphs, SEM images, EDX analysis results) corresponding to this Appendix E can be accessed on this link:

[APPENDIX E Autoclave Results](#)